# Anaerobic digestion of nut and coffee wastes: different pretreatment techniques to enhance methane production

A thesis submitted to the National University of Ireland Galway (NUIG) as fulfilment of the requirements for the degree of Doctor of Philosophy

by

Armando Oliva

Supervisor: Prof. Piet N. L. Lens

School of Natural Sciences

May 2022

**Declaration**

I, Armando Oliva, declare that this thesis or any part thereof has not been, or not currently being, submitted for any degree at the National University of Ireland, or any other University. I further declare that the work embodied is my own.

**Armando Oliva**

**Summary**

Lignocellulosic materials (LMs) are the most abundant residues on the planet and have a great potential for methane production. Nevertheless, the energy potential of LMs for biofuel production is limited by their complex structure. LMs are composed of cellulose, hemicellulose, lignin and non-bound matter, which include free sugars, polyphenols, protein and lipids. This PhD thesis investigated the impact of organosolv, N-methylmorpholine N-oxide (NMMO)-driven, and ultrasounds pretreatment on the methane production potential of hazelnut skin (HS), almond shell (AS), and spent coffee grounds (SCG).

The first experimental phase (Chapter 3) investigated a methanol-organosolv pretreatment performed at 130, 160, and 200 °C with and without catalyst addition. The biochemical methane potential (BMP) of HS increased up to 18-folds, and the catalyst addition allowed lowering of the pretreatment temperature. On the contrary, all pretreatment conditions failed to enhance the BMP of SCG and AS. In Chapter 4, a swelling mode NMMO pretreatment was performed for 1, 3, and 5 h. The NMMO pretreatment enhanced the BMP of AS up to 58%. The pretreated SCG showed increased porosity (up to 63%) and a higher sugar percentage (up to 27%) despite failing to increase the methane production. All pretreatment conditions were effective on HS, achieving the highest methane production of 400.4 mL $CH_4$/g VS after increasing the sugar (up to 112%) and reducing the lignin (up to 29%) content. Chapter 5 focused on ultrasound pretreatment. The liquid fraction of ultrasound pretreated HS was particularly rich in polyphenols (up to 11.5 g/L) and sugars (up to 13.2 g/L), showing great potential for biomolecules recovery. The liquid fraction from ultrasound pretreated AS and SCG are suitable for valorisation through anaerobic digestion (AD). The solid residues recovered after ultrasounds were used for methane production and a similar BMP compared to the raw LMs was obtained.

Chapter 6 investigated the fed-batch AD of raw, macerated, and methanol-organosolv pretreated HS, focusing on the factors impacting the process in the long term. An efficient reactor configuration was proposed to increase the substrate load while reducing the solid retention time during the fed-batch AD of HS. Maceration and methanol-organosolv pretreatment were used to remove polyphenols from HS (i.e. 82 and 97% removal, respectively) and improve HS biodegradation. Additionally, organosolv pretreatment removed 9% of the lignin. The organosolv-pretreated HS showed an increment in methane production potential of 21%, while macerated HS produced less methane than the raw substrate, probably due to the loss of non-structural sugars during maceration.

**Acknowledgement**

First, I would like to thank the Science Foundation of Ireland (SFI) for supporting the SFI Research Professorship Programme entitled Energy Technologies for Biofuels, Bioenergy and a Sustainable Irish Bioeconomy (IETSBIO3). It has been a privilege for me to be part of the international group built by Professor Piet N. L. Lens at the National University of Ireland Galway (NUIG).

I particularly thank Professor Piet Lens for giving me the freedom to develop my research project under his careful guidance. He allowed me to work in a fantastic lab and meet all the people involved in this research project. I will always be grateful to Professor Giovanni Esposito (University of Naples Federico II), who introduced me to the research world, enabling me to work in the laboratory of the University of Cassino and Southern Lazio during my Bachelor's and Master's thesis. A special thank certainly goes to Stefano Papirio, who made me love the research since my Bachelor's and still keeps helping me through my PhD.

An important role in choosing to start this PhD was played by the research group I met in Seville in 2018 during my internship. I worked with Fernando, Juan, Angeles, Rafael, Paco, Adrian, Ainoa, and Gema. During that experience, I understood how enjoyable the lab work can be when you are surrounded by the right people.

I thank all the colleagues I met at the University of Naples II during my internship. My mentor Lea, for all the help she gave me, especially in the first year of my PhD. Thank you, great "god of the lab" Borja, for being the best research assistant ever! Manuel, Leah, and Marlee for the research support. Simone, Federica, Carlos, Laura, Paolo, Fabiano, Marco (both tall and short), Juan, Peyman, Jewel, Yaxue, George, Ana Maria, Mohan, and Sudeshna for the moments we spent together in Galway. I also want to thank all the research groups collaborating with us for the help that never missed at NUIG when needed.

I thank my great friends Francesco (FB) and Egidio for the moments we shared. I hope that a lot more will follow. Finally, I thank my parents, my brother Matteo, and my girlfriend Camilla for supporting my choices. It was not easy to be so far away, especially during the pandemic, but we made it through, and I hope it was worth it.

*Per aspera ad astra*

**Table of contents**

## List of figures

## List of tables

**List of publications and chapters contribution**

The work contained in this thesis consists of the following publications in international peer-reviewed journals and books:

| Publication | Author contribution |
|---|---|
| **Chapter 2:** Oliva A., Papirio S., Esposito G., Lens P.N.L., 2022. Pretreatment of Lignocellulosic Materials to Enhance their Methane Potential. In: Sinharoy A., Lens P.N.L. (eds) Renewable Energy Technologies for Energy Efficient Sustainable Development. Applied Environmental Science and Engineering for a Sustainable Future. Springer, Pages 85–120. https://doi.org/10.1007/978-3-030-87633-3_4 | **A. Oliva:** conceptualization, investigation, methodology, writing - original draft, writing - review & editing. **S. Papirio:** supervision, writing - review & editing. **G. Esposito:** supervision, writing - review & editing. **P.N.L. Lens:** supervision, writing - review & editing, project administration, funding acquisition. |
| **Chapter 3:** Oliva A., Tan L.C., Papirio S., Esposito G., Lens P.N.L., 2021. Effect of methanol-organosolv pretreatment on anaerobic digestion of lignocellulosic materials, Renewable Energy, Volume 169, Pages 1000–1012. https://doi.org/10.1016/j.renene.2020.12.095 | **A. Oliva:** conceptualization, data curation, investigation, resources, methodology, formal analysis, writing - original draft, writing - review & editing. **L.C. Tan:** supervision, writing – review & editing, project administration. **S. Papirio:** supervision, writing - review & editing. **G. Esposito:** supervision, writing - review & editing. **P.N.L. Lens:** supervision, project administration, funding acquisition. |
| **Chapter 6:** Oliva A., Tan L.C., Papirio S., Esposito G., Lens P.N.L., 2022. Fed-batch anaerobic digestion of raw and pretreated hazelnut skin over long-term operation, Bioresource Technology (In press). https://doi.org/10.1016/j.biortech.2022.127372 | **A. Oliva:** conceptualization, data curation, formal analysis, investigation, validation, visualization, writing - original draft, and writing - review & editing. **L.C. Tan:** supervision, writing - review & editing. **S. Papirio:** supervision, resources, writing - review & editing, and project administration. **G. Esposito:** supervision, resources, and writing - review & editing. **P.N.L. Lens:** supervision, resources, writing - review & editing, project administration, and funding acquisition. |

The following manuscripts are currently submitted for publication in international peer-reviewed journals:

| Submitted manuscript | Author contribution |
|---|---|
| **Chapter 4:** Oliva A., Tan L.C., Papirio S., Esposito G., Lens P.N.L., 2022. Use of N-Methylmorpholine N-oxide (NMMO) pretreatment to enhance the bioconversion of lignocellulosic residues to methane. | **A. Oliva:** conceptualization, data curation, formal analysis, investigation, validation, visualization, writing - original draft, and writing - review & editing. **L.C. Tan:** supervision and writing - review & editing. **S. Papirio:** supervision, resources, writing - review & editing, and project administration. **G. Esposito:** supervision, resources, and writing - review & editing. **P.N.L. Lens:** supervision, resources, writing - review & editing, project administration, and funding acquisition. |
| **Chapter 5:** Oliva A., Papirio S., Esposito G., Lens P.N.L., 2022. Ultrasounds application for nut and coffee wastes valorisation via biomolecules solubilisation and methane production | **A. Oliva:** conceptualization, data curation, formal analysis, investigation, validation, visualization, writing - original draft, and writing - review & editing. **S. Papirio:** supervision, resources, writing - review & editing, and project administration. **G. Esposito:** supervision, resources, and writing - review & editing. **P.N.L. Lens:** supervision, resources, writing - review & editing, project administration, and funding acquisition. |

**Funding**

This PhD thesis was supported by Science Foundation Ireland (SFI) through the SFI Research Professorship Programme entitled *Innovative Energy Technologies for Biofuels, Bioenergy and a Sustainable Irish Bioeconomy* (IETSBIO3; grant number 15/RP/2763) and the SFI Research Infrastructure research grant *Platform for Biofuel Analysis* (Grant Number 16/RI/3401).

**Nomenclature**

IPCC: Intergovernmental Panel on Climate Change

AD: anaerobic digestion

$CH_4$: methane

$CO_2$: carbon dioxide

REN21: Renewables 2021 Global Status Report

VFAs: volatile fatty acids

LMs: lignocellulosic materials

HS: hazelnut skin

SCG: spent coffee grounds

AS: almond shell

NMMO: N-Methylmorpholine N-oxide

NaOH: sodium hydroxide

KOH: potassium hydroxide

$Ca(OH)_2$:calcium hydroxide

TCI: total crystallinity index

LOI: lateral order index

WSC: water swelling capacity

f: frequency

$P_d$: power density

P: ultrasonic power

t: time

V: volume

$TS_0$: initial total solid content

CrI: crystallinity index

TS: total solid

VS: volatile solid

C: carbon

H: hydrogen

N: nitrogen

S: sulfur

O: oxigen

UASB: upflow anaerobic sludge blanket

MeOH: methanol

EtOH: ethanol

S/L: solid to liquid ratio

BMP: batch biochemical methane potential

$N_2$: nitrogen gas

SEM: scanning electron microscopic

TCD: thermal conductivity detector

HPLC: high-performance liquid chromatograph

RID: refractive index detector

Cp: specific heat capacity

$E_P$: specific energy production

SMY: specific methane yield

ξ: lower heating value of methane

CHP: combined heat and power

$E_R$: specific energy recovery

ANOVA: analysis of variance

$r_{lign\text{-}CH4}$: correlation between lignin content and cumulative methane production

G: cumulative methane production

$G_m$: maximum methane production yields estimated

$t_b$: crossover point

$R_m$: rate of methane production

λ: lag phase

$E_{R,\ eff}$: effective energy recovery

FTIR: Fourier transform infrared

H: heat loss

U: thermal conductivity

T: temperature

Δx: thickness

SMP: specific methane potential

$r^2$: correlation coefficient

ΔE: energy balance

DBM: digestate from baffalo manure

WRC: water retention capacity

r: Pearson coefficient

SWRT: solid waste retention time

SSMC: stainless steel mesh container

$Na_2CO_3$: sodium carbonate

PBS: phosphate-buffered saline

PCR: polymerase chain reaction

TA: total alkalinity

PA: partial alkalinity

IA: intermediate alkalinity

F-C: Folin-Ciocalteu

SBRT: solid biomass retention time

*Chapter 1*

# General introduction

## 1.1 Background and problem statement

### *1.1.1 Renewable energy*

The interest in renewable energy started in the 1970s when the world experienced an energy crisis, and fossil fuels seemed to be depleting. Nowadays, the interest in renewable energy is more focused on global environmental quality protection and sustainability. The main concern is global warming caused by the increase of carbon dioxide emissions and other atmospheric pollutants resulting from anthropogenic activities. The Intergovernmental Panel on Climate Change (IPCC) stated that the human impact on global warming is worse than expected. In 2017, the warming caused by anthropogenic activities reached 1 °C compared to the temperature of the pre-industrial levels. The Paris Agreement in 2015 aims to limit global warming below 1.5 °C than pre-industrial levels (Hansen et al., 2019).

Several strategies have been developed to replace fossil fuels. Among the others, the use of biomass for energy production emerged as a viable alternative due to the abundance and renewability of these materials. In the first place, biomass has been used for heat generation via burning. The most employed technology is cogeneration, which allows reusing the lost heat to generate electricity. Biomass is considered a carbon-neutral energy source since they absorb carbon dioxide during their growth that is then released back to the atmosphere during combustion (Perea-Moreno et al., 2019). Nevertheless, the gaseous biomass industry showed a more effective path for biomass utilisation, which allows producing energy with limited and controlled emissions in the atmosphere. In this perspective, anaerobic digestion (AD) is the most employed process to produce gaseous sources for energy generation from biomass feedstocks. The biogas produced is a mixture of methane ($CH_4$), carbon dioxide ($CO_2$) and other gases that can be employed in many applications at various degrees of purity. Biogas can be used either directly for heating and power generation, or methane can be separated and used to replace fossil fuels in gas pipeline distribution or for transport purposes (Chynoweth et al., 2001).

Despite the great potential and wide range of possible substrates for AD, the Renewables 2021 Global Status Report (REN21) stated that biomethane production covered only 1% of the global fossil gas demand in 2018. Advantageously, the number of biogas and biomethane plants is rapidly growing in Europe, reaching 18855 biogas and 726 biomethane plants with a total capacity of 64 PJ in 2020 (Renewables 2021 Global Status Report, 2021).

*1.1.2 Anaerobic digestion process*

Environmental protection and the need to find renewable energy sources to replace fossil fuels have prompted the AD technology from an initial concept of only extensive organic matter stabilisation to an industrial process focused on maximising biogas production (Mao et al., 2015; Zamri et al., 2021). AD is an attractive waste treatment management practice, as it can mitigate pollution while producing renewable energy in the form of methane and other valuable products (Satchwell et al., 2018). The AD process involves complex metabolic reactions carried out by several microbial groups. Therefore, understanding the metabolic pathways of AD is the key to optimising the process (Meegoda et al., 2018).

AD consists of four stages: hydrolysis, acidogenesis, acetogenesis and methanogenesis. In the first stage, hydrolytic bacteria secrete enzymes capable of decomposing complex organic polymers, i.e. carbohydrates, proteins and lipids, into soluble monomers, i.e. sugars, amino acids, and long-chain fatty acids. Acidogenesis is the second stage, during which the soluble monomers are fermented to volatile fatty acids (VFAs), i.e. formic, acetic, propionic, butyric, isovaleric, valeric, isocaproic, and caproic acid, as well as hydrogen and alcohols, i.e. mainly ethanol. During the subsequent acetogenesis stage, those compounds are furtherly converted into acetate, carbon dioxide, and hydrogen by acetogenic bacteria. In the final phase, archaea convert acetic acid and hydrogen into methane via, respectively, acetotrophic and hydrogenotrophic methanogenic pathways (Bianco et al., 2021; Luo et al., 2019).

The microorganisms responsible for acids and methane production require different operating conditions to achieve their maximum potential. These conditions, e.g. pH, temperature, alkalinity, and solid content, differ depending on the microorganism's physiology, nutritional needs, growth kinetics, and sensitivity to environmental conditions. The balance failure between the multiple groups of microorganisms involved in the AD process is the primary cause of reactor instability (Chen et al., 2008). Depending on the substrate fed into the anaerobic digester, the limiting group of microorganisms differ (Kainthola et al., 2019). The AD of sugars-rich substrates, e.g. food and vegetables, is generally limited by the methanogenesis step (Srisowmeya et al., 2020). For those substrates, the first three phases of the AD process are usually faster than methanogenesis, leading to acid compounds accumulation, pH decrease, and, ultimately, failure of the entire AD process (Bajpai, 2017). Acidogenic and acetogenic bacteria work within a pH range of 4.0 - 8.0, while a limiting range of 6.5 - 7.2 is suitable for the growth of methanogenic archaea (Chen et al., 2008). On the other hand, hydrolysis is the limiting stage

for more recalcitrant substrates, such as lignocellulosic materials (LMs) (Schroyen et al., 2018). The recalcitrance of LMs prevails on the effectiveness of hydrolytic bacteria to reduce the substrate hydrolysis rate, which often results in low methane production rates, prolonged AD time and incomplete biodegradation of the substrate (Li et al., 2019; Xu et al., 2019).

### *1.1.3 Lignocellulosic biomass and biogas*

LMs management and valorisation has become a hot topic in the last years, lignocelluloses being the most abundant renewable biomasses on earth (Cai et al., 2017). LMs have been discharged for decades before realising that they are a valuable source for renewable energy production (Tarasov et al., 2017). LMs derive from urban, industrial and agricultural activities and can be divided into six categories, i.e. agricultural residues, forest residues, animal wastes, waste from processing industries, biomasses from energy crops, and the organic fraction of municipal solid waste (Mancini et al., 2016; Xu et al., 2019).

The abundance and low cost of LMs inspired different strategies for their valorisation. The most employed methods for LMs valorisation involve thermochemical, biological and physicochemical processes. The thermochemical processes, e.g. pyrolysis, convert the LMs into fuels or directly into thermal energy. On the other hand, biological processes, e.g. AD, use different microorganisms to produce biofuels from LMs under particular conditions. Finally, physicochemical processes use the LMs to produce fuels through chemical reactions after preliminary physical treatments, e.g. microwave processing (Yu et al., 2021).

The biological stabilisation of organic wastes reduces greenhouse gas emissions, which are otherwise largely produced in combustion processes or biomass decomposition in landfills or other open environment strategies (Kristanto and Koven, 2019; Uddin et al., 2021). LMs can be converted into several biofuels, such as hydrogen, ethanol, and methane. The path depends on multiple factors, such as conversion efficiency, energy transport, the need for direct heat or steam, and environmental impact (Haldar and Purkait, 2020; Vu et al., 2020). In many aspects, methane seems to be an ideal fuel since its utilisation produces few atmospheric pollutants and generates less carbon dioxide per unit of energy compared to other fossil fuels (Chynoweth et al., 2001). Therefore, its use for vehicles fuel, industrial applications, and power generation is increasing. Methane can be used at different stages of purity, and its efficiencies of transport and energy conversion can be compared to electricity. In addition, an extensive pipeline distribution system is already in place worldwide for methane use (Chynoweth et al., 2001).

Despite the large LM potential for AD, the use of LMs is still limited by the complex and resistant structure, consisting of three main polymers, i.e. cellulose, hemicellulose, and lignin. The complex structure of LMs results in their resistance to biological degradation (Xu et al., 2019). Several studies have been conducted to overcome the recalcitrance of the most common LMs and enhance their methane production potential. Nevertheless, the wide variety of LMs, with different chemical composition and physical characteristics, continue attracting the interest of research activities.

The interest in LMs valorisation initially focused on straws and forest residues (Ferreira et al., 2013; Kabir et al., 2015), but several researchers are now investigating selected substrates, such as nut residues, wastes from the confectionary industry, coffee residues, and grass and flower wastes (Agarwal et al., 2021; Antonopoulou et al., 2020; Mancini et al., 2018; Zhang et al., 2021). However, traditional AD is usually not effective on LMs and pretreatments are required to increase the efficiency of lignocellulose hydrolysis. Pretreatment techniques are commonly classified into physical, chemical, physico-chemical and biological ones (Xu et al., 2019).

Pretreatments generally aim to separate the most recalcitrant component, i.e. lignin, from the cellulose and hemicellulose structural sugars (Mancini et al., 2016). In this perspective, pretreatments can either aim to keep the fermentable sugars into the solid matrix by dissolving the lignin or, on the other hand, allow sugar hydrolysis, keeping the lignin in the solid fraction (Figure 1.1). In addition, some pretreatments focus on improving the physical characteristics of the substrate (Figure 1.1), e.g. porosity, facilitating the subsequent AD process (Mancini et al., 2016). In any case, the sugars-rich and the easy-biodegradable matrix is selected for AD, while the extracted lignin can be used for several applications, such as combustion, source of aromatic compounds, ink additive, or component for resins and foam (Jędrzejczak et al., 2021; Matsakas et al., 2019).

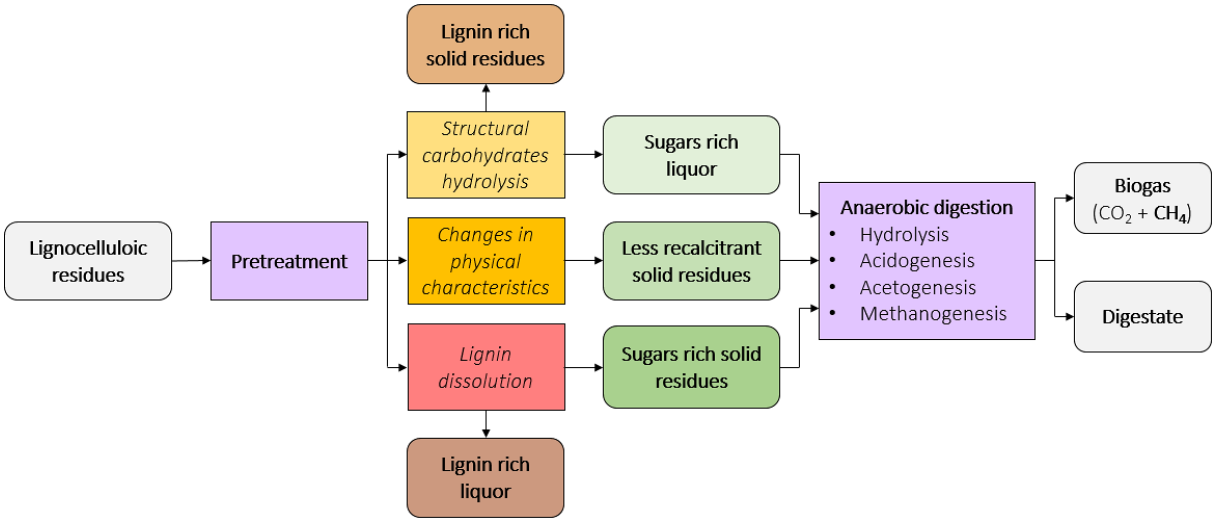


**Figure 1.1 –** Process flow diagram of the possible paths to enhance the conversion of lignocellulosic materials into methane by performing pretreatments before anaerobic digestion.

## 1.2 Research objectives

The overall objective of this PhD thesis is to reveal the potential of recalcitrant waste materials for energetic valorisation through AD. Three LMs, i.e. hazelnut skin (HS), spent coffee grounds (SCG), and almond shell (AS), were selected for the present study. The three LMs were pretreated using different techniques to increase their methane production potential. The following main aspects were investigated:

i) The effects of chemical, i.e. methanol-organosolv and N-Methylmorpholine N-oxide (NMMO), and physical, i.e. ultrasounds, pretreatments on the AD of HS, SCG, and AS. In particular, this research discussed the effect of each pretreatment on methane production, AD kinetics, and VFAs evolution along with the AD process. Particular attention was given to the differences in chemical composition, i.e. cellulose, hemicellulose, and lignin content, and physical characteristics, i.e. porosity, crystallinity, and external surface, prior to and after pretreatment.

ii) The performance in terms of methane production of one of the three LMs, i.e. HS, under fed-batch AD operation conditions. HS load, HS retention time, and pH control, among other parameters, were monitored and optimised. In addition, the impact of digesting raw, macerated, and organosolv pretreated HS on the bioreactor performance was investigated.

### 1.3 Thesis outline

This PhD thesis is divided into seven chapters, including an introduction, literature review, four research chapters, and a general discussion and perspective for LMs.

Chapter 1 gives an overview of the thesis, focusing on the background and problem statement of renewable energy and, in particular, methane as a biofuel. This chapter states the main goals of the research project and outlines the structure of the PhD thesis (Figure 1.2).

Chapter 2 overviewed the characteristics and potential of LMs for AD, with a specific focus on three emerging pretreatment methods used to enhance the conversion of LMs into methane, i.e. organosolv, NMMO, and ultrasound pretreatment.

Chapter 3 discussed on the experimental results obtained by pretreating HS, SCG, and AS with an organic solvent before undergoing AD. In particular, the use of methanol as a solvent was investigated at different pretreatment temperatures, i.e. 130, 160, and 200 °C, with and without catalyst addition, i.e. 0.1% (*w/v*) sulfuric acid. This chapter discussed the improvement in methane production, with particular attention to the changes in the chemical composition and physical characteristics of the three LMs.

Chapter 4 investigated the use of NMMO pretreatment to valorise HS, SCG, and AS via AD. NMMO effectiveness was studied varying the pretreatment time, i.e. 1, 3, and 5 h. The discussion focused on the changes in cellulose, hemicellulose, lignin, and extractives content, as well as porosity and other physical characteristics of the substrates used, and on how this reflected on the methane production potential of the LMs.

Chapter 5 debated the changes in the chemical composition of HS, SCG, and AS after undergoing ultrasound pretreatment. The effectiveness of ultrasonic waves at different temperatures, i.e. ambient and 80 °C, and through different media, i.e. distilled water and 50% (*v/v*) water-methanol solution, was studied. The methane production potential of the solid residues and liquor phase was investigated, paying particular attention to potential valuable molecules extracted in the liquid phase.

Chapter 6 focused on the optimisation of the AD process for HS. The process was optimised in HS load, HS retention time, and pH control. The impact of different strategies to adjust the pH was monitored, focusing on the interaction between the chemical employed and polyphenolic compounds. Raw, macerated, and organosolv pretreated HS was fed during the experimental period to investigate and discuss their impact on the AD process.

Chapter 7 highlighted the main findings of the research project and discussed their relevance and perspective for the valorisation of LMs. Recommendations for future work are given in this chapter to conclude this PhD dissertation.

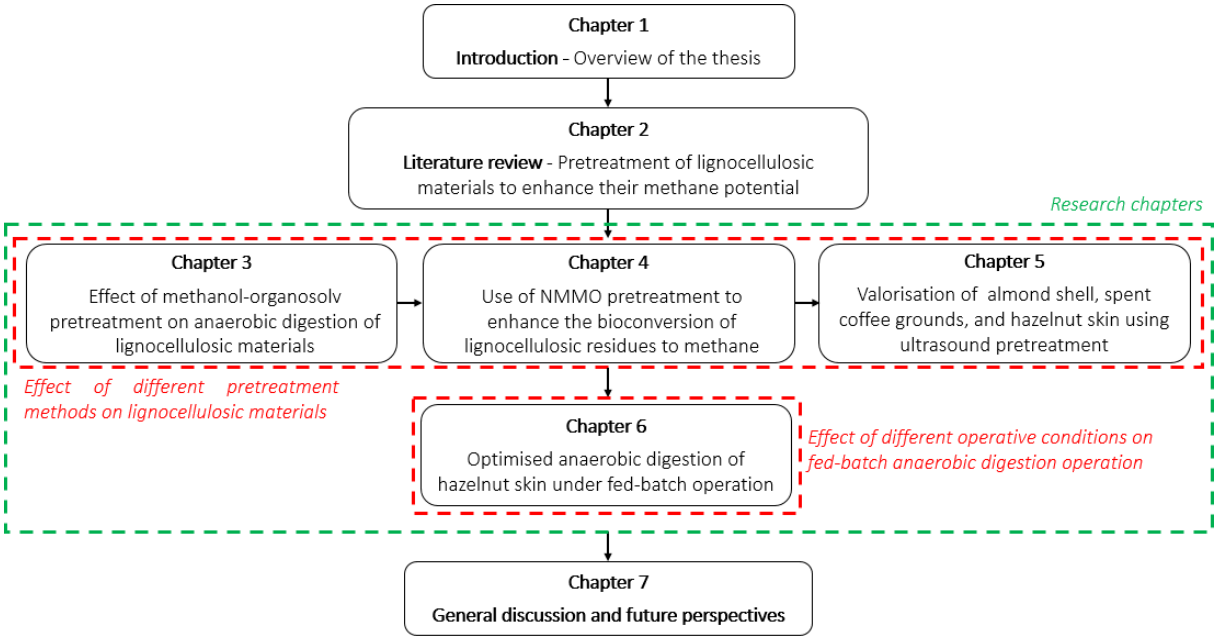


**Figure 1.2 –** Outline of this PhD thesis on anaerobic digestion of lignocellulosic materials.

## 1.4 References


Agarwal, A., Paritosh, K., Dangayach, P., Gehlot, P., Pareek, N., Vivekanand, V., 2021. Hydrothermal, acidic, and alkaline pretreatment of waste flower-mix for enhanced biogas production: a comparative assessment. Biomass Convers. Biorefinery 1–9. https://doi.org/10.1007/s13399-021-01607-6

Antonopoulou, G., Vayenas, D., Lyberatos, G., 2020. Biogas production from physicochemically pretreated grass lawn waste: Comparison of different process schemes. Molecules 25, 1–14. https://doi.org/10.3390/molecules25020296

Bajpai, P., 2017. Basics of Anaerobic Digestion Process, in: Anaerobic Technology in Pulp and Paper Industry. Springer, Singapore, pp. 7–12. https://doi.org/10.1007/978-981-10-4130-3

Bianco, F., Race, M., Forino, V., Pacheco-Ruiz, S., Rene, E.R., 2021. Bioreactors for wastewater to energy conversion : from pilot to full scale, in: Waste Biorefinery. Elsevier Inc., pp. 103–124. https://doi.org/10.1016/B978-0-12-821879-2/00004-1

Cai, J., He, Y., Yu, X., Banks, S.W., Yang, Y., Zhang, X., Yu, Y., Liu, R., Bridgwater, A. V., 2017. Review of physicochemical properties and analytical characterization of

lignocellulosic biomass. Renew. Sustain. Energy Rev. 76, 309–322. https://doi.org/10.1016/j.rser.2017.03.072

Chen, Y., Cheng, J.J., Creamer, K.S., 2008. Inhibition of anaerobic digestion process: A review. Bioresour. Technol. 99, 4044–4064. https://doi.org/10.1016/j.biortech.2007.01.057

Chynoweth, D.P., Owens, J.M., Legrand, R., 2001. Renewable methane from anaerobic digestion of biomass. Renew. Energy 22, 1–8. https://doi.org/10.1016/S0960-1481(00)00019-7

Ferreira, L.C., Donoso-Bravo, A., Nilsen, P.J., Fdz-Polanco, F., Pérez-Elvira, S.I., 2013. Influence of thermal pretreatment on the biochemical methane potential of wheat straw. Bioresour. Technol. 143, 251–257. https://doi.org/10.1016/j.biortech.2013.05.065

Haldar, D., Purkait, M.K., 2020. Lignocellulosic conversion into value-added products: A review. Process Biochem. 89, 110–133. https://doi.org/10.1016/j.procbio.2019.10.001

Hansen, K., Breyer, C., Lund, H., 2019. Status and perspectives on 100% renewable energy systems. Energy 175, 471–480. https://doi.org/10.1016/j.energy.2019.03.092

Jędrzejczak, P., Collins, M.N., Jesionowski, T., Klapiszewski, Ł., 2021. The role of lignin and lignin-based materials in sustainable construction – A comprehensive review. Int. J. Biol. Macromol. 187, 624–650. https://doi.org/10.1016/j.ijbiomac.2021.07.125

Kabir, M.M., Rajendran, K., Taherzadeh, M.J., Sárvári Horváth, I., 2015. Experimental and economical evaluation of bioconversion of forest residues to biogas using organosolv pretreatment. Bioresour. Technol. 178, 201–208. https://doi.org/10.1016/j.biortech.2014.07.064

Kainthola, J., Kalamdhad, A.S., Goud, V. V., 2019. A review on enhanced biogas production from anaerobic digestion of lignocellulosic biomass by different enhancement techniques. Process Biochem. 84, 81–90. https://doi.org/10.1016/j.procbio.2019.05.023

Kristanto, G.A., Koven, W., 2019. Estimating greenhouse gas emissions from municipal solid waste management in Depok, Indonesia. City Environ. Interact. 4, 100027. https://doi.org/10.1016/j.cacint.2020.100027

Li, Y., Chen, Y., Wu, J., 2019. Enhancement of methane production in anaerobic digestion process: A review. Appl. Energy 240, 120–137. https://doi.org/10.1016/j.apenergy.2019.01.243

Luo, L., Kaur, G., Wong, J.W.C., 2019. A mini-review on the metabolic pathways of food waste two-phase anaerobic digestion system. SAGE. https://doi.org/10.1177/0734242X18819954

Mancini, G., Papirio, S., Lens, P.N.L., Esposito, G., 2018. Anaerobic Digestion of Lignocellulosic Materials Using Ethanol-Organosolv Pretreatment. Environ. Eng. Sci. 35, 953–960. https://doi.org/10.1089/ees.2018.0042

Mancini, G., Papirio, S., Lens, P.N.L., Esposito, G., 2016. Solvent Pretreatments of Lignocellulosic Materials to Enhance Biogas Production: A Review. Energy and Fuels 30, 1892–1903. https://doi.org/10.1021/acs.energyfuels.5b02711

Mao, C., Feng, Y., Wang, X., Ren, G., 2015. Review on research achievements of biogas from anaerobic digestion. Renew. Sustain. Energy Rev. 45, 540–555. https://doi.org/10.1016/j.rser.2015.02.032

Matsakas, L., Raghavendran, V., Yakimenko, O., Persson, G., Olsson, E., Rova, U., Olsson, L., Christakopoulos, P., 2019. Lignin-first biomass fractionation using a hybrid organosolv – Steam explosion pretreatment technology improves the saccharification and fermentability of spruce biomass. Bioresour. Technol. 273, 521–528. https://doi.org/10.1016/j.biortech.2018.11.055

Meegoda, J.N., Li, B., Patel, K., Wang, L.B., 2018. A review of the processes, parameters, and optimization of anaerobic digestion. Int. J. Environ. Res. Public Health 15. https://doi.org/10.3390/ijerph15102224

Perea-Moreno, M.A., Samerón-Manzano, E., Perea-Moreno, A.J., 2019. Biomass as renewable energy: Worldwide research trends. Sustain. 11. https://doi.org/10.3390/su11030863

Renewables 2021 Global Status Report, 2021. . Paris: REN21 Secretariat.

Satchwell, A.J., Scown, C.D., Smith, S.J., Amirebrahimi, J., Jin, L., Kirchstetter, T.W., Brown, N.J., Preble, C. V., 2018. Accelerating the Deployment of Anaerobic Digestion to Meet Zero Waste Goals. Environ. Sci. Technol. 52, 13663–13669. https://doi.org/10.1021/acs.est.8b04481

Schroyen, M., Vervaeren, H., Raes, K., Van Hulle, S.W.H., 2018. Modelling and simulation of anaerobic digestion of various lignocellulosic substrates in batch reactors: Influence of lignin content and phenolic compounds II. Biochem. Eng. J. 134, 80–87. https://doi.org/10.1016/j.bej.2018.03.017

Srisowmeya, G., Chakravarthy, M., Nandhini Devi, G., 2020. Critical considerations in two-stage anaerobic digestion of food waste – A review. Renew. Sustain. Energy Rev. 119, 109587. https://doi.org/10.1016/j.rser.2019.109587

Tarasov, D., Leitch, M., Fatehi, P., 2017. Thermal properties of lignocellulosic precipitates from neutral sulfite semichemical pulping process. Fuel Process. Technol. 158, 146–153.

https://doi.org/10.1016/j.fuproc.2016.12.017

Uddin, M.N., Siddiki, S.Y.A., Mofijur, M., Djavanroodi, F., Hazrat, M.A., Show, P.L., Ahmed, S.F., Chu, Y.M., 2021. Prospects of Bioenergy Production From Organic Waste Using Anaerobic Digestion Technology: A Mini Review. Front. Energy Res. 9. https://doi.org/10.3389/fenrg.2021.627093

Vu, H.P., Nguyen, L.N., Vu, M.T., Johir, M.A.H., McLaughlan, R., Nghiem, L.D., 2020. A comprehensive review on the framework to valorise lignocellulosic biomass as biorefinery feedstocks. Sci. Total Environ. 743, 140630. https://doi.org/10.1016/j.scitotenv.2020.140630

Xu, N., Liu, S., Xin, F., Zhou, J., Jia, H., Xu, J., Jiang, M., Dong, W., 2019. Biomethane production from lignocellulose: Biomass recalcitrance and its impacts on anaerobic digestion. Front. Bioeng. Biotechnol. 7, 1–12. https://doi.org/10.3389/fbioe.2019.00191

Yu, I.K.M., Chen, H., Abeln, F., Auta, H., Fan, J., Budarin, V.L., Clark, J.H., Parsons, S., Chuck, C.J., Zhang, S., Luo, G., Tsang, D.C.W., 2021. Chemicals from lignocellulosic biomass: A critical comparison between biochemical, microwave and thermochemical conversion methods. Crit. Rev. Environ. Sci. Technol. 51, 1479–1532. https://doi.org/10.1080/10643389.2020.1753632

Zamri, M.F.M.A., Hasmady, S., Akhiar, A., Ideris, F., Shamsuddin, A.H., Mofijur, M., Fattah, I.M.R., Mahlia, T.M.I., 2021. A comprehensive review on anaerobic digestion of organic fraction of municipal solid waste. Renew. Sustain. Energy Rev. 137, 110637. https://doi.org/10.1016/j.rser.2020.110637

Zhang, T., Tonouchi, K., Kong, Z., Li, Y., Cheng, H., Qin, Y., Li, Y.Y., 2021. Improvement of coffee grounds high solid thermophilic methane fermentation by co-digestion with in-situ produced waste activated sludge: Performance and stability. Sci. Total Environ. 765, 142551. https://doi.org/10.1016/j.scitotenv.2020.142551

*Chapter 2*

# Pretreatment of lignocellulosic materials to enhance their methane production potential

A modified version of this chapter has been published as:

Oliva A., Papirio S., Esposito G., Lens P.N.L., 2022. Pretreatment of Lignocellulosic Materials to Enhance their Methane Potential. In: Sinharoy A., Lens P.N.L. (eds) Renewable Energy Technologies for Energy Efficient Sustainable Development. Applied Environmental Science and Engineering for a Sustainable Future. Springer, Pages 85–120. https://doi.org/10.1007/978-3-030-87633-3_4.

**Abstract**

Lignocellulosic materials (LMs) are the most abundant residues on the planet and have a huge potential for methane production. Several strategies have been tested to enhance the methane production potential of LMs, with a particular emphasis on environmentally friendly and economically convenient pretreatments. This chapter revisits the potential of two chemical, i.e. organosolv and N-methylmorpholine N-oxide (NMMO)-driven, and one physical, i.e. ultrasounds, pretreatment. Organosolv pretreatment enables to obtain a pure lignin fraction from LMs, leaving most of the fermentable sugars in the solid matrix. The result is a lignin-poor material with an increased porosity and a higher bioavailability of the sugar fraction. Another advantage is the cost-effectiveness and the easy recovery of the chemicals involved. NMMO pretreatment focuses on the cellulosic component of the biomass, aiming to reduce its crystallinity and to increase the porosity of the substrate. The main advantage of NMMO lies in its high recovery percentage, which reaches up to 99%. Ultrasound pretreatment involves ultrasonic waves that allow fractionating LMs, breaking the linkages between lignin, cellulose and hemicellulose, generally leaving cellulose and most of the hemicellulose in the solid fraction and dissolving the lignin in the liquor. Ultrasound pretreatment does not require chemicals and can be easily combined with other pretreatments to enhance its effectiveness.

## 2.1 Introduction

Lignocellulosic materials (LMs) are generated from industrial, agricultural and municipal activities. Disposal of these wastes is often difficult due to the enormous volumes produced, especially during the harvesting season (Barbu et al., 2020; Oh et al., 2018). Anaerobic digestion (AD) is a viable and green alternative to landfill disposal or combustion for these LMs (Alonso-Fariñas et al., 2020). The use of LMs for AD is, however, still limited by their resistance to biological and chemical degradation. The main issue of AD of LMs is the complex and resistant structure, mainly consisting of cellulose, hemicellulose, and lignin (Bhatia et al., 2020). Various strategies have been explored to increase the biodegradability of LMs (Bianco et al., 2021b; Kohli et al., 2020; Mancini et al., 2018c; Papirio, 2020; Yao et al., 2018). Pretreatments of LMs aim to increase the efficacy of lignocellulose hydrolysis by improving the accessibility of microorganisms to the sugar fraction (cellulose and hemicellulose) of LMs. This can be achieved by removing lignin and/or hemicellulose or by decreasing the degree of polymerisation and crystallinity of the cellulosic component of the biomass (Kumar and Sharma, 2017).

This chapter aims to overview the characteristics and potential of LMs for AD, with a specific focus on three emerging pretreatment technologies to enhance the conversion of LMs into methane, i.e. organosolv, N-methylmorpholine N-oxide (NMMO), and ultrasound pretreatment. The principles of each pretreatment will be thoroughly discussed, pointing out advantages and drawbacks. Particular attention will be given to the effect of the three pretreatments on the physical characteristics and chemical composition of LMs, focusing on the subsequent valorisation of the pretreated solid residues through the AD process.

## 2.2 Lignocellulosic materials: structure and potential

Biomass is one of the most abundant resources on the planet, with a global production of $2\times10^{11}$ tons per year (Reddy and Yang, 2005). Biomass can be converted into fuels and provide renewable materials at the same time, offering a viable alternative to fossil fuels. Biomass is produced via photosynthesis, by fixing atmospheric carbon dioxide and converting solar energy to chemical energy to build up the carbon backbone of plant cells (Zhang, 2008). LMs represent more than 60% of the global biomass and serve as a cheap and abundant feedstock (Bilal et al., 2017). Agricultural, municipal, and industrial activities generate LMs as waste, generally at low cost (Table 2.1). Also, the use of LMs for biofuel production does not create conflicts between land use for food and energy production (Kucharska et al., 2018). Depending on the origin,

LMs are classified as forest residues, municipal solid waste, waste paper, or crop residue resources (Balat, 2011).

**Table 2.1 –** Chemical composition (in terms of cellulose, hemicellulose, and lignin content) of the most employed lignocellulosic materials for methane production.

| **Biomass origin** | **Substrate** | **Cellulose[a]** (%) | **Hemicellulose[b]** (%) | **Lignin[c]** (%) | **Reference** |
|---|---|---|---|---|---|
| Agricultural residues | Maize straw | 38.3 | 29.8 | 3.8 | Khatri et al. (2015) |
| | Wheat straw | 31.0 | 18.4 | 18.3 | Mancini et al. (2018a) |
| | Rice straw | 28.6 | 19.5 | 17.3 | Mancini et al. (2018b) |
| | Barley straw | 39.1 | 25.7 | 15.2 | Duque et al. (2013) |
| | Sweet sorghum straw | 37.7 | 28.1 | 21.5 | Dong et al. (2019) |
| | Oat straw | 35.0 | 28.2 | 4.1 | Gomez-Tovar et al. (2012) |
| | Rye straw | 42.1 | 23.8 | 19.5 | Ingram et al. (2011) |
| | Triticale straw | 33.0 | 23.0 | 29.0 | Teghammar et al. (2012) |
| | Sugarcane bagasse | 47.6 | 22.6 | 27.6 | Hashemi et al. (2019) |
| | Sunflower stalks | 34.1 | 26.2 | 26.8 | Hesami et al. (2015) |
| Nuts residues | Peanut shell | 23.6 | 12.2 | 40.0 | Shen et al. (2018) |
| | Almond shell | 23.4 | 21.9 | 30.6 | Oliva et al. (2021) |
| | Walnut shell | 25.6 | 23.0 | 46.7 | Şenol (2021) |
| | Pistachio shell | 20.1 | 23.2 | 24.3 | Shen et al. (2018) |
| | Chestnut shell | 26.8 | 24.5 | 36.8 | Bianco et al. (2021b) |
| | Hazelnut shell | 18.0 | 17.2 | 39.1 | Shen et al. (2018) |
| | Hazelnut skin | 10.2 | 3.6 | 39.7 | Oliva et al. (2021) |
| Industrial wastes | Spent coffee grounds | 8.8 | 33.6 | 20.3 | Oliva et al. (2021) |
| | Brewery spent grain | 19.2 | 26.9 | 30.5 | Ravindran et al. (2018) |
| | Cocoa bean shell | 13.5 | 7.0 | 29.9 | Mancini et al. (2018b) |
| | Rubber wood waste | 43.6 | 8.3 | 31.0 | Tongbuekeaw et al. (2020) |
| | Oil palm empty fruit bunch | 36.1 | 22.4 | 26.4 | Tang et al. (2018) |
| | Olive pomace | 12.3 | 8.9 | 34.0 | Elalami et al. (2020) |
| | Grape pomace | 15.8 | 8.6 | 35.4 | Bordiga et al. (2019) |
| Forest residues | Switch grass | 42.0 | 19.0 | 24.0 | Larnaudie et al. (2019) |
| | Spruce wood | 42.0 | 20.0 | 27.0 | Teghammar et al. (2012) |
| | Poplar wood | 49.0 | 23.0 | 27.0 | Rego et al. (2019) |
| | Birch wood | 40.1 | 26.8 | 24.5 | Goshadrou et al. (2013) |
| | Pine wood | 44.5 | 28.0 | 26.8 | Mirmohamadsadeghi et al. (2014) |
| | Elm wood | 46.4 | 26.3 | 26.2 | Mirmohamadsadeghi et al. (2014) |

[a] Cellulose content (g/100 g dry matter) was considered equal to the glucan content (Mussatto et al., 2011).
[b] Hemicellulose content (g/100 g dry matter) is reported as the sum of xylan, mannan, galactan, arabinan, galactan, and rhamnan (Mussatto et al., 2011).
[c] Lignin content (g/100 g dry matter) is reported as the sum of acid soluble and acid-insoluble lignin (Sluiter et al., 2008).

The structural and chemical composition of LMs is extremely variable (Table 2.1) due to various genetic and environmental factors. The chemical composition of LMs includes mainly cellulose, hemicellulose, and lignin, arranged in a three-dimensional and complex structure (Figure 2.1) (Zhang et al., 2019). Depending on the specific substrate, a significant part of LMs may consist of non-structural compounds. The most common extractives present in LMs are free sugars (sucrose, glucose, and fructose), phenolic compounds, proteins, lipids, waxes, chlorophyll, essential oils, starches, and fatty acids (Tajmirriahi et al., 2021a, 2021b).

The complex structure of lignocelluloses results in its resistance to biological and chemical degradation, with hydrolysis being the limiting step (Kainthola et al., 2019a). Hydrolysis of lignocellulose requires several enzymes to work together, including cellulases, hemicellulases, and lignin-degrading enzymes (Xu et al., 2019). The main reason for biomass recalcitrance is the low accessibility of crystalline cellulose fibers, which prevents cellulases from working efficiently. Equally, the presence of lignin and hemicellulose prevents cellulase from accessing the substrate efficiently (Mancini et al., 2016a; Xu et al., 2019; Zoghlami and Paës, 2019).

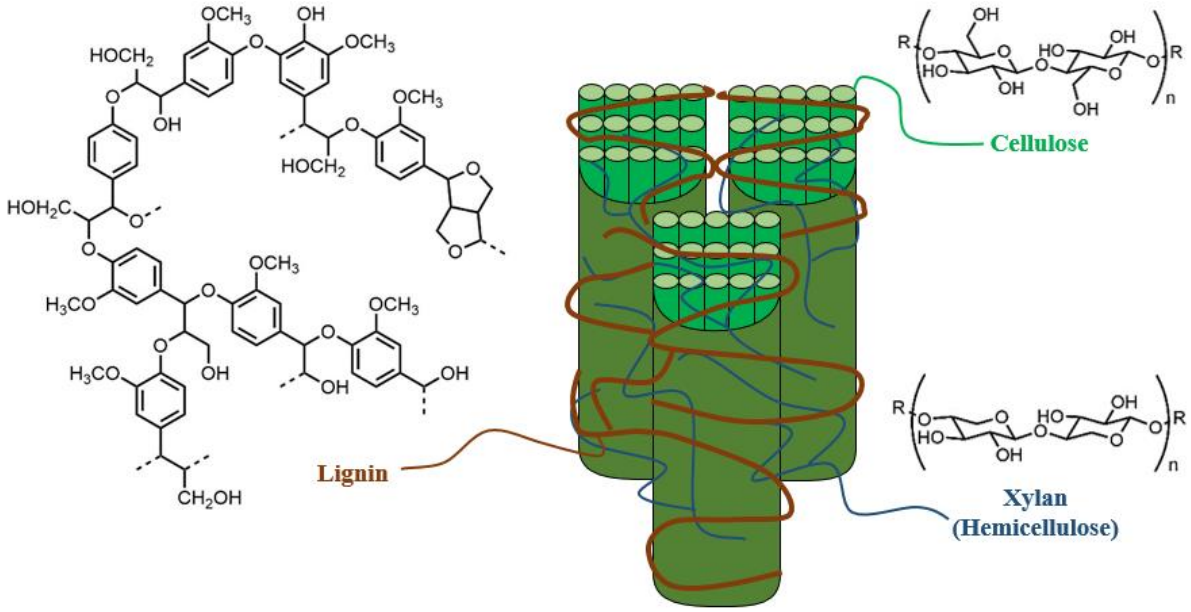


**Figure 2.1 –** Schematic representation of the structure of lignocellulosic materials containing cellulose, hemicellulose, and lignin.

### *2.2.1 Cellulose*

Cellulose is a linear polysaccharide consisting of a repeated unit called cellobiose consisting of D-glucose subunits linked to one another by *β*-(1,4)-glycosidic bonds (Su et al., 2018). The cellobiose units are composed of long-chain cellulose polymers, linked together by van der Waals and hydrogen bonds. Cellulose is packed into microfibrils, which reduce the access of

the enzymes and complicate cellulose degradation (Kumar et al., 2009; Zhang et al., 2019). Cellulose alternates crystalline and amorphous regions, with the latter being the weakness for chemical and biological attack. Cellulose degradation aims to decompose the polysaccharide into free sugar molecules. The resulting product is glucose, a six-carbon sugar (Singhvi and Gokhale, 2019).

Cellulose crystallinity presents several structures (i.e. $I_\alpha$, $I_\beta$, II, III, and IV), depending on the crystallites disposition (Blanco et al., 2018). Native cellulose has a parallel chain disposition and exists in nature as cellulose $I_\alpha$ and $I_\beta$. Cellulose $I_\alpha$ shows one-chain triclinic cells and abounds in bacterial cellulose and algae (Nishiyama, 2009). Cellulose $I_\beta$ is present in cotton and wood materials and reveals two-chain monoclinic cells (Blanco et al., 2018). Cellulose $I_\alpha$ conversion to cellulose $I_\beta$ is a non-reversible process requiring high temperatures (260 - 280 °C) (Matthews et al., 2012). Cellulose II is obtained by maceration or dissolution and subsequent regeneration of cellulose I using solvent-based processes (Corrêa et al., 2010). Cellulose II presents an antiparallel chain disposition, making it more appreciated for textile applications and easily accessible for enzymes and microorganisms (Wikandari et al., 2016). Only very low or high pH allows cellulose solubilisation in water, whereas solvents like NMMO or ionic liquids dissolve cellulose at neutral pH (Baruah et al., 2018). Cellulose III is obtained by treating cellulose I and II with an ammonia solution, whereas cellulose IV derives from cellulose III treatment in glycerol over 260 °C (Corrêa et al., 2010). The transformation to cellulose III and IV can be reverted using thermal or chemical processes (Isogai et al., 1989; Wada et al., 2006). In contrast, cellulose II is non-reversible to cellulose I (Nagarajan et al., 2017).

### *2.2.2 Hemicellulose*

Hemicellulose does not have a fixed structure. Its backbone can be either a homopolymer or a hetero-polymer with short branches linked by β-1,4-glucan bonds and, occasionally, by β-1,3-glucan bonds (Zhang et al., 2019). These branches consist of five-carbon sugars (i.e. xylose, rhamnose, and arabinose), six-carbon sugars (i.e. glucose, mannose, and galactose), and uronic acids. Generally, xylose is the dominant sugar for hardwoods and agricultural residues, while mannose prevails in softwoods (Baruah et al., 2018; Singhvi and Gokhale, 2019). Contrary to cellulose, the polymers present in hemicelluloses are easily degradable, due to the amorphous (non-crystalline) structure and the lower degree of polymerisation. Hemicellulose, together with lignin, represents a barrier around the cellulose (Figure 2.1), reducing the access of

cellulases enzymes (Baruah et al., 2018; Zoghlami and Paës, 2019). The most common pretreatments for hemicellulose hydrolysis are dilute acid or alkaline compounds, steam explosion or enzymes (Zoghlami and Paës, 2019).

*2.2.3 Lignin*

Lignin is the third most abundant polymer in nature, after cellulose and hemicelluloses, and generally represents 10 - 25% of the total feedstock dry matter (Balat, 2011). Lignin is an aromatic, complex, three-dimensional cross-linked polymer synthesised from phenylpropanoid precursors (Figure 2.1). The lignin structure consists of phenyl propane structural units, liked by aryl ether linkages. The structural variableness is given by the substitution of the methoxyl groups present in the aromatic rings (Baruah et al., 2018). The lignin content ranges from 10 to 20% in various LMs, such as straws, hulls, bagasse, and stalks, and can increase to 30 - 40% for nut shells and pinewood (Ponnusamy et al., 2019). The three most common monomers present in lignin are sinapyl alcohol, coniferyl alcohol, and p-coumaryl alcohol, corresponding to the three main structural units, which are syringyl, guaiacyl, and hydroxyphenyl, respectively (Ralph et al., 2019).

Lignin protects the plants from microbial attack and oxidation and gives rigidity and impermeability to their structure (Ponnusamy et al., 2019). The presence of lignin is one of the main drawbacks of using LMs in fermentation and AD, as it makes lignocelluloses resistant to chemical and biological degradation by reducing the hydrolysis rate (Reddy and Yang, 2005). Organic solvents, thermal, and fungal pretreatment are generally suggested for efficient lignin removal (Amin et al., 2017; Singhvi and Gokhale, 2019).

## 2.3 Parameters affecting lignocellulose conversion to biofuels

The biodegradation of LMs is influenced by four main factors, i.e. i) accessible surface, ii) crystallinity and degree of polymerisation of cellulose, as well as the iii) lignin and iv) hemicellulose content (Mancini et al., 2016a). Cellulose accessibility is a key factor in the bioconversion of LMs to fermentable sugars. Thus, the contact between cellulose and cellulase is one of the most critical factors affecting the enzymatic hydrolysis yield and rate. The contact area depends on biomass porosity and particle size (Meng and Ragauskas, 2014; Xu et al., 2019). Cellulase accessibility to cellulose mainly depends on porosity, rather than the external surface of the substrate (Siqueira et al., 2017). Over 90% of the cellulose enzymatic digestibility depends on the substrate porosity (Wang et al., 2012). In AD, a limited access to cellulose results in a scarce contact between biomass and hydrolytic bacteria, which reduces the release

of fermentable sugars for the subsequent degradation steps. The accessible surface increases along the AD process proportionally with the degradation of the cell wall components (Xu et al., 2019). The microorganisms-substrate contact controls the hydrolysis efficiency, especially during the first days of AD. On the contrary, other factors prevail later, such as the compact structure and the degree of crystallinity of the remaining cellulose (Oliva et al., 2021; Xu et al., 2019).

The ordered structure and high crystallinity of cellulose are the main deterrents to convert it to biofuels. Nevertheless, amorphous regions, which are more accessible to enzymatic attack, are randomly present in the cellulose structure (Zoghlami and Paës, 2019). The cellulose becomes more accessible by decreasing the crystallinity degree, enhancing the biofuel production from cellulose-rich materials (Jeihanipour et al., 2011). As described in Section 2.2.1, cellulose is a linear homopolymer composed of microfibrils, joint together to form fibrils and finally fibers. The degree of polymerisation refers to the average length of the polysaccharide chains. An increase in the degree of polymerisation is reflected in a higher density and tensile strength of the cellulosic component of LMs, making cellulose hydrolysis more difficult (Hallac and Ragauskas, 2011; Mattonai et al., 2018).

A further factor affecting the hydrolysis of LMs is the presence of hemicellulose and lignin. Hemicellulose and lignin form a physical barrier around cellulose. It is important to remove or alter them, while avoiding the degradation of the hemicellulose sugars to obtain a high sugar yield (Singhvi and Gokhale, 2019; Xu et al., 2019; Zoghlami and Paës, 2019). Hemicellulose contributes to the resistance of the plant cell wall and reduces the overall hydrolysis rate of LMs (Xu et al., 2019). Nevertheless, hydrolysis and acidification of hemicellulose alone are faster than those of cellulose, suggesting that the methane production from hemicellulose can be optimised by controlling the organic loading rate (Li et al., 2018). Other studies reported that the hemicellulose-cellulose linkages contribute to reducing the crystallinity of cellulose, enhancing the hydrolysis step (Li et al., 2015; Xu et al., 2012). On the other hand, lignin is well known to negatively affect the AD process by reducing the biodegradability of LMs and the overall methane yield (Li et al., 2018). Lignin consolidates the cell wall structure and prevents contact of hydrolytic enzymes with carbohydrates. In addition, lignin is capable of adsorbing cellulase enzymes, further protecting the cellulosic component of LMs (Lu et al., 2016).

## 2.4 Pretreatment methods to enhance methane production from lignocellulosic materials

The use of LMs for methane production is limited due to their resistance to the enzymatic attack (Mahmood et al., 2019). Therefore, many studies have focused on developing cost-effective pretreatments to reduce the recalcitrance of LMs (Table 2.2) (Lee et al., 2021; Matsakas et al., 2020; Oliva et al., 2021). Pretreatments aim to increase the efficacy of lignocellulose hydrolysis by improving the accessibility to cellulose. This scope can be achieved by removing or altering the lignin and hemicellulose fraction of LMs (Figure 2.2) (Ali et al., 2020; Haldar and Purkait, 2021).

To be efficient and economically advantageous, pretreatment methods should meet the following features: (i) high recovery of carbohydrates, (ii) high digestibility of the cellulose in the subsequent enzymatic hydrolysis, (iii) high solid concentrations as well as a high concentration of free sugars in the liquid fraction, (iv) no destruction of hemicelluloses and cellulose, (v) no formation of possible inhibitors for hydrolytic enzymes and fermenting microorganisms, (vi) cost-effectiveness and low consumption of chemicals, (vii) low generation of residues, and (viii) low capital and operational costs (Kumari and Singh, 2018; Taherzadeh and Karimi, 2008).

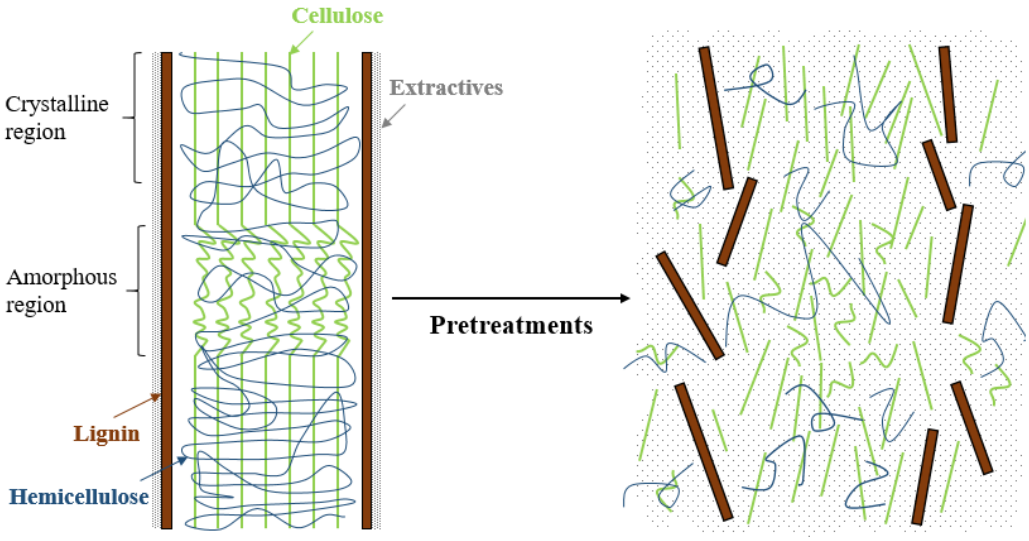


**Figure 2.2 –** Schematisation of the effect of pretreatment on the lignocellulosic structure.

Pretreatment techniques can be differently classified. A first classification concerns the pH maintained during the process, with pretreatments grouped in acidic, neutral and alkaline (Ravindran and Jaiswal, 2016). Nevertheless, the most common classification categorises pretreatments into physical, chemical, physicochemical and biological (Table 2.2) (Singh et al., 2015).

*2.4.1 Physical pretreatments*

The most common physical pretreatments include different milling (e.g. ball, colloid, vibro-energy, roller, and hammer), extrusion and irradiation, with the primary objective of increasing the accessible surface area and decreasing cellulose crystallinity and degree of polymerisation (Amin et al., 2017).

Milling is a size reduction technique employed to increase the surface/volume ratio and alter the structure and the degree of crystallinity of LMs, making pretreated substrates more amenable to cellulase attack (Ravindran and Jaiswal, 2016).

Irradiation pretreatments involve gamma rays, electron beam, ultrasounds (see Section 2.7) and microwaves, intending to improve the enzymatic hydrolysis of lignocelluloses (Taherzadeh and Karimi, 2008). The pretreatment effectiveness is proportional to the lignin content, resulting in a lower efficiency on less recalcitrant (i.e. low lignin) substrates (Keikhosor et al., 2013).

Extrusion pretreatment relies on the spinning of a single or twin screw into a temperature-controlled barrel. The mechanical action causes strong shearing forces between the substrate, the screw, and the barrel, locally increasing pressure and temperature. Apart from the particle size reduction, those forces alter also the biomass structure and change the crystallinity of the cellulosic component of the biomass (Duque et al., 2017; Zheng and Rehmann, 2014).

*2.4.2 Chemical pretreatments*

Chemical pretreatments act directly on the main components of the biomass, removing lignin and hemicellulose or decreasing the crystallinity degree of the cellulose (Ponnusamy et al., 2019). The chemical agents employed are divided into four main categories: alkali, acids, salts, and organic solvents.

Alkaline pretreatment involves basic solutions, e.g. sodium hydroxide (NaOH), potassium hydroxide (KOH), and calcium hydroxide ($Ca(OH)_2$), aiming to enhance the digestibility of LMs. The main effects on LMs are lignin and hemicellulose removal, an increase in porosity and the reduction of polymerisation and crystallinity degree of the cellulose (Tu and Hallett, 2019). Alkaline pretreatments occur at mild conditions, i.e. ambient pressure and temperature, but generally last over 24 hours (Amin et al., 2017). NaOH and KOH are the most employed basic solutions for alkaline pretreatment, having particular effectiveness for lignin removal from low lignin content LMs (Baruah et al., 2018). Nevertheless, the recycling of alkaline solutions is challenging, and $Na^+$ and $K^+$ ions can inhibit the subsequent AD process (Bianco

et al., 2021b). On the other hand, a $Ca(OH)_2$ solution can be more easily recovered but is less effective than NaOH and KOH based solutions (Amin et al., 2017).

Acid pretreatment is performed with diluted or concentrated solutions. Organic acids, such as formic acid, as well as inorganic acids, i.e. sulfuric, nitric, phosphoric, and hydrochloric, are widely employed (Baruah et al., 2018). Dilute acid pretreatment (0.1 - 5%) aims to remove the hemicellulosic component of the biomass and is effective at high temperatures (100 - 250 °C). On the other hand, acids concentrated at 30 - 70% hydrolise both cellulose and hemicellulose and require temperatures below 100 °C (Solarte-Toro et al., 2019). Acid solutions are unable to dissolve lignin but alter the cellulose-hemicellulose-lignin linkages, which increases the biodegradability of the solid residues (Amin et al., 2017). Nevertheless, the formation of inhibitory compounds can occur. Phenolic compounds, aldehydes and furfurals are the most know inhibitory compounds observed after acid pretreatments (Ali et al., 2020). Acid-pretreated solid residues of LMs require abundant washing to be ready for AD or other biological processes (Rajan and Carrier, 2014). On the other hand, before undergoing fermentation processes, the pH of the hydrolysate has to be neutralised with alkaline solutions (Gonzales et al., 2017), which increases the overall process costs (Castilla-Archilla et al., 2021) and can create further inhibition (Bianco et al., 2021b).

Ionic liquids and NMMO (see Section 2.6) act on the cellulosic component of LMs (Halder et al., 2019; Mancini et al., 2016b). Ionic liquids are salts in the liquid state at room temperature in which isolated ions and cations interact by Coulomb forces. NMMO is a zwitterion containing localised positive and negative charges in a single molecule (Böhmdorfer et al., 2017). Ionic liquids and NMMO dissolve cellulose, which can then be regenerated using an anti-solvent (Mancini et al., 2016a). The regenerated cellulose shows a lower crystallinity which is a critical factor for the bioconversion of LMs (Xu et al., 2019). NMMO is effective at different concentrations in aqueous solutions (Wikandari et al., 2016), the mechanisms of which are thoroughly discussed in Section 2.6.

Organosolv pretreatment (see Section 2.5) involves organic solvents such as ethanol, methanol, and acetic acid, heated to high temperature to remove lignin and reduce the recalcitrance of LMs. Lignin is a valuable product and can be recovered at high purity levels after organosolv pretreatment (Ferreira and Taherzadeh, 2020).

*2.4.3 Physicochemical pretreatments*

Physicochemical pretreatment methods combine chemical and physical approaches. This category includes several pretreatment methods such as liquid hot water, wet oxidation, ammonia fiber explosion, steam explosion, and $CO_2$ explosion. Steam explosion and liquid hot water are the two most studied strategies.

Steam explosion combines thermal and pressure effects to hydrolyse the hemicellulosic component of the biomass (Jacquet et al., 2015). LMs undergo high-pressure (5 - 50 atm) saturated steam at temperatures between 160 and 260 °C. The pretreatment time is generally short (1 - 10 min) and inversely related to temperature (Amin et al., 2017). Water molecules firstly penetrate LMs and explosively escape once pressure is released, causing cell wall disruption (Ravindran and Jaiswal, 2016). Higher temperatures lead to substantial hemicellulose hydrolysis into glucose and xylose monomers, liberating acetic acid, which acts as a catalyst to hydrolyse the remaining sugars (Baruah et al., 2018). However, harsh pretreatment conditions can generate inhibitors such as phenolic compounds, formic and levulinic acid (Cantarella et al., 2004; Martín et al., 2018). Alternatively, an external catalyst (e.g. $H_2SO_4$, $SO_2$, $H_3PO_4$, and $CO_2$) allows lowering the pretreatment temperature while maintaining a high hemicellulose hydrolysis rate (Duque et al., 2016).

Liquid hot water pretreatment, similarly to steam explosion, requires high temperature and pressure to remove hemicellulose and disrupt lignin bonds making the remaining cellulose more available for AD (Hashemi et al., 2019b; Qiao et al., 2011). Contrary to steam explosion pretreatment, water remains in the liquid state, and pressure allows maintaining this status at high temperatures (Ruiz et al., 2020). The hemicellulose sugars, together with other hydrolysable compounds, are hydrolysed, making liquid hot water pretreatment ideal for LMs rich in non-structural sugars (Ravindran and Jaiswal, 2016). pH has to be controlled to avoid the formation of inhibitory compounds (Yang et al., 2018). Liquid hot water pretreatment does not need particle size comminution but demands a large amount of water (Baruah et al., 2018).

*2.4.4 Biological pretreatments*

Biological pretreatments include enzymes, microbial consortia, and fungal strains (Baruah et al., 2018). Compared with physical and chemical methods, a biological pretreatment has various advantages, such as no requirement for chemicals and a lower energy input (Taherzadeh and Karimi, 2008). Biological pretreatment methods are performed under mild environmental conditions, which reduce the risk of generating inhibitory compounds (Ravindran and Jaiswal,

2016). Nevertheless, the long pretreatment time and the competition for carbohydrates between organisms carrying out pretreatment and biogas production limit biological pretreatments in commercial applications (Tu and Hallett, 2019).

Several wood-decay fungi have been studied, and white-rot strains are most interesting for the biological pretreatment of LMs, since they can selectively metabolise lignin from LMs with low carbohydrate consumption (Amin et al., 2017). In contrast, soft-rot and brown-rot fungi use enzymes to degrade cellulose and hemicellulose with minimal lignin removal (Ravindran and Jaiswal, 2016). White rot fungi have two enzyme systems: the oxidative ligninolytic system and the hydrolytic system. The first one makes use of three enzymes, i.e. lignin peroxide, manganese peroxide and laccase, which attack the phenyl rings in lignin. The second one degrades cellulose and hemicellulose to release fermentable sugars using cellulase and hemicellulase enzymes (Nadir et al., 2019). White-rot fungi degrade lignin with two modes of action, namely selective and non-selective decay. In selective decay mode, fungi selectively degrade the lignin and hemicellulose fractions, while the cellulose fraction is essentially unaffected. Non-selective degradation consumes similar amounts of cellulose, hemicellulose, and lignin for fungal growth (Baruah et al., 2018).

Microbial consortia employ mixed cultures to increase the total sugar yield and reduce the lignin content of LMs (Ali et al., 2020; Wen et al., 2015; Zhong et al., 2016). Similarly to fungal pretreatment, enzymatic pretreatment uses pure enzymes (e.g. laccase, manganese peroxidase, cellulase, and xylanase) to achieve the same goals (Koupaie et al., 2019). Nevertheless, microbial consortia and enzymatic pretreatment are still attempting to meet a cost-effective balance beyond the laboratory scale (Koupaie et al., 2019; Wen et al., 2015).

**Table 2.2 –** Effectiveness of different pretreatment methods on the enhancement of the methane production potential of lignocellulosic materials.

| Category | Pretreatment | Substrate | Δ $CH_4$ | Reference |
|---|---|---|---|---|
| Physical | Ball milling | Wheat straw | + 49% | Dell'Omo and Spena (2020) |
| | Microwave | Energy crop (*Sida hermaphrodita*) | + 39% | Zieliński et al. (2019) |
| | Extrusion | Rice straw | + 72% | (Chen et al., 2014) |
| Chemical | Alkaline (NaOH) | Wheat straw | + 15% | Mancini et al. (2018a) |
| | Acid ($H_2SO_4$) | Cassava residues | + 57% | Zhang et al. (2011) |
| | Ionic liquid ([C4mim]Cl/DMSO) | Rice straw | + 137% | Gao et al. (2013) |
| Physicochemical | Steam explosion | Rubber wood waste | + 670% | Eom et al. (2019) |
| | Liquid hot water | Sunflower residues | + 173% | Lee and Park (2020) |
| Biological | Fungal (white-rot) | Rice straw | + 114% | Kainthola et al. (2019b) |
| | Microbial consortia (WSD-5) | Napier grass | + 49% | Wen et al. (2015) |
| | Microbial consortia (CS-5) | Catalpa sawdust | + 76% | Ali et al. (2020) |

## 2.5 Organosolv pretreatment

### *2.5.1 Mechanism and process parameters of organosolv pretreatment*

Organosolv pretreatment is the most efficient pretreatment method to remove lignin, which protects the polysaccharides against degradation (Ostovareh et al., 2015). Organosolv is a chemical pretreatment in which the LMs are mixed with an organic or aqueous organic solvent and heated to dissolve the lignin component. Besides, depending on the operating conditions, partial hemicellulose hydrolysis can occur (Oliva et al., 2021). After pretreatment, lignin can be extracted from the solvent by precipitation, membrane filtration (Arkell et al., 2014), and water electrolysis (Jin et al., 2013). Precipitation is the most employed strategy and is performed via acidification of the lignin-rich liquor (Mussatto et al., 2007).

A wide range of organic or aqueous organic solvents has been explored to pretreat LMs, with or without the addition of inorganic or organic acid catalysts (Table 2.3). The optimal process temperature depends on the type of biomass, solvent, and catalyst, and usually ranges from 150 to 200 °C (Taherzadeh and Karimi, 2008). Organic solvents are classified into low boiling point alcohols (e.g. methanol and ethanol), higher boiling point alcohols (e.g. ethylene glycol and glycerol), and other classes of organic compounds (e.g. dimethyl sulfoxide, ethers and ketones) (Borand and Karaosmanoğlu, 2018). In the choice of the solvent, the price and easiness of recovery should also be considered. The solvent should be separated and reused to reduce the

operational costs of the process (Zhou et al., 2018). Also, solvent residues must be removed from the pretreated material to avoid the inhibition of the subsequent AD process (Behera et al., 2014; Harmsen et al., 2010). Due to the high cost of the solvents, ethanol and methanol are preferred over alcohols with a higher boiling point. The most employed catalysts to enhance the pretreatment effectiveness are hydrochloric, sulfuric, and phosphoric acid (Ferreira and Taherzadeh, 2020), but organic acids such as acetic and formic acid have also been investigated (Borand and Karaosmanoğlu, 2018).

After organosolv pretreatment, three separate components are obtained: a pure cellulose fraction, an aqueous hemicellulose stream, and a highly pure lignin fraction (Meng et al., 2020). Further, similarly to other pretreatments, organosolv causes a decrease in the crystallinity of LMs and enhances the accessibility of carbohydrates for microbial degradation (Mancini et al., 2016a). At higher temperatures, the cellulose fraction of the biomass is also degraded. Furthermore, to be effective, the pretreatment time varies between 0.5 and a few hours. Under these process conditions, organosolv is well suitable to dissolve hemicellulose, recover cellulose, and make it more susceptible to enzymatic hydrolysis (Ferreira and Taherzadeh, 2020). Typically, an uncatalysed organosolv pretreatment is efficient only towards low-density hardwoods and agricultural residues. Softwoods or high-density hardwoods require more severe pretreatment conditions (Harmsen et al., 2010).

### *2.5.2 Benefits and drawbacks*

The benefits of organosolv pretreatment include: (i) production of high-quality lignin, which can be used for several applications, (ii) reduced amount of waste produced, (iii) lower energy use, (iv) increase in porosity, (v) removal of lignin and the reduction of the hemicellulose fraction, which may shorten the hydrolysis stage, (vi) low formation of inhibitory compounds, compared to the industrially most employed pretreatments, and (vii) easy solvent recovery. On the contrary, potential drawbacks of the organosolv pretreatment are the high operational and investment costs, as well as the risk of explosion due to the use of organic solvents and the high temperatures employed (Ferreira and Taherzadeh, 2020; Meng et al., 2020; Zhou et al., 2018).

### *2.5.3 Effectiveness of organosolv pretreatment on different lignocellulosic materials*

Organosolv pretreatment, performed with 75% ethanol using sulfuric acid as a catalyst, improves the methane production from hardwood elm, softwood pine, and rice straw (Mirmohamadsadeghi et al., 2014). The optimal process parameters vary depending on the substrate. Rice straw increases its methane production potential by 32% when pretreated at 150

°C for 60 min. Instead, 30 min pretreatment is sufficient to enhance the methane production from pinewood by 84%. On the other hand, a higher pretreatment temperature (i.e. 180 °C) has a positive effect on elmwood (Mirmohamadsadeghi et al., 2014). Ostovareh et al. (2015) improved the bioconversion of sweet sorghum stalks to ethanol and biogas by organosolv pretreatment. Nevertheless, the use of the acid catalyst improves the methane yield only at lower pretreatment temperatures.

The organic solvent selection plays a key role when pretreating hazelnut skin (Table 2.3). The use of methanol and catalysed-methanol is more efficient than ethanol organosolv pretreatment (Mancini et al., 2018b; Oliva et al., 2021). In contrast, methanol-organosolv pretreatment is not strong enough to overcome the recalcitrance of nut shells, such as almond shell, and causes a loss of biodegradable matter from spent coffee grounds, decreasing the methane production (Oliva et al., 2021). On the other hand, ethanol-organosolv pretreatment is particularly effective on rice straw and wheat straw, raising the methane production potential of the two LMs to 332 and 316 mL $CH_4$/g VS, respectively (Mancini et al., 2018a, 2018b).

Organosolv pretreatment was effective on forest residues using three different organic solvents (i.e. ethanol, methanol, and acetic acid) with or without 1% w/w sulfuric acid, acetic acid, and hydrochloric acid as catalysts (Kabir et al., 2015). The methane production potential of catalyst-free pretreated forest residues achieves 300, 230, and 330 mL $CH_4$/g VS for ethanol, methanol, and acetic acid pretreated LM, respectively, rather than the untreated biomass that reaches only 50 mL $CH_4$/g VS. The use of catalysts significantly improved methane production only when coupled with methanol (Kabir et al., 2015). The low performance of the forest residues treated with only methanol can be attributed to the presence of methanol residues in the pretreated substrate that may have negatively affected the AD process. Only a few methanogen groups utilise methanol as precursors for methane production, and the catalyst addition was necessary to balance this adverse effect. In contrast, methanogens can easily convert ethanol and acetic acid to methane (Kabir et al., 2015). The economic analysis performed in that study showed that the methanol supply and recovery were cheaper than for the other two solvents (Kabir et al., 2015). Ethanol-organosolv pretreatment can also be combined with steam explosion to enhance the AD of birch and spruce woodchips (Matsakas et al., 2020).

Recent studies have focused on rubber wood waste valorisation using organosolv pretreatment under a biorefinery approach (Charnnok et al., 2020; Tongbuekeaw et al., 2020). Organosolv pretreatment (75% ethanol) significantly increases the methane production from rubber wood

waste from 59 to 166 mL $CH_4$/g VS, reducing the lignin content by 74% (Tongbuekeaw et al., 2020). Sequential ethanol-organosolv and enzymatic pretreatments enhance the methane production potential of rubber wood waste. The organosolv step removes almost 50% of the lignin, obtaining a glucose-rich hydrolysate for the subsequent enzyme-assisted AD (Charnnok et al., 2020).

**Table 2.3 –** Effectiveness of organosolv pretreatment for lignin removal (Δlignin) and increment of the methane production potential ($\Delta CH_4$) of different lignocellulosic materials.

| Substrate | Optimal pretreatment condition | Pretreatment effectiveness[a] | Reference |
|---|---|---|---|
| Rice straw | 50% EtOH, 180 °C, 1 h | Δlignin: -18%<br>$\Delta CH_4$: +41% | Mancini et al. (2018b) |
| Rice straw | 75% EtOH, 150 °C, 1 h, catalyst | Δlignin: -22%<br>$\Delta CH_4$: +32% | Mirmohamadsadeghi et al. (2014) |
| Wheat straw | 50% EtOH, 180 °C, 1 h | Δlignin: -14%<br>$\Delta CH_4$: +15% | Mancini et al. (2018a) |
| Sugarcane bagasse | 25% EtOH + 10% Ammonia, 70 °C, 12 h | Δlignin: -49%<br>$\Delta CH_4$: +135% | Sajad Hashemi et al. (2019) |
| Sweet sorghum stalks | 50% PrOH, 160 °C, 0.5 h, catalyst | Δlignin: -25%<br>$\Delta CH_4$: +107% | Ostovareh et al. (2015) |
| Sunflower stalks | 50% EtOH, 160 °C, 0.5 h | Δlignin: -26%<br>$\Delta CH_4$: +124% | Hesami et al. (2015) |
| Hazelnut skin | 50% MeOH, 130 °C, 1 h, catalyst | Δlignin: -9%<br>$\Delta CH_4$: +1700% | Oliva et al. (2021) |
| Hazelnut skin | 50% EtOH, 180 °C, 1 h | Δlignin: N.O.<br>$\Delta CH_4$: +10% | Mancini et al. (2018b) |
| Almond shell | 50% MeOH, 200 °C, 1 h | Δlignin: N.O.<br>$\Delta CH_4$: +7% | Oliva et al. (2021) |
| Cocoa bean shell | 50% EtOH, 180 °C, 1 h | Δlignin: N.O.<br>$\Delta CH_4$: N.O. | Mancini et al. (2018b) |
| Spent coffee grounds | 50% MeOH, 200 °C, 1 h, catalyst | Δlignin: N.O.<br>$\Delta CH_4$: +10% | Oliva et al. (2021) |
| Forest residues | 50% MeOH, 190 °C, 1 h, catalyst | Δlignin: -4%<br>$\Delta CH_4$: +320% | Kabir et al. (2015) |
| Elmwood | 75% EtOH, 180 °C, 1 h, catalyst | Δlignin: -27%<br>$\Delta CH_4$: +73% | Mirmohamadsadeghi et al. (2014) |
| Pinewood | 75% EtOH, 150 °C, 0.5 h, catalyst | Δlignin: N.O.<br>$\Delta CH_4$: +84% | Mirmohamadsadeghi et al. (2014) |
| Rubber wood waste | 75% EtOH, 210 °C, 0.5 h | Δlignin: -74%<br>$\Delta CH_4$: +179% | Tongbuekeaw et al. (2020) |

[a] N.O. means that no significant effect on the specific parameter was observed.

## 2.6 N-methylmorpholine N-oxide pretreatment

### *2.6.1 Mechanisms and process parameters of the NMMO pretreatment*

NMMO is a cyclic, tertiary amine, aliphatic oxide capable of dissolving cellulose by disrupting the original hydrogen bonds and creating new linkages with the dissolved polymer (Sari and Budiyono, 2014; Satari et al., 2019). The effect on cellulose depends on the NMMO hydration (Figure 2.3). A water content lower than 17% completely dissolves cellulose, while an NMMO content of 76 - 82% leads to the swelling of the cellulose fibers by creating balloons, in which the cellulose starts to dissolve. A further increase of the water content (25 - 30%) reduces the cellulose dissolution and mainly results in the swelling of the cellulose fibers. An NMMO content lower than 65% proportionally decreases cellulose swelling, with no dissolution observed (Cuissinat and Navard, 2006). The ability of NMMO in dissolving cellulose is attributed to its chemical structure, presenting weak polar N-O bonds with a negative charge on oxygen and positively charged on nitrogen. NMMO tends to form new hydrogen bonds with both water and cellulose, preferentially with cellulose until the water content of the aqueous solution is below 17% (Mancini et al., 2016a; Wikandari et al., 2016).

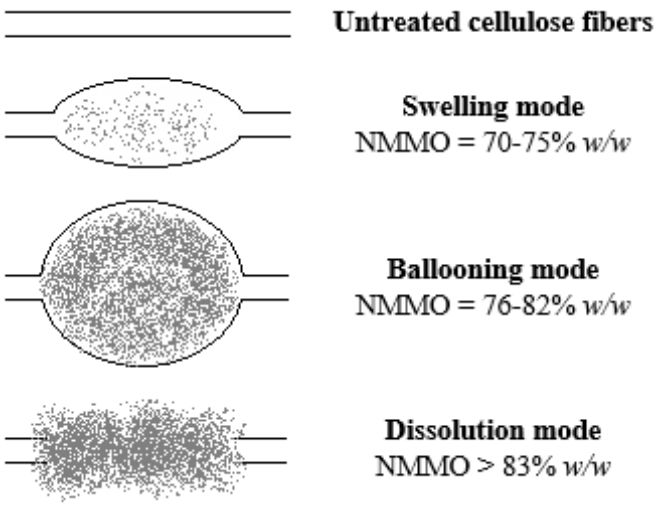


**Figure 2.3 –** Effect of NMMO pretreatment on cellulose fibers.

The interest in NMMO started in the early 20$^{th}$ century with applications in the textile industry and culminating with its usage in the Lyocell process (Sayyed et al., 2019). Recently, the effectiveness of NMMO on cellulose has allowed its use as a pretreatment for LMs (Table 2.4) (Khoshnevisan et al., 2016; Shafiei et al., 2011; Sołowski et al., 2020). The dissolution mode (85% NMMO) is recommended for ethanol production, while a lower NMMO concentration results in a better improvement in terms of methane production (Jeihanipour et al., 2010). The dissolution mode foresees the complete solubilisation and subsequent regeneration of the

cellulosic component of the biomass. The rate of cellulose dissolution is inversely related to the cellulose concentration and degree of polymerisation (Wikandari et al., 2016). The regeneration of cellulose occurs by adding an anti-solvent, such as boiling water (Cuissinat and Navard, 2006). The regenerated cellulose shows a lower total crystallinity index (TCI) and lateral order index (LOI), which facilitate the microbial attack. On the other hand, NMMO pretreatment in swelling/ballooning mode allows a higher increase in porosity, with a lower decrease of the crystallinity indexes (Jeihanipour et al., 2010).

TCI and LOI of cellulose-based materials can be estimated by Fourier-transform infrared spectroscopy. TCI is expressed as the ratio of the absorbance value at 1375 and 2902 $cm^{-1}$ and is proportional to the entire crystallinity of the sample. LOI is representative of the ratio between cellulose I and cellulose II, and is calculated as the infrared spectral ratio 1420/893 $cm^{-1}$. The LOI increases with the crystallinity of cellulose I and decreases with the increasing crystallinity of cellulose II (Carrillo et al., 2004; Nelson and O'Connor, 1964a, 1964b).

*2.6.2 Benefits and drawbacks*

NMMO is often recommended as the most advantageous cellulose solvent compared to the well-known phosphoric acid, alkaline solutions, and other ionic liquids. NMMO offers the advantage of acting directly on the cellulosic component of the biomass, reducing the risk of losing carbohydrates, in contrast with other pretreatments such as steam explosion, alkaline, phosphoric acid, and biological pretreatments (Wikandari et al., 2016). Depending on the stage of hydration, NMMO acts differently on the cellulosic component of the biomass, by increasing the porosity or reducing the crystallinity of LMs (Jeihanipour et al., 2010). NMMO pretreatment can be operated in relatively mild conditions, with temperature ranging from 90 and 130 °C and pretreatment times between 20 min and 30 h (Mancini et al., 2016a).

The pretreatment feasibility strongly depends on solvent recovery and recycling. The solvent recovery takes place by treating the liquid stream of the NMMO pretreatment with ion-exchange resins to remove contaminants and subsequent evaporation of the water, obtaining the monohydrate form of NMMO (Satari et al., 2019). NMMO pretreatment non-recyclable liquid waste streams can be treated with ozone, with ozonation products being easily biodegradable at neutral pH (Stockinger et al., 1996). The loss of NMMO during recovery is less than 2% (Sari and Budiyono, 2014). Nevertheless, the use of NMMO as a pretreatment for LMs on a large scale is still limited because of the considerable amount of water required for the washing step (Mancini et al., 2016a).

The efficacy of recovered NMMO depends on the chemical composition of the LMs. In particular, the pretreatment of lignin-rich LMs reduces the efficiency of recovered NMMO (Millati et al., 2020), most likely due to negative side reactions and release of by-products such as tannins, resin acids, and phenolic compounds (Kabir et al., 2014). The NMMO action during pretreatment does not produce furans, reducing the risk of inhibition in the subsequent biofuel production processes (Wikandari et al., 2016). However, leftover NMMO after pretreatment can inhibit the AD process, even at low (0.5 - 1%) concentrations (Millati et al., 2020).

*2.6.3 Effectiveness of NMMO pretreatment on different lignocellulosic materials*

Recent studies show the effects of 85% NMMO pretreatment at 120 °C on rice straw, wheat straw, and hazelnut skin (Mancini et al., 2018a, 2016b). The pretreatment is particularly effective on rice straw, increasing the methane production by 82%, even though no significant effect on the LOI was observed. On the other hand, NMMO pretreatment significantly reduces the crystallinity index of pretreated hazelnut skin, resulting in a higher methane production during the first days of AD (Mancini et al., 2016b). Similarly to hazelnut skin, NMMO pretreatment increases the porosity of wheat straw, enhancing the specific rate constant $R_m$ from 21 to 32 mL $CH_4$/g VS/d (Mancini et al., 2018a).

Teghammar et al. (2012) investigated the effect of 85% NMMO pretreatment on spruce wood, rice straw and triticale straw, observing that only for rice straw a longer pretreatment time (i.e. 15 h) leads to an inhibition of the AD process. On the other hand, 15 h NMMO pretreatment is particularly efficient for spruce wood and triticale straw, especially when no comminution is performed. The negative effect of a longer pretreatment time is due to the loss of glucan and xylan during pretreatment (Teghammar et al., 2012). On the contrary, all investigated pretreatment times (i.e. 1, 3, and 15 h) can positively affect the AD of pinewood, confirming that a longer time is required when larger particle size substrates undergo NMMO pretreatment (Shafiei et al., 2014). The dissolution mode pretreatment (i.e. 85% NMMO) increases the porosity and reduces the crystallinity of birch wood after 3 h pretreatment, enhancing the methane production potential by 47% (Goshadrou et al., 2013).

To the authors' knowledge, only Purwandari et al. (2013) studied the effect of the NMMO concentration on pretreatment of LMs, although it is reported to be a key factor for cellulose hydrolysis and subsequent conversion to methane (Jeihanipour et al., 2010). The authors investigated 73, 79, and 85% NMMO pretreatment at 90 and 120 °C. A longer pretreatment time at 90 °C positively affects the subsequent AD of oil palm empty fruit bunches. In contrast,

increasing the pretreatment temperature to 120 °C, the optimal pretreatment time is 3 hours, and the significance of the NMMO concentration is attenuated (Purwandari et al., 2013).

**Table 2.4 –** Effectiveness of NMMO pretreatment on glucan or total carbohydrates content (Δglucan, Δcarbo), crystallinity index (ΔLOI), water swelling capacity (ΔWSC), and increment of the methane production potential ($\Delta CH_4$) of various lignocellulosic materials.

| Substrate | Optimal pretreatment condition | Pretreatment effectiveness[a] | Reference |
|---|---|---|---|
| Cotton linters | 73% NMMO, 90 °C, 1 h | ΔLOI: -22%<br>ΔWSC: -23%<br>$\Delta CH_4$: +17% | Jeihanipour et al. (2010) |
| Rice straw | 85% NMMO, 120 °C, 3 h | ΔLOI: N.O.<br>$\Delta CH_4$: +81% | Mancini et al. (2016b) |
| Triticale straw | 85% NMMO, 130 °C, 15 h | Δglucan: +35%<br>$\Delta CH_4$: +583% | Teghammar et al. (2012) |
| Wheat straw | 85% NMMO, 120 °C, 3 h | Δglucan: N.O.<br>ΔWSC: +46%<br>$\Delta CH_4$: +11% | Mancini et al. (2018a) |
| Barley straw | 85% NMMO, 90 °C, 7 h | Δcarbo: +5%<br>$\Delta CH_4$: +92% | Kabir et al. (2014) |
| Hazelnut skin | 85% NMMO, 120 °C, 3 h | ΔLOI: -9%<br>$\Delta CH_4$: N.O. | Mancini et al. (2016b) |
| Cocoa bean shell | 85% NMMO, 120 °C, 3 h | ΔLOI: +15%<br>$\Delta CH_4$: +14% | Mancini et al. (2016b) |
| Oil palm empty fruit bunch | 85% NMMO, 120 °C, 3 h | Δglucan: N.O.<br>ΔLOI: -76%<br>$\Delta CH_4$: +48% | Purwandari et al. (2013) |
| Forest residues | 85% NMMO, 90 °C, 30 h | Δcarbo: +7%<br>$\Delta CH_4$: +114% | Kabir et al. (2014) |
| Forest residues | 85% NMMO, 120 °C, 3 h | Δcarbo: +10%<br>$\Delta CH_4$: +162% | Aslanzadeh et al. (2014) |
| Birch wood (milled) | 85% NMMO, 130 °C, 3 h | Δglucan: +8%<br>ΔWSC: +57%<br>ΔLOI: -18%<br>$\Delta CH_4$: +48% | Goshadrou et al. (2013) |
| Softwood spruce chips | 85% NMMO, 130 °C, 15 h | Δglucan: +12%<br>$\Delta CH_4$: +1088% | Teghammar et al. (2012) |
| Pinewood chips | 85% NMMO, 120 °C, 30 h | Δglucan: +12%<br>ΔWSC: +280%<br>ΔLOI: -6%<br>$\Delta CH_4$: +580% | Shafiei et al. (2014) |
| Cassava residues | 85% NMMO, 90 °C, 2 h | ΔLOI: -19%<br>$\Delta CH_4$: +28% | Cheng et al. (2017) |

[a] N.O. means that no significant effect on the specific parameter was observed.

## 2.7 Ultrasound pretreatment

*2.7.1 Mechanism and process parameters of ultrasound pretreatment*

Ultrasound, or sonication, techniques have been widely employed in medical applications as well as chemical and food processing for decades using different frequencies depending on the purpose (Chemat et al., 2011; Miller et al., 2012; Suslick, 1999). Recently, ultrasounds are getting attention as pretreatment method to enhance the bioconversion of lignocellulosic and other waste materials due to their environmental friendly approach (Table 2.5) (Bussemaker and Zhang, 2013). Ultrasound pretreatment relies on diffusion of sound waves (> 20 kHz) in liquid media, creating alternations of compression and rarefaction phenomena (Figure 2.4a) (Yang et al., 2017). The alternation of high and low pressurised zones gives rise to gas bubbles that grow up with the sound waves diffusion until imploding for cavitation (Figure 2.4b). The bubbles collapse releases a considerable amount of energy, creating zones with high temperature (2000 - 5000 K) and pressure (up to 1800 atm) (Hassan et al., 2018; Luo et al., 2014).

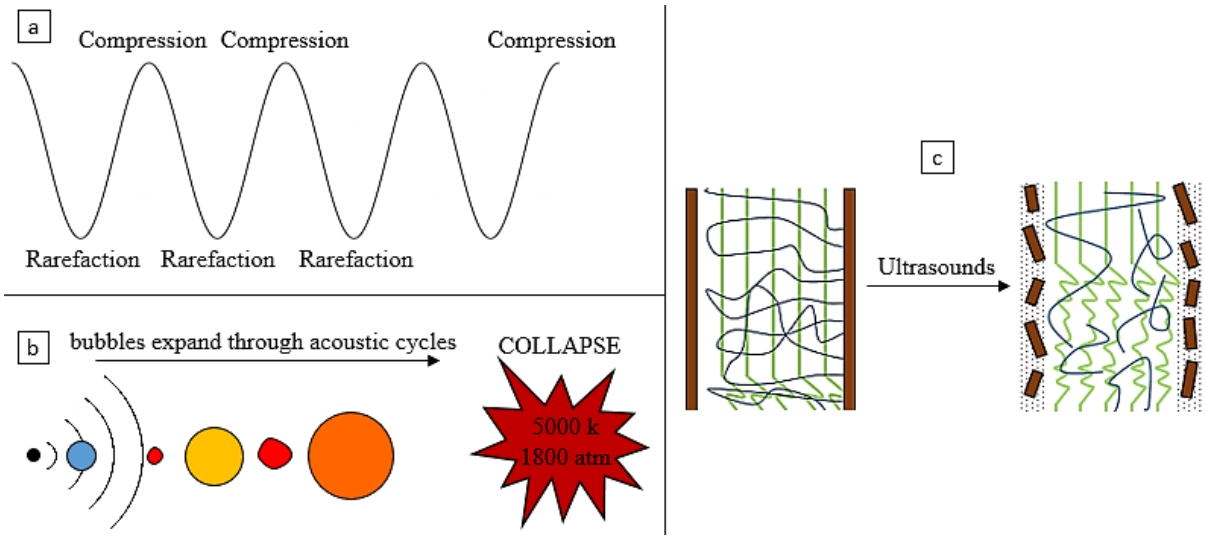


**Figure 2.4 –** Mechanisms of ultrasound pretreatment: a) alternation of compression and rarefaction zones in the liquid media, b) effect of ultrasonic waves on gas bubbles, c) effect of ultrasounds on lignocellulosic structure.

Ultrasonic cavitation is affected by several parameters. Firstly, the frequency (f) emitted by the ultrasonic device plays a key role. It is reported that a higher intensity is required to obtain cavitation at high sonic frequencies, overwhelming the cohesive forces of the medium (Luo et al., 2014; Santos et al., 2009). The intensity of sonication is proportional to the amplitude of vibration of the ultrasonic source. Generally, high amplitudes are not recommended, since they can easily lead to deterioration of the ultrasonic transducer. The optimal amplitude also depends

on the viscosity of the medium. Higher amplitudes are required when the resistance of the sample to the movement of the ultrasonic device increases (Santos et al., 2009). Another important parameter to take into account when performing ultrasound pretreatment is the power density ($P_d$) (Zou et al., 2016b), calculated following Eq. (2.1):

$$P_d = \frac{P \cdot t}{V \cdot TS_0} \quad (2.1)$$

where P is the ultrasonic power (W), t is the pretreatment time (t), V is the volume (L) of the slurry undergoing ultra-sonication, and $TS_0$ is the initial total solid content (kg) of the slurry.

Apart from the characteristics of the ultrasonic wave, the operating conditions also impact the cavitation phenomenon. Temperature has a contrasting effect during ultrasound pretreatment. High temperatures break down the interactions between the solute and matrix, such as hydrogen bonds, Van der Waals forces, and dipole attractions. Nevertheless, the vapour pressure increases with the temperature of the solvent, with the solvent vapour filling the cavitation bubbles, thus reducing their power of collapse (Bussemaker and Zhang, 2013). While water is the most employed medium for ultrasound pretreatment, other liquids with a lower polarity (e.g. organic liquids) are also expected to be efficient. On the other hand, viscous liquids (e.g. oils) make cavitation harder (Santos et al., 2009).

*2.7.2 Benefits and drawbacks*

Cavitation has both thermal and physical effects on the solid particles present in the media, contributing to the fractionation of the lignocellulosic structure and lysing of the membranes and cell walls of the LMs (Figure 2.4c) (Rehman et al., 2013; Santos et al., 2009). Ultrasound pretreatment reduces the crystallinity and degree of polymerisation of cellulose, enhancing its hydrolysis and the solubilisation of the overall organic matter. Besides, ultrasound pretreatment modifies the surface of LMs and disrupts the lignin linkages, separating the lignin fraction from the cellulose and hemicellulose sugars (Bundhoo and Mohee, 2018; Bussemaker and Zhang, 2013; Hassan et al., 2018).

The main concern on ultrasounds techniques regards cost end energy aspects. Although some researchers reported the unfeasibility of ultrasound pretreatment on a laboratory scale (Bundhoo and Mohee, 2018), other studies show its energetic convenience when employing commercial technologies on a larger scale (Cano et al., 2015). Apart from the energy and economic aspect, the possible degradation of cellulose and hemicellulose sugars should be considered when

performing ultrasound pretreatment for LMs valorisation. Nevertheless, this aspect highly depends on the lignocellulosic substrate (Bussemaker and Zhang, 2013).

*2.7.3 Effectiveness of ultrasound pretreatment on different substrates*

Several authors report that ultrasounds can reduce the particle size and increase the surface area of sewage sludge (Bougrier et al., 2006; Cho et al., 2013; Chu et al., 2001; Na et al., 2007) and manures (Elbeshbishy et al., 2011). Recently, the same effect has been observed on LMs, showing that the pretreatment duration is proportional to the substrate disruption. Scanning electron microscopic (SEM) images show that the damages to the external surface of wheat straw and maize straw increase with the pretreatment time. Therefore, ultrasound pretreatment improves the vulnerability of LMs, thus increasing the available contact surface for the subsequent AD process (Zou et al., 2016b, 2016a).

Ultrasound pretreatment also acts on the chemical composition of LMs. The cavitation phenomena lead to the formation of radicals that contribute to increased oxidative stress during pretreatment (Santos et al., 2009). This aspect, together with high pressure and temperature, reduces the lignin content of LMs, generally leaving the cellulosic component of the biomass unaffected. On the other hand, the removal of hemicellulose sugars is observed, most likely due to their amorphous structure and weak linkages (Perrone et al., 2016). Therefore, ultrasonic waves enable to obtain cellulose-rich materials, increasing the digestability of LMs during AD. Imam and Capareda (2012) investigated the effect of hot water and ultrasound-assisted hot water pretreatment on sweet sorghum residues. Hot water pretreatment alone is not effective on lignin removal. On the other hand, the ultrasonic implementation reduced the lignin content by 48%, compared to the untreated sweet sorghum. Similarly, ultrasound pretreatment of sugarcane bagasse reduced the lignin content from 27 to 21%, with minor effects on the cellulose and hemicellulose content (Ramadoss and Muthukumar, 2014). Ultrasound-ammonia pretreatment removed 70% of the lignin from sugarcane bagasse (Velmurugan and Incharoensakdi, 2016).

While ultrasound pretreatment generally does not change the cellulose content, ultrasonic waves may affect the cellulosic hydrogen bonds (Nakashima et al., 2016). In particular, ultrasounds reduce the crystallinity of the cellulosic part of LMs by rearranging the cellulose structure, leaving a more amorphous polymer, vulnerable to enzymatic attack (Bussemaker and Zhang, 2013). On the other hand, some studies report an increase in the crystallinity index after

ultrasound pretreatment. This is likely a consequence of the high lignin removal, resulting in a higher cellulose content remaining in the solid phase after the pretreatment.

The methane production potential increases as a consequence of the changed structural and chemical characteristics of the ultrasound pretreated LMs (Subhedar and Gogate, 2014). Qi et al. (2021) investigated the effectiveness of ultrasound pretreatment on the co-digestion of cannabis straw and municipal wastewater, obtaining a 77% increment of the methane production after 30 min pretreatment at 100 W. Zou et al. (2016b, 2016a) observed a positive effect on methane production from wheat and maize straw co-digested with dairy manure after ultrasound pretreatment.

Interestingly, ultrasound pretreatment shows a great potential when combined with alkaline pretreatment (Hassan et al., 2017). The combination can occur using an alkaline solution as the medium of the ultrasound pretreatment or, simply, when ultrasonic irradiation follows the previously performed alkaline pretreatment (Hassan et al., 2017; Korai and Li, 2020). Sequential NaOH-ultrasound pretreatment enhances the methane production potential of corn stover from 148 up to 320 mL $CH_4$/g VS (Hassan et al., 2017). Similarly, ultrasound pretreatment of wheat straw using 2, 5 and 6% KOH as the medium allows a 47% increment of methane production (Korai and Li, 2020). Despite the promising effects, other studies did not observe a significant effect on methane production after ultrasound pretreatment, most likely due to the low specific energy applied, which lowers the rate of sugar solubilisation (Elalami et al., 2020; Passos et al., 2015).

**Table 2.5 –** Effectiveness of ultrasound pretreatment on reducing sugars (Δsugars), crystallinity index (ΔCrI), lignin removal (Δlignin), and increment of methane production potential ($\Delta CH_4$) for different lignocellulosic materials.

| Substrate | Optimal pretreatment condition | Effectiveness[a] | Reference |
|---|---|---|---|
| Wheat straw (co-digestion with dairy manure) | f: 40 kHz, P: 200 W, t: 20min | Δsugars: +24%<br>$\Delta CH_4$: +80% | Zou et al. (2016a) |
| Maize straw (co-digestion with dairy manure) | f: 50 kHz, P: 250 W, t: 30min | Δsugars: +16%<br>$\Delta CH_4$: +70% | Zou et al. (2016b) |
| Wheat straw | f: 20 kHz, P: 450 W, t: 10min (ultrasound assisted with KOH) | $\Delta CH_4$: +47% | Korai and Li (2020) |
| Cannabis straw | f: 40 kHz, P: 100 W, t: 30min | ΔCrI: +21%<br>$\Delta CH_4$: +77% | Qi et al. (2021) |
| Corn stover | f: 40 kHz, P: 200 W, t: 90min | $\Delta CH_4$: +15% | Hassan et al. (2017) |
| Grape pomace | f: 50 kHz, P: 60 W, t: 70min | Δlignin: -18%<br>$\Delta CH_4$: +10% | El Achkar et al. (2018) |
| Olive pomace | f: 20 kHz, P: 450 W, t: 10min | Δlignin: -10%<br>$\Delta CH_4$: N.O. | Elalami et al. (2020) |
| *Sida hermaphrodita* (L.) Rusby (codigestion with cattle manure) | f: 25 kHz, P: 300 W, t: 10min | $\Delta CH_4$: +127% | Kisielewska et al. (2020) |
| Vinegar residues (grinded) | f: 40 kHz, P: 50W, t: 60 min | $\Delta CH_4$: +30% | Kong et al. (2021) |

[a] N.O. means that no significant effect on the specific parameter was observed.

## 2.8 References


Ali, N., Zhang, Q., Liu, Z.Y., Li, F.L., Lu, M., Fang, X.C., 2020. Emerging technologies for the pretreatment of lignocellulosic materials for bio-based products. Appl. Microbiol. Biotechnol. 104, 455–473. https://doi.org/10.1007/s00253-019-10158-w

Ali, S.S., Kornaros, M., Manni, A., Sun, J., El-Shanshoury, A.E.R.R., Kenawy, E.R., Khalil, M.A., 2020. Enhanced anaerobic digestion performance by two artificially constructed microbial consortia capable of woody biomass degradation and chlorophenols detoxification. J. Hazard. Mater. 389. https://doi.org/10.1016/j.jhazmat.2020.122076

Alonso-Fariñas, B., Oliva, A., Rodríguez-Galán, M., Esposito, G., García-Martín, J.F., Rodríguez-Gutiérrez, G., Serrano, A., Fermoso, F.G., 2020. Environmental assessment of olive mill solid waste valorization via anaerobic digestion versus olive pomace oil extraction. Processes 8. https://doi.org/10.3390/PR8050626

Amin, F.R., Khalid, H., Zhang, H., Rahman, S., Zhang, R., Liu, G., Chen, C., 2017. Pretreatment methods of lignocellulosic biomass for anaerobic digestion. AMB Express 7. https://doi.org/10.1186/s13568-017-0375-4

Arkell, A., Olsson, J., Wallberg, O., 2014. Process performance in lignin separation from softwood black liquor by membrane filtration. Chem. Eng. Res. Des. 92, 1792–1800. https://doi.org/10.1016/j.cherd.2013.12.018

Aslanzadeh, S., Berg, A., Taherzadeh, M.J., Sárvári Horváth, I., 2014. Biogas production from N-Methylmorpholine-N-oxide (NMMO) pretreated forest residues. Appl. Biochem. Biotechnol. 172, 2998–3008. https://doi.org/10.1007/s12010-014-0747-z

Balat, M., 2011. Production of bioethanol from lignocellulosic materials via the biochemical pathway: A review. Energy Convers. Manag. 52, 858–875. https://doi.org/10.1016/j.enconman.2010.08.013

Barbu, M.C., Sepperer, T., Tudor, E.M., Petutschnigg, A., 2020. Walnut and hazelnut shells: Untapped industrial resources and their suitability in lignocellulosic composites. Appl. Sci. 10, 1–11. https://doi.org/10.3390/APP10186340

Baruah, J., Nath, B.K., Sharma, R., Kumar, S., Deka, R.C., Baruah, D.C., Kalita, E., 2018. Recent trends in the pretreatment of lignocellulosic biomass for value-added products. Front. Energy Res. 6, 1–19. https://doi.org/10.3389/fenrg.2018.00141

Behera, S., Arora, R., Nandhagopal, N., Kumar, S., 2014. Importance of chemical pretreatment for bioconversion of lignocellulosic biomass. Renew. Sustain. Energy Rev. 36, 91–106. https://doi.org/10.1016/j.rser.2014.04.047

Bharathiraja, B., Sudharsana, T., Jayamuthunagai, J., Praveenkumar, R., Chozhavendhan, S., Iyyappan, J., 2018. Biogas production – A review on composition, fuel properties, feed stock and principles of anaerobic digestion. Renew. Sustain. Energy Rev. 90, 570–582. https://doi.org/10.1016/j.rser.2018.03.093

Bhatia, S.K., Jagtap, S.S., Bedekar, A.A., Bhatia, R.K., Patel, A.K., Pant, D., Rajesh Banu, J., Rao, C. V., Kim, Y.G., Yang, Y.H., 2020. Recent developments in pretreatment technologies on lignocellulosic biomass: Effect of key parameters, technological improvements, and challenges. Bioresour. Technol. 300, 122724. https://doi.org/10.1016/j.biortech.2019.122724

Bianco, F., Race, M., Forino, V., Pacheco-Ruiz, S., Rene, E.R., 2021a. Bioreactors for wastewater to energy conversion : from pilot to full scale, in: Waste Biorefinery. Elsevier Inc., pp. 103–124. https://doi.org/10.1016/B978-0-12-821879-2/00004-1

Bianco, F., Şenol, H., Papirio, S., 2021b. Enhanced lignocellulosic component removal and biomethane potential from chestnut shell by a combined hydrothermal–alkaline pretreatment. Sci. Total Environ. 762. https://doi.org/10.1016/j.scitotenv.2020.144178

Bilal, M., Asgher, M., Iqbal, H.M.N., Hu, H., Zhang, X., 2017. Biotransformation of lignocellulosic materials into value-added products—A review. Int. J. Biol. Macromol. 98, 447–458. https://doi.org/10.1016/j.ijbiomac.2017.01.133

Blanco, A., Monte, M.C., Campano, C., Balea, A., Merayo, N., Negro, C., 2018. Nanocellulose for industrial use: Cellulose nanofibers (CNF), cellulose nanocrystals (CNC), and bacterial cellulose (BC), Handbook of Nanomaterials for Industrial Applications. Elsevier Inc. https://doi.org/10.1016/B978-0-12-813351-4.00005-5

Böhmdorfer, S., Hosoya, T., Röder, T., Potthast, A., Rosenau, T., 2017. A cautionary note on thermal runaway reactions in mixtures of 1-alkyl-3-methylimidazolium ionic liquids and N-methylmorpholine-N-oxide. Cellulose 24, 1927–1932. https://doi.org/10.1007/s10570-017-1257-2

Borand, M.N., Karaosmanoğlu, F., 2018. Effects of organosolv pretreatment conditions for lignocellulosic biomass in biorefinery applications: A review. J. Renew. Sustain. Energy 10. https://doi.org/10.1063/1.5025876

Bordiga, M., Travaglia, F., Locatelli, M., 2019. Valorisation of grape pomace: an approach that is increasingly reaching its maturity – a review. Int. J. Food Sci. Technol. 54, 933–942. https://doi.org/10.1111/ijfs.14118

Bougrier, C., Albasi, C., Delgenès, J.P., Carrère, H., 2006. Effect of ultrasonic, thermal and ozone pre-treatments on waste activated sludge solubilisation and anaerobic biodegradability. Chem. Eng. Process. Process Intensif. 45, 711–718. https://doi.org/10.1016/j.cep.2006.02.005

Bundhoo, Z.M.A., Mohee, R., 2018. Ultrasound-assisted biological conversion of biomass and waste materials to biofuels: A review. Ultrason. Sonochem. 40, 298–313. https://doi.org/10.1016/j.ultsonch.2017.07.025

Bussemaker, M.J., Zhang, D., 2013. Effect of ultrasound on lignocellulosic biomass as a pretreatment for biorefinery and biofuel applications. Ind. Eng. Chem. Res. 52, 3563–3580. https://doi.org/10.1021/ie3022785

Cano, R., Pérez-Elvira, S.I., Fdz-Polanco, F., 2015. Energy feasibility study of sludge pretreatments: A review. Appl. Energy 149, 176–185. https://doi.org/10.1016/j.apenergy.2015.03.132

Cantarella, M., Cantarella, L., Alberto Gallifuoco, A.S., Alfani, F., 2004. Effect of Inhibitors Released during Steam-Explosion Treatment of Poplar Wood on Subsequent Enzymatic Hydrolysis and SSF. Biotechnol. Prog. 20, 200–206. https://doi.org/10.1021/bp0257978

Carrillo, F., Colom, X., Suñol, J.J., Saurina, J., 2004. Structural FTIR analysis and thermal characterisation of lyocell and viscose-type fibres. Eur. Polym. J. 40, 2229–2234. https://doi.org/https://doi.org/10.1016/j.eurpolymj.2004.05.003

Castilla-Archilla, J., Papirio, S., Lens, P.N.L., 2021. Two step process for volatile fatty acid production from brewery spent grain: Hydrolysis and direct acidogenic fermentation using anaerobic granular sludge. Process Biochem. 100, 272–283. https://doi.org/10.1016/j.procbio.2020.10.011

Charnnok, B., Sawangkeaw, R., Chaiprapat, S., 2020. Integrated process for the production of fermentable sugar and methane from rubber wood. Bioresour. Technol. 302. https://doi.org/10.1016/j.biortech.2020.122785

Chemat, F., Zill-E-Huma, Khan, M.K., 2011. Applications of ultrasound in food technology: Processing, preservation and extraction. Ultrason. Sonochem. 18, 813–835. https://doi.org/10.1016/j.ultsonch.2010.11.023

Chen, X., Zhang, Y.L., Gu, Y., Liu, Z., Shen, Z., Chu, H., Zhou, X., 2014. Enhancing methane production from rice straw by extrusion pretreatment. Appl. Energy 122, 34–41. https://doi.org/10.1016/j.apenergy.2014.01.076

Chen, Y., Cheng, J.J., Creamer, K.S., 2008. Inhibition of anaerobic digestion process: A review. Bioresour. Technol. 99, 4044–4064. https://doi.org/10.1016/j.biortech.2007.01.057

Cheng, J., Zhang, J., Lin, R., Liu, J., Zhang, L., Cen, K., 2017. Ionic-liquid pretreatment of cassava residues for the cogeneration of fermentative hydrogen and methane. Bioresour. Technol. 228, 348–354. https://doi.org/10.1016/j.biortech.2016.12.107

Cho, S.K., Hwang, Y.H., Kim, D.H., Jeong, I.S., Shin, H.S., Oh, S.E., 2013. Low strength ultrasonication positively affects the methanogenic granules toward higher AD performance. Part I: Physico-chemical characteristics. Bioresour. Technol. 136, 66–72. https://doi.org/10.1016/j.biortech.2013.02.111

Chu, C.P., Chang, B.V., Liao, G.S., Jean, D.S., Lee, D.J., 2001. Observations on changes in ultrasonically treated waste-activated sludge. Water Res. 35, 1038–1046. https://doi.org/10.1016/S0043-1354(00)00338-9

Chynoweth, D.P., Owens, J.M., Legrand, R., 2000. Renewable methane from anaerobic digestion of biomass. Renew. Energy 22, 1–8. https://doi.org/10.1016/S0960-1481(00)00019-7

Corrêa, A.C., de Teixeira, E.M., Pessan, L.A., Mattoso, L.H.C., 2010. Cellulose nanofibers from curaua fibers. Cellulose 17, 1183–1192. https://doi.org/10.1007/s10570-010-9453-3

Cuissinat, C., Navard, P., 2006. Swelling and dissolution of cellulose part 1: Free floating cotton and wood fibres in N-methylmorpholine-N-oxide-water mixtures. Macromol. Symp. 244, 1–18. https://doi.org/10.1002/masy.200651201

Dell'Omo, P.P., Spena, V.A., 2020. Mechanical pretreatment of lignocellulosic biomass to improve biogas production: Comparison of results for giant reed and wheat straw. Energy 203, 1–9. https://doi.org/10.1016/j.energy.2020.117798

Dong, M., Wang, S., Xu, F., Wang, J., Yang, N., Li, Q., Chen, J., Li, W., 2019. Pretreatment of sweet sorghum straw and its enzymatic digestion: Insight into the structural changes and visualization of hydrolysis process. Biotechnol. Biofuels 12, 1–11. https://doi.org/10.1186/s13068-019-1613-6

Duque, A., Manzanares, P., Ballesteros, I., Ballesteros, M., 2016. Steam Explosion as Lignocellulosic Biomass Pretreatment, in: Biomass Fractionation Technologies for a Lignocellulosic Feedstock Based Biorefinery. Elsevier Inc., pp. 349–368. https://doi.org/10.1016/B978-0-12-802323-5.00015-3

Duque, A., Manzanares, P., Ballesteros, I., Negro, M.J., Oliva, J.M., Saez, F., Ballesteros, M., 2013. Optimization of integrated alkaline-extrusion pretreatment of barley straw for sugar production by enzymatic hydrolysis. Process Biochem. 48, 775–781. https://doi.org/10.1016/j.procbio.2013.03.003

Duque, A., Manzanares, P., Ballesteros, M., 2017. Extrusion as a pretreatment for lignocellulosic biomass: Fundamentals and applications. Renew. Energy 114, 1427–1441. https://doi.org/10.1016/j.renene.2017.06.050

El Achkar, J.H., Lendormi, T., Salameh, D., Louka, N., Maroun, R.G., Lanoisellé, J.L., Hobaika, Z., 2018. Influence of pretreatment conditions on lignocellulosic fractions and methane production from grape pomace. Bioresour. Technol. 247, 881–889. https://doi.org/10.1016/j.biortech.2017.09.182

Elalami, D., Carrere, H., Abdelouahdi, K., Garcia-Bernet, D., Peydecastaing, J., Vaca-Medina, G., Oukarroum, A., Zeroual, Y., Barakat, A., 2020. Mild microwaves, ultrasonic and alkaline pretreatments for improving methane production: Impact on biochemical and structural properties of olive pomace. Bioresour. Technol. 299, 122591. https://doi.org/10.1016/j.biortech.2019.122591

Elbeshbishy, E., Aldin, S., Hafez, H., Nakhla, G., Ray, M., 2011. Impact of ultrasonication of hog manure on anaerobic digestability. Ultrason. Sonochem. 18, 164–171. https://doi.org/10.1016/j.ultsonch.2010.04.011

Eom, T., Chaiprapat, S., Charnnok, B., 2019. Enhanced enzymatic hydrolysis and methane production from rubber wood waste using steam explosion. J. Environ. Manage. 235, 231–239. https://doi.org/10.1016/j.jenvman.2019.01.041

Ferreira, J.A., Taherzadeh, M.J., 2020. Improving the economy of lignocellulose-based biorefineries with organosolv pretreatment. Bioresour. Technol. 299, 122695. https://doi.org/10.1016/j.biortech.2019.122695

Gao, J., Chen, L., Yuan, K., Huang, H., Yan, Z., 2013. Ionic liquid pretreatment to enhance the anaerobic digestion of lignocellulosic biomass. Bioresour. Technol. 150, 352–358. https://doi.org/10.1016/j.biortech.2013.10.026

Gomez-Tovar, F., Celis, L.B., Razo-Flores, E., Alatriste-Mondragón, F., 2012. Chemical and enzymatic sequential pretreatment of oat straw for methane production. Bioresour. Technol. 116, 372–378. https://doi.org/10.1016/j.biortech.2012.03.109

Gonzales, R.R., Kumar, G., Sivagurunathan, P., Kim, S.H., 2017. Enhancement of hydrogen production by optimization of pH adjustment and separation conditions following dilute acid pretreatment of lignocellulosic biomass. Int. J. Hydrogen Energy 42, 27502–27511. https://doi.org/10.1016/j.ijhydene.2017.05.021

Goshadrou, A., Karimi, K., Taherzadeh, M.J., 2013. Ethanol and biogas production from birch by NMMO pretreatment. Biomass and Bioenergy 49, 95–101. https://doi.org/10.1016/j.biombioe.2012.12.013

Gür, T.M., 2016. Comprehensive review of methane conversion in solid oxide fuel cells: Prospects for efficient electricity generation from natural gas. Prog. Energy Combust. Sci. 54, 1–64. https://doi.org/10.1016/j.pecs.2015.10.004

Haldar, D., Purkait, M.K., 2021. A review on the environment-friendly emerging techniques for pretreatment of lignocellulosic biomass: Mechanistic insight and advancements. Chemosphere 264, 1–16. https://doi.org/10.1016/j.chemosphere.2020.128523

Halder, P., Kundu, S., Patel, S., Setiawan, A., Atkin, R., Parthasarthy, R., Paz-Ferreiro, J., Surapaneni, A., Shah, K., 2019. Progress on the pre-treatment of lignocellulosic biomass employing ionic liquids. Renew. Sustain. Energy Rev. 105, 268–292. https://doi.org/10.1016/j.rser.2019.01.052

Hallac, B.B., Ragauskas, A.J., 2011. Analyzing cellulose degree of polymerization and its relevancy to cellulosic ethanol. Biofuels, Bioprod. Biorefining 5, 215–225. https://doi.org/10.1002/bbb

Harmsen, P., Huijgen, W., Bermudez, L., Bakker, R., López, L., Bakker, R., 2010. Literature

Review of Physical and Chemical Pretreatment Processes for Lignocellulosic Biomass, Energy. https://doi.org/10.1016/j.psep.2011.08.004

Hashemi, S.S., Karimi, K., Majid Karimi, A., 2019a. Ethanolic ammonia pretreatment for efficient biogas production from sugarcane bagasse. Fuel 248, 196–204. https://doi.org/10.1016/j.fuel.2019.03.080

Hashemi, S.S., Karimi, K., Mirmohamadsadeghi, S., 2019b. Hydrothermal pretreatment of safflower straw to enhance biogas production. Energy 172, 545–554. https://doi.org/10.1016/j.energy.2019.01.149

Hassan, M., Umar, M., Mamat, T., Muhayodin, F., Talha, Z., Mehryar, E., Ahmad, F., Ding, W., Zhao, C., 2017. Methane Enhancement through Sequential Thermochemical and Sonication Pretreatment for Corn Stover with Anaerobic Sludge. Energy and Fuels 31, 6145–6153. https://doi.org/10.1021/acs.energyfuels.7b00478

Hassan, S.S., Williams, G.A., Jaiswal, A.K., 2018. Emerging technologies for the pretreatment of lignocellulosic biomass. Bioresour. Technol. 262, 310–318. https://doi.org/10.1016/j.biortech.2018.04.099

Hesami, S.M., Zilouei, H., Karimi, K., Asadinezhad, A., 2015. Enhanced biogas production from sunflower stalks using hydrothermal and organosolv pretreatment. Ind. Crops Prod. 76, 449–455. https://doi.org/10.1016/j.indcrop.2015.07.018

Imam, T., Capareda, S., 2012. Ultrasonic and high-temperature pretreatment, enzymatic hydrolysis and fermentation of lignocellulosic sweet sorghum to bio-ethanol. Int. J. Ambient Energy 33, 152–160. https://doi.org/10.1080/01430750.2012.686195

Ingram, T., Wörmeyer, K., Lima, J.C.I., Bockemühl, V., Antranikian, G., Brunner, G., Smirnova, I., 2011. Comparison of different pretreatment methods for lignocellulosic materials. Part I: Conversion of rye straw to valuable products. Bioresour. Technol. 102, 5221–5228. https://doi.org/10.1016/j.biortech.2011.02.005

Isogai, A., Usuda, M., Kato, T., Uryu, T., Atalla, R.H., 1989. Solid-State CP / MAS NMR Study of Cellulose Polymorphs. Macromolecules 22, 3168–3172. https://doi.org/10.1021/ma00197a045

Jacquet, N., Maniet, G., Vanderghem, C., Delvigne, F., Richel, A., 2015. Application of Steam Explosion as Pretreatment on Lignocellulosic Material: A Review. Ind. Eng. Chem. Res. 54, 2593–2598. https://doi.org/10.1021/ie503151g

Jeihanipour, A., Karimi, K., Taherzadeh, M.J., 2010. Enhancement of ethanol and biogas production from high-crystalline cellulose by different modes of NMO pretreatment.

Biotechnol. Bioeng. 105, 469–476. https://doi.org/10.1002/bit.22558

Jeihanipour, A., Niklasson, C., Taherzadeh, M.J., 2011. Enhancement of solubilization rate of cellulose in anaerobic digestion and its drawbacks. Process Biochem. 46, 1509–1514. https://doi.org/10.1016/j.procbio.2011.04.003

Jin, W., Tolba, R., Wen, J., Li, K., Chen, A., 2013. Efficient extraction of lignin from black liquor via a novel membrane-assisted electrochemical approach. Electrochim. Acta 107, 611–618. https://doi.org/10.1016/j.electacta.2013.06.031

Kabir, M.M., Niklasson, C., Taherzadeh, M.J., Horváth, I.S., 2014. Biogas production from lignocelluloses by N-methylmorpholine-N-oxide (NMMO) pretreatment: Effects of recovery and reuse of NMMO. Bioresour. Technol. 161, 446–450. https://doi.org/10.1016/j.biortech.2014.03.107

Kabir, M.M., Rajendran, K., Taherzadeh, M.J., Sárvári Horváth, I., 2015. Experimental and economical evaluation of bioconversion of forest residues to biogas using organosolv pretreatment. Bioresour. Technol. 178, 201–208. https://doi.org/10.1016/j.biortech.2014.07.064

Kainthola, J., Kalamdhad, A.S., Goud, V. V., 2019a. A review on enhanced biogas production from anaerobic digestion of lignocellulosic biomass by different enhancement techniques. Process Biochem. 84, 81–90. https://doi.org/10.1016/j.procbio.2019.05.023

Kainthola, J., Kalamdhad, A.S., Goud, V. V., Goel, R., 2019b. Fungal pretreatment and associated kinetics of rice straw hydrolysis to accelerate methane yield from anaerobic digestion. Bioresour. Technol. 286, 1–9. https://doi.org/10.1016/j.biortech.2019.121368

Keikhosor, K., Shafiei, M., Kumar, R., 2013. Progress in Physical and Chemical Pretreatment of Lignocellulosic Biomass, in: Gupta, V.K., Tuohy, M.G. (Eds.), Biofuel Technologies: Recent Developments. Springer, Berlin, Heidelberg, pp. 53–96. https://doi.org/10.1007/978-3-642-34519-7_3

Khatri, S., Wu, S., Kizito, S., Zhang, W., Li, J., Dong, R., 2015. Synergistic effect of alkaline pretreatment and Fe dosing on batch anaerobic digestion of maize straw. Appl. Energy 158, 55–64. https://doi.org/10.1016/j.apenergy.2015.08.045

Khoshnevisan, B., Shafiei, M., Rajaeifar, M.A., Tabatabaei, M., 2016. Biogas and bioethanol production from pinewood pre-treated with steam explosion and N-methylmorpholine-N-oxide (NMMO): A comparative life cycle assessment approach. Energy 114, 935–950. https://doi.org/10.1016/j.energy.2016.08.024

Kisielewska, M., Rusanowska, P., Dudek, M., Nowicka, A., Krzywik, A., Dębowski, M.,

Joanna, K., Zieliński, M., 2020. Evaluation of Ultrasound Pretreatment for Enhanced Anaerobic Digestion of *Sida hermaphrodita*. Bioenergy Res. 13, 824–832. https://doi.org/10.1007/s12155-020-10108-9

Kohli, K., Katuwal, S., Biswas, A., Sharma, B.K., 2020. Effective delignification of lignocellulosic biomass by microwave assisted deep eutectic solvents. Bioresour. Technol. 303. https://doi.org/10.1016/j.biortech.2020.122897

Kong, X., Defemur, Z., Li, M., Zhang, Q., Li, H., Yue, X., 2021. Effects of combined ultrasonic and grinding pre-treatments on anaerobic digestion of vinegar residue: organic solubilization, hydrolysis, and $CH_4$ production. Environ. Technol. https://doi.org/10.1080/09593330.2020.1870572

Korai, R.M., Li, X., 2020. Effect of ultrasonic assisted KOH pretreatment on physiochemical characteristic and anaerobic digestion performance of wheat straw. Chinese J. Chem. Eng. 28, 2409–2416. https://doi.org/10.1016/j.cjche.2020.06.022

Koupaie, E.H., Dahadha, S., Bazyar Lakeh, A.A., Azizi, A., Elbeshbishy, E., 2019. Enzymatic pretreatment of lignocellulosic biomass for enhanced biomethane production-A review. J. Environ. Manage. 233, 774–784. https://doi.org/10.1016/j.jenvman.2018.09.106

Kucharska, K., Rybarczyk, P., Hołowacz, I., Łukajtis, R., Glinka, M., Kamiński, M., 2018. Pretreatment of lignocellulosic materials as substrates for fermentation processes. Molecules 23, 1–32. https://doi.org/10.3390/molecules23112937

Kumar, A.K., Sharma, S., 2017. Recent updates on different methods of pretreatment of lignocellulosic feedstocks: a review. Bioresour. Bioprocess. 4, 1–19. https://doi.org/10.1186/s40643-017-0137-9

Kumar, P., Barrett, D.M., Delwiche, M.J., Stroeve, P., 2009. Methods for pretreatment of lignocellulosic biomass for efficient hydrolysis and biofuel production. Ind. Eng. Chem. Res. 48, 3713–3729. https://doi.org/10.1021/ie801542g

Kumari, D., Singh, R., 2018. Pretreatment of lignocellulosic wastes for biofuel production: A critical review. Renew. Sustain. Energy Rev. 90, 877–891. https://doi.org/10.1016/j.rser.2018.03.111

Kweku, D., Bismark, O., Maxwell, A., Desmond, K., Danso, K., Oti-Mensah, E., Quachie, A., Adormaa, B., 2018. Greenhouse Effect: Greenhouse Gases and Their Impact on Global Warming. J. Sci. Res. Reports 17, 1–9. https://doi.org/10.9734/jsrr/2017/39630

Larnaudie, V., Ferrari, M.D., Lareo, C., 2019. Techno-economic analysis of a liquid hot water pretreated switchgrass biorefinery: Effect of solids loading and enzyme dosage on

enzymatic hydrolysis. Biomass and Bioenergy 130, 1–11. https://doi.org/10.1016/j.biombioe.2019.105394

Lee, J., Park, K.Y., 2020. Impact of hydrothermal pretreatment on anaerobic digestion efficiency for lignocellulosic biomass: Influence of pretreatment temperature on the formation of biomass-degrading byproducts. Chemosphere 256, 1–7. https://doi.org/10.1016/j.chemosphere.2020.127116

Lee, K.M., Hong, J.Y., Tey, W.Y., 2021. Combination of ultrasonication and deep eutectic solvent in pretreatment of lignocellulosic biomass for enhanced enzymatic saccharification. Cellulose 28, 1513–1526. https://doi.org/10.1007/s10570-020-03598-5

Li, F., Zhang, M., Guo, K., Hu, Z., Zhang, R., Feng, Y., Yi, X., Zou, W., Wang, L., Wu, C., Tian, J., Lu, T., Xie, G., Peng, L., 2015. High-level hemicellulosic arabinose predominately affects lignocellulose crystallinity for genetically enhancing both plant lodging resistance and biomass enzymatic digestibility in rice mutants. Plant Biotechnol. J. 13, 514–525. https://doi.org/10.1111/pbi.12276

Li, W., Khalid, H., Zhu, Z., Zhang, R., Liu, G., Chen, C., Thorin, E., 2018. Methane production through anaerobic digestion: Participation and digestion characteristics of cellulose, hemicellulose and lignin. Appl. Energy 226, 1219–1228. https://doi.org/10.1016/j.apenergy.2018.05.055

Lu, X., Zheng, X., Li, X., Zhao, J., 2016. Adsorption and mechanism of cellulase enzymes onto lignin isolated from corn stover pretreated with liquid hot water. Biotechnol. Biofuels 9, 1–12. https://doi.org/10.1186/s13068-016-0531-0

Luo, J., Fang, Z., Smith, R.L., 2014. Ultrasound-enhanced conversion of biomass to biofuels. Prog. Energy Combust. Sci. 41, 56–93. https://doi.org/10.1016/j.pecs.2013.11.001

Luo, L., Kaur, G., Wong, J.W.C., 2019. A mini-review on the metabolic pathways of food waste two-phase anaerobic digestion system. SAGE. https://doi.org/10.1177/0734242X18819954

Mahmood, H., Moniruzzaman, M., Iqbal, T., Khan, M.J., 2019. Recent advances in the pretreatment of lignocellulosic biomass for biofuels and value-added products. Curr. Opin. Green Sustain. Chem. 20, 18–24. https://doi.org/10.1016/j.cogsc.2019.08.001

Mancini, G., Papirio, S., Lens, P.N.L., Esposito, G., 2018a. Increased biogas production from wheat straw by chemical pretreatments. Renew. Energy 119, 608–614. https://doi.org/10.1016/j.renene.2017.12.045

Mancini, G., Papirio, S., Lens, P.N.L., Esposito, G., 2018b. Anaerobic Digestion of

Lignocellulosic Materials Using Ethanol-Organosolv Pretreatment. Environ. Eng. Sci. 35, 953–960. https://doi.org/10.1089/ees.2018.0042

Mancini, G., Papirio, S., Lens, P.N.L., Esposito, G., 2016a. Solvent Pretreatments of Lignocellulosic Materials to Enhance Biogas Production: A Review. Energy and Fuels 30, 1892–1903. https://doi.org/10.1021/acs.energyfuels.5b02711

Mancini, G., Papirio, S., Lens, P.N.L., Esposito, G., 2016b. Effect of N-methylmorpholine-N-oxide Pretreatment on Biogas Production from Rice Straw, Cocoa Shell, and Hazelnut Skin. Environ. Eng. Sci. 33, 843–850. https://doi.org/10.1089/ees.2016.0138

Mancini, G., Papirio, S., Riccardelli, G., Lens, P.N.L., Esposito, G., 2018c. Trace elements dosing and alkaline pretreatment in the anaerobic digestion of rice straw. Bioresour. Technol. 247, 897–903. https://doi.org/10.1016/j.biortech.2017.10.001

Martín, C., Wu, G., Wang, Z., Stagge, S., Jönsson, L.J., 2018. Formation of microbial inhibitors in steam-explosion pretreatment of softwood impregnated with sulfuric acid and sulfur dioxide. Bioresour. Technol. 262, 242–250. https://doi.org/10.1016/j.biortech.2018.04.074

Martins, F., Felgueiras, C., Smitkova, M., Caetano, N., 2019. Analysis of fossil fuel energy consumption and environmental impacts in european countries. Energies 12, 1–11. https://doi.org/10.3390/en12060964

Matsakas, L., Sarkar, O., Jansson, S., Rova, U., Christakopoulos, P., 2020. A novel hybrid organosolv-steam explosion pretreatment and fractionation method delivers solids with superior thermophilic digestibility to methane. Bioresour. Technol. 316, 1–10. https://doi.org/10.1016/j.biortech.2020.123973

Matthews, J.F., Himmel, M.E., Crowley, M.F., 2012. Conversion of cellulose Iα to Iβ via a high temperature intermediate (I-HT) and other cellulose phase transformations. Cellulose 19, 297–306. https://doi.org/10.1007/s10570-011-9608-x

Mattonai, M., Pawcenis, D., del Seppia, S., Łojewska, J., Ribechini, E., 2018. Effect of ball-milling on crystallinity index, degree of polymerization and thermal stability of cellulose. Bioresour. Technol. 270, 270–277. https://doi.org/10.1016/j.biortech.2018.09.029

Meng, X., Bhagia, S., Wang, Y., Zhou, Y., Pu, Y., Dunlap, J.R., Shuai, L., Ragauskas, A.J., Yoo, C.G., 2020. Effects of the advanced organosolv pretreatment strategies on structural properties of woody biomass. Ind. Crops Prod. 146, 112144. https://doi.org/10.1016/j.indcrop.2020.112144

Meng, X., Ragauskas, A.J., 2014. Recent advances in understanding the role of cellulose

accessibility in enzymatic hydrolysis of lignocellulosic substrates. Curr. Opin. Biotechnol. 27, 150–158. https://doi.org/10.1016/j.copbio.2014.01.014

Millati, R., Wikandari, R., Ariyanto, T., Putri, R.U., Taherzadeh, M.J., 2020. Pretreatment technologies for anaerobic digestion of lignocelluloses and toxic feedstocks. Bioresour. Technol. 304, 122998. https://doi.org/10.1016/j.biortech.2020.122998

Miller, D.L., Smith, N.B., Bailey, M.R., Czarnota, G.J., Hynynen, K., Makin, I.R.S., 2012. Overview of therapeutic ultrasound applications and safety considerations. J. Ultrasound Med. 31, 623–634. https://doi.org/10.7863/jum.2012.31.4.623

Mirmohamadsadeghi, S., Karimi, K., Zamani, A., Amiri, H., Horváth, I.S., 2014. Enhanced solid-state biogas production from lignocellulosic biomass by organosolv pretreatment. Biomed Res. Int. 2014. https://doi.org/10.1155/2014/350414

Mussatto, S.I., Carneiro, L.M., Silva, J.P.A., Roberto, I.C., Teixeira, J.A., 2011. A study on chemical constituents and sugars extraction from spent coffee grounds. Carbohydr. Polym. 83, 368–374. https://doi.org/10.1016/j.carbpol.2010.07.063

Mussatto, S.I., Fernandes, M., Roberto, I.C., 2007. Lignin recovery from brewer's spent grain black liquor. Carbohydr. Polym. 70, 218–223. https://doi.org/10.1016/j.carbpol.2007.03.021

Na, S., Kim, Y.U., Khim, J., 2007. Physiochemical properties of digested sewage sludge with ultrasonic treatment. Ultrason. Sonochem. 14, 281–285. https://doi.org/10.1016/j.ultsonch.2006.06.004

Nadir, N., Ismail, N.L., Hussain, A.S., 2019. Fungal pretreatment of lignocellulosic biomass, in: Biomass for Bioenergy-Recent Trends and Future Challenges. IntechOpen, pp. 39–57. https://doi.org/10.5772/intechopen.84239

Nagarajan, S., Skillen, N.C., Irvine, J.T.S., Lawton, L.A., Robertson, P.K.J., 2017. Cellulose II as bioethanol feedstock and its advantages over native cellulose. Renew. Sustain. Energy Rev. 77, 182–192. https://doi.org/10.1016/j.rser.2017.03.118

Nakashima, K., Ebi, Y., Kubo, M., Shibasaki-Kitakawa, N., Yonemoto, T., 2016. Pretreatment combining ultrasound and sodium percarbonate under mild conditions for efficient degradation of corn stover. Ultrason. Sonochem. 29, 455–460. https://doi.org/10.1016/j.ultsonch.2015.10.017

Nelson, M.L., O'Connor, R.T., 1964a. Relation of certain infrared bands to cellulose crystallinity and crystal lattice type. Part I. Spectra of lattice types I, II, III and of amorphous cellulose. J. Appl. Polym. Sci. 8, 1311–1324.

https://doi.org/10.1002/app.1964.070080322

Nelson, M.L., O'Connor, R.T., 1964b. Relation of certain infrared bands to cellulose crystallinity and crystal lattice type. Part II. A new infrared ratio for estimation of crystallinity in celluloses I and II. J. Appl. Polym. Sci. 8, 1325–1341. https://doi.org/10.1002/app.1964.070080323

Nishiyama, Y., 2009. Structure and properties of the cellulose microfibril. J. Wood Sci. 55, 241–249. https://doi.org/10.1007/s10086-009-1029-1

Oh, W. Da, Lisak, G., Webster, R.D., Liang, Y.N., Veksha, A., Giannis, A., Moo, J.G.S., Lim, J.W., Lim, T.T., 2018. Insights into the thermolytic transformation of lignocellulosic biomass waste to redox-active carbocatalyst: Durability of surface active sites. Appl. Catal. B Environ. 233, 120–129. https://doi.org/10.1016/j.apcatb.2018.03.106

Oliva, A., Tan, L.C., Papirio, S., Esposito, G., Lens, P.N.L., 2021. Effect of methanol-organosolv pretreatment on anaerobic digestion of lignocellulosic materials. Renew. Energy 169, 1000–1012. https://doi.org/10.1016/j.renene.2020.12.095

Ostovareh, S., Karimi, K., Zamani, A., 2015. Efficient conversion of sweet sorghum stalks to biogas and ethanol using organosolv pretreatment. Ind. Crops Prod. 66, 170–177. https://doi.org/10.1016/j.indcrop.2014.12.023

Papirio, S., 2020. Coupling acid pretreatment and dosing of Ni and Se enhances the biomethane potential of hazelnut skin. J. Clean. Prod. 262, 121407. https://doi.org/10.1016/j.jclepro.2020.121407

Passos, F., Carretero, J., Ferrer, I., 2015. Comparing pretreatment methods for improving microalgae anaerobic digestion: Thermal, hydrothermal, microwave and ultrasound. Chem. Eng. J. 279, 667–672. https://doi.org/10.1016/j.cej.2015.05.065

Perrone, O.M., Colombari, F.M., Rossi, J.S., Moretti, M.M.S., Bordignon, S.E., Nunes, C. da C.C., Gomes, E., Boscolo, M., Da-Silva, R., 2016. Ozonolysis combined with ultrasound as a pretreatment of sugarcane bagasse: Effect on the enzymatic saccharification and the physical and chemical characteristics of the substrate. Bioresour. Technol. 218, 69–76. https://doi.org/10.1016/j.biortech.2016.06.072

Ponnusamy, V.K., Nguyen, D.D., Dharmaraja, J., Shobana, S., Banu, J.R., Saratale, R.G., Chang, S.W., Kumar, G., 2019. A review on lignin structure, pretreatments, fermentation reactions and biorefinery potential. Bioresour. Technol. 271, 462–472. https://doi.org/10.1016/j.biortech.2018.09.070

Purwandari, F.A., Sanjaya, A.P., Millati, R., Cahyanto, M.N., Horváth, I.S., Niklasson, C.,

Taherzadeh, M.J., 2013. Pretreatment of oil palm empty fruit bunch (OPEFB) by N-methylmorpholine-N-oxide (NMMO) for biogas production: Structural changes and digestion improvement. Bioresour. Technol. 128, 461–466. https://doi.org/10.1016/j.biortech.2012.10.088

Qazi, A., Hussain, F., Rahim, N.A.B.D., Hardaker, G., Alghazzawi, D., Shaban, K., Haruna, K., 2019. Towards Sustainable Energy: A Systematic Review of Renewable Energy Sources, Technologies, and Public Opinions. IEEE Access 7, 63837–63851. https://doi.org/10.1109/ACCESS.2019.2906402

Qi, N., Zhao, X., Zhang, L., Gao, M., Yu, N., Liu, Y., 2021. Performance assessment on anaerobic co-digestion of Cannabis ruderalis and blackwater: Ultrasonic pretreatment and kinetic analysis. Resour. Conserv. Recycl. 169, 105506. https://doi.org/10.1016/j.resconrec.2021.105506

Qiao, W., Yan, X., Ye, J., Sun, Y., Wang, W., Zhang, Z., 2011. Evaluation of biogas production from different biomass wastes with/without hydrothermal pretreatment. Renew. Energy 36, 3313–3318. https://doi.org/10.1016/j.renene.2011.05.002

Rajan, K., Carrier, D.J., 2014. Effect of dilute acid pretreatment conditions and washing on the production of inhibitors and on recovery of sugars during wheat straw enzymatic hydrolysis. Biomass and Bioenergy 62, 222–227. https://doi.org/10.1016/j.biombioe.2014.01.013

Ralph, J., Lapierre, C., Boerjan, W., 2019. Lignin structure and its engineering. Curr. Opin. Biotechnol. 56, 240–249. https://doi.org/10.1016/j.copbio.2019.02.019

Ramadoss, G., Muthukumar, K., 2014. Ultrasound assisted ammonia pretreatment of sugarcane bagasse for fermentable sugar production. Biochem. Eng. J. 83, 33–41. https://doi.org/10.1016/j.bej.2013.11.013

Ravindran, R., Jaiswal, A.K., 2016. A comprehensive review on pre-treatment strategy for lignocellulosic food industry waste: Challenges and opportunities. Bioresour. Technol. 199, 92–102. https://doi.org/10.1016/j.biortech.2015.07.106

Ravindran, R., Jaiswal, S., Abu-Ghannam, N., Jaiswal, A.K., 2018. A comparative analysis of pretreatment strategies on the properties and hydrolysis of brewers' spent grain. Bioresour. Technol. 248, 272–279. https://doi.org/10.1016/j.biortech.2017.06.039

Reddy, N., Yang, Y., 2005. Biofibers from agricultural byproducts for industrial applications. Trends Biotechnol. 23, 22–27. https://doi.org/10.1016/j.tibtech.2004.11.002

Rego, F., Soares Dias, A.P., Casquilho, M., Rosa, F.C., Rodrigues, A., 2019. Fast determination

of lignocellulosic composition of poplar biomass by thermogravimetry, in: Biomass and Bioenergy. Elsevier Ltd, pp. 375–380. https://doi.org/10.1016/j.biombioe.2019.01.037

Rehman, M.S.U., Kim, I., Chisti, Y., Han, J.I., 2013. Use of ultrasound in the production of bioethanol from lignocellulosic biomass. Energy Educ. Sci. Technol. Part A Energy Sci. Res. 30, 1391–1410.

Ruiz, H.A., Conrad, M., Sun, S.N., Sanchez, A., Rocha, G.J.M., Romaní, A., Castro, E., Torres, A., Rodríguez-Jasso, R.M., Andrade, L.P., Smirnova, I., Sun, R.C., Meyer, A.S., 2020. Engineering aspects of hydrothermal pretreatment: From batch to continuous operation, scale-up and pilot reactor under biorefinery concept. Bioresour. Technol. 299, 1–16. https://doi.org/10.1016/j.biortech.2019.122685

Santos, H.M., Lodeiro, C., Capelo-Martínez, J.L., 2009. The Power of Ultrasound, in: Ultrasound in Chemistry: Analytical Applications. pp. 1–16. https://doi.org/10.1002/9783527623501.ch1

Sari, F.P., Budiyono, B., 2014. Enhanced biogas production from rice straw with various pretreatment : a review. Waste Technol. 2, 17–25. https://doi.org/10.12777/wastech.2.1.17-25

Satari, B., Karimi, K., Kumar, R., 2019. Cellulose solvent-based pretreatment for enhanced second-generation biofuel production: A review, Sustainable Energy and Fuels. Royal Society of Chemistry. https://doi.org/10.1039/c8se00287h

Sayyed, A.J., Deshmukh, N.A., Pinjari, D. V., 2019. A critical review of manufacturing processes used in regenerated cellulosic fibres: viscose, cellulose acetate, cuprammonium, LiCl/DMAc, ionic liquids, and NMMO based lyocell. Cellulose 26, 2913–2940. https://doi.org/10.1007/s10570-019-02318-y

Sen, S., Ganguly, S., 2017. Opportunities, barriers and issues with renewable energy development – A discussion. Renew. Sustain. Energy Rev. 69, 1170–1181. https://doi.org/10.1016/j.rser.2016.09.137

Şenol, H., 2021. Effects of NaOH, thermal, and combined NaOH-thermal pretreatments on the biomethane yields from the anaerobic digestion of walnut shells. Environ. Sci. Pollut. Res. https://doi.org/10.1007/s11356-020-11984-6

Shafiei, M., Karimi, K., Taherzadeh, M.J., 2011. Techno-economical study of ethanol and biogas from spruce wood by NMMO-pretreatment and rapid fermentation and digestion. Bioresour. Technol. 102, 7879–7886. https://doi.org/10.1016/j.biortech.2011.05.071

Shafiei, M., Karimi, K., Zilouei, H., Taherzadeh, M.J., 2014. Enhanced ethanol and biogas

production from pinewood by NMMO pretreatment and detailed biomass analysis. Biomed Res. Int. 2014. https://doi.org/10.1155/2014/469378

Shen, J., Yan, H., Zhang, R., Liu, G., Chen, C., 2018. Characterization and methane production of different nut residue wastes in anaerobic digestion. Renew. Energy 116, 835–841. https://doi.org/10.1016/j.renene.2017.09.018

Singh, A., Agrawal, M., 2008. Acid rain and its ecological consequences. J. Environ. Biol. 29, 15–24.

Singh, J., Suhag, M., Dhaka, A., 2015. Augmented digestion of lignocellulose by steam explosion, acid and alkaline pretreatment methods: A review. Carbohydr. Polym. 117, 624–631. https://doi.org/10.1016/j.carbpol.2014.10.012

Singhvi, M.S., Gokhale, D. V., 2019. Lignocellulosic biomass: Hurdles and challenges in its valorization. Appl. Microbiol. Biotechnol. 103, 9305–9320. https://doi.org/10.1007/s00253-019-10212-7

Siqueira, G., Arantes, V., Saddler, J.N., Ferraz, A., Milagres, A.M.F., 2017. Limitation of cellulose accessibility and unproductive binding of cellulases by pretreated sugarcane bagasse lignin. Biotechnol. Biofuels 10, 1–12. https://doi.org/10.1186/s13068-017-0860-7

Sluiter, A., Hames, B., Ruiz, R., Scarlata, C., Sluiter, J., Templeton, D., Crocker, D., 2008. Determination of Structural Carbohydrates and Lignin in Biomass. Natl. Renew. Energy Lab. Tech. Rep. NREL/ TP -510 -42618.

Solarte-Toro, J.C., Romero-García, J.M., Martínez-Patiño, J.C., Ruiz-Ramos, E., Castro-Galiano, E., Cardona-Alzate, C.A., 2019. Acid pretreatment of lignocellulosic biomass for energy vectors production: A review focused on operational conditions and techno-economic assessment for bioethanol production. Renew. Sustain. Energy Rev. 107, 587–601. https://doi.org/10.1016/j.rser.2019.02.024

Sołowski, G., Konkol, I., Cenian, A., 2020. Production of hydrogen and methane from lignocellulose waste by fermentation. A review of chemical pretreatment for enhancing the efficiency of the digestion process. J. Clean. Prod. 267. https://doi.org/10.1016/j.jclepro.2020.121721

Stockinger, H., Kut, O.M., Heinzle, E., 1996. Ozonation of wastewater containing N-methylmorpholine-N-oxide. Water Res. 30, 1745–1748. https://doi.org/10.1016/0043-1354(95)00320-7

Su, J., Qiu, M., Shen, F., Qi, X., 2018. Efficient hydrolysis of cellulose to glucose in water by

agricultural residue-derived solid acid catalyst. Cellulose 25, 17–22. https://doi.org/10.1007/s10570-017-1603-4

Subhedar, P.B., Gogate, P.R., 2014. Alkaline and ultrasound assisted alkaline pretreatment for intensification of delignification process from sustainable raw-material. Ultrason. Sonochem. 21, 216–225. https://doi.org/10.1016/j.ultsonch.2013.08.001

Suslick, K.S., 1999. Application of ultrasound to materials chemistry. Annu. Rev. Mater. Sci. 29, 295–326. https://doi.org/10.1146/annurev.matsci.29.1.295

Taherzadeh, M.J., Karimi, K., 2008. Pretreatment of lignocellulosic wastes to improve ethanol and biogas production: A review. Int. J. Mol. Sci. 9, 1621–1651. https://doi.org/10.3390/ijms9091621

Tajmirriahi, M., Karimi, K., Kumar, R., 2021a. Effects of pinewood extractives on bioconversion of pinewood. Fuel 283, 119302. https://doi.org/10.1016/j.fuel.2020.119302

Tajmirriahi, M., Momayez, F., Karimi, K., 2021b. The critical impact of rice straw extractives on biogas and bioethanol production. Bioresour. Technol. 319, 124167. https://doi.org/10.1016/j.biortech.2020.124167

Tang, P.L., Abdul, P.M., Engliman, N.S., Hassan, O., 2018. Effects of pretreatment and enzyme cocktail composition on the sugars production from oil palm empty fruit bunch fiber (OPEFBF). Cellulose 25, 4677–4694. https://doi.org/10.1007/s10570-018-1894-0

Teghammar, A., Karimi, K., Sárvári Horváth, I., Taherzadeh, M.J., 2012. Enhanced biogas production from rice straw, triticale straw and softwood spruce by NMMO pretreatment. Biomass and Bioenergy 36, 116–120. https://doi.org/10.1016/j.biombioe.2011.10.019

Tongbuekeaw, T., Sawangkeaw, R., Chaiprapat, S., Charnnok, B., 2020. Conversion of rubber wood waste to methane by ethanol organosolv pretreatment. Biomass Convers. Biorefinery. https://doi.org/10.1007/s13399-020-00710-4

Tu, W.C., Hallett, J.P., 2019. Recent advances in the pretreatment of lignocellulosic biomass. Curr. Opin. Green Sustain. Chem. 20, 11–17. https://doi.org/10.1016/j.cogsc.2019.07.004

Vasco-Correa, J., Khanal, S., Manandhar, A., Shah, A., 2018. Anaerobic digestion for bioenergy production: Global status, environmental and techno-economic implications, and government policies. Bioresour. Technol. 247, 1015–1026. https://doi.org/10.1016/j.biortech.2017.09.004

Velmurugan, R., Incharoensakdi, A., 2016. Proper ultrasound treatment increases ethanol production from simultaneous saccharification and fermentation of sugarcane bagasse. RSC Adv. 6, 91409–91419. https://doi.org/10.1039/c6ra17792a

Wada, M., Nishiyama, Y., Langan, P., 2006. X-ray structure of ammonia-cellulose I: New insights into the conversion of cellulose i to cellulose III i. Macromolecules 39, 2947–2952. https://doi.org/10.1021/ma060228s

Wang, Q.Q., He, Z., Zhu, Z., Zhang, Y.H.P., Ni, Y., Luo, X.L., Zhu, J.Y., 2012. Evaluations of cellulose accessibilities of lignocelluloses by solute exclusion and protein adsorption techniques. Biotechnol. Bioeng. 109, 381–389. https://doi.org/10.1002/bit.23330

Wen, B., Yuan, X., Li, Q.X., Liu, J., Ren, J., Wang, X., Cui, Z., 2015. Comparison and evaluation of concurrent saccharification and anaerobic digestion of Napier grass after pretreatment by three microbial consortia. Bioresour. Technol. 175, 102–111. https://doi.org/10.1016/j.biortech.2014.10.043

Wikandari, R., Millati, R., Taherzadeh, M.J., 2016. Pretreatment of Lignocelluloses With Solvent N-Methylmorpholine N-oxide, in: Biomass Fractionation Technologies for a Lignocellulosic Feedstock Based Biorefinery. Elsevier Inc., pp. 255–280. https://doi.org/10.1016/B978-0-12-802323-5.00012-8

Xu, N., Liu, S., Xin, F., Zhou, J., Jia, H., Xu, J., Jiang, M., Dong, W., 2019. Biomethane production from lignocellulose: Biomass recalcitrance and its impacts on anaerobic digestion. Front. Bioeng. Biotechnol. 7, 1–12. https://doi.org/10.3389/fbioe.2019.00191

Xu, N., Zhang, W., Ren, S., Liu, F., Zhao, C., Liao, H., Xu, Z., Huang, J., Li, Q., Tu, Y., Yu, B., Wang, Y., Jiang, J., Qin, J., Peng, L., 2012. Hemicelluloses negatively affect lignocellulose crystallinity for high biomass digestibility under NaOH and $H_2SO_4$ pretreatments in *Miscanthus*. Biotechnol. Biofuels 5, 1–12. https://doi.org/10.1186/1754-6834-5-58

Yang, B., Tao, L., Wyman, C.E., 2018. Strengths, challenges, and opportunities for hydrothermal pretreatment in lignocellulosic biorefi neries. Biofuels, Bioprod. Biorefining 1, 125–138. https://doi.org/10.1002/bbb.1825

Yang, X., Li, Y., Li, S., Oladejo, A.O., Ruan, S., Wang, Y., Huang, S., Ma, H., 2017. Effects of ultrasound pretreatment with different frequencies and working modes on the enzymolysis and the structure characterization of rice protein. Ultrason. Sonochem. 38, 19–28. https://doi.org/10.1016/j.ultsonch.2017.02.026

Yao, Y., Bergeron, A.D., Davaritouchaee, M., 2018. Methane recovery from anaerobic digestion of urea-pretreated wheat straw. Renew. Energy 115, 139–148. https://doi.org/10.1016/j.renene.2017.08.038

Zhang, C., Su, H., Baeyens, J., Tan, T., 2014. Reviewing the anaerobic digestion of food waste

for biogas production. Renew. Sustain. Energy Rev. 38, 383–392. https://doi.org/10.1016/j.rser.2014.05.038

Zhang, Q., Tang, L., Zhang, J., Mao, Z., Jiang, L., 2011. Optimization of thermal-dilute sulfuric acid pretreatment for enhancement of methane production from cassava residues. Bioresour. Technol. 102, 3958–3965. https://doi.org/10.1016/j.biortech.2010.12.031

Zhang, Y., He, H., Liu, Y., Wang, Y., Huo, F., Fan, M., Adidharma, H., Li, X., Zhang, S., 2019. Recent progress in theoretical and computational studies on the utilization of lignocellulosic materials. Green Chem. 21, 9–35. https://doi.org/10.1039/c8gc02059k

Zhang, Y.H.P., 2008. Reviving the carbohydrate economy via multi-product lignocellulose biorefineries. J. Ind. Microbiol. Biotechnol. 35, 367–375. https://doi.org/10.1007/s10295-007-0293-6

Zheng, J., Rehmann, L., 2014. Extrusion pretreatment of lignocellulosic biomass: A review. Int. J. Mol. Sci. 15, 18967–18984. https://doi.org/10.3390/ijms151018967

Zhong, C., Wang, C., Wang, F., Jia, H., Wei, P., Zhao, Y., 2016. Enhanced biogas production from wheat straw with the application of synergistic microbial consortium pretreatment. RSC Adv. 6, 60187–60195. https://doi.org/10.1039/c5ra27393e

Zhou, Z., Lei, F., Li, P., Jiang, J., 2018. Lignocellulosic biomass to biofuels and biochemicals: A comprehensive review with a focus on ethanol organosolv pretreatment technology. Biotechnol. Bioeng. 115, 2683–2702. https://doi.org/10.1002/bit.26788

Zieliński, M., Kisielewska, M., Dudek, M., Rusanowska, P., Nowicka, A., Krzemieniewski, M., Kazimierowicz, J., Dębowski, M., 2019. Comparison of microwave thermohydrolysis and liquid hot water pretreatment of energy crop *Sida hermaphrodita* for enhanced methane production. Biomass and Bioenergy 128, 0–10. https://doi.org/10.1016/j.biombioe.2019.105324

Zoghlami, A., Paës, G., 2019. Lignocellulosic Biomass: Understanding Recalcitrance and Predicting Hydrolysis. Front. Chem. 7, 874. https://doi.org/10.3389/fchem.2019.00874

Zou, S., Wang, H., Wang, X., Zhou, S., Li, X., Feng, Y., 2016a. Application of experimental design techniques in the optimization of the ultrasonic pretreatment time and enhancement of methane production in anaerobic co-digestion. Appl. Energy 179, 191–202. https://doi.org/10.1016/j.apenergy.2016.06.120

Zou, S., Wang, X., Chen, Y., Wan, H., Feng, Y., 2016b. Enhancement of biogas production in anaerobic co-digestion by ultrasonic pretreatment. Energy Convers. Manag. 112, 226–235. https://doi.org/10.1016/j.enconman.2015.12.087

*Chapter 3*

# Effect of methanol-organosolv pretreatment on anaerobic digestion of lignocellulosic materials

A modified version of this chapter has been published as:

Oliva A., Tan L.C., Papirio S., Esposito G., Lens P.N.L., 2021. Effect of methanol-organosolv pretreatment on anaerobic digestion of lignocellulosic materials, Renewable Energy, Volume 169, Pages 1000–1012. https://doi.org/10.1016/j.renene.2020.12.095.

**Abstract**

Lignocellulosic materials are the most abundant biomass on the planet, representing a great opportunity for energy valorisation. This work investigated the effect of methanol-organosolv pretreatment on the methane production from hazelnut skin (HS), spent coffee grounds (SCG), and almond shell (AS). The pretreatment on the three lignocellulosic materials was performed at 130, 160, and 200 °C for 60 min using a 50% (*v/v*) methanol solution, with and without the addition of sulfuric acid as a catalyst. The biochemical methane potential of raw and pretreated substrates was evaluated under wet-mesophilic conditions in batch reactors, achieving 17.3 (± 32.3), 293.4 (± 46.6), and 23.2 (± 9.6) mL $CH_4$/g VS for HS, SCG, and AS, respectively. The methanol-organosolv pretreatment was particularly effective on HS, increasing its methane production potential up to 310.6 (± 22.2) $CH_4$/g VS. On the contrary, all pretreatment conditions were ineffective on SCG and AS in terms of cumulative methane production. Among the three substrates, only HS showed significant composition changes due to the pretreatment, with the lignin content decreasing from 39.66 to 34.73% and the amount of bioavailable sugars increasing. An energy assessment confirmed the pretreatment efficacy on HS, with a maximum net positive energy recovery of 1.35 kWh/kg VS.

## 3.1 Introduction

Lignocellulosic materials (LMs) are the most abundant bioresources on the planet, with approximately 200 billion tons of plant biomass produced every year and 5 - 10% of the primary biomass still accessible for biorefinery applications after the primary use (Reddy and Yang, 2005; Saini et al., 2015). The use of LMs for biofuel production does not compete with food production, since LMs are treated as wastes from agricultural, municipal, or industrial activities and generally have a low cost (Galbe and Zacchi, 2012).

The energy valorisation of LMs represents a great opportunity for the transition from a fossil fuel-based economy to a sustainable carbon-neutral bioeconomy, with anaerobic digestion (AD) being one of the most well-established technologies (Paul and Dutta, 2018). AD is an alternative to landfilling and combustion, with the advantages of avoiding uncontrolled emissions and producing methane ($CH_4$) which, once combusted, generates a lower amount of carbon dioxide ($CO_2$) per unit of energy compared to other fossil fuels and few other atmospheric pollutants. The World Bioenergy Association reported a domestic supply of biogas of approximately 1.33 EJ, with Europe accounting for half of the global supply (World Bioenergy Association, 2019). The energy content of biogas, described by the lower calorific value, ranges from 20 to 36 $MJ/Nm^3$ biogas depending on the methane content (Angelidaki et al., 2018; Chynoweth et al., 2001).

The use of LMs for AD is, nevertheless, still limited due to their complex and resistant structure, which mainly consists of cellulose, hemicellulose, lignin, and other non-structural components, called extractives (Sawatdeenarunat et al., 2015). The main reason for biomass recalcitrance seems to be the low accessibility of cellulose fibers, caused by the presence of lignin and hemicellulose, which prevents cellulase enzymes from reaching and attacking cellulose (Vats et al., 2020).

Pretreatments can be used to increase the hydrolysis of LMs and improve the accessibility to cellulose. The most commonly used classification categorizes the different pretreatments into physical, chemical, physico-chemical, and biological (Zheng et al., 2014). Chemical pretreatments improve the biodegradability of cellulose by removing lignin and, where appropriate, hemicelluloses, increasing the accessible surface area, and reducing the degree of polymerization and crystallinity of the cellulosic biomass components. The chemical agents can be classified into four main categories: acids, alkali, organic solvent, and salts (Amin et al., 2017).

Organosolv pretreatment has been reported as one of the most efficient methods for lignin removal. In this pretreatment, the LMs are mixed with an aqueous organic solvent, and heated to dissolve the lignin and part of the hemicellulose, leaving the cellulose in the solid phase. The process temperature usually ranges from 120 to 200 °C, depending on the type of biomass, catalyst, and solvent. The duration varies between 0.5 and 3.0 hours (Zhang et al., 2016). The organosolv pretreatment is well suited to be integrated into a biorefinery concept, combining the advantages of an easy solvent recycling and the recovery of a highly pure lignin fraction (Ferreira and Taherzadeh, 2020; Gunasekaran et al., 2020). Several authors studied the effect of ethanol-organosolv pretreatment for ethanol and biogas production, as well as recovery of sugars and other valuable compounds (Choi et al., 2019; Jiang et al., 2019; Kim et al., 2018; Sulbarán-Rangel et al., 2020). Nevertheless, only a few studies investigated the use of other alternative solvents such as methanol, acetone, and butanol, which can result in a more efficient lignin removal and subsequent a higher methane production (Katsimpouras et al., 2018; Salapa et al., 2017; Yuan et al., 2018). Methanol is considered an environmentally friendly solvent due to a low accumulation capacity in soils in case of accidental losses, and a high biodegradability under both aerobic and anaerobic conditions (Medina et al., 2017).

This study aims to investigate the effects of organosolv pretreatment on the methane yield obtained from the AD of three LMs materials, namely hazelnut skin, spent coffee grounds, and almond shell. In addition to this, the changes in lignocellulosic composition and physical structure were also studied. The organosolv pretreatment was carried out using methanol as the organic solvent at a 50% (*v/v*) water-methanol solution, with and without catalyst (sulfuric acid) addition. The pretreatment was conducted at 130, 160, and 200 °C for 1 hour. The experimental methane production results were validated by fitting them with a modified Gompertz model. An energy balance was performed to assess the feasibility of the organosolv pretreatment.

## 3.2 Materials and methods

### *3.2.1 Raw materials*

Three raw materials were used as substrates: hazelnut skin (HS), spent coffee grounds (SCG), and almond shell (AS). The HS came from the industrial roasting of imported Turkish hazelnuts performed by a local food farming company in the Campania region (Italy). SCG were directly collected from a coffee bar in Galway (Ireland). The initial moisture content of SCG was 63.2 (± 0.3) wt%. Due to the high water content and to prevent spoilage due to microbial formation during storage, the SCG was dehydrated at 60 °C for about 48 h before use (Pellera and

Gidarakos, 2018). Almonds were commercially purchased from a local market in the Lazio region (Italy), crushed manually, and separated from the edible kernel to obtain the AS. Both HS and AS were cut down and sieved to screen for a particle size ranging from 1.0 and 2.5 mm. The raw materials were stored at 4 °C when not used. The concentration of total (TS) and volatile (VS) solids of the raw materials, as well as the thermal ultimate analyses, i.e. carbon (C), hydrogen (H), nitrogen (N), sulfur (S), and oxigen (O) content, of the raw LMs, is reported in Table 3.1.

**Table 3.1 –** TS and VS concentration, as well as the ultimate analyses of the raw substrates employed in this study.

| | **HS** | **SCG** | **AS** |
|---|---|---|---|
| **TS**[a] (%) | 94.3 ± 0.1 | 68.3 ± 0.2 | 91.1 ± 0.1 |
| **VS**[a] (%) | 91.6 ± 0.1 | 67.0 ± 0.5 | 89.9 ± 0.1 |
| **C**[b] (%) | 59.72 ± 0.04 | 55.08 ± 0.10 | 50.91 ± 0.06 |
| **H**[b] (%) | 6.38 ± 0.04 | 7.09 ± 0.02 | 5.98 ± 0.04 |
| **N**[b] (%) | 0.98 ± 0.01 | 2.41 ± 0.00 | 0.27 ± 0.01 |
| **S**[b] (%) | 0.10 ± 0.00 | 0.12 ± 0.01 | 0.07 ± 0.01 |
| **O**[b]$_{diff}$ (%) | 32.82 ± 0.00 | 35.30 ± 0.12 | 42.76 ± 0.01 |

[a] *TS and VS are based on the wet matter (g/100 g).*

[b] *Content of C, H, N, S, and O is reported on a dry ash-free basis.*

### *3.2.2 Inoculum*

The inoculum used in this study was a granular sludge obtained from a full-scale upflow anaerobic sludge blanket (UASB) digester, operated at ambient temperature for the treatment of dairy wastewater and located in Kilconnell (Ireland). The TS and VS content of the inoculum was 6.0 (± 0.1) and 5.2 (± 0.1)%, respectively. The total and volatile suspended solid concentration of the sludge was reported by Castilla-Archilla et al. (2020), who used the same sludge as an inoculum in their acidogenic experiments. The inoculum was stored at 4 °C while waiting to be used.

### *3.2.3 Organosolv pretreatment*

The organosolv pretreatment was performed on HS, SCG, and AS using a 50% (*v/v*) water-methanol solution as the solvent, with and without the addition of sulfuric acid as the catalyst. As pretreatment temperature, 130, 160 and 200 °C were investigated. The pretreatment duration was 60 min. Table 3.2 summarises the pretreatment conditions applied on the three substrates.

**Table 3.2 –** Methanol (MeOH)-organosolv pretreatment conditions applied on hazelnut skin, spent coffee grounds, and almond shell used as substrates for anaerobic digestion in this study.

| **Pretreatment condition** | **Solvent** | **Catalyst** | **T** (°C) | **t** (min) |
|---|---|---|---|---|
| A | Untreated | - | - | - |
| B | 50% MeOH | none | 130 | 60 |
| C | 50% MeOH | none | 160 | 60 |
| D | 50% MeOH | none | 200 | 60 |
| E | 50% MeOH | 0.01M $H_2SO_4$ | 130 | 60 |
| F | 50% MeOH | 0.01M $H_2SO_4$ | 160 | 60 |
| G | 50% MeOH | 0.01M $H_2SO_4$ | 200 | 60 |

The pretreatment was performed using a high-pressure stainless-steel vessel (Sigma-Aldrich, Germany) with a working volume of 300 mL (Mancini et al., 2018a). First, 20 g (dry weight) of the LMs were mixed with 200 g of 50% (*v/v*) methanol solution, keeping a solid to liquid ratio (S/L) of 1:10 (Ferreira and Taherzadeh, 2020). In the case of catalyst addition, sulfuric acid was added to the solution to obtain a sulfuric acid concentration of 0.1% (*w/v*). The procedure was identically repeated to pretreat all three LMs.

The vessel was then sealed, placed in a convective oven (UN110, Memmert, Germany), and heated to the desired temperature, which was kept for 60 min. After the pretreatment, the vessel was cooled in an ice bath. The pretreated LMs were removed from the vessel, washed with 100 mL fresh 50% (*v/v*) methanol, and rinsed with abundant distilled water until obtaining a clear liquor with neutral pH. The pretreated LMs were dehydrated at 60 °C for about 2 days and stored in plastic bags at 4 °C until use.

*3.2.4 Biochemical methane potential tests*

Batch biochemical methane potential (BMP) tests were carried out under mesophilic (~ 37 °C) conditions in 250 mL serum glass bottles (OCHS, Germany) (Figure 3.1). Temperature was kept using an orbital water bath (OLS26, Grant, UK), which continuously maintained the bottles at 100 rpm. Each bottle was filled with the inoculum and the raw or pretreated LMs. The inoculum to substrate ratio was kept at 1.5 in terms of g VS. Distilled water was added to adjust the final volume to 150 mL in all bottles, leaving 100 mL as headspace volume for the biogas accumulation. The final solid content was 1.8% TS in order to operate AD under wet conditions (Nagao et al., 2012). To ensure anaerobic conditions, each bottle was flushed with nitrogen gas ($N_2$) and then vented to reach atmospheric pressure. Control biochemical tests, containing only inoculum and distilled water, were simultaneously carried out to evaluate the methane production obtained from the inoculum alone. Results are all reported as net cumulative

methane production obtained after subtracting the amount of methane produced with the substrate-free controls. All experiments were performed in triplicate and methane production was recorded for 45 days.

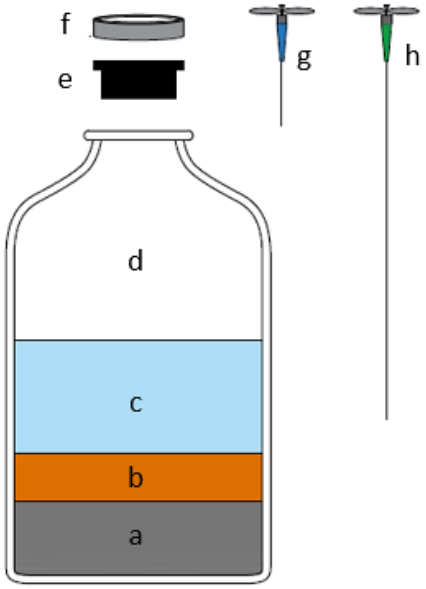


**Figure 3.1 –** Schematic design of 250 mL serum bottles used to perform the biochemical methane potential assays: inoculum (a), substrate (b), distilled water (c), headspace (d), rubber septum (e), aluminium crimp (f), needles equipped with 1-way stopcocks (Masterflex, Germany) for gas (g) and liquid (h) sampling.

### *3.2.5 Analytical methods*

TS and VS of the inoculum, raw and pretreated materials were determined according to Sluiter et al. (2008b, 2008a) by using a convective oven (UN110, Memmert, Germany) incubated overnight at 105 °C and a muffle furnace (BWF 11/13, Carbolite, UK) at 575 °C for 4 hours, respectively.

Water swelling capacity (WSC) or water-holding capacity was evaluated as an indicator of porosity before and after the pretreatment following the protocols described by Jeihanipour et al. (2010). The external surface of raw and pretreated substrates was observed using a scanning electron microscope (SEM) (S2600N, Hitachi, Japan) at an acceleration voltage of 15 kV. All LMs were preliminarily made conductive by gold coating (Yarbrough et al., 2009) with a sputter coater (K550, Emitech, UK).

The ultimate analysis of raw LMs, as well as full characterisation of raw and pretreated LMs, were carried out by Celignis Limited (Limerick, Ireland). The ultimate analysis was done following the procedure outlined in European Standard EN 15104:2011 using an elemental analyser (Vario MACRO cube, Elementar, Germany) to determine the carbon, hydrogen,

nitrogen, and sulfur content of the raw samples, with the oxygen content obtained by subtraction from 100 of the values of the other elements. The full characterisation of raw and pretreated LMs in terms of full extractives, lignocellulosic sugars, lignin, and ash was performed in duplicate according to the procedure described by Sluiter et al. (2008d, 2008c).

Biogas accumulation in the headspace volume was monitored with a pressure-meter (Leo 1, Keller, Switzerland) and calculated as pressure difference using the ideal gas law, according to Li et al. (2018). The gas composition was evaluated with a gas chromatograph (7890B, Agilent, USA), equipped with a thermal conductivity detector (TCD) heated at 250 °C, able to detect $CH_4$, $CO_2$, $N_2$, $O_2$, and $H_2$. Helium was used as the carrier gas with a flow rate of 10 mL/min. The headspace was regularly sampled and then restored at atmospheric pressure.

The volatile fatty acids (VFAs) accumulation during the AD process was monitored by using a high-performance liquid chromatograph (HPLC) (1260 Infinity II, Agilent, USA) equipped with a Hi-Plex H (300x7.7 mm) column, heated at 60 °C and a refractive index detector (RID) set at 55 °C. A 0.005M $H_2SO_4$ solution was used as the mobile phase at a flow rate of 0.7 mL/min. For analysis of VFAs, 2.5 mL of the liquid phase was sampled from each bottle during the first 20 days of the experiment, following the same timing of the gaseous samples. Before being analysed, the samples for VFAs analysis were centrifuged for 10 min at 14,500 rpm and filtered with 0.2µm polyethersulfone membranes (Filtropur S 0.2, Sarstedt, Germany). The pH of liquid samples was measured with a pH meter (300 pH/ORP, Cole Parmer, USA).

### 3.3 Calculations

*3.3.1 Theoretical methane production*

The theoretical BMP of raw substrates was estimated considering their elemental composition (C, H, O, N) according to Pellera and Gidarakos (2016). The following Boswell-Boyle's Eq. (3.1) and Eq. (3.2) describe the stoichiometry of the degradation reaction and the theoretical BMP, respectively:

$$C_aH_bO_cN_dS_e + \left(a - \frac{b}{4} - \frac{c}{2} + \frac{3d}{4} + \frac{e}{2}\right)H_2O \rightarrow \left(\frac{a}{2} + \frac{b}{8} - \frac{c}{4} - \frac{3d}{8} - \frac{e}{4}\right)CH_4 + \left(\frac{a}{2} - \frac{b}{8} + \frac{c}{4} + \frac{3d}{8} + \frac{e}{4}\right)CO_2 + dNH_3 + eH_2S \quad (3.1)$$

$$BMP_{th}\left[\frac{NmL}{g\,VS}\right] = 22.4 \cdot \frac{\left(\frac{a}{2}+\frac{b}{8}-\frac{c}{4}-\frac{3d}{8}-\frac{e}{4}\right)}{12a+b+16c+14d+32e} \cdot 1000 \quad (3.2)$$

The elemental composition enables a fast estimation of the maximum BMP. However, this equation does not consider the presence of non-biodegradable matter, including lignin. It is also based on the assumption of perfect mixing, constant temperature, ideal conditions for the microbial activity, and no ashes accumulation. Despite that the theoretical BMP is never achieved, it gives an estimation of the maximum accessible methane production of a substrate (Codignole Luz et al., 2018; Nielfa et al., 2015).

*3.3.2 Model fitting*

Methane production was modelled by fitting the experimental data with a modified Gompertz model, in two stages, using the Origin2018 software (OriginLab Corporation, USA). The end of the first stage was defined as the last steady-state point observed followed by an exponential increase in methane production, assigned as the start of the second stage. The precision of fitting was evaluated with the Excel 2016 RSQ (Pearson product-moment correlation coefficient) function (Microsoft Corporation, USA).

The Gompertz model, used by several authors (Donoso-Bravo et al., 2010; Li et al., 2011; Pellera and Gidarakos, 2016) to evaluate methane production through AD, is described by Eq. (3.3) and Eq. (3.4), respectively:

$$G_1 = G_{m1} \cdot \exp\left\{-exp\left[\frac{R_{m1} \cdot e}{G_{m1}} \cdot (\lambda_1 - t) + 1\right]\right\} \qquad t < t_b \tag{3.3}$$

$$G_f = G_1 + G_{m2} \cdot \exp\left\{-exp\left[\frac{R_{m2} \cdot e}{G_{m2}} \cdot (\lambda_2 - t) + 1\right]\right\} \quad t > t_b \tag{3.4}$$

where t (d) is time, the independent variable of the model, and $t_b$ (d) is the crossover point between the two stages, observed experimentally. $G_1$ and $G_f$ (mL $CH_4$/g VS) are the cumulative methane productions during the first stage and at the end of the process, respectively. $G_{m1}$ and $G_{m2}$ (mL $CH_4$/g VS) are the maximum methane production yields estimated for the two stages. $R_{m1}$ and $R_{m2}$ (mL $CH_4$/g VS·d) are the maximum methane production rates. $\lambda_1$ and $\lambda_2$ are the lag phases (d).

*3.3.3 Energy balance*

The energy balance of the organosolv pretreatment on HS, SCG, and AS was roughly estimated. The specific energy consumption H (kWh/kg VS) required for the pretreatment was calculated according to Mancini et al. (2016a) using Eq. (3.5):

$$H = \frac{m \cdot C_p \cdot \Delta T}{3600} \tag{3.5}$$

where m (kg) is the mass of aqueous-organic solvent required to treat 1 kg VS of the raw substrate, $C_p$ (2.83 kJ/(kg·°C) (Thermtest Inc., 2017)) is the solvent specific heat capacity, ΔT is the difference between ambient (25 °C) and pretreatment temperature, and 3600 is the conversion factor between kJ and kWh.

The specific energy production $E_P$ (kWh/kg VS) from the methane produced was obtained using Eq. (3.6), as reported by Bianco et al. (2020):

$$E_P = (SMY_{treated} - SMY_{raw}) \cdot \xi \cdot 0.5 \quad (3.6)$$

where $SMY_{treated}$ and $SMY_{raw}$ (kg $CH_4$/kg VS) are the specific methane yields from pretreated and raw substrates, ξ is the lower heating value of methane (13.9 kWh/kg $CH_4$), and 0.5 represents the efficiency of a combined heat and power unit (CHP), equal to 50%. The specific energy recovery $E_R$ was obtained by subtracting H from $E_P$.

*3.3.4 Statistical analysis*

The cumulative methane production data from each substrate under the different pretreatment conditions were compared by one-way analysis of variance (ANOVA) followed by the Tukey post hoc test (Lee and Lee, 2018). The same statistical analysis was performed for the porosity index of raw and pretreated LMs. The correlation between lignin content and cumulative methane production ($r_{lign\text{-}CH4}$) was evaluated using the Pearson product-moment correlation. All analyses were performed with Minitab 17 Statistical Software (Minitab LCC, USA), where a difference marked with a p-value lower than 0.05 was considered statistically significant.

## 3.4 Results

*3.4.1 Methane production and energy balance assessment*

Table 3.3 shows the methane production after 45 days of AD from HS, SCG, and AS. The theoretical BMP calculation showed a maximum achievable methane production of 613.8, 573.0, and 490.0 mL/g VS, respectively for raw HS, SCG, and AS.

The organosolv pretreatment significantly increased the methane production from HS ($p < 0.05$) (Table 3.3) under all the pretreatment conditions (Figure 3.2a-b). The methane yield increased from 17.3 up to 310.6 mL $CH_4$/g VS. The energy balance assessment showed a positive energy gain for the methanol-organosolv pretreated HS, with the net energy production ($E_R$) ranging from 0.08 and 0.75 kWh/kg VS (Table 3.3), depending on the pretreatment condition used. On the other hand, no significant difference ($p > 0.05$) in methane production was observed with the pretreated SCG compared to the raw material (Figure 3.2c-d), with the methane content in

the biogas steadily ranging from 62.7 to 68.8% and the net methane production between 175.8 and 322.9 mL $CH_4$/g VS. All the applied pretreatment conditions on AS were ineffective in terms of increased cumulative methane production (Figure 3.2e-f). Nevertheless, by treating AS at 200 °C without catalyst addition, the methane content in biogas rose from 57.1 to 77.4%.

No significant VFAs accumulation was observed for both raw and pretreated materials (Figure 3.3), with pH always ranging from 6.3 and 7.5 during the AD process.

**Table 3.3 –** Cumulative specific net methane production followed by statistical comparison, methane percentage in biogas, and specific energy recovery (ER) from untreated and methanol-organosolv pretreated LMs after 45 days of anaerobic digestion.

| **Substrate** | **Pretreatment condition**[a] | **Methane production** (mL $CH_4$/g VS) | **Statistical information**[b] | **Methane percentage**[c] (% $CH_4$) | **$E_R$** (kWh/kg VS) |
|---|---|---|---|---|---|
| HS | A | 17.3 ± 32.3 | c | 36.3 | - |
| | B | 259.7 ± 1.5 | ab | 72.4 | 0.49 |
| | C | 253.5 ± 9.8 | b | 72.8 | 0.26 |
| | D | 272.9 ± 1.6 | ab | 72.9 | 0.08 |
| | E | 310.6 ± 22.2 | a | 69.1 | 0.75 |
| | F | 297.9 ± 6.9 | ab | 69.7 | 0.48 |
| | G | 296.9 ± 12.5 | ab | 69.0 | 0.20 |
| SCG | A | 293.4 ± 46.6 | a | 62.7 | - |
| | B | 175.8 ± 28.6 | b | 68.8 | -1.49 |
| | C | 243.2 ± 14.5 | ab | 64.8 | -1.41 |
| | D | 302.4 ± 41.4 | a | 64.2 | -1.46 |
| | E | 273.5 ± 20.9 | a | 62.6 | -1.07 |
| | F | 321.3 ± 43.4 | a | 62.0 | -1.11 |
| | G | 322.9 ± 19.5 | a | 62.1 | -1.48 |
| AS | A | 23.2 ± 9.6 | a | 57.1 | - |
| | B | 8.8 ± 3.9 | bc | 65.1 | -0.80 |
| | C | 3.7 ± 3.4 | c | 55.2 | -1.03 |
| | D | 24.8 ± 2.6 | ab | 77.4 | -1.20 |
| | E | 17.1 ± 3.8 | abc | 56.3 | -0.76 |
| | F | 12.0 ± 1.6 | abc | 48.4 | -0.99 |
| | G | 10.9 ± 5.8 | abc | 48.7 | -0.30 |

[a] *The pretreatment conditions are defined in Table 3.2.*

[b] *The same letter represents no significant differences ($p > 0.05$) with the compared condition.*

[c] *Calculated as cumulative methane to cumulative biogas ratio.*

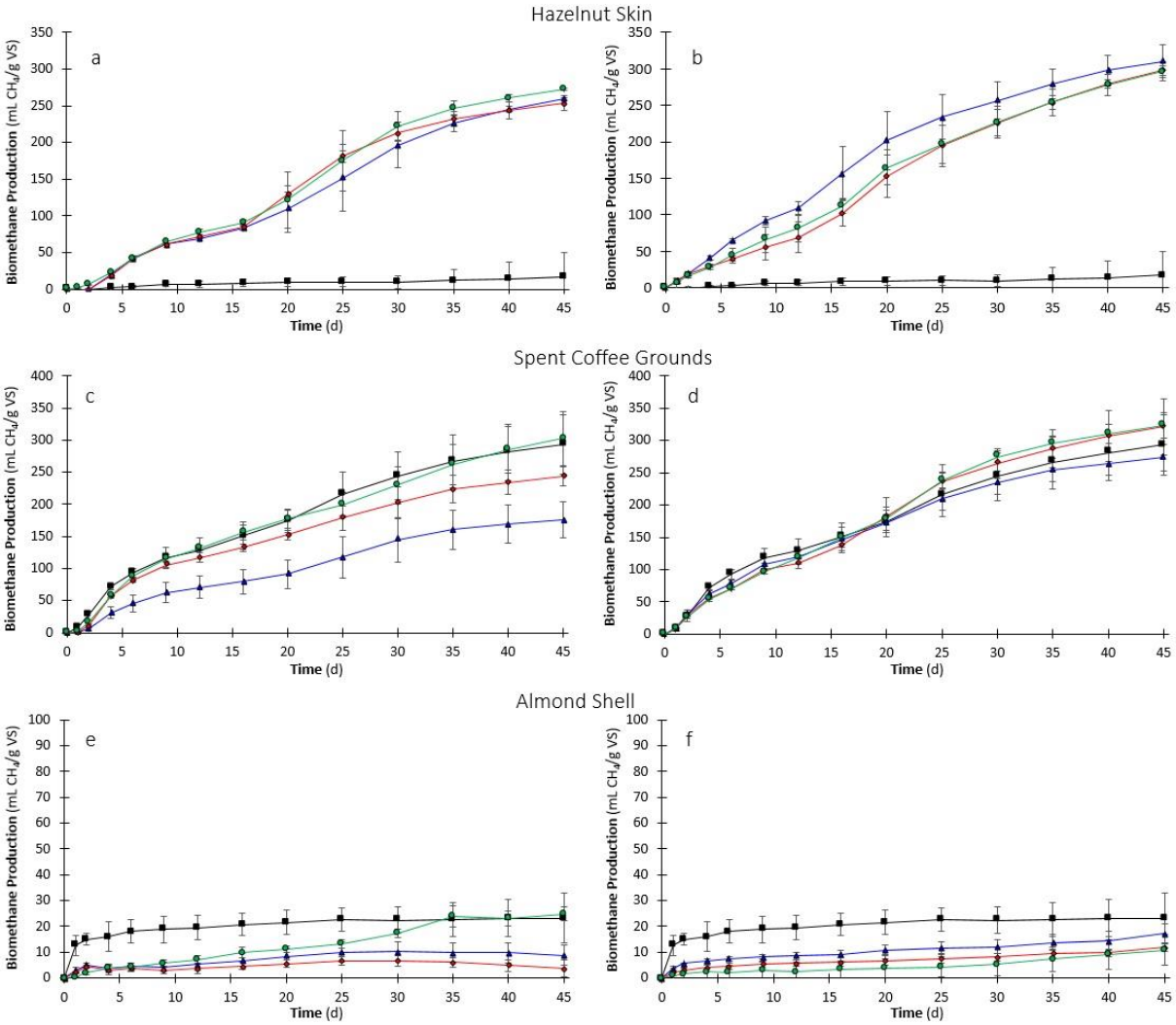


**Figure 3.2 –** Cumulative methane production from AD of HS, SCG and AS: untreated (■); organosolv at 130 °C (▲), 160 °C (◆), and 200 °C (●) without (a, c, e) and with (b, d, f) catalyst addition.

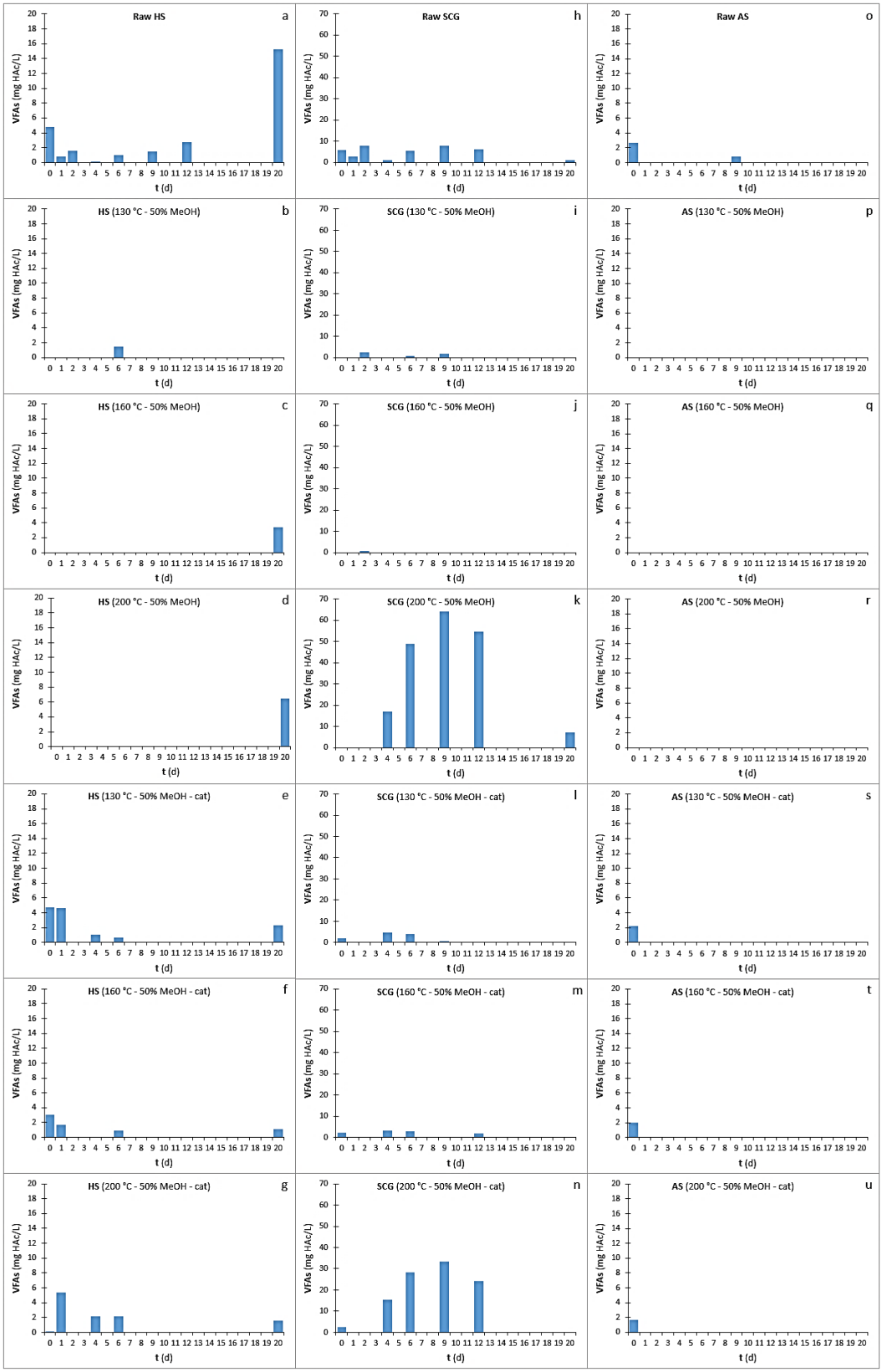


**Figure 3.3 –** VFAs evolution during the AD process. Raw HS (a) and HS treated at 130, 160, and 200 °C without (b, c, d) and with catalyst raw (e, f, g). Raw SCG (h) and SCG treated at 130, 160, and 200 °C without (i, j, k) and with catalyst raw (l, m, o). Raw AS (o) and HS treated at 130, 160, and 200 °C without (p, q, r) and with catalyst raw (s, t, u).

*3.4.2 Effect of pretreatments on the chemical composition of lignocellulosic materials*

The compositional analysis revealed the remarkable recalcitrant nature of the three raw substrates (Table 3.4). The total lignin content was 39.66 (± 0.09), 20.31 (± 0.29), and 30.58 (± 0.13) g/100 g TS, respectively for HS, SCG, and AS. On the other hand, the sugar content and composition were significantly different between the three LMs. Raw HS resulted in a significantly lower sugar content (13.72%), mainly consisting of glucan (10.15%), mostly associated with the total cellulose content (Table 3.4). On the contrary, raw SCG showed a high content of six-carbon hemicellulose sugars, such as mannan (23.14%) and galactan (8.79%), with cellulose being only 8.77% of the dry mass composition (Table 3.4). Lastly, the compositional analysis of raw AS resulted in a more balanced composition between cellulose, hemicellulose, and total lignin, with glucan (23.35%) and xylan (19.74%) being the most abundant sugars (Table 3.4). The lignocellulosic compositional analysis also revealed the presence of extractives, especially in HS and SCG.

Organosolv pretreatment reduced the lignin content of HS by 7 - 12%, with total sugars increasing from 13.72 up to 17.34%. The SCG glucan and mannan content increased to 8.86 - 10.05 and 24.25 - 26.24%, depending on the pretreatment condition, with a maximum lignin reduction of 10%, associated with the highest pretreatment temperature with no catalyst addition. On the other hand, the pretreatment has not reduced the lignin content of AS, with a slight increase in the total sugars content. Besides, all pretreatment conditions removed part of the extractives from the three LMs.

The Pearson's test showed a strong inverse correlation between the lignin content and cumulative methane production from HS ($r_{lign\text{-}CH4} = - 0.927$) with a p-value of 0.003. In contrast, no significant correlation was observed between the lignin content and the cumulative methane production for AS and SCG ($p > 0.05$).

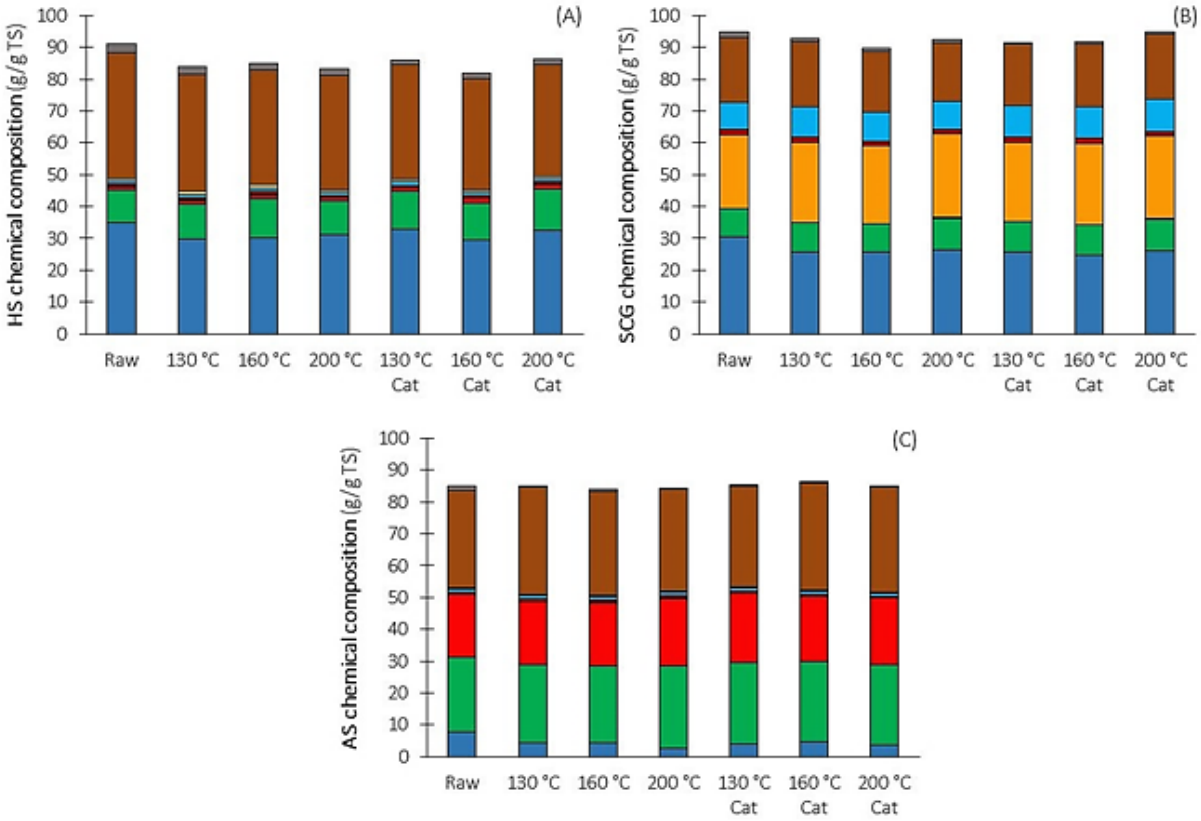


**Figure 3.4 –** Chemical composition of raw and pretreated substrates: full extractives (■), glucan (■), xylan (■), mannan (■), arabinan (■), galactan (■), rhamnan (■), total lignin (■), and ashes (■). AS: almond shell, SCG: spent coffee grounds, and HS: hazelnut skin. Pretreatment time exposure: 1, 3, 5 h.

**Table 3.4 –** Chemical composition of raw and pretreated substrates expressed as ashes, full extractives, total lignin and structural sugars content.

| Substrate | Pretreatment condition[a] | Lignocellulosic materials characterisation | | | | Total sugars composition | | | | | |
|---|---|---|---|---|---|---|---|---|---|---|---|
| | | Ashes[b] (%) | Full extractives[b] (%) | Total lignin[b,c] (%) | Total sugars[b,d] (%) | Glucan[b] (%) | Xylan[b] (%) | Mannan[b] (%) | Arabinan[b] (%) | Galactan[b] (%) | Rhamnan[b] (%) |
| HS | A | 2.71 ± 0.06 | 35.02 ± 0.02 | 39.66 ± 0.09 | 13.72 ± 0.08 | 10.15 ± 0.05 | 0.98 ± 0.01 | 0.29 ± 0.02 | 0.70 ± 0.01 | 0.91 ± 0.02 | 0.69 ± 0.00 |
| | B | 2.37 ± 0.10 | 29.87 ± 0.65 | 36.90 ± 0.38 | 14.80 ± 0.04 | 10.78 ± 0.01 | 1.06 ± 0.02 | 0.29 ± 0.02 | 0.82 ± 0.01 | 1.06 ± 0.01 | 0.79 ± 0.00 |
| | C | 2.35 ± 0.20 | 30.07 ± 0.65 | 35.95 ± 0.21 | 16.74 ± 0.04 | 12.23 ± 0.05 | 1.18 ± 0.07 | 0.32 ± 0.02 | 0.92 ± 0.02 | 1.22 ± 0.01 | 0.87 ± 0.06 |
| | D | 1.89 ± 0.07 | 31.03 ± 0.69 | 36.30 ± 0.72 | 14.04 ± 0.01 | 10.57 ± 0.07 | 1.00 ± 0.01 | 0.26 ± 0.02 | 0.66 ± 0.02 | 0.94 ± 0.02 | 0.61 ± 0.02 |
| | E | 1.51 ± 0.13 | 32.91 ± 0.17 | 36.04 ± 0.06 | 15.64 ± 0.12 | 11.80 ± 0.01 | 0.98 ± 0.04 | 0.28 ± 0.03 | 0.69 ± 0.00 | 1.07 ± 0.01 | 0.83 ± 0.05 |
| | F | 1.74 ± 0.06 | 29.44 ± 0.07 | 35.04 ± 0.39 | 15.79 ± 0.11 | 11.68 ± 0.03 | 1.14 ± 0.01 | 0.29 ± 0.00 | 0.76 ± 0.02 | 1.07 ± 0.03 | 0.85 ± 0.03 |
| | G | 1.98 ± 0.10 | 32.38 ± 0.59 | 34.73 ± 0.16 | 17.34 ± 0.03 | 13.06 ± 0.01 | 1.38 ± 0.02 | 0.39 ± 0.00 | 0.70 ± 0.02 | 1.05 ± 0.01 | 0.76 ± 0.01 |
| SCG | A | 1.69 ± 0.10 | 30.47 ± 0.83 | 20.31 ± 0.29 | 42.38 ± 0.04 | 8.77 ± 0.06 | 0.15 ± 0.01 | 23.14 ± 0.00 | 1.53 ± 0.01 | 8.79 ± 0.04 | nd[e] |
| | B | 0.98 ± 0.15 | 25.67 ± 0.18 | 20.52 ± 0.11 | 45.68 ± 0.28 | 9.25 ± 0.04 | 0.14 ± 0.01 | 25.14 ± 0.12 | 1.64 ± 0.03 | 9.51 ± 0.10 | nd[e] |
| | C | 0.96 ± 0.09 | 25.74 ± 0.07 | 19.22 ± 0.15 | 43.76 ± 0.08 | 8.86 ± 0.02 | 0.14 ± 0.00 | 24.25 ± 0.04 | 1.56 ± 0.00 | 8.94 ± 0.02 | nd[e] |
| | D | 1.07 ± 0.19 | 26.34 ± 0.13 | 18.33 ± 0.38 | 46.81 ± 0.40 | 10.01 ± 0.04 | 0.16 ± 0.01 | 26.24 ± 0.25 | 1.46 ± 0.01 | 8.92 ± 0.09 | nd[e] |
| | E | 0.65 ± 0.08 | 25.75 ± 0.45 | 19.30 ± 0.26 | 45.88 ± 0.15 | 9.36 ± 0.03 | 0.15 ± 0.03 | 24.96 ± 0.09 | 1.66 ± 0.01 | 9.74 ± 0.04 | nd[e] |
| | F | 0.39 ± 0.01 | 24.55 ± 0.46 | 19.85 ± 0.17 | 46.83 ± 0.21 | 9.58 ± 0.01 | 0.15 ± 0.01 | 25.42 ± 0.23 | 1.70 ± 0.06 | 9.99 ± 0.03 | nd[e] |
| | G | 0.70 ± 0.08 | 26.04 ± 0.87 | 20.38 ± 0.23 | 47.68 ± 0.15 | 10.05 ± 0.19 | 0.14 ± 0.02 | 25.81 ± 0.31 | 1.62 ± 0.01 | 10.07 ± 0.02 | nd[e] |
| AS | A | 1.45 ± 0.04 | 7.78 ± 0.63 | 30.58 ± 0.13 | 45.20 ± 0.07 | 23.35 ± 0.18 | 19.74 ± 0.16 | 0.08 ± 0.01 | 0.66 ± 0.01 | 1.08 ± 0.03 | 0.30 ± 0.00 |
| | B | 0.48 ± 0.01 | 4.14 ± 0.15 | 33.67 ± 0.28 | 46.77 ± 0.36 | 24.63 ± 0.13 | 19.82 ± 0.14 | 0.09 ± 0.03 | 0.77 ± 0.03 | 1.19 ± 0.02 | 0.27 ± 0.01 |
| | C | 0.73 ± 0.05 | 4.26 ± 0.50 | 32.60 ± 0.36 | 46.46 ± 0.56 | 24.35 ± 0.19 | 19.72 ± 0.44 | 0.09 ± 0.00 | 0.80 ± 0.04 | 1.17 ± 0.02 | 0.32 ± 0.00 |
| | D | 0.48 ± 0.02 | 2.68 ± 0.18 | 31.80 ± 0.33 | 49.39 ± 0.12 | 25.69 ± 0.16 | 21.34 ± 0.19 | 0.10 ± 0.04 | 0.77 ± 0.05 | 1.18 ± 0.07 | 0.30 ± 0.00 |
| | E | 0.33 ± 0.00 | 3.96 ± 0.61 | 31.64 ± 0.12 | 49.48 ± 0.75 | 25.61 ± 0.24 | 21.67 ± 0.53 | 0.09 ± 0.01 | 0.66 ± 0.01 | 1.14 ± 0.01 | 0.31 ± 0.00 |
| | F | 0.47 ± 0.08 | 4.80 ± 0.20 | 33.56 ± 0.22 | 47.55 ± 0.44 | 25.05 ± 0.13 | 20.37 ± 0.60 | 0.17 ± 0.05 | 0.59 ± 0.01 | 1.08 ± 0.03 | 0.29 ± 0.01 |
| | G | 0.43 ± 0.12 | 3.78 ± 0.79 | 33.01 ± 0.46 | 47.84 ± 0.49 | 24.98 ± 0.09 | 21.02 ± 0.37 | 0.08 ± 0.01 | 0.49 ± 0.00 | 1.01 ± 0.02 | 0.26 ± 0.00 |

[a] *The pretreatment conditions are defined in Table 3.2.*

[b] *Based on dry matter (g/100 g TS).*

[c] *Total lignin is reported as the sum of Klason lignin and acid soluble lignin according to Sluiter et al. (2008c).*

[d] *Total sugars are obtained as the sum of glucan, xylan, mannan, arabinan, galactan, and rhamnan.*

[e] *nd: not detected.*

*3.4.3 Effect of pretreatments on porosity and external surface area of lignocellulosic materials*

WSC was measured as a representative parameter of the LMs porosity, showing a significant difference among the three substrates (Table 3.5). HS resulted in the higher WSC, ranging from 4.80 to 6.20 g $H_2O$/g TS depending on the pretreatment conditions. Opposite, SCG and AS showed WSC values ranging from 2.76 to 3.41 g $H_2O$/g TS and from 1.07 to 1.45 g $H_2O$/g TS, respectively. Among the pretreatment conditions, no significant positive effect on WSC was observed for HS and AS ($p > 0.05$), while organosolv pretreatment under all conditions significantly increased the swelling capacity of SCG ($p < 0.05$) from 2.76 (± 0.06) up to 3.41 (± 0.08) g $H_2O$/g TS.

Figure 3.5 shows the structure of the external surface area of raw (panel a, b and c) and pretreated LMs at 130 °C with catalyst addition (panel d, e and f) using SEM images. The breakdown of cell walls was evident for HS when comparing the SEM images before (Figure 3.5a) and after (Figure 3.5d) the pretreatment, showing a major exposure of cellulosic fibers after pretreatment. Raw AS (Figure 3.5c) presented a series of vascular bundles, while pretreatment destroyed the original structure showing a craggy surface, with deep fissures (Figure 3.5f). On the other hand, organosolv pretreatment slightly affected the external surface of SCG (Figure 3.5b and e) but mainly kept the original compact structure, in contrast with what was observed for pretreated HS.

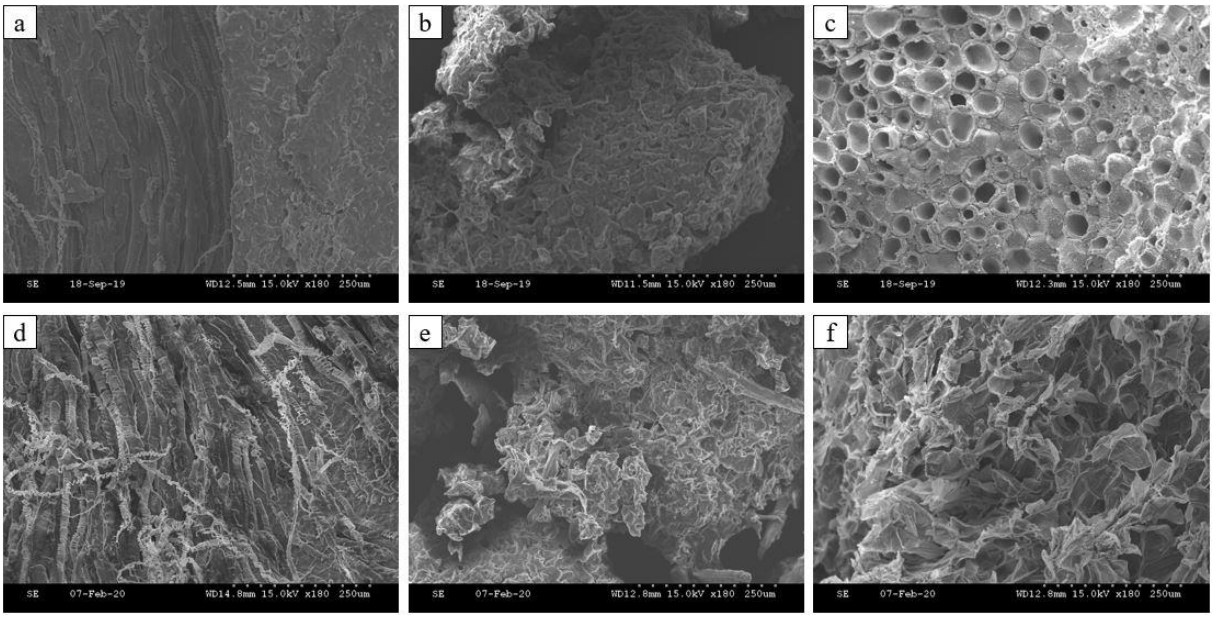


**Figure 3.5 –** Scanning electron microscopic images of untreated and pretreated materials at 130 °C with catalyst addition: (a) raw AS, (b) raw SCG, (c) raw HS, (d) pretreated AS, (e) pretreated SCG, (f) pretreated HS.

**Table 3.5 –** Water swelling capacity and statistical comparison of raw and pretreated LMs.

| Substrate | Pretreatment condition[a] | Water swelling capacity (g $H_2O$/g TS) | Statistical information[b] |
|---|---|---|---|
| HS | A | 5.53 ± 0.49 | ab |
| | B | 5.34 ± 0.65 | ab |
| | C | 5.31 ± 0.25 | ab |
| | D | 6.20 ± 0.69 | a |
| | E | 5.28 ± 0.44 | ab |
| | F | 4.81 ± 0.30 | ab |
| | G | 4.80 ± 0.52 | b |
| SCG | A | 2.76 ± 0.06 | d |
| | B | 3.07 ± 0.06 | b |
| | C | 3.41 ± 0.08 | a |
| | D | 3.04 ± 0.04 | b |
| | E | 2.87 ± 0.03 | cd |
| | F | 2.96 ± 0.09 | bc |
| | G | 3.05 ± 0.01 | b |
| AS | A | 1.40 ± 0.10 | a |
| | B | 1.45 ± 0.07 | a |
| | C | 1.14 ± 0.08 | bc |
| | D | 1.07 ± 0.06 | c |
| | E | 1.30 ± 0.02 | ab |
| | F | 1.13 ± 0.03 | bc |
| | G | 1.30 ± 0.14 | abc |

*[a] The pretreatment conditions are defined in Table 3.2.*

*[b] The same letter represents no significant differences ($p > 0.05$) with the compared condition.*

### *3.4.4 Modified Gompertz model fitting of the experimental data*

The modified Gompertz model was applied to fit the experimental methane production obtained from raw and pretreated SCG and HS (Figure 3.6), which achieved a significantly higher biogas production than that observed in the substrate-free controls. On the contrary, no fitting was achieved when AS was used as a substrate for AD, due to the low and fluctuating methane production.

Two stages of methane production were identified, with 12 days ($t_b$) being the crossover point for all the substrates except for raw HS, where $t_b$ was 20 days. Table 3.6 shows that all pretreatment conditions considerably increased the rate of methane production ($R_m$) from HS for both the first and second stages. Besides, the catalyst addition reduced the lag phase $\lambda_1$ from 2 - 3 days to less than 1 day, as well as $\lambda_2$, with the distinction of the two stages being less noticeable with the increase in pretreatment temperature and the use of catalyst.

With regards to SCG, the pretreatments at 160 and 200 °C with catalyst addition showed a reduction of the rate $R_{m1}$ in the first stage and an increase of $R_{m2}$, compared to the raw SCG. In any case, the catalyst addition had a positive effect on the lag phase λ.

**Table 3.6 –** Parameters obtained by modelling the experimental data of HS and SCF from Figure 3.2 with the modified Gompertz model. No fitting was achieved when AS was used as a substrate for AD.

| **Substrate** | **Pretreatment condition**[a] | **$t_b$**[b] (d) | **Stage 1** | | **Stage 2** | | **RSQ**[e] |
|---|---|---|---|---|---|---|---|
| | | | **$R_{m1}$**[c] (mL $CH_4$/g VS·d) | **$\lambda_1$**[d] (d) | **$R_{m2}$**[c] (mL $CH_4$/g VS·d) | **$\lambda_2$**[d] (d) | |
| HS | A | 20 | 0.98 | 2.4 | 0.65 | 12.6 | 0.9951 |
| | B | 12 | 12.51 | 2.5 | 9.22 | 3.9 | 0.9999 |
| | C | 12 | 12.26 | 2.6 | 11.04 | 3.0 | 0.9994 |
| | D | 12 | 9.82 | 1.8 | 11.01 | 4.1 | 0.9999 |
| | E | 12 | 12.80 | 0.8 | 9.34 | 0.0 | 0.9972 |
| | F | 12 | 6.90 | 0.0 | 10.04 | 0.8 | 0.9977 |
| | G | 12 | 8.60 | 0.7 | 9.16 | 0.5 | 0.9973 |
| SCG | A | 12 | 20.70 | 0.8 | 7.54 | 0.5 | 0.9991 |
| | B | 12 | 11.17 | 1.6 | 5.54 | 4.2 | 0.9991 |
| | C | 12 | 20.98 | 1.5 | 5.75 | 2.3 | 0.9989 |
| | D | 12 | 20.47 | 1.4 | 6.30 | 2.0 | 0.9991 |
| | E | 12 | 16.30 | 0.5 | 7.61 | 1.3 | 0.9986 |
| | F | 12 | 14.43 | 0.4 | 10.72 | 1.6 | 0.9984 |
| | G | 12 | 13.65 | 0.5 | 10.74 | 2.0 | 0.9986 |

[a] *The pretreatment conditions are defined in Table 3.2.*

[b] *$t_b$ identifies the crossover point between the two stages of the AD process.*

[c] *$R_{m1}$ and $R_{m2}$ are the maximum methane production rates of the two stages.*

[d] *$\lambda_1$ and $\lambda_2$ are the lag phases of stage 1 and stage 2, respectively.*

[e] *RSQ is the Excel function used to measure the correlation between experimental and model data.*

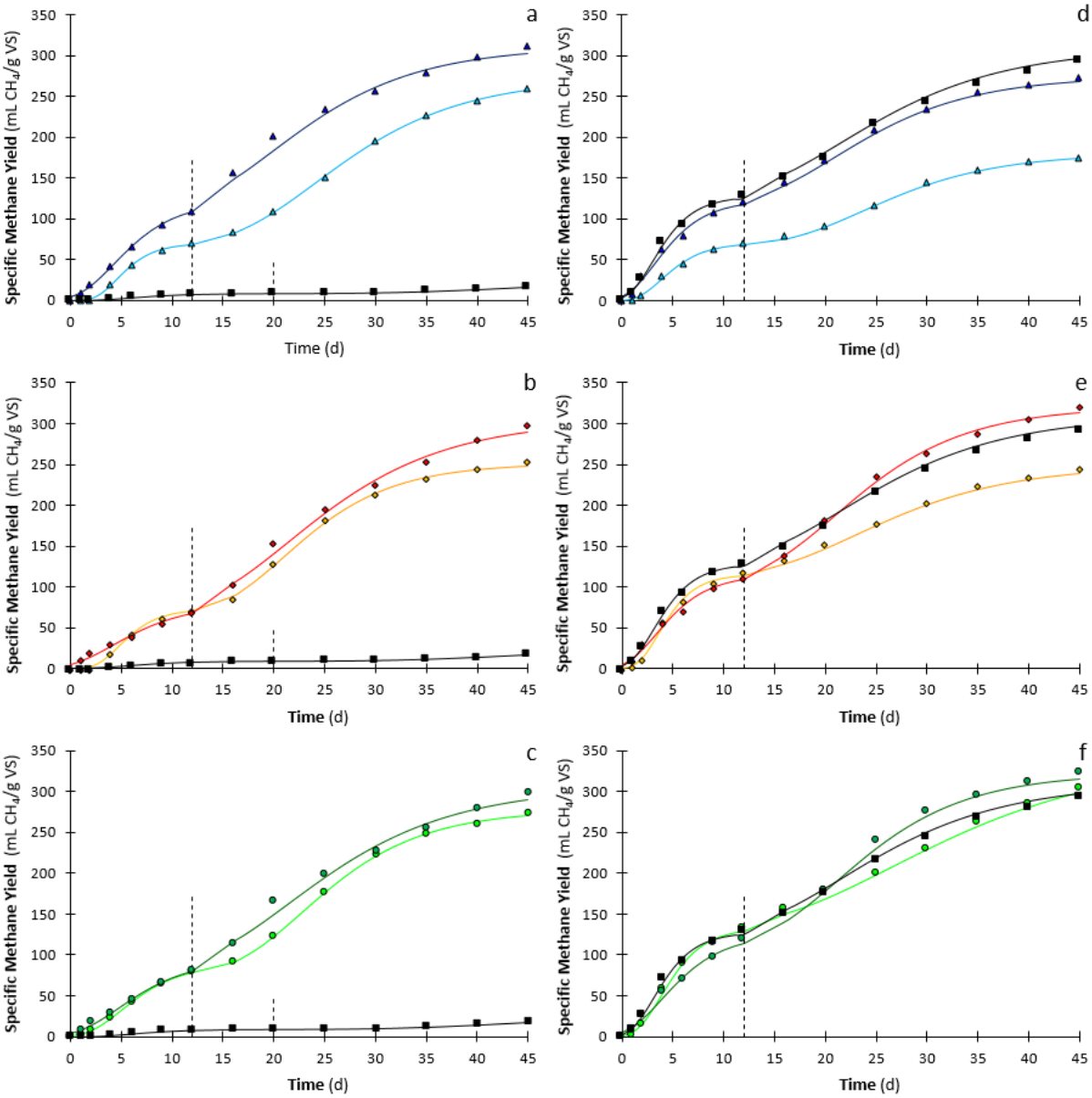


**Figure 3.6 –** Fitting of the experimental methane production values from hazelnut skin (a, b, c) and spent coffee grounds (d, e, f), raw (■) and treated at 130 °C (▲), 130 °C with the catalyst (▲), 160 °C (◆), 160 °C with the catalyst (◆), 200 °C (●), and 200 °C with the catalyst (●), by a modified Gompertz model. The dashed line identifies the crossover point $t_b$ between the two stages of methane production. No fitting was achieved when AS was used as a substrate for AD.

## 3.5 Discussion

### *3.5.1 Effect of organosolv pretreatment on the AD process of the three LMs*

This study showed for the first time the effect of methanol as an organic solvent for the pretreatment of HS, SCG, and AS. Several studies investigated the efficiency of organosolv pretreatment to enhance biogas production, with BMP improvement being associated with lignin removal and an increase in the availability of polysaccharides (Table 3.7). Most of the

previous studies on organosolv used ethanol as a solvent (Mirmohamadsadeghi et al., 2014; Ostovareh et al., 2015; Tongbuekeaw et al., 2020). However, to the best of the authors' knowledge, only Kabir et al. (2015) investigated the methanol-organosolv pretreatment to enhance methane production from LMs. That study compared the effects of the most employed organic solvents on forestry residues, with and without catalyst addition, showing that catalysed-methanol pretreatment was the most performing and cost-effective alternative, with a recovery rate of the solvent up to 98.2% (Kabir et al., 2015).

The BMP tests clearly showed the effectiveness of methanol-organosolv pretreatment on HS (Table 3.3). On the contrary, no remarkable positive effect of pretreatment on cumulative biogas production was observed for SCG and AS (Table 3.3). In particular, the highest methane yield from HS (310.6 mL $CH_4$/g VS) was obtained with the HS pretreated with the catalyst at the lowest temperature, achieving 50.6% of the theoretical methane yield calculated from the elemental composition of the raw substrate. On the other hand, the BMP of raw HS only represents 2.8% of the theoretical methane yield. The catalyst addition during the pretreatment at 130 °C resulted in a significant benefit for the AD of HS by increasing the methane production of 20% compared with the catalyst-free pretreated HS. The benefit of catalyst addition is reduced by increasing the pretreatment temperature. Previous studies showed a similar synergy between catalyst and pretreatment temperature, regardless of the organic solvent employed (Hesami et al., 2015; Ostovareh et al., 2015). At high temperatures, LMs self-catalyse the pretreatment by releasing acids (Zhou et al., 2018). Instead, when a lower temperature pretreatment is performed, external catalyst addition is required to optimise the cost-benefit balance and reduce the energy consumption during pretreatment (Zhou et al., 2018). Moreover, the catalyst addition during the pretreatment is reported to be particularly beneficial in terms of methane production when methanol and isopropanol are used as organic solvents, being less advantageous in combination with ethanol and acetic acid (Hesami et al., 2015; Kabir et al., 2015; Ostovareh et al., 2015).

Figure 3.6 shows the evolution of the methane production for both raw and pretreated SCG and HS according to the modified Gompertz model, by which the biogas production rate is proportional to the microbial activity (Altaş, 2009). Two stages of digestion can be identified: the first stage within the first 12 days, in which the easily degradable materials are digested, and a second phase, where the less readily and more recalcitrant materials start to be degraded. This was particularly observed in catalyst-free conditions, where the double "S" shape methane

production profile is more evident (Figure 3.6). A similar pattern was previously observed by Rincón et al. (2013) during the AD of two-phase olive mill solid waste and by Pellera and Gidarakos (2016) for different agroindustrial wastes. In the present study, the crossover point was less noticeable when sulfuric acid was used as a catalyst during the pretreatment, resulting in a reduction of the lag phases, especially in the case of treated HS. The catalyst addition is reported to be the most important factor for both lignin fractionation and hemicellulose hydrolysis during pretreatment (Ferreira and Taherzadeh, 2020). With regards to SCG, the pretreatment lowered the methane production rate of the first stage but enabled a more efficient use of the more recalcitrant materials, resulting in a higher rate of methane production in the second stage, when SCG was pretreated at 160 and 200 °C with the catalyst (Table 3.6).

Interestingly, the methane production from raw HS obtained in the present study was considerably different to that reported by Mancini et al. (2018a), who observed a much higher methane yield (261 mL $CH_4$/g VS) for raw HS, with organosolv pretreatment being only slightly effective on HS. The different effectiveness of pretreatment on HS can be ascribed to the use of a different organic solvent. Methanol is reported to be a better solvent for lignin, compared to ethanol (Sameni et al., 2017). On the other hand, the difference in methane production from raw HS is most likely attributed to the use of a different inoculum, which was a digestate from buffalo manure and dairy factory in the work of Mancini et al. (2018a). This hypothesis is supported by the study of Gu et al. (2014), in which a digestate from dairy manure was significantly more efficient than anaerobic granular sludge to promote the AD of untreated rice straw. The use of granular sludge, together with the limited mixing, likely led to a scarce contact between the solid substrates and the methanogenic population (McHugh et al., 2003). The intimate contact between the cellulose and cellulase enzymes is one of the most critical factors affecting the enzymatic hydrolysis yield and rate, with particle size being responsible for the external accessible surface area (Meng and Ragauskas, 2014). This may explain the low BMP observed for AS and raw HS. On the other hand, although pretreatment was not effective, the AD of raw SCG allowed a high cumulative methane yield (293.4 mL $CH_4$/g VS) in line with previous studies (Girotto et al., 2018; Kim et al., 2017) and corresponding to the 51.2% of the maximum theoretical methane yield.

**Table 3.7 –** Comparison of methane yield enhancement by organosolv pretreatment on different LMs reported by various studies.

| Substrate | Raw – pretreated composition | | | Organosolv pretreatment | Optimal conditions | | | | Methane production (mL $CH_4$/g VS) | | Reference |
|---|---|---|---|---|---|---|---|---|---|---|---|
| | Cellulose[a] (%) | Hemicellulose[a] (%) | Lignin[a] (%) | | S/L[a] (g/g) | T (°C) | Solvent (%) | t (h) | Raw – pretreated | Increment (%) | |
| Sugarcane bagasse | 47.6 – 60.9 | 22.6 – 28.9 | 27.6 – 14.0 | Ethanol-Ammonia | 1:14 | 70 | 25-10 | 12 | 106 – 249 | 135 | Hashemi et al., 2019 |
| Rice straw | 28.6 – 32.0 | 19.5 – 16.0 | 17.3 – 14.1 | | | 180 | | | 235 – 332 | 41 | |
| Hazelnut skin | 11.4 – 12.5 | 5.9 – 4.7 | 34.4 – 32.5 | Ethanol | 1:10 | 180 | 50 | 1 | 261 – 288 | 10 | Mancini et al., 2018a |
| Cocoa bean shell | 13.5 – 15.0 | 7.0 – 5.8 | 29.9 – 26.3 | | | 180 | | | 231 – 219 | -5 | |
| Wheat straw | 31 – 36.3 | 18.4 – 9.4 | 18.3 – 15.8 | Ethanol | 1:10 | 180 | 50 | 1 | 274 – 316 | 15 | Mancini et al., 2018b |
| Elm hardwood | 46.4 – 58.1 | 26.3 – 21.3 | 26.2 – 19.1 | | | 180 | | 1 | 54[c] – 94[c] | 73 | Mirmohamadsadeghi et al., 2014 |
| Pine softwood | 44.5 – 51.3 | 28.0 – 20.2 | 26.8 – 27.8 | Ethanol (Catalyst) | 1:8 | 150 | 75 | 0.5 | 39[c] – 71[c] | 84 | |
| Rice straw | 21.5 – 28.7 | 50.1 – 45.3 | 17.1 – 13.4 | | | 150 | | 1 | 116[c] – 153[c] | 32 | |
| Forest residues | 22.3 – 43.1 | 20.0 – 11.5 | 44.7 – 40.7 | Ethanol (Catalyst) | 1:10 | 190 | 50 | 1 | 50 – 190 | 280 | Kabir et al., 2015 |
| | 22.3 – 35.2 | 20.0 – 17.2 | 44.7 – 43.0 | Methanol (Catalyst) | | | | | 50 – 210 | 320 | |
| | 22.3 – 31.2 | 20.0 – 15.5 | 44.7 – 42.1 | Acetic Acid | | | | | 50 – 200 | 300 | |
| Sunflower stalks | 34.1 – 59.6 | 26.2 – 17.6 | 26.8 – 21.2 | Isopropanol (Catalyst) | 1:10 | 160 | 50 | 0.5 | 124 – 278 | 124 | Hesami et al., 2015 |
| Sorghum stalks | 35.5 – 40.2 | 17.3 – 14.9 | 15.5 – 11.6 | Ethanol | 1:10 | 160 | 50 | 0.5 | 75 – 155 | 106 | Ostovareh et al., 2015 |
| Rubberwood waste | 43.6 – 68.1 | 8.3 – 5.2 | 31.0 – 8.1 | Ethanol | 1:10 | 210 | 75 | N/A[d] | 59 – 166 | 179 | Tongbuekeaw et al., 2020 |
| Hazelnut skin | 10.2 – 11.8 | 3.6 – 3.8 | 39.7 – 36.0 | Methanol | | 200 | | | 17 – 311 | 1729 | This study |
| Spent coffee grounds | 8.8 – 10.1 | 33.6 – 37.6 | 20.3 – 20.4 | Methanol (Catalyst) | 1:10 | 200 | 50 | 1 | 293 – 323 | 10 | |
| Almond shell | 23.4 – 25.7 | 21.9 – 23.7 | 30.6 – 31.8 | Methanol (Catalyst) | | 130 | | | 23 – 25 | 9 | |

[a] *Based on dry matter (g/100 g TS).*

[b] *S/L stands for solid to liquid ratio.*

[c] *Mirmohamadsadeghi et al. (2014) reported the methane production potential as mL $CH_4$/g carbohydrates.*

[d] *N/A: not available.*

*3.5.2 Change of LMs composition by methanol pretreatment*

HS, SCG, and AS largely differ in their composition (Table 3.4). HS is particularly rich in lignin (40%) but lacks in polysaccharides (14%), similarly to what was reported by Mancini et al. (2018a). The AS composition is balanced in glucose (23%), xylose (20%), and lignin (31%) as elsewhere observed (Queirós et al., 2020). The chemical composition of SCG reported in the literature is more variable, with a lignin content ranging from 20 to 30% and a cellulose and hemicellulose content of 10 and 30 - 40%, respectively (Kovalcik et al., 2018). However, some studies reported a lower lignin content for SCG (Girotto et al., 2018; Mata et al., 2018). This study showed SCG as a hemicellulose-rich material (34%), with cellulose and lignin being 9 and 20% of the dry matter, respectively. The variation in chemical composition might be attributed to the different origin of the coffee beans, and different processing during the production of coffee grounds (Kovalcik et al., 2018).

The main aim of organosolv pretreatment is lignin removal (Ferreira and Taherzadeh, 2020). Given this, a positive effect was expected for AS and HS, both particularly rich in lignin. Despite this, only the HS composition significantly changed due to the pretreatment, showing a lignin decrease and increase in total sugar content (Table 3.4 and Figure 3.4). Lignin is considered the most relevant factor for LMs recalcitrance (Ferreira and Taherzadeh, 2020), and lignin removal showed a positive effect on the methane yield in several studies on different LMs (Mancini et al., 2018a; Mirmohamadsadeghi et al., 2014; Ostovareh et al., 2015).

The ineffectiveness of organosolv pretreatment on SCG is most likely attributed to the loss of non-structural compounds during the pretreatment and subsequent washing steps (Table 3.4). These compounds include free sugars, such as sucrose, glucose, and fructose, which are excellent substrates for biofuel production through fermentation pathways (Ostovareh et al., 2015). However, the catalyst addition and a higher pretreatment temperature allowed to compensate for this loss by increasing the structural sugar bioavailability. This is supported by the fact that methane production from pretreated SCG increased with the severity of pretreatment, from 175.8 up to 322.9 mL $CH_4$/g VS. Nevertheless, the pretreatment was not effective enough to significantly balance this loss.

None of the pretreatment conditions had a positive effect on the cumulative methane production from AS, likely due to the hard structure of the substrate, which should be tackled by a different pretreatment. In particular, the authors hint to explore a pretreatment that can be performed for longer, without the risk of losing the biodegradable sugars. In this perspective, the ionic liquid

is suggested as an alternative to the organosolv pretreatment tested in the present study. The ionic liquid pretreatment duration ranges from 1 and 24 hours (Halder et al., 2019), which is expected to be sufficient for a complete soaking of the AS. This pretreatment acts directly on the cellulosic part of the LMs, by decreasing the crystallinity index and swelling up the cellulose, reducing the risk of losing biodegradable substances as a result of the longer duration of the pretreatment (Halder et al., 2019).

Besides, the compositional analysis highlights the potential of HS and SCG for a deeper biorefinery approach, using a preliminary extraction step to remove the non-structural compounds. HS and SCG are extremely extractives-rich materials, with organosolv pretreatment able to remove only a maximum of 24 and 19% of them, respectively (Table 3.4 and Figure 3.4 ). The extractives are defined as non-bound substances, soluble in water or ethanol, mainly composed of non-structural sugars, proteins, fats, chlorophyll, and waxes (Karimi and Taherzadeh, 2016; Sluiter et al., 2008d). The early separation of these substances provides the dual advantage of recovered valuable compounds and removal of inhibitors for the AD process. Non-structural compounds such as cell wall proteins, pectin, and lipids are also involved in the recalcitrance of LMs. Their degradation results in the accumulation of ammonia and long-chain fatty acids, which are inhibitors of the microorganisms involved in the AD (Chen et al., 2008; Xu et al., 2019).

*3.5.3 Impact of the pretreatment on LMs structure and water swelling capacity*

WSC is defined as the amount of water retained by the biomass with no external force application. Water contributes to increasing the accessible surface area, but also affects cellulose crystallinity and lignin bonds, solubilises part of the hemicellulose, and promotes the hydrolysis step (Sanchez et al., 2019). The ineffectiveness of pretreatment on AS and SCG might be attributed to the low porosity of these materials.

The WSC was 1.45 and 2.76 g $H_2O$/g TS, respectively, for raw AS and SCG, while it was 5.53 g $H_2O$/g TS for raw HS (Table 3.5). A low WSC shows a low capacity of the substrates to retain water molecules in the cell wall pores, thus indicating that also solvents have difficulty in penetrating the material. The WSC is used as an indicator of the interior accessible surface area for enzymatic hydrolysis, based on the principle that no enzymes can enter the pores of LMs if water cannot (Mancini et al., 2018a). Thus, the lower accessible surface area might explain the ineffectiveness of a solvent-based pretreatment on AS and SCG, due to a low substrate-solvent contact. The lack of contact might be overcomed by combining a pre-milling step to the

organosolv pretreatment to increase the accessible surface area of the AS. Alternatively, a more intrusive pretreatment, such as steam explosion, might be considered on AS to penetrate its hard external surface. Despite steam explosion often leads to sugar loss into the liquor, it is capable of disrupting the cell wall structure of agricultural residues (Amin et al., 2017). On the other hand, the already small particle size of SCG suggests to use an alternative pretreatment, such as e.g., ionic liquid that is reported to be effective on cellulose swelling up (Jeihanipour et al., 2010).

To the best of the authors' knowledge, the WSC prior to and after pretreatment has never been reported for HS, SCG, and AS. Sanchez et al. (2019) studied the hydration of different straws and bagasses, reporting WSC values ranging between 4 and 10 (g $H_2O$/g TS). The experimental procedure for WSC determination is often missing details, which makes comparison between different works difficult. Despite this, a study on high-crystalline cellulose revealed the relation between porosity and methane production, showing that the BMP was proportional to the WSC of the cellulose (Jeihanipour et al., 2010). However, in this study, no correlation was observed between WSC and methane production, most likely due to the low cellulose content of the three LMs.

SEM analysis showed the strong and dense external surface of raw AS (Figure 3.5c), in contrast with raw SCG (Figure 3.5b) and raw HS (Figure 3.5a). The methanol-organosolv pretreatment drastically affected the surface of HS (Figure 3.5a-d) by exposing the cellulose fibers, as similarly observed by Papirio (2020) who treated the same material with a 1.6% (w/w) NaOH solution. The external surface of pretreated SCG (Figure 3.5e) appeared weaker and softer than the raw material after the pretreatment (Figure 3.5b). In the case for AS, the pretreatment seemingly destroyed the original external pores (Figure 3.5c), with the treated samples exhibiting more fragile bundles and a higher accessible surface (Figure 3.5f). However, the changes in AS structure after pretreatment were still not enough to improve the methane production. The organosolv pretreatment has been reported to be effective on several LMs by causing lignin disruption and an increase of the available surface area (Ebrahimi et al., 2017; Hesami et al., 2015; Ostovareh et al., 2015). The increased accessible surface, together with the higher porosity and lignin content reduction, leads to an easier digestibility and subsequent enhanced methane production (Xu et al., 2019). In this study, the methanol-organosolv pretreatment disrupted the linkages between cellulose, hemicellulose, and lignin of HS (Fig 3.5d), exposing the cellulose fibers to the enzymatic attack. The increased cellulose

bioavailability, coupled to the partial removal of lignin and extractives, led to a significant ($p < 0.05$) increment of the BMP from HS.

Apart from the lack of major changes in the AS chemical composition and porosity after the pretreatment here used, the recalcitrance of AS also largely depends on the material processing in the production process of almonds before being discarded. While both SCG and HS are roasted during the production chain, AS remains a raw material. Oliveros et al. (2017) studied the effects of the roasting process on coffee beans, showing an increase of the void fraction from 9.88 to 34.24%, compared to the unroasted beans. Those authors noticed that the volume of the coffee beans increased up to 1.8 times, with the SEM images showing a more fragile material after roasting. The increase in pore volume during the roasting process was also confirmed by Perren and Escher (2013) in their study on nuts quality, including almonds and hazelnuts. Overall, the low porosity (Table 3.5) and compact external surface area (Figure 3.5c-f), coupled with the particle size of AS (1 - 2.5 mm), justify the low BMP of AS as substrate, both raw and pretreated (Table 3.3).

*3.5.4 Energy assessment and waste stream management*

The energy balance assessment showed that only the HS pretreatment led to a positive energy balance (Table 3.3), due to the low improvement in methane production obtained by treating SCG and AS. The optimal net heat energy gain was achieved by treating HS at 130 °C with catalyst addition, resulting in an energy production of 1.46 kWh/kg VS. Despite the pretreatment temperature did not show a particular effectiveness on the methane production itself, it is an important factor in keeping the energy consumption low. The pretreatment energy demand was reduced from 1.19 to 0.71 kWh/kg VS of HS by reducing the pretreatment temperature from 200 to 130 °C. However, several authors include heat recovery by heat exchangers in the energy assessment. The recoverable energy is widely assumed to be 85% of the energy consumption (Yuan et al., 2019). Considering the heat recovery, the effective energy recovery ($E_{R,\ eff}$) of the process achieves a positive value of 1.35 kWh/kg VS under the pretreatment condition at 130 °C, which maximised the methane production from HS. Finally, to take into account the difference between laboratory and real scale, a scale-up factor of 0.85 can be applied to adjust the final cumulative methane production value (Alonso-Fariñas et al., 2020).

The recycling and utilisation of the spent liquid waste stream after pretreatment are required to further improve the assessment of cost effectiveness of the entire process chain and to close the

energy loop of organosolv pretreatment. In this perspective, the optimisation of the S/L ratio during the pretreatment might offset the processing costs by reducing the amount of waste and producing a liquid stream richer in valuable compounds (Ferreira and Taherzadeh, 2020). Unlike other solvents (i.e. ionic liquids, sodium hydroxide, and sodium carbonate), organic solvents do not generally create inhibition during the AD process if present in moderate concentrations, since they are intermediates of the process, or useable by methanogens for methane production (Kabir et al., 2015; Mancini et al., 2016b). This results in a low water volume to use in the washing step of the pretreated materials, which, together with the easy solvent recovery by evaporation, makes the organosolv pretreatment more cost-effective compared to other chemical pretreatments (Kabir et al., 2015). Besides, methanol has been successfully tested as an electron donor for several environmental technological applications, such as denitrification (Di Capua et al., 2019) and selenate bioreduction (Eregowda et al., 2019), offering an alternative use to the organosolv pretreated waste stream.

### 3.6 Conclusion

Methanol-organosolv pretreatment is an effective technique for enhancing the AD of HS, attaining an 18-fold increase in methane production compared to the untreated material. The lignocellulosic compositional analysis on HS showed a reduction of the lignin content from 35.0 to 29.4%. In particular, the lowest pretreatment temperature and the addition of catalyst resulted in the highest methane production from HS (310.6 mL $CH_4$/g VS). An energy-saving of about 62% can be achieved by lowering the pretreatment temperature from 200 to 130 °C. For SCG and AS, no significant improvement in methane production was observed under all pretreatment conditions investigated, most likely due to the lower porosity of the raw substrate and loss of non-structural compounds during the washing steps.

### 3.7 References

Alonso-Fariñas, B., Oliva, A., Rodríguez-Galán, M., Esposito, G., García-Martín, J.F., Rodríguez-Gutiérrez, G., Serrano, A., Fermoso, F.G., 2020. Environmental assessment of olive mill solid waste valorization via anaerobic digestion versus olive pomace oil extraction. Processes 8. https://doi.org/10.3390/PR8050626

Altaş, L., 2009. Inhibitory effect of heavy metals on methane-producing anaerobic granular sludge. J. Hazard. Mater. 162, 1551–1556. https://doi.org/10.1016/j.jhazmat.2008.06.048

Amin, F.R., Khalid, H., Zhang, H., Rahman, S., Zhang, R., Liu, G., Chen, C., 2017. Pretreatment methods of lignocellulosic biomass for anaerobic digestion. AMB Express

7:72. https://doi.org/10.1186/s13568-017-0375-4

Angelidaki, I., Treu, L., Tsapekos, P., Luo, G., Campanaro, S., Wenzel, H., Kougias, P.G., 2018. Biogas upgrading and utilization: Current status and perspectives. Biotechnol. Adv. 36, 452–466. https://doi.org/10.1016/j.biotechadv.2018.01.011

Bianco, F., Monteverde, G., Race, M., Papirio, S., Esposito, G., 2020. Comparing performances, costs and energy balance of ex situ remediation processes for PAH-contaminated marine sediments. Environ. Sci. Pollut. Res. https://doi.org/10.1007/s11356-020-08379-y

Castilla-Archilla, J., Papirio, S., Lens, P.N.L., 2020. Two step process for volatile fatty acid production from brewery spent grain: hydrolysis and direct acidogenic fermentation using anaerobic granular sludge. Process Biochem. https://doi.org/10.1016/j.procbio.2020.10.011

Chen, Y., Cheng, J.J., Creamer, K.S., 2008. Inhibition of anaerobic digestion process: A review. Bioresour. Technol. 99, 4044–4064. https://doi.org/10.1016/j.biortech.2007.01.057

Choi, J.H., Jang, S.K., Kim, J.H., Park, S.Y., Kim, J.C., Jeong, H., Kim, H.Y., Choi, I.G., 2019. Simultaneous production of glucose, furfural, and ethanol organosolv lignin for total utilization of high recalcitrant biomass by organosolv pretreatment. Renew. Energy 130, 952–960. https://doi.org/10.1016/j.renene.2018.05.052

Chynoweth, D.P., Owens, J.M., Legrand, R., 2001. Renewable methane from anaerobic digestion of biomass. Renew. Energy 22, 1–8. https://doi.org/10.1016/S0960-1481(00)00019-7

Codignole Luz, F., Volpe, M., Fiori, L., Manni, A., Cordiner, S., Mulone, V., Rocco, V., 2018. Spent coffee enhanced biomethane potential via an integrated hydrothermal carbonization-anaerobic digestion process. Bioresour. Technol. 256, 102–109. https://doi.org/10.1016/j.biortech.2018.02.021

Di Capua, F., Pirozzi, F., Lens, P.N.L., Esposito, G., 2019. Electron donors for autotrophic denitrification. Chem. Eng. J. 362, 922–937. https://doi.org/10.1016/j.cej.2019.01.069

Donoso-Bravo, A., Pérez-Elvira, S.I., Fdz-Polanco, F., 2010. Application of simplified models for anaerobic biodegradability tests. Evaluation of pre-treatment processes. Chem. Eng. J. 160, 607–614. https://doi.org/10.1016/j.cej.2010.03.082

Ebrahimi, M., Caparanga, A.R., Ordono, E.E., Villaflores, O.B., 2017. Evaluation of organosolv pretreatment on the enzymatic digestibility of coconut coir fibers and bioethanol production via simultaneous saccharification and fermentation. Renew. Energy

109, 41–48. https://doi.org/10.1016/j.renene.2017.03.011

Eregowda, T., Rene, E.R., Lens, P.N.L., 2019. Bioreduction of selenate in an anaerobic biotrickling filter using methanol as electron donor. Chemosphere 225, 406–413. https://doi.org/10.1016/j.chemosphere.2019.02.158

Ferreira, J.A., Taherzadeh, M.J., 2020. Improving the economy of lignocellulose-based biorefineries with organosolv pretreatment. Bioresour. Technol. 299, 122695. https://doi.org/10.1016/j.biortech.2019.122695

Galbe, M., Zacchi, G., 2012. Pretreatment: The key to efficient utilization of lignocellulosic materials. Biomass and Bioenergy 46, 70–78. https://doi.org/10.1016/j.biombioe.2012.03.026

Girotto, F., Lavagnolo, M.C., Pivato, A., 2018. Spent Coffee Grounds Alkaline Pre-treatment as Biorefinery Option to Enhance their Anaerobic Digestion Yield. Waste and Biomass Valorization 9, 2565–2570. https://doi.org/10.1007/s12649-017-0033-8

Gu, Y., Chen, X., Liu, Z., Zhou, X., Zhang, Y., 2014. Effect of inoculum sources on the anaerobic digestion of rice straw. Bioresour. Technol. 158, 149–155. https://doi.org/10.1016/j.biortech.2014.02.011

Gunasekaran, V., Ramesh, S., Sathiasivan, K., Shankar, M., Rajesh, M., Tamilarasan, K., 2020. Simultaneous organosolv pretreatment and detoxification of agro-biomass for efficient lignin extraction and characterization. Chem. Pap. 74, 273–283. https://doi.org/10.1007/s11696-019-00876-w

Halder, P., Kundu, S., Patel, S., Setiawan, A., Atkin, R., Parthasarthy, R., Paz-Ferreiro, J., Surapaneni, A., Shah, K., 2019. Progress on the pre-treatment of lignocellulosic biomass employing ionic liquids. Renew. Sustain. Energy Rev. 105, 268–292. https://doi.org/10.1016/j.rser.2019.01.052

Hashemi, S.S., Karimi, K., Majid Karimi, A., 2019. Ethanolic ammonia pretreatment for efficient biogas production from sugarcane bagasse. Fuel 248, 196–204. https://doi.org/10.1016/j.fuel.2019.03.080

Hesami, S.M., Zilouei, H., Karimi, K., Asadinezhad, A., 2015. Enhanced biogas production from sunflower stalks using hydrothermal and organosolv pretreatment. Ind. Crops Prod. 76, 449–455. https://doi.org/10.1016/j.indcrop.2015.07.018

Jeihanipour, A., Karimi, K., Taherzadeh, M.J., 2010. Enhancement of ethanol and biogas production from high-crystalline cellulose by different modes of NMO pretreatment. Biotechnol. Bioeng. 105, 469–476. https://doi.org/10.1002/bit.22558

Jiang, Y., Liu, X., Yang, S., Song, X., Wang, S., 2019. Combining organosolv pretreatment with mechanical grinding of sugarcane bagasse for the preparation of nanofibrillated cellulose in a novel green approach. BioResources 14, 313–335. https://doi.org/10.15376/biores.14.1.313-335

Kabir, M.M., Rajendran, K., Taherzadeh, M.J., Sárvári Horváth, I., 2015. Experimental and economical evaluation of bioconversion of forest residues to biogas using organosolv pretreatment. Bioresour. Technol. 178, 201–208. https://doi.org/10.1016/j.biortech.2014.07.064

Karimi, K., Taherzadeh, M.J., 2016. A critical review of analytical methods in pretreatment of lignocelluloses: Composition, imaging, and crystallinity. Bioresour. Technol. 200, 1008–1018. https://doi.org/10.1016/j.biortech.2015.11.022

Katsimpouras, C., Dedes, G., Bistis, P., Kekos, D., Kalogiannis, K.G., Topakas, E., 2018. Acetone/water oxidation of corn stover for the production of bioethanol and prebiotic oligosaccharides. Bioresour. Technol. 270, 208–215. https://doi.org/10.1016/j.biortech.2018.09.018

Kim, J., Kim, H., Baek, G., Lee, C., 2017. Anaerobic co-digestion of spent coffee grounds with different waste feedstocks for biogas production. Waste Manag. 60, 322–328. https://doi.org/10.1016/j.wasman.2016.10.015

Kim, S.J., Um, B.H., Im, D.J., Lee, J.H., Oh, K.K., 2018. Combined ball milling and ethanol organosolv pretreatment to improve the enzymatic digestibility of three types of herbaceous biomass. Energies 11. https://doi.org/10.3390/en11092457

Kovalcik, A., Obruca, S., Marova, I., 2018. Valorization of spent coffee grounds: A review. Food Bioprod. Process. 110, 104–119. https://doi.org/10.1016/j.fbp.2018.05.002

Lee, S., Lee, D.K., 2018. What is the proper way to apply the multiple comparison test? Korean J. Anesthesiol. 71, 353–360. https://doi.org/10.4097/kja.d.18.00242

Li, C., Champagne, P., Anderson, B.C., 2011. Evaluating and modeling biogas production from municipal fat, oil, and grease and synthetic kitchen waste in anaerobic co-digestions. Bioresour. Technol. 102, 9471–9480. https://doi.org/10.1016/j.biortech.2011.07.103

Li, W., Khalid, H., Zhu, Z., Zhang, R., Liu, G., Chen, C., Thorin, E., 2018. Methane production through anaerobic digestion: Participation and digestion characteristics of cellulose, hemicellulose and lignin. Appl. Energy 226, 1219–1228. https://doi.org/10.1016/j.apenergy.2018.05.055

Mancini, G., Papirio, S., Lens, P.N.L., Esposito, G., 2018a. Anaerobic Digestion of

Lignocellulosic Materials Using Ethanol-Organosolv Pretreatment. Environ. Eng. Sci. 00, 1–8. https://doi.org/10.1089/ees.2018.0042

Mancini, G., Papirio, S., Lens, P.N.L., Esposito, G., 2018b. Increased biogas production from wheat straw by chemical pretreatments. Renew. Energy 119, 608–614. https://doi.org/10.1016/j.renene.2017.12.045

Mancini, G., Papirio, S., Lens, P.N.L., Esposito, G., 2016a. Effect of N-methylmorpholine-N-oxide Pretreatment on Biogas Production from Rice Straw, Cocoa Shell, and Hazelnut Skin. Environ. Eng. Sci. 33, 843–850. https://doi.org/10.1089/ees.2016.0138

Mancini, G., Papirio, S., Lens, P.N.L., Esposito, G., 2016b. Solvent Pretreatments of Lignocellulosic Materials to Enhance Biogas Production: A Review. Energy and Fuels 30, 1892–1903. https://doi.org/10.1021/acs.energyfuels.5b02711

Mata, T.M., Martins, A.A., Caetano, N.S., 2018. Bio-refinery approach for spent coffee grounds valorization. Bioresour. Technol. 247, 1077–1084. https://doi.org/10.1016/j.biortech.2017.09.106

McHugh, S., O'Reilly, C., Mahony, T., Colleran, E., O'Flaherty, V., 2003. Anaerobic granular sludge bioreactor technology. Rev. Environ. Sci. Biotechnol. 2, 225–245. https://doi.org/10.1023/B:RESB.0000040465.45300.97

Medina, E., Wellon, G.C., Evegren, F., 2017. Methanol Safe Handling Manual, 4th ed. Alexandria, USA.

Meng, X., Ragauskas, A.J., 2014. Recent advances in understanding the role of cellulose accessibility in enzymatic hydrolysis of lignocellulosic substrates. Curr. Opin. Biotechnol. 27, 150–158. https://doi.org/10.1016/j.copbio.2014.01.014

Mirmohamadsadeghi, S., Karimi, K., Zamani, A., Amiri, H., Sárvári Horváth, I., 2014. Enhanced solid-state biogas production from lignocellulosic biomass by organosolv pretreatment. Biomed Res. Int. 2014. https://doi.org/10.1155/2014/350414

Nagao, N., Tajima, N., Kawai, M., Niwa, C., Kurosawa, N., Matsuyama, T., Yusoff, F.M., Toda, T., 2012. Maximum organic loading rate for the single-stage wet anaerobic digestion of food waste. Bioresour. Technol. 118, 210–218. https://doi.org/10.1016/j.biortech.2012.05.045

Nielfa, A., Cano, R., Fdz-Polanco, M., 2015. Theoretical methane production generated by the co-digestion of organic fraction municipal solid waste and biological sludge. Biotechnol. Reports. https://doi.org/10.1016/j.btre.2014.10.005

Oliveros, N.O., Hernández, J.A., Sierra-Espinosa, F.Z., Guardián-Tapia, R., Pliego-Solórzano,

R., 2017. Experimental study of dynamic porosity and its effects on simulation of the coffee beans roasting. J. Food Eng. 199, 100–112. https://doi.org/10.1016/j.jfoodeng.2016.12.012

Ostovareh, S., Karimi, K., Zamani, A., 2015. Efficient conversion of sweet sorghum stalks to biogas and ethanol using organosolv pretreatment. Ind. Crops Prod. 66, 170–177. https://doi.org/10.1016/j.indcrop.2014.12.023

Papirio, S., 2020. Coupling acid pretreatment and dosing of Ni and Se enhances the biomethane potential of hazelnut skin. J. Clean. Prod. 262, 121407. https://doi.org/10.1016/j.jclepro.2020.121407

Paul, S., Dutta, A., 2018. Challenges and opportunities of lignocellulosic biomass for anaerobic digestion. Resour. Conserv. Recycl. 130, 164–174. https://doi.org/10.1016/j.resconrec.2017.12.005

Pellera, F.M., Gidarakos, E., 2018. Chemical pretreatment of lignocellulosic agroindustrial waste for methane production. Waste Manag. 71, 689–703. https://doi.org/10.1016/j.wasman.2017.04.038

Pellera, F.M., Gidarakos, E., 2016. Effect of substrate to inoculum ratio and inoculum type on the biochemical methane potential of solid agroindustrial waste. J. Environ. Chem. Eng. 4, 3217–3229. https://doi.org/10.1016/j.jece.2016.05.026

Perren, R., Escher, F.E., 2013. Impact of roasting on nut quality, in: Improving the Safety and Quality of Nuts. Woodhead Publishing Limited, pp. 173–197. https://doi.org/10.1533/9780857097484.2.173

Queirós, C.S.G.P., Cardoso, S., Lourenço, A., Ferreira, J., Miranda, I., Lourenço, M.J. V., Pereira, H., 2020. Characterization of walnut, almond, and pine nut shells regarding chemical composition and extract composition. Biomass Convers. Biorefinery 10, 175–188. https://doi.org/10.1007/s13399-019-00424-2

Reddy, N., Yang, Y., 2005. Biofibers from agricultural byproducts for industrial applications. Trends Biotechnol. 23, 22–27. https://doi.org/10.1016/j.tibtech.2004.11.002

Rincón, B., Bujalance, L., Fermoso, F.G., Martín, A., Borja, R., 2013. Biochemical methane potential of two-phase olive mill solid waste: Influence of thermal pretreatment on the process kinetics. Bioresour. Technol. 140, 249–255. https://doi.org/10.1016/j.biortech.2013.04.090

Saini, J.K., Saini, R., Tewari, L., 2015. Lignocellulosic agriculture wastes as biomass feedstocks for second-generation bioethanol production: concepts and recent

developments. 3 Biotech 5, 337–353. https://doi.org/10.1007/s13205-014-0246-5

Salapa, I., Katsimpouras, C., Topakas, E., Sidiras, D., 2017. Organosolv pretreatment of wheat straw for efficient ethanol production using various solvents. Biomass and Bioenergy 100, 10–16. https://doi.org/10.1016/j.biombioe.2017.03.011

Sameni, J., Krigstin, S., Sain, M., 2017. Solubility of Lignin and Acetylated Lignin in Organic Solvents. BioResources 12. https://doi.org/10.15376/biores.12.1.1548-1565

Sanchez, A., Hernández-Sánchez, P., Puente, R., 2019. Hydration of lignocellulosic biomass. Modelling and experimental validation. Ind. Crops Prod. 131, 70–77. https://doi.org/10.1016/j.indcrop.2019.01.029

Sawatdeenarunat, C., Surendra, K.C., Takara, D., Oechsner, H., Khanal, S.K., 2015. Anaerobic digestion of lignocellulosic biomass: Challenges and opportunities. Bioresour. Technol. 178, 178–186. https://doi.org/10.1016/j.biortech.2014.09.103

Sluiter, A., Hames, B., Hyman, D., Payne, C., Ruiz, R., Scarlata, C., Sluiter, J., Templeton, D., Wolfe J., 2008a. Determination of Total Solids in Biomass and Total Dissolved Solids in Liquid Process Samples. Natl. Renew. Energy Lab. Tech. Rep. NREL/TP-510-42621.

Sluiter, A., Hames, B., Ruiz, R., Scarlata, C., Sluiter, J., Templeton, D., 2008b. Determination of Ash in Biomass. Natl. Renew. Energy Lab. Tech. Rep. NREL/TP-510-42622.

Sluiter, A., Hames, B., Ruiz, R., Scarlata, C., Sluiter, J., Templeton, D., Crocker, D., 2008c. Determination of Structural Carbohydrates and Lignin in Biomass. Natl. Renew. Energy Lab. Tech. Rep. NREL/ TP -510 -42618.

Sluiter, A., Ruiz, R., Scarlata, C., Sluiter, J., Templeton, D., 2008d. Determination of Extractives in Biomass. Natl. Renew. Energy Lab. Tech. Rep. NREL/TP-510-42619.

Sulbarán-Rangel, B., Alarcón Aguirre, J.S., Breton-Deval, L., del Real-Olvera, J., Gurubel Tun, K.J., 2020. Improvement of Anaerobic Digestion of Hydrolysed Corncob Waste by Organosolv Pretreatment for Biogas Production. Appl. Sci. 10, 2785. https://doi.org/10.3390/app10082785

Thermtest Inc., 2017. Rule of Mixtures Calculator for Specific Heat Capacity [WWW Document]. URL https://thermtest.com/thermal-resources/rule-of-mixtures (accessed 5.20.20).

Tongbuekeaw, T., Sawangkeaw, R., Chaiprapat, S., Charnnok, B., 2020. Conversion of rubber wood waste to methane by ethanol organosolv pretreatment. Biomass Convers. Biorefinery. https://doi.org/https://doi.org/10.1007/s13399-020-00710-4

Vats, N., Khan, A.A., Ahmad, K., 2020. Options for Enhanced Anaerobic Digestion of Waste

and Biomass - a Review. J. Biosyst. Eng. 45, 1–15. https://doi.org/https://doi.org/10.1007/s42853-019-00040-y

World Bioenergy Association, 2019. Global bioenergy statistics.

Xu, N., Liu, S., Xin, F., Zhou, J., Jia, H., Xu, J., Jiang, M., Dong, W., 2019. Biomethane production from lignocellulose: Biomass recalcitrance and its impacts on anaerobic digestion. Front. Bioeng. Biotechnol. 7, 1–12. https://doi.org/10.3389/fbioe.2019.00191

Yarbrough, J.M., Himmel, M.E., Ding, S.Y., 2009. Plant cell wall characterization using scanning probe microscopy techniques. Biotechnol. Biofuels 2, 1–11. https://doi.org/10.1186/1754-6834-2-17

Yuan, T., Cheng, Y., Zhang, Z., Lei, Z., Shimizu, K., 2019. Comparative study on hydrothermal treatment as pre- and post-treatment of anaerobic digestion of primary sludge: Focus on energy balance, resources transformation and sludge dewaterability. Appl. Energy 239, 171–180. https://doi.org/10.1016/j.apenergy.2019.01.206

Yuan, W., Gong, Z., Wang, G., Zhou, W., Liu, Y., Wang, X., Zhao, M., 2018. Alkaline organosolv pretreatment of corn stover for enhancing the enzymatic digestibility. Bioresour. Technol. 265, 464–470. https://doi.org/10.1016/j.biortech.2018.06.038

Zhang, K., Pei, Z., Wang, D., 2016. Organic solvent pretreatment of lignocellulosic biomass for biofuels and biochemicals: A review. Bioresour. Technol. 199, 21–33. https://doi.org/10.1016/j.biortech.2015.08.102

Zheng, Y., Zhao, J., Xu, F., Li, Y., 2014. Pretreatment of lignocellulosic biomass for enhanced biogas production. Prog. Energy Combust. Sci. 42, 35–53. https://doi.org/10.1016/j.pecs.2014.01.001

Zhou, Z., Lei, F., Li, P., Jiang, J., 2018. Lignocellulosic biomass to biofuels and biochemicals: A comprehensive review with a focus on ethanol organosolv pretreatment technology. Biotechnol. Bioeng. 115, 2683–2702. https://doi.org/10.1002/bit.26788

*Chapter 4*

# Use of N-Methylmorpholine N-Oxide (NMMO) pretreatment to enhance the bioconversion of lignocellulosic materials to methane

A modified version of this chapter has been submitted for publication in *Biomass Conversion and Biorefinery* journal.

**Abstract**

Lignocellulosic materials (LMs) are one of the most abundant wastes produced worldwide. Nevertheless, unlocking the full energy potential from LMs for biofuel production is limited by their complex structure. This study investigated the effect of N-Methylmorpholine N-oxide (NMMO) pretreatment on almond shell (AS), spent coffee grounds (SCG), and hazelnut skin (HS) to improve their bioconversion to methane. The pretreatment was performed using a 73% NMMO solution heated at 120 °C for 1, 3, and 5 h. The baseline methane productions achieved from raw AS, SCG, and HS were 54.7 (± 5.3), 337.4 (± 16.5), and 265.4 (± 10.4) mL $CH_4$/g VS, respectively. The NMMO pretreatment enhanced the methane production potential of AS up to 58%, despite no changes in chemical composition and external surface were observed after pretreatment. Opposite to this, pretreated SCG showed increased porosity (up to 63%) and a higher sugar percentage (up to 27%) after pretreatment despite failing to increase methane production. All pretreatment conditions were effective on HS, achieving the highest methane production of 400.4 (± 9.5) mL $CH_4$/g VS after 5 h pretreatment. The enhanced methane production was due to the increased sugar percentage (up to 112%), lignin removal (up to 29%), and loss of inhibitory compounds during the pretreatment. An energy assessment revealed that the NMMO pretreatment is an attractive technology to be implemented on an industrial scale for energy recovery from HS residues.

## 4.1 Introduction

Anaerobic digestion (AD) is one of the most employed and successful strategies for biofuel production (Bianco et al., 2021a). The gaseous output of AD is biogas, a gas mixture mainly composed of carbon dioxide and methane that can be used for several applications depending on the purity and volume (Kapoor et al., 2020). The biogas produced has the advantage of being re-used on-site to maintain the digester temperature, as well as to ensure the energy self-sufficiency of the entire AD plant (Li et al., 2019).

Several substrates are employed for AD, including lignocellulosic materials (LMs). LMs mainly originate from farming crops, land management, agricultural and municipal activities, but also confectionery industry and commercial activities, such as bars and cafés (Battista et al., 2016; Lama et al., 2021b; Mancini et al., 2018a). These biomasses types generate disposal and management issues, impacting rural and urban areas (Lama et al., 2021a; Roy et al., 2021). Being among the most abundant wastes worldwide (Zoghlami and Paës, 2019) and due to their low supply cost (Lee and Park, 2020), LMs are highly favourable for bioenergy generation, with an estimated energy potential of 30 EJ per year (Dahunsi and Enyinnaya, 2019). However, the complex LM structure, mainly composed of cellulose, hemicellulose, and lignin, makes them often ill-suited for AD (Xu et al., 2019). For this reason, pretreatments are frequently employed to enhance the hydrolysis of cellulose and hemicellulose sugars, allowing a more profitable AD (Haldar and Purkait, 2021).

Among several LMs, nut residues are attracting the attention of many researchers due to their huge output and potential for biofuel production (Maestri et al., 2020). Global tree nut production has steadily increased in the last decade, reaching over 5.3 million metric tons in the harvesting season 2020/2021 (International Nut and Dried Fruit Council Foundation, 2021). The top producing countries are the USA, Turkey, and China, but nuts are exported all over the world, both shelled and unshelled. In particular, European countries cover over 30% of the global nuts consumption. The tree nut supply value rises year by year, reaching a value of 38.8 billion dollars in the 2020/2021 season (International Nut and Dried Fruit Council Foundation, 2021). However, the tree nut network also generates millions of tons of residues, causing environmental and disposal problems (Sharma et al., 2020). Indeed, most of the nut residues are nowadays still landfilled or incinerated (Sharma et al., 2020), losing significant amounts of high organic content to be alternatively valorised (Shen et al., 2018). Apart from nuts, the coffee production chain is also attractive for residue valorisation via AD (Ballesteros et al., 2014). In

particular, spent coffee grounds, representing the final waste produced during coffee production/consumption, is an opportunity for AD, with over 6 million tons of wastes produced every year (Ballesteros et al., 2014).

This study aims to investigate (i) the AD process and methane production potential of three raw LMs, i.e. almond shell (AS), spent coffee grounds (SCG), and hazelnut skin (HS) and (ii) the effect of N-Methylmorpholine N-oxide (NMMO) pretreatment on the LMs looking at the impact on both chemical composition and biochemical methane potential (BMP). NMMO is an organic solvent able to modify the cellulosic part of the biomass after being mixed with the LMs and heated at 90 - 130 °C (Satari et al., 2019). The effect on cellulose depends on the NMMO concentration, with cellulose fibres swelling up by creating balloons when increasing the NMMO concentration (Jeihanipour et al., 2010). The presence of swelled fibres enhances the biomass porosity, which is one of the most relevant factors for efficient anaerobic digestion, being an index of the accessible surface area for microbial attack (Oliva et al., 2022). When using 79% NMMO purity, the cellulose dissolution inside balloons occurs until the balloons break out, releasing the dissolved cellulose when the NMMO concentration exceeds 85% (Cuissinat and Navard, 2006). The dissolved cellulose can be regenerated by adding boiling water as an anti-solvent, obtaining a cellulose-rich material, with lower crystallinity and higher porosity (Mancini et al., 2016a). While 85% NMMO pretreatment leads to a lower degree of cellulose crystallinity, swelling (73%) and ballooning (79%) modes are more efficient in increasing the porosity of the cellulose (Jeihanipour et al., 2010). On the other hand, pretreatments with NMMO at concentrations lower than 70% are less effective on the cellulose swelling (Cuissinat and Navard, 2006).

A few studies investigated NMMO pretreatment to enhance the biodegradability of LMs, mainly focusing on straws and forest residues. However, the growing demand for alternative sources of (bio)energy triggers the exploration of untapped organic substrates, such as nut and coffee residues. Contrary to the most studied LMs, these substrates show higher lignin content and richness in non-structural compounds. The difference in chemical composition can result in different AD performance and effectiveness of pretreatment. In addition, most previous studies investigated the effect of NMMO at 85% concentration (Cheng et al., 2017; Kabir et al., 2014; Mancini et al., 2016b). However, a lower NMMO concentration not only allows a greater swelling of the cellulose fibres but can also reduce the overall costs of the pretreatment by decreasing the NMMO amount required for the process. Therefore, the present study focused

on investigating the efficiency of a low-NMMO concentration (i.e. 73%) pretreatment on the methane production from AS, SCG, and HS compared to the baseline performance, varying the pretreatment time from 1 to 3 and 5 h. The correlation between the BMP, chemical composition, and physical characteristics of the substrate was discussed. The kinetics of the AD process were studied by fitting the experimental data with a modified Gompertz model. An energy gain assessment was carried out to validate the viability of the NMMO pretreatment on a larger scale. Furthermore, economic, energetic and environmental aspects are discussed in the perspective of implementing the NMMO technology on an industrial scale.

## 4.2 Materials and methods

### *4.2.1 Substrate and inoculum*

Three LMs were used as substrates for AD, i.e. AS, SCG, and HS. The substrates were collected and prepared for AD as previously described by Oliva et al. (2021). HS and AS were cut down and sieved to select a particle size between 1 and 2.5 mm. The three substrates were stored in plastic bags at 4 °C prior to being pretreated or directly used in the AD experiments. The inoculum used as a source of microorganisms was a digestate from buffalo manure (DBM) obtained from a full-scale AD plant located in Eboli (Italy). The characterisation of the raw LMs and inoculum in terms of total (TS) and volatile solid (VS) is reported in Table 4.1. The DBM was characterised in detail in previous studies, where the same inoculum was used (Bianco et al., 2020a; Papirio, 2020).

**Table 4.1 –** Total (TS) and volatile (VS) solid of raw substrates, i.e. almond shell (AS), spent coffee grounds (SCG), hazelnut skin (HS), and inoculum, i.e. digestate from buffalo manure (DBM).

| | **AS** | **SCG** | **HS** | **DBM** |
|---|---|---|---|---|
| **TS** [a] (%) | 89.6 ± 0.1 | 87.4 ± 0.6 | 89.2 ± 0.3 | 4.8 ± 0.1 |
| **VS** [a] (%) | 88.1 ± 0.3 | 85.8 ± 0.5 | 86.6 ± 0.3 | 2.9 ± 0.0 |
| **VS/TS** (g/g) | 0.98 | 0.98 | 0.97 | 0.6 |

[a]TS and VS are based on g/100 g wet matter.

### *4.2.2 N-Methylmorpholine N-oxide pretreatment*

The NMMO pretreatment was performed by mixing 30 g of each substrate with 300 g of 73% (*w/w*) NMMO solution in 1000 mL Erlenmeyer flasks, keeping a substrate to solvent ratio of 1:10 (*w/w*) (Mancini et al., 2016b). The 73% NMMO solution was obtained by concentrating the commercial 50% (*w/w*) NMMO (Sigma-Aldrich, St. Louis, USA) using a R210/R215 rotary evaporator (Büchi, Flawil, Switzerland). The flasks containing the mixture LMs-NMMO were

heated and kept at 120 °C for 1, 3, and 5 h using an ONE22 oil bath (Memmert, Schwabach, Germany). Propyl gallate (ACROS organics, Dublin, Ireland) was added before heating the mixture to avert the oxidation of NMMO during the pretreatment (Mancini et al., 2016b). The mixing was done manually every 10 min using a glass stirring rod. After the pretreatment, boiling deionised water was added as an anti-solvent to break the reaction (Satari et al., 2019). The solid residues were placed in a textile cloth and washed with abundant boiling deionised water till a clear filtrate was obtained. The pretreated LMs were dried at 40 °C before undergoing AD.

*4.2.3 BMP tests and calculation of biogas production*

BMP batch tests were performed under mesophilic (37 ±1 °C) conditions in 250 mL serum glass bottles (OCHS, Bovenden, Germany). Each bottle was loaded with 1.5 g VS from DBM and 1 g VS from raw or pretreated AS, SCG, or HS. Demineralised water was added to adjust the final working volume to 150 mL, leaving 100 mL as headspace volume for the biogas accumulation. The final solids content of the AD process was 2.3% TS. Control biochemical tests were simultaneously carried out to evaluate the methane production obtained from the inoculum only. Each bottle was flushed for 2 min with argon gas (flow rate of 5 L/min) to ensure anaerobic conditions and then left at atmospheric pressure. All the experiments were performed in triplicate, and the bottles were shaken manually once per day.

The biogas production was quantified by measuring the pressure difference of the headspace volume between two sampling points using a Leo 1 pressure reader (Keller, Winterthur, Switzerland). The pressure value was then converted into volume following the ideal gas law (W. Li et al., 2018). The carbon dioxide and methane content were evaluated through an Einhorn saccharometer (Glass studio, Naples, Italy), filled with 12% NaOH solution and thymolphthalein (Sigma-Aldrich, St. Louis, USA) as pH indicator (Yazdani et al., 2019; Zeynali et al., 2017). The net cumulative methane production achieved from the AD of raw and NMMO pretreated LMs was calculated as the average of the biological triplicates after subtracting the methane production of the controls. The methane production was recorded regularly until the daily accumulation in all bottles was below 1% of the cumulative methane production (Holliger et al., 2016).

*4.2.4 Analytical methods*

TS and VS of raw and pretreated LMs as well as of the inoculum and the final digestate were determined as described by Sluiter at al. (2008a, 2008b), using a TCN115 convection oven

(Argo Lab, Carpi, Italy) and a BWF 11/13 muffle furnace (Carbolite, Sheffield, UK), respectively. VS degradation during AD was estimated by comparing the initial and final VS content measured for each bottle.

The water retention capacity (WRC), an indicator of the accessible interior surface area, of raw and pretreated LMs was measured as suggested by Sanchez et al. (2019). The external surface area of raw and pretreated LMs was observed through scanning electron microscopic (SEM) images, using the procedure and the equipment previously described by Oliva et al. (2021). The untreated and NMMO pretreated LMs were analysed with a Nicolet iS5 Fourier-transform infrared (FTIR) spectrometer (Thermo Fisher Scientific, Waltham, USA) to evaluate the crystalline structure of the cellulose by determining the lateral order index (LOI) of the samples. LOI was obtained as the ratio between the absorbance at 1420 $cm^{-1}$, representative of the crystalline fraction of the cellulose, and the absorbance at 898 $cm^{-1}$, representative of the amorphous cellulose (Carrillo et al., 2004). The analysis was done in triplicate, and the data were averaged over 16 runs with a resolution of 4 $cm^{-1}$ in the 4000 - 400 $cm^{-1}$ region.

The characterisation of raw and pretreated LMs in terms of extractives, structural carbohydrates, total lignin and ashes was performed as previously reported by Oliva et al. (2021), following the protocols of Sluiter at al. (2008c, 2008d). Firstly, the extractives were removed with a sequential extraction using water and 95% ethanol solution as solvents. Afterwards, the extractives-free LMs underwent a two-step acid hydrolysis using 72 and 4% (*w/w*) $H_2SO_4$ at 30 and 121 °C, respectively. Liquor and acid-insoluble residues were separated by filtration. The acid-soluble lignin was determined spectrophotometrically at 205 nm. The Klason lignin was estimated gravimetrically by subtracting the acid-insoluble ash from the acid-insoluble residues. The speciation of the structural carbohydrates solubilised in the two-step hydrolysis was obtained with a ICS-3000 Ion Chromatography System (DIonex, Sunnyvale, USA).

Volatile fatty acids (VFAs) accumulation and degradation during the AD process were monitored by sampling 1.5 mL of the liquid phase from each bottle seven times during the first 14 days of the experiment. The samples were stored and prepared for analysis as described by Papirio (2020). The method and equipment used for VFAs analysis are reported by Bianco et al. (2020b). The pH of the liquid samples was measured using a HI-98103 pH meter (Hanna Instruments, Woonsocket, USA).

*4.2.5 Kinetic model*

The kinetics of methane production obtained from raw and pretreated HS, SCG, and AS were evaluated by fitting the experimental data with a modified Gompertz model (Hassan et al., 2017), using Eq. (4.1):

$$G(t) = G_m \cdot \exp\left\{-exp\left[\frac{R_m \cdot e}{G_m} \cdot (\lambda - t) + 1\right]\right\} \quad (4.1)$$

where t (d) is the time of the AD process, G(t) (mL $CH_4$/g VS) is the cumulative specific methane production achieved at t (d), $G_m$ (mL $CH_4$/g VS) and $R_m$ (mL $CH_4$/g VS·d) are the maximum specific methane production potential and rate estimated by the model, respectively, e = exp (1), and λ (d) is the lag phase time.

The model fitting was performed using the Origin2018 software (OriginLab Corporation, Northampton, USA). The correlation coefficient ($r^2$) between experimental and model data was evaluated with the Excel 2016 software (Microsoft Corporation, Redmond, USA).

*4.2.6 Energy assessment*

In this study, an energy balance of the whole process was performed using the following hypotheses:

a) 1 $m^3$ (1 m long by 1 m wide by 1 m high) stainless steel tank (Figure 4.1) was used to perform the NMMO pretreatment.
b) The tank can treat 90 kg of LMs immersed in 900 kg of NMMO solution, following the substrate to solvent ratio used in the present study (i.e. 1:10 *w/w*).
c) The sides and the bottom surface of the tank are thermally insulated with cork layers (thickness = 20 cm). The heat loss through these surfaces is negligible due to the low thermal conductivity of cork, i.e. 0.045 W/(m·°C) (Knapic et al., 2016).
d) The upper surface of the tank is covered with a polyethylene plate (thickness = 3 cm) during the NMMO pretreatment to limit heat loss.
e) The tank is already at working temperature (i.e. 120 °C). The ambient temperature is 20 °C.

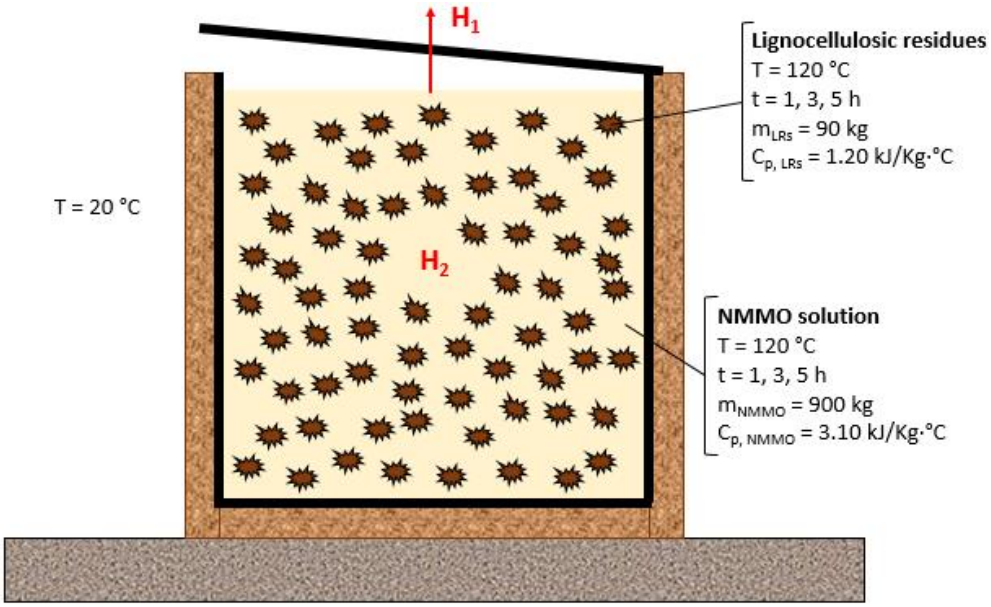


**Figure 4.1 –** Operating parameters, specific heat capacity values, and a schematic representation of the tank assumed to be used for the NMMO pretreatment while performing the energetic assessment.

Under these conditions, the energy required to keep the stainless steel tank at the operating temperature depends on the heat loss from the upper surface to the environment ($H_1$) and on the energy used to heat the NMMO solution and the LMs immersed in the tank ($H_2$). The two aliquots were calculated using Eq. (4.2) and Eq. (4.3):

$$H_1 = U \cdot A \cdot \frac{\Delta T}{\Delta x} \cdot t_p \quad (4.2)$$

$$H_2 = \left(m_{NMMO} \cdot C_{p,NMMO} + m_{LRs} \cdot C_{p,LRs}\right) \cdot \frac{\Delta T}{3600} \quad (4.3)$$

where U (0.45 W/(m·°C) (Curry and Pillay, 2015)) is the thermal conductivity of the upper surface of the tank, A (1 $m^2$) is the upper surface of the cubic tank, ΔT (100 °C) is the difference between operating and ambient temperature, Δx (0.03 m) is the thickness of the insulating plate used to cover the tank, $t_p$ (h) is the pretreatment time, $m_{NMMO}$ (900 kg) and $m_{LMs}$ (90 kg) are the masses of the 73% NMMO solution and LMs, respectively, $C_{p,\,NMMO}$ (3.10 kJ/kg·°C) is the specific heat capacity of the 73% NMMO solution, calculated considering the $C_p$ of water and an 85% NMMO solution (Mancini et al., 2016b), $C_{p,\,LMs}$ (1.20 kJ/kg·°C (Lo et al., 2017)) is the specific heat capacity of LMs, and 3600 is the conversion factor between kJ and kWh.

The energy gain ($E_p$) from the increment of methane production after the NMMO pretreatment was calculated according to Mancini et al. (2018a), considering the difference in methane production between pretreated and raw substrates according to Eq. (4.4). The specific methane

production potential was rectified using an upscale factor of 0.85 to account for the difference between laboratory and real scale AD conditions (Alonso-Fariñas et al., 2020).

$$E_P = \left(SMP_{pretreated} - SMP_{raw}\right) \cdot \xi \cdot CHP \quad (4.4)$$

where $SMP_{pretreated}$ and $SMP_{raw}$ (kg $CH_4$/kg VS) are the specific methane production potential from pretreated and raw substrates, $\xi$ is the lower heating value of methane (13.9 kWh/kg $CH_4$), and CHP (0.5) is the efficiency of a combined heat and power unit, equal to 50%.

About 85% of the energy used to reach and maintain the pretreatment temperature (i.e. $H_1$ + $H_2$) can be recovered by heat exchangers (Mancini et al., 2018a), accounting for a positive aliquot ($E_{r,H}$) in the energy balance here proposed. The overall energy balance ($\Delta E$) is therefore described by Eq. (4.5):

$$\Delta E = E_p - H_1 - H_2 + E_{r,H} \quad (4.5)$$

*4.2.7 Statistical analysis*

The BMP, WRC, and LOI of raw and pretreated substrates were compared by one-way analysis of variance (ANOVA) followed by the Tukey post hoc test. The Pearson correlation coefficient (r) between BMP and pretreatment time, the changes in lignocellulosic composition (i.e. extractives, sugars, and lignin content) and WRC of each substrate was evaluated with the Pearson test. The correlation was considered strong when r was higher than 0.8 (Akoglu, 2018). All analyses were performed with Minitab 17 Statistical Software (Minitab LCC, USA). The difference was considered statistically significant when p was < 0.05.

## 4.3 Results

*4.3.1 Changes in lignocellulosic composition after the NMMO pretreatment*

Raw and pretreated substrates were characterised in terms of cellulose and hemicellulose sugars, lignin, and extractive content. The chemical composition analysis (Figure 4.2 and Table 4.2) showed that raw AS, SCG, and HS have a lignin content of 29.2, 18.8, and 44.2% (based on the dry matter), respectively. Raw AS showed a 43% total sugar percentage, mainly constituted by glucan (22%) and xylan (19%). On the other hand, raw SCG sugars were primarily composed of mannan (24%) and galactan (9%), while glucan represented only 9% of the overall sugar content. The total sugar percentage of raw HS was lower than that of raw AS and raw SCG, representing only 14% of the dry matter, with glucan being the main constituent (10%). The compositional analysis also revealed abundant extractives in the raw substrates, in particular for SCG (30%) and HS (28%).

The NMMO treatment affected the composition of the substrates differently (Table 4.2). AS lost up to 45% of the extractives during the NMMO pretreatment, but no significant effect was observed on the cellulose, hemicellulose, and lignin content. NMMO pretreated SCG showed a higher sugar percentage (+ 27%) compared to the raw SCG, mainly related to glucan (+ 57%). As regards to HS, the NMMO pretreatment removed up to 30% of the total lignin content. Also, the glucan percentage increased by 120% in the most performing pretreatment condition. SCG and HS respectively lost up to 37 and 49% of the extractives during the pretreatment.

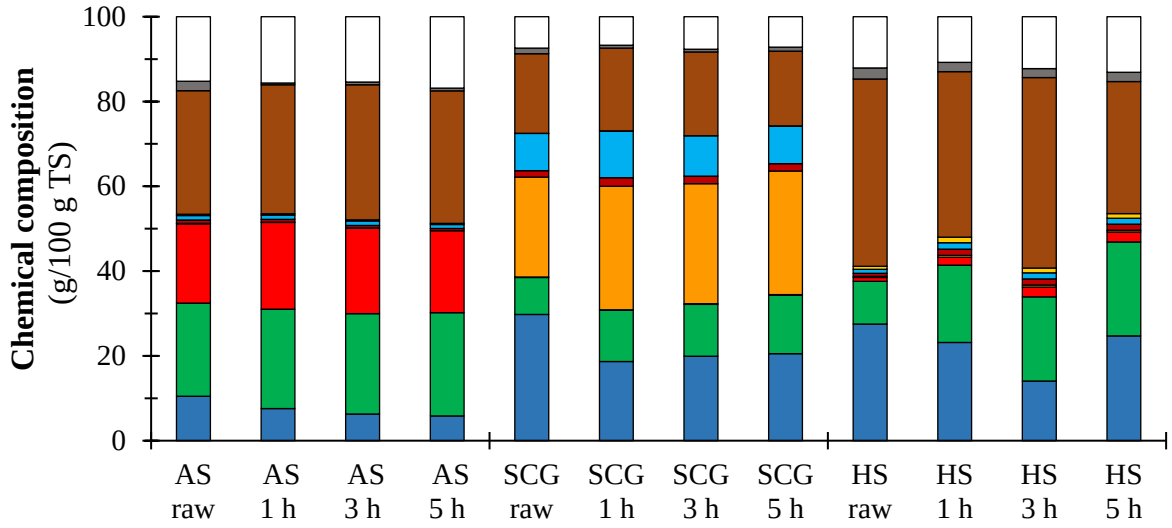


**Figure 4.2 –** Chemical composition of raw and NMMO pretreated substrates: full extractives (■), glucan (■), xylan (■), mannan (■), arabinan (■), galactan (■), rhamnan (■), total lignin (■), ashes (■), and unknown matter (□). AS: almond shell, SCG: spent coffee grounds, and HS: hazelnut skin. Pretreatment time exposure: 1, 3, 5 h.

**Table 4.2 –** Chemical composition of raw and NMMO pretreated substrates expressed as full extractives, structural sugars (glucan, xylan, mannan, arabinan, galactan, and rhamnan), total lignin (Klason lignin and acid soluble lignin), and ashes content. AS: almond shell, SCG: spent coffee grounds, and HS: hazelnut skin. Pretreatment time exposure: 1, 3, and 5 h.

| **Substrate** | **Full Extractives[a]** (%) | **Total Sugars[a, c]** (%) | **Total Lignin[a, b]** (%) | **Ashes[a]** (%) | **Unknown[d]** (%) | **Glucan[a]** (%) | **Xylan[a]** (%) | **Mannan[a]** (%) | **Arabinan[a]** (%) | **Galactan[a]** (%) | **Rhamnan[a]** (%) | **Klason Lignin[a]** (%) | **Acid Soluble Lignin[a]** (%) |
|---|---|---|---|---|---|---|---|---|---|---|---|---|---|
| AS raw | 10.5 ± 0.1 | 42.9 ± 0.1 | 29.2 ± 0.2 | 2.2 ± 0.1 | 15.2 | 22.0 ± 0.3 | 18.7 ± 0.5 | 0.1 ± 0.0 | 0.8 ± 0.0 | 1.1 ± 0.0 | 0.3 ± 0.0 | 27.7 ± 0.2 | 1.5 ± 0.0 |
| AS 1 h | 7.6 ± 0.0 | 45.9 ± 0.1 | 30.4 ± 0.1 | 0.4 ± 0.0 | 15.6 | 23.4 ± 0.1 | 20.5 ± 0.2 | 0.1 ± 0.0 | 0.6 ± 0.0 | 1.0 ± 0.0 | 0.3 ± 0.0 | 28.4 ± 0.1 | 2.1 ± 0.0 |
| AS 3 h | 6.3 ± 0.2 | 45.8 ± 0.7 | 31.9 ± 0.7 | 0.7 ± 0.2 | 15.4 | 23.7 ± 0.3 | 20.2 ± 0.4 | 0.1 ± 0.0 | 0.6 ± 0.0 | 1.0 ± 0.0 | 0.3 ± 0.0 | 29.8 ± 0.7 | 2.0 ± 0.0 |
| AS 5 h | 5.8 ± 0.2 | 45.4 ± 0.3 | 31.3 ± 0.1 | 0.7 ± 0.0 | 16.8 | 24.3 ± 0.2 | 19.3 ± 0.1 | 0.0 ± 0.0 | 0.5 ± 0.0 | 1.0 ± 0.1 | 0.3 ± 0.0 | 29.6 ± 0.1 | 1.7 ± 0.0 |
| SCG raw | 29.8 ± 0.4 | 42.8 ± 0.1 | 18.8 ± 0.1 | 1.3 ± 0.1 | 7.4 | 8.7 ± 0.0 | 0.1 ± 0.0 | 23.5 ± 0.0 | 1.5 ± 0.0 | 8.8 ± 0.1 | 0.1 ± 0.0 | 16.8 ± 0.1 | 1.9 ± 0.0 |
| SCG 1 h | 18.7 ± 0.1 | 54.4 ± 0.2 | 19.5 ± 0.1 | 0.7 ± 0.0 | 6.7 | 12.1 ± 0.1 | 0.1 ± 0.0 | 29.1 ± 0.3 | 2.0 ± 0.0 | 11.0 ± 0.0 | 0.1 ± 0.0 | 16.8 ± 0.1 | 2.7 ± 0.0 |
| SCG 3 h | 19.9 ± 0.0 | 52.0 ± 0.3 | 19.8 ± 0.3 | 0.6 ± 0.0 | 7.7 | 12.2 ± 0.3 | 0.1 ± 0.0 | 28.3 ± 0.1 | 1.8 ± 0.0 | 9.5 ± 0.0 | 0.0 ± 0.0 | 17.7 ± 0.3 | 2.1 ± 0.0 |
| SCG 5 h | 20.5 ± 0.1 | 53.7 ± 0.4 | 17.6 ± 0.2 | 0.9 ± 0.2 | 7.2 | 13.8 ± 0.1 | 0.1 ± 0.1 | 29.2 ± 0.2 | 1.7 ± 0.0 | 8.9 ± 0.0 | 0.1 ± 0.0 | 16.1 ± 0.2 | 1.5 ± 0.1 |
| HS raw | 27.5 ± 0.4 | 13.6 ± 0.3 | 44.2 ± 0.3 | 2.6 ± 0.1 | 12.1 | 10.1 ± 0.2 | 0.9 ± 0.0 | 0.3 ± 0.0 | 0.7 ± 0.0 | 0.9 ± 0.0 | 0.7 ± 0.0 | 42.7 ± 0.3 | 1.5 ± 0.0 |
| HS 1 h | 23.2 ± 0.2 | 24.8 ± 0.1 | 39.0 ± 0.5 | 2.2 ± 0.0 | 10.8 | 18.2 ± 0.1 | 1.8 ± 0.0 | 0.5 ± 0.1 | 1.5 ± 0.0 | 1.5 ± 0.0 | 1.3 ± 0.1 | 37.5 ± 0.4 | 1.5 ± 0.1 |
| HS 3 h | 14.1 ± 0.6 | 26.6 ± 0.3 | 44.9 ± 0.3 | 2.1 ± 0.2 | 12.2 | 19.8 ± 0.2 | 2.3 ± 0.1 | 0.5 ± 0.1 | 1.4 ± 0.0 | 1.4 ± 0.0 | 1.1 ± 0.0 | 43.5 ± 0.2 | 1.5 ± 0.0 |
| HS 5 h | 24.7 ± 0.5 | 28.8 ± 0.5 | 31.2 ± 0.2 | 2.2 ± 0.1 | 13.1 | 22.1 ± 0.3 | 2.4 ± 0.1 | 0.4 ± 0.0 | 1.4 ± 0.1 | 1.4 ± 0.1 | 1.1 ± 0.1 | 29.5 ± 0.2 | 1.7 ± 0.0 |

[a] *Based on the dry matter (g/100 g TS).*

[b] *Total lignin is calculated as the sum of acid soluble lignin and Klason lignin* (Sluiter et al., 2008c).

[c] *Total sugars are obtained as the sum of glucan, xylan, mannan, arabinan, galactan, and rhamnan.*

[d] *The unknown matter is calculated as the complement to 100 of the other components.*

*4.3.2 Effect of the NMMO pretreatment on external surface area, porosity and crystallinity*

The SEM images reported in Figure 4.3 illustrate the structural changes observed in the external surface between raw and pretreated LMs. Raw AS (Figure 4.3A) shows a slivered, hard and compact surface. The NMMO pretreatment appears to be able to smooth the AS outer surface (Figure 4.3B, 4.3C, 4.3D), although looking still dense and tough. Raw SCG (Figure 4.3E) shows a stringy surface, which remains nearly untouched by the pretreatment (Figure 4.3F, 4.3G, and 4.3H). On the other hand, HS shows the most appreciable effects of the cellulose swelling caused by the NMMO pretreatment, among the three substrates. The external surface of raw HS (Figure 4.3I) is compact, and the cellulose filaments appear thin and embodied in the lignocellulosic structure. The NMMO pretreatment (Figure 4.3J, 4.3K, and 4.3L) swelled the filaments, increasing the exposure of the cellulosic part of HS to the enzymatic attack. In particular, the 5 h pretreatment seems able to break down part of the cell wall of HS. Some of the cellulose filaments are more exposed and appear crimped and vulnerable (Figure 4.3L).

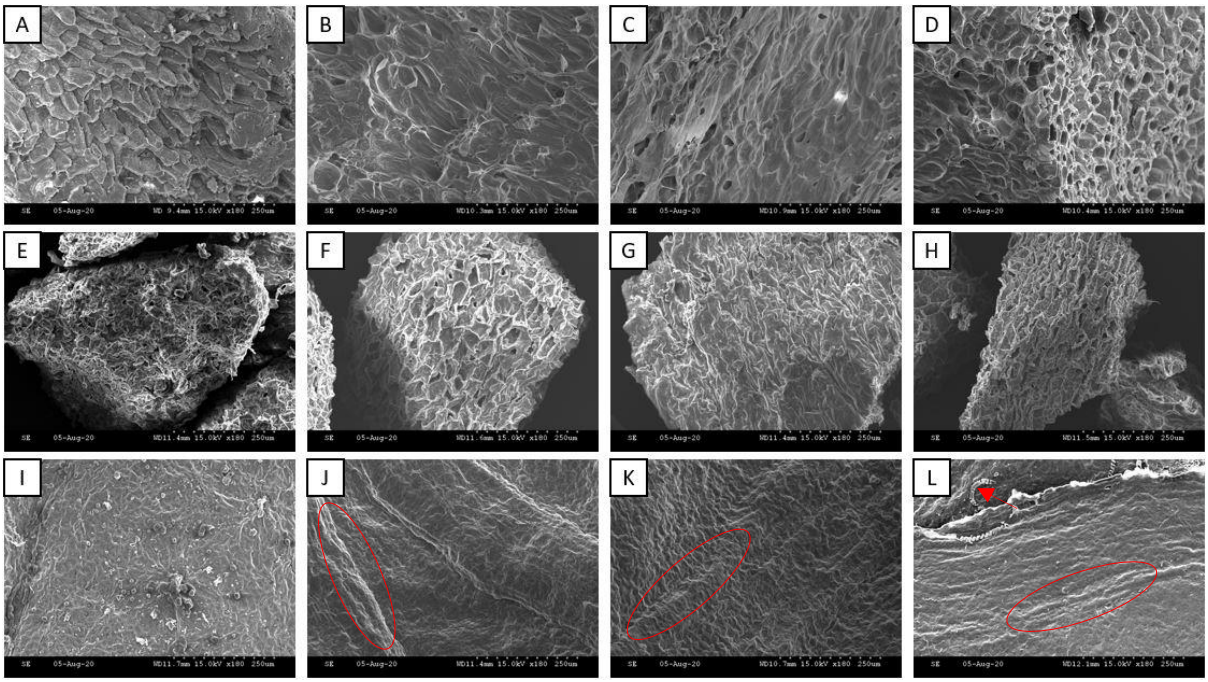


**Figure 4.3 –** Scanning electron microscopic images of the external surface area of raw and NMMO pretreated substrates. Raw AS (A), 1 h pretreated AS (B), 3 h pretreated AS (C), and 5 h pretreated AS (D). Raw SCG (E), 1 h pretreated SCG (F), 3 h pretreated SCG (G), and 5 h pretreated SCG (H). Raw HS (I), 1 h pretreated HS (J), 3 h pretreated HS (K), and 5 h pretreated HS (L). AS: almond shell, SCG: spent coffee grounds, and HS: hazelnut skin. Pretreatment time exposure: 1, 3, and 5 h.

To further inspect the bioaccessible surface area of the LMs, the WRC of the raw and pretreated substrates was measured, as an indicator of porosity. Table 4.3 shows that the 5 h NMMO

pretreatment significantly increased ($p < 0.05$) the WRC of AS from 0.53 to 0.59 g $H_2O$/g TS. On the other hand, all the other pretreatment conditions lowered the AS porosity. The WRC of SCG was significantly higher ($p < 0.05$) after the NMMO pretreatment. The highest porosity was observed for the 3 h NMMO pretreated SCG, increasing the WRC by 63%. Finally, in the case of HS, the porosity significantly increased ($p < 0.05$) proportionally to the pretreatment time. The WRC of HS rose from 1.76 to 2.20 g $H_2O$/g TS in the most performing pretreatment condition (i.e. 5 h).

The FTIR analysis shows a significant reduction ($p < 0.05$) of the LOI for AS and HS under all pretreatment conditions tested. On the other hand, no significant change ($p > 0.05$) in the crystallinity index of SCG was observed (Table 4.3). The spectra of the FTIR analysis are reported in Figure 4.4.

**Table 4.3 –** Water retention capacity (WRC) and lateral order index (LOI) followed by statistical comparison of raw and pretreated substrates with 73% NMMO solution. AS: almond shell, SCG: spent coffee grounds, and HS: hazelnut skin. Pretreatment time exposure: 1, 3, and 5 h.

| **Substrate** | **WRC** (g $H_2O$/g TS) | **Statistical information** [a] | **LOI** (A1420/A898) | **Statistical information** [a] |
|---|---|---|---|---|
| AS raw | 0.53 ± 0.00 | b | 2.18 ± 0.24 | a |
| AS 1 h | 0.45 ± 0.02 | c | 1.02 ± 0.03 | c |
| AS 3 h | 0.47 ± 0.03 | c | 1.03 ± 0.02 | c |
| AS 5 h | 0.59 ± 0.02 | a | 1.38 ± 0.04 | b |
| SCG raw | 1.12 ± 0.03 | c | 1.39 ± 0.13 | a |
| SCG 1 h | 1.81 ± 0.01 | ab | 1.57 ± 0.30 | a |
| SCG 3 h | 1.83 ± 0.06 | a | 1.56 ± 0.23 | a |
| SCG 5 h | 1.72 ± 0.02 | b | 1.46 ± 0.06 | a |
| HS raw | 1.76 ± 0.04 | c | 3.89 ± 0.40 | a |
| HS 1 h | 1.77 ± 0.05 | c | 1.38 ± 0.12 | b |
| HS 3 h | 2.01 ± 0.06 | b | 1.31 ± 0.24 | b |
| HS 5 h | 2.20 ± 0.11 | a | 1.40 ± 0.07 | b |

[a] Not sharing letters means that the condition was significantly different ($p < 0.05$) with the compared condition.

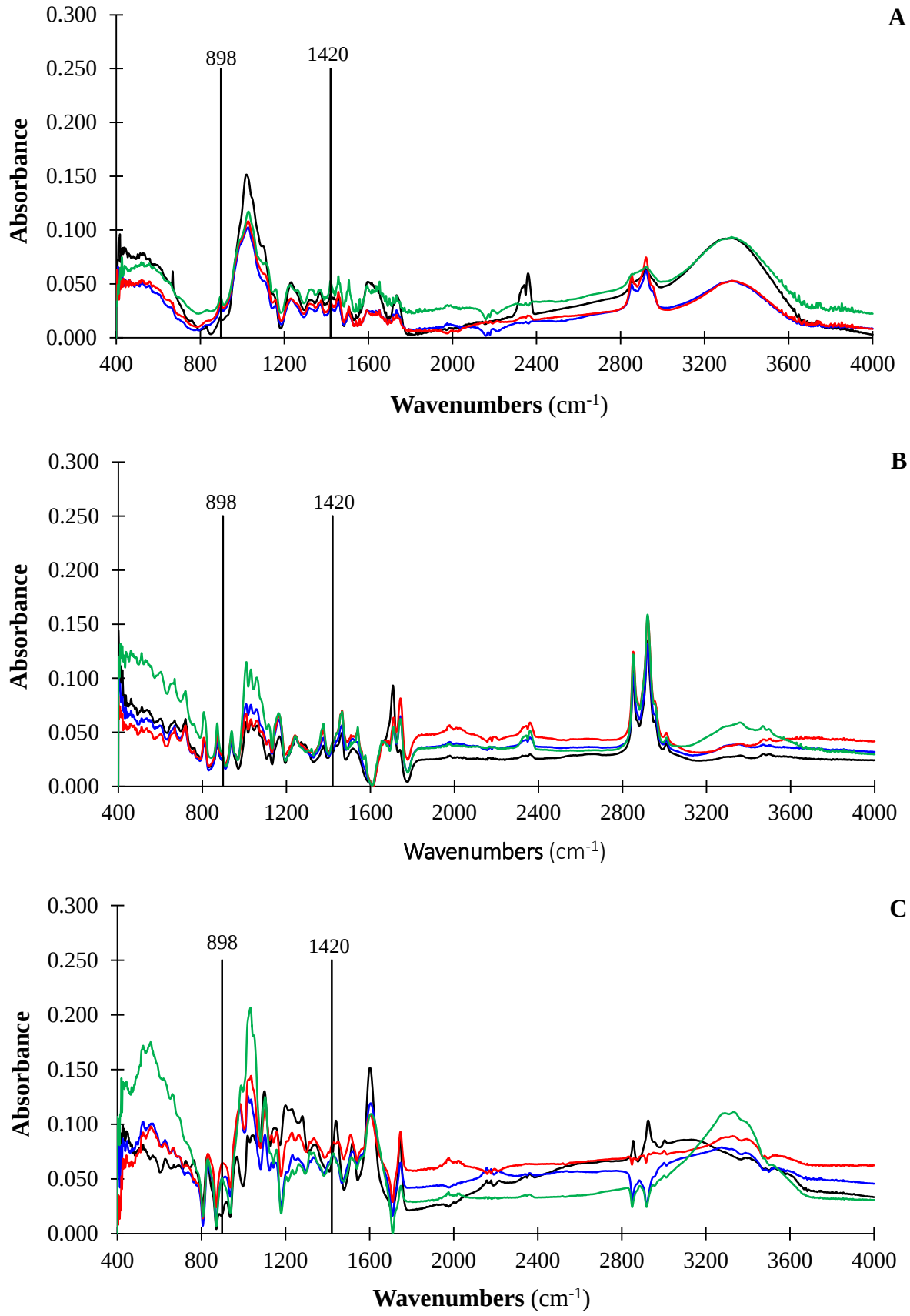


**Figure 4.4 –** Spectra obtained from the FTIR analysis of raw (▬) and NMMO pretreated, i.e. 1 h (▬), 3 h (▬), 5 h (▬), almond shell (A), spent coffee grounds (B), and hazelnut skin (C). Pretreatment time exposure: 1, 3, 5 h.

*4.3.3 Impact of the NMMO pretreatment on methane production and kinetics*

The net cumulative methane production achieved from the AD of raw and NMMO pretreated LMs is given in Table 4.4. Figure 4.5 shows the methane production evolution over the 45 days of AD. The AD of untreated LMs showed the high BMP of raw SCG and raw HS, which reached 337.4 (± 16.5) and 265.4 (± 10.4) mL $CH_4$/g VS, respectively. On the other hand, the BMP of raw AS was only 54.7 (± 5.3) mL $CH_4$/g VS.

The NMMO pretreatment was significantly ($p < 0.05$) effective on AS by increasing the BMP up to 86.1 (± 2.0) mL $CH_4$/g VS (Figure 4.5A). The best pretreatment condition corresponded to the longer pretreatment time. Nevertheless, a pretreatment of 3 h also showed an appreciable ($p < 0.05$) enhancement (25%) of the methane production from AS. Similarly, the 3 h and 5 h NMMO pretreatment improved the BMP of HS by 31 and 51%, respectively, reaching a maximum BMP of 400.4 (± 9.5) mL $CH_4$/g VS (Figure 4.5C). Regarding HS, the 1 h pretreatment also showed a significant ($p < 0.05$) enhancement in methane production, i.e. by 14%. On the contrary, none of the pretreatment conditions tested in this study was significantly effective on SCG in terms of methane production (Figure 4.5B). A slight 8% increase of the BMP was observed for the 3 h and 5 h pretreated SCG, not being statistically significant ($p > 0.05$).

The kinetic analysis showed a high correlation with the modified Gompertz model used to fit the experimental data (Table 4.4). The model fitting confirmed the pretreatment effectiveness on AS and HS, with the experimental BMP achieving 98% of the maximum methane production potential ($G_m$) estimated by the model. The 73% NMMO pretreatment enhanced the maximum specific methane production rate ($R_m$) of AS from 2.95 to 3.15, 3.76, and 4.58 mL $CH_4$/g VS/d for the 1, 3, and 5 h pretreated AS, respectively. However, all the pretreatment conditions increased the lag phase ($\lambda$) of AD for AS. The $R_m$ of HS increased up to 34% when the NMMO pretreatment lasted 5 h. No significant change of $\lambda$ was observed by pretreating the HS, apart from the 3 h pretreatment, which resulted in a decreased $\lambda$ to 3.7 days. Interestingly, the experimental data showed that the NMMO pretreatment led to a delay of the peak of methane production rate only in the case of HS.

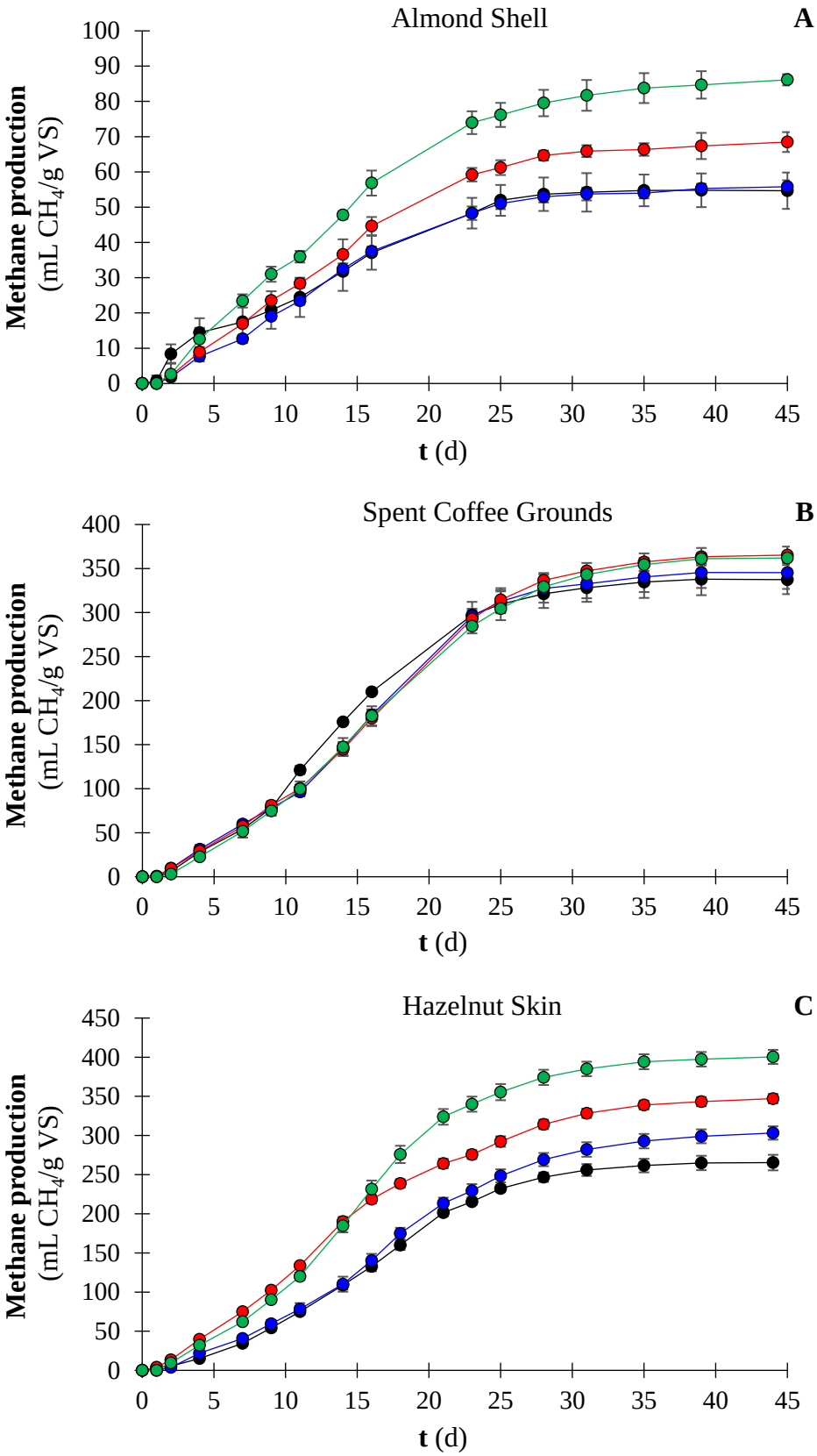


**Figure 4.5 –** Cumulative methane production from anaerobic digestion of almond shell (A), spent coffee grounds (B), and hazelnut skin (C): untreated (●), 1 h NMMO (●), 3 h NMMO (●), 5 h NMMO (●) exposure. Pretreatment time exposure: 1, 3, and 5 h.

**Table 4.4 –** Biochemical methane potential (BMP) followed by statistical comparison and kinetic parameters, i.e. maximum specific methane production potential (Gm), maximum specific methane production rate (Rm), lag phase (λ), and correlation coefficient (r2), obtained from the anaerobic digestion process of raw and pretreated substrates with 73% NMMO solution. AS: almond shell, SCG: spent coffee grounds, and HS: hazelnut skin. Pretreatment time exposure: 1, 3, and 5 h.

| **Substrate** | **BMP** (mL $CH_4$/g VS) | **Statistical information** [a] | **Methane production increment** (%) | **$G_m$** [b] (mL $CH_4$/g VS·d) | **$R_m$** [b] (mL $CH_4$/g VS·d) | **λ** [b] (d) | **$r^2$** [c] |
|---|---|---|---|---|---|---|---|
| AS raw | 54.7 ± 5.3 | c | - | 55.90 | 2.95 | 1.7 | 0.9852 |
| AS 1 h | 55.8 ± 2.2 | c | 2.1 | 55.81 | 3.15 | 3.3 | 0.9982 |
| AS 3 h | 68.5 ± 3.1 | b | 25.2 | 68.51 | 3.76 | 3.3 | 0.9970 |
| AS 5 h | 86.1 ± 2.0 | a | 57.5 | 86.01 | 4.58 | 3.0 | 0.9962 |
| SCG raw | 337.4 ± 16.5 | a | - | 339.69 | 21.10 | 5.0 | 0.9981 |
| SCG 1 h | 345.3 ± 18.5 | a | 2.3 | 348.22 | 20.47 | 5.2 | 0.9904 |
| SCG 3 h | 365.2 ± 9.7 | a | 8.3 | 369.52 | 19.76 | 5.3 | 0.9939 |
| SCG 5 h | 361.9 ± 4.9 | a | 7.3 | 366.84 | 19.64 | 5.8 | 0.9973 |
| HS raw | 265.4 ± 10.4 | d | - | 269.58 | 14.56 | 5.4 | 0.9953 |
| HS 1 h | 303.2 ± 9.0 | c | 14.2 | 308.97 | 15.01 | 5.7 | 0.9971 |
| HS 3 h | 347.1 ± 6.7 | b | 30.8 | 351.62 | 17.30 | 3.7 | 0.9972 |
| HS 5 h | 400.4 ± 9.5 | a | 50.9 | 403.18 | 23.18 | 5.1 | 0.9973 |

[a] Not sharing letters means that the condition was significantly different ($p < 0.05$) with the compared condition.

[b] Predicted by fitting the experimental data with a modified Gompertz model.

[c] Correlation coefficient between experimental and model data.

*4.3.4 Volatile solid degradation and volatile fatty acids evolution during anaerobic digestion*

The percentage of VS degraded during the AD process (Figure 4.6) accounted for 13, 71, and 24% for raw AS, SCG, and HS, respectively. The pretreatment with 73% NMMO significantly ($p < 0.05$) enhanced the VS biodegradation of AS up to 21%. On the other hand, no significant difference ($p > 0.05$) was observed in VS degraded from raw and pretreated SCG. Regarding HS, all pretreatment durations considerably increased the amount of biodegradable matter ($p < 0.05$), with the increment being positively correlated with the pretreatment time and reaching 54% in the case of 5 h NMMO pretreatment.

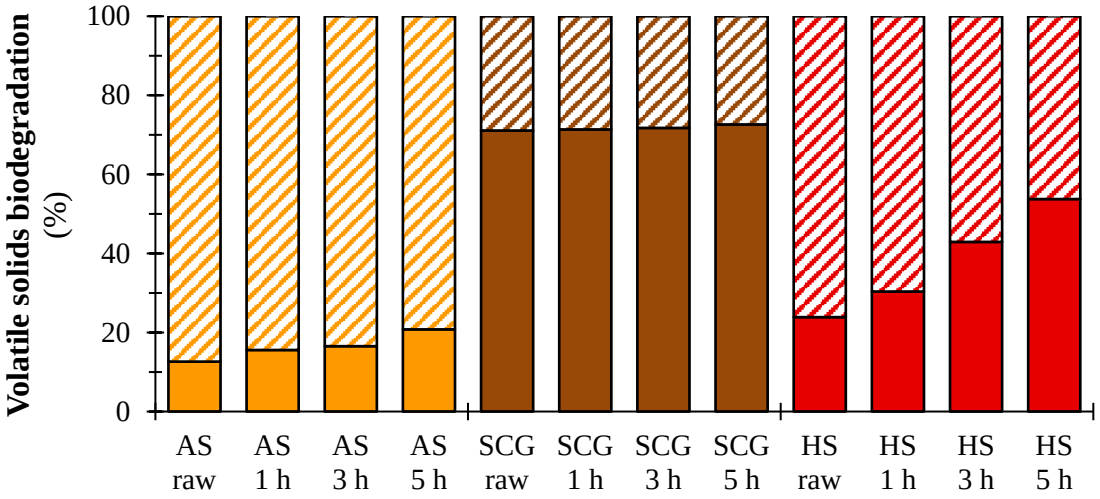


**Figure 4.6 –** Biodegraded (full bars) and leftover (dashed bars) volatile solids of raw and pretreated substrates after 45 days of anaerobic digestion: AS (), SCG (), and HS (). AS: almond shell, SCG: spent coffee grounds, and HS: hazelnut skin. Pretreatment time exposure: 1, 3, and 5 h.

The VFAs evolution was monitored along with the AD process of raw and pretreated substrates. The total VFAs concentration is reported in Figure 4.7 as acetic acid equivalent. Acetic and propionic acid were the main acids produced during the AD of SCG and HS (data not shown). On the contrary, acetic acid was the sole VFA detected during AD of AS (data not shown), which entailed the maximum VFAs concentration on day 0 of the experiment (Figure 4.7A). In particular, the VFAs concentration on day 0 of AD of AS was significantly higher when digesting raw (i.e. 317 mg $HAc_{eq}$/L) rather than pretreated (i.e. 31 mg $HAc_{eq}$/L) substrates. The VFAs evolution was similar for raw and pretreated SCG (Figure 4.7B). The maximum concentration was observed on day 7 for untreated (i.e. 390 mg $HAc_{eq}$/L), 3 h (i.e. 292 mg $HAc_{eq}$/L) and 5 h (i.e. 207 mg $HAc_{eq}$/L) NMMO pretreated SCG. On the other hand, in the case of 1 h NMMO pretreated SCG, the VFAs concentration was almost stable between day 7 (i.e. 327 mg $HAc_{eq}$/L) and 14 (i.e. 371 mg $HAc_{eq}$/L). As regards to HS (Figure 4.7C), the highest

VFAs accumulation was observed on day 4 for the 3 h NMMO pretreated HS (i.e. 211 mg $HAc_{eq}$/L), while the peak was obtained on day 7 for the other pretreatment conditions.

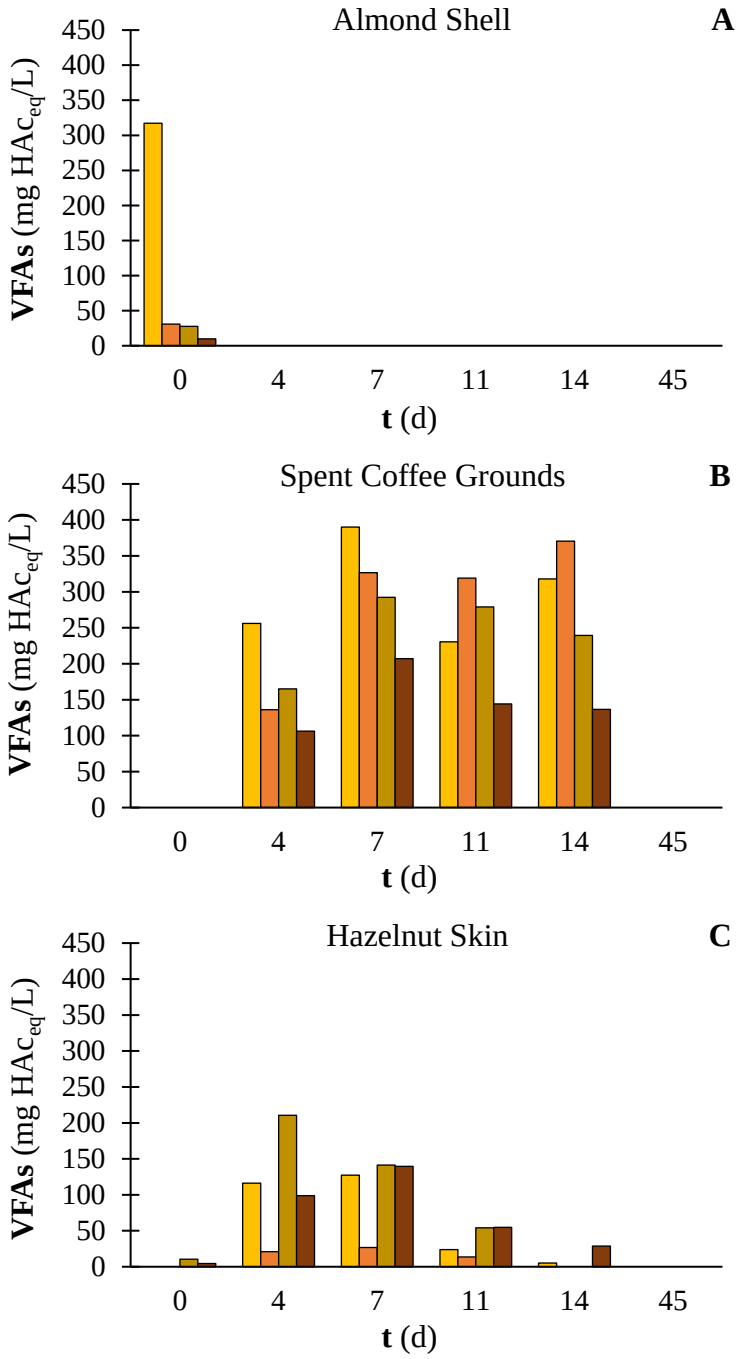


**Figure 4.7 –** Volatile fatty acids (VFAs) accumulation during the AD of untreated and pretreated AS (A), SCG (B), and HS (C): untreated (■), 1 h NMMO (■), 3 h NMMO (■), 5 h NMMO (■) exposure. AS: almond shell, SCG: spent coffee grounds, and HS: hazelnut skin. Pretreatment time exposure: 1, 3, and 5 h.

*4.3.5 Energy saving*

The energy balance performed in this study (Table 4.5) revealed the feasibility of applying the NMMO pretreatment for HS, giving an energy gain of 0.18 and 0.40 kWh/kg VS after 3 h and 5 h pretreatment, respectively. On the other hand, the energy assessment returned a negative energy balance for pretreated AS and SCG.

**Table 4.5 –** Energy balance (ΔE) calculated considering energy costs (H1 and H2), energy recovered by heat exchangers (Er, H), and energy gain from the extra methane produced (EP) from pretreated substrates. AS: almond shell, SCG: spent coffee grounds, and HS: hazelnut skin. Pretreatment time exposure ($t_p$): 1, 3, and 5 h.

| **Substrate** | **$t_p$** (h) | **$H_1$** (kWh) | **$H_2$** (kWh) | **$E_{r,H}$** (kWh) | **$E_P$** (kWh) | **ΔE** (kWh) | **ΔE** (kWh/kg VS) |
|---|---|---|---|---|---|---|---|
| AS 1 h | 1 | 1.5 | 80.47 | 69.67 | 0.38 | -11.92 | -0.15 |
| AS 3 h | 3 | 4.5 | 80.47 | 72.22 | 4.63 | -8.12 | -0.10 |
| AS 5 h | 5 | 7.5 | 80.47 | 74.77 | 10.55 | -2.64 | -0.03 |
| SCG 1 h | 1 | 1.5 | 80.47 | 69.67 | 2.57 | -9.72 | -0.13 |
| SCG 3 h | 3 | 4.5 | 80.47 | 72.22 | 9.09 | -3.65 | -0.05 |
| SCG 5 h | 5 | 7.5 | 80.47 | 74.77 | 8.00 | -5.19 | -0.07 |
| HS 1 h | 1 | 1.5 | 80.47 | 69.67 | 12.46 | 0.17 | 0.00 |
| HS 3 h | 3 | 4.5 | 80.47 | 72.22 | 26.95 | 14.20 | 0.18 |
| HS 5 h | 5 | 7.5 | 80.47 | 74.77 | 44.52 | 31.32 | 0.40 |

## 4.4 Discussion

*4.4.1 Anaerobic digestion of untreated almond shells, spent coffee grounds, and hazelnut skin*

The AD of the three raw LMs under investigation showed that SCG and HS had a high BMP compared to most studied agricultural and industrial LMs (Li et al., 2013; Shen et al., 2018), producing 337.4 and 265.4 mL $CH_4$/g VS, respectively (Table 4.4). On the other hand, raw AS only produced 54.7 mL $CH_4$/g VS (Table 4.4), being in the range of methane production from that of other nut shells observed by Shen et al. (2018).

One of the most important factors hindering the AD of LMs is the lignin content (Zoghlami and Paës, 2019). The three substrates used in this study showed different chemical compositions, but all have a rather high lignin content (Table 4.2), i.e. 29.2, 18.8 and, 44.2% (based on the dry matter), respectively for AS, SCG, and HS. Based on the lignin content only, HS was expected to be the most recalcitrant substrate among the three. Nevertheless, the experimental evidence showed that many other factors affect the AD of LMs.

AS was indeed the least suitable substrate for AD, resulting in the lowest methane production among the raw substrates (Figure 4.5). This result is consistent with previous studies, where a

methane production of 45.4 (± 8.7) mL $CH_4$/g VS was achieved (Shen et al., 2018). Other studies reported an even lower BMP of AS, i.e. 20.2 (± 13.0) mL $CH_4$/g VS (Nitsos et al., 2015) and 23.2 (± 9.6) mL $CH_4$/g VS (Oliva et al., 2021). The low BMP did not reflect the cellulose (22.0%) and hemicellulose (21.0%) content of the AS here used, suggesting a greater potential of AS for AD (Paul and Dutta, 2018). Nevertheless, the scarce WRC (0.53 g $H_2O$/g TS), the high LOI (i.e. 2.18), and the hard external surface of AS (Table 4.3 and Figure 4.3A) most likely prevented the microorganisms to attack the substrate, resulting in slow and inefficient AD (Mancini et al., 2018b). The VFAs evolution observed in the present study (Figure 4.7A) suggests that AS has a remarkable aliquot of extractives easily soluble in aqueous solution, which immediately hydrolysed and were likely converted into VFAs peaking at 317.3 (± 24.0) mg $HAc_{eq}$/L on day 0 (Figure 4.7A). On the other hand, the absence of VFAs accumulated during the subsequent days of AD indicates that the hydrolysis of cellulose and hemicellulose from AS is slow, with methanogenic archaea acting at the same speed of hydrolytic and acidogenic bacteria (Li et al., 2019).

On the contrary, SCG and HS showed a higher BMP (Table 4.4). In particular, in this study, HS produced 265.4 (± 10.4) mL $CH_4$/g VS. This result is comparable with previous studies where the same substrate was used (Mancini et al., 2018a, 2016b; Papirio, 2020). A significantly lower methane production was obtained from HS (i.e. 17.3 mL $CH_4$/g VS) when using a granular sludge as the source of microorganisms (Oliva et al., 2021). This evidence highlighted that not only the physical and chemical characteristics of the substrate but also the type of inoculum greatly affects the AD process, as previously observed by Gu et al. (2014) for rice straw. The methane obtained from SCG was 337.4 (± 16.5) mL $CH_4$/g VS. This value is comparable with the available literature regarding the AD of SCG under similar operative conditions (Girotto et al., 2018; Kim et al., 2017). Contrary to HS, the AD of SCG seems to be less susceptible to the type of inoculum since no significant difference was observed with Chapter 3 where a granular sludge was used (Oliva et al., 2021). The VFAs analysis (Figure 4.7B, 4.7C) reflected the usual trend of LMs, with slow hydrolysis and maximum VFAs accumulation after a few days of AD (Annamalai et al., 2020). In particular, the maximum VFAs accumulation was observed on day 7, with a concentration of 389.9 (± 33.2) and 127.4 (± 86.7) mg $HAc_{eq}$/L for SCG and HS, respectively (Figure 4.7B, 4.7C).

The higher biodegradability of SCG and HS is due to the physical characteristics of the substrates. SCG and HS showed a significantly higher WRC than AS (Table 4.3). The LOI

indicates that mainly crystalline cellulose prevails in HS, while SCG is composed of both crystalline and amorphous cellulose (Table 4.3 and Figure 4.4). Besides, the external surface of SCG and HS appeared smoother than that of AS (Figure 4.3). The results obtained in this study are in accordance with previous works (Yu et al., 2019), where the porosity and other physical characteristics of LMs were key factors for efficient AD (Hernández-Shek et al., 2020). As a further aspect, the measurement of the leftover VS at the end of the experiment confirmed the recalcitrance of AS and HS (Figure 4.6). Only 12.6 and 23.9% of the overall volatile matter was degraded after 45 days of AD for raw AS and HS, respectively (Figure 4.6). On the other hand, 71.1% of the VS from SCG was degraded during the AD process (Figure 4.6).

### *4.4.2 NMMO pretreatment effectiveness on lignocellulosic substrates*

#### *4.4.2.1 Almond shell*

The pretreatment with a 73% NMMO solution was effective on AS, achieving the maximum BMP (86.1 mL/g VS) from the 5 h pretreated AS and increased by 58% compared with the raw AS (Table 4.3). The effect of the pretreatment increased with its duration (Figure 4.5A), showing a strong direct correlation, i.e. r = 0.980. Nevertheless, the maximum methane production obtained in this study is still far from the theoretical methane production potential, i.e. 490 mL/g VS (Oliva et al., 2021). The low methane production is reflected by the limited VS degradation (Figure 4.6). The highest VS degradation (21%) occurred for the 5 h NMMO pretreated AS after 45 days of AD, meaning that the microorganisms did not degrade most of the available VS. The non-degraded VS (Figure 4.6) certainly includes lignin, which represents 31.3% of the 5 h pretreated AS composition (Table 4.2). Only fungi and specific strains of bacteria are able to decompose lignin thanks to their selective enzymatic system (Mei et al., 2020; Schneider et al., 2020). Thus, it is very likely that most of the initial lignin content remained unaltered after AD (Li et al., 2021), eventually accounting for non-degraded VS, which is one of the aspects contributing to the low BMP of raw and pretreated AS.

The NMMO pretreatment did not lead to significant changes in sugars and lignin content of AS (Table 4.2 and Figure 4.2), in line with the results obtained for other substrates such as flower waste (Gopal et al., 2021) and wheat straw (Mancini et al., 2018b). Thus, the enhanced methane production observed with the pretreated substrate is attributed to other aspects. In particular, the NMMO pretreatment reduced the ratio between crystalline and amorphous cellulose, i.e. LOI, under all pretreatment conditions (Table 4.3 and Figure 4.4), indicating a higher biodegradability of the pretreated AS (Purwandari et al., 2013). Also, the WRC of AS increased

from 0.53 to 0.59 g $H_2O$/g TS after 5 h of pretreatment (Table 4.3). Mancini et al. (2018b) obtained similar results for wheat straw using an 85% NMMO pretreatment for 3 h. In that study, WRC increased from 1.30 to 1.90 g $H_2O$/g TS resulting in an 11% increment in methane production. On the other hand, in the present study, no effect was observed on the 3 h and 1 h pretreated AS in terms of WRC. The increment in methane production from 3 h pretreated AS (i.e. 25.2%) might be, therefore, associated with the strength of the cellulose-hemicellulose-lignin linkage that is likely weakened by the NMMO pretreatment, as previously observed by Cheng et al. (2017) for cassava residues. In addition, a moderate inverse correlation, i.e. r = -0.776, was observed between the extractives content and BMP of AS. This correlation could be due to inhibitory compounds initially present in the extractives of AS that were lost during the pretreatment (Tajmirriahi et al., 2021a).

Although the outer surface of the pretreated AS is smoother than for the raw substrate (Figure 4.3A-D), it looks resistant and leathery, confirming that the pretreatment did not significantly alter the physical structure of the substrate. In a previous study, Oliva et al. (2021) investigated the effectiveness of methanol-organosolv pretreatment on AS. In that case, the pretreatment affected neither the external surface nor the porosity of the substrate, resulting in no increment in the methane production. A longer NMMO pretreatment or a different, more aggressive pretreatment, such as acid or alkaline pretreatment, may be tested to disrupt the hard and compact structure of AS. Nevertheless, previous studies reported that longer NMMO pretreatment may result in loss of hemicellulose sugars (Shafiei et al., 2014; Teghammar et al., 2012). Overall, the low porosity and the highly resistant outer surface, together with the high lignin content, explain the low BMP of raw and pretreated AS.

As regards to the trend of VFAs (Figure 4.7A), the higher concentration observed on day 0 reflects the methane production of the following days (1 - 4) from raw AS. Methane production from raw AS was higher compared to the pretreated AS (Figure 4.5A) until day 4, resulting in a shorter lag-phase (Table 4.4). The lower VFAs concentration observed on day 0 in the bottles with the pretreated AS was likely due to the loss of non-structural sugars during NMMO pretreatment. Acidogenic bacteria can easily convert free sugars in VFAs, allowing faster methane production in the first days of AD (Wainaina et al., 2019). The failure to accumulate VFAs during the AD progress probably suggests that the hydrolysis rate was still low, despite the NMMO pretreatment enhancing the VS biodegradability of AS (Figure 4.6).

*4.4.2.2 Spent coffee grounds*

The cumulative methane production obtained from SCG was similar for the raw and pretreated substrate (Figure 4.5B), showing that NMMO pretreatment was ineffective for SCG. In this study, depending on the pretreatment condition, the BMP of SCG ranged between 337.4 and 365.3 mL $CH_4$/g VS (Table 4.4). Several studies focused on SCG for biofuels or valuable biomolecules production (Battista et al., 2021; Kim et al., 2019). Nevertheless, only Girotto et al. (2018) reported a methane production slightly higher than that here obtained, showing that an 8% NaOH pretreatment allowed to produce 392 mL $CH_4$/g VS from SCG. The VFAs evolution (Figure 4.7B) follows the trend previously observed during AD of LMs, i.e. a peak within the first 10 days of the process followed by a gradual decrease in VFAs concentration (Zuo et al., 2020). The maximum VFAs concentration was observed on day 7, i.e. 390 mL $HAc_{eq}$/L (Figure 4.7B) and is significantly below the overall VFAs inhibitory threshold of 6000 mg/L (Lee et al., 2017).

The WRC of SCG significantly increased after the NMMO pretreatment (Table 4.3), with the maximum porosity (i.e. 1.83 g $H_2O$/g TS) corresponding to the 3 h NMMO pretreated SCG. This is in agreement with the increment of porosity reported by Shafiei et al. (2014) for pinewood. In addition, the pretreatment allowed increasing the sugar percentage by up to 25% (mainly glucan and mannan) along with the pretreatment duration (Table 4.2) due to the loss of other components, i.e. extractives. Teghammar et al. (2012) obtained similar results performing an 85% NMMO pretreatment on spruce and triticale straw, increasing the methane production potential of these substrates but also observing a loss of hemicellulose sugars when increasing the pretreatment time. On the other hand, Teghammar et al. (2012) showed that pretreatment times longer than 1 h reduced the glucan content and lowered the methane production potential of rice straw. On the contrary, in the present study, the higher sugar percentage achieved with NMMO pretreatment did not affect the methane production from SCG. The loss of extractives from 30 to 37% during the pretreatment can explain this result. SCG are rich in free sugars, proteins and fatty acids that microorganisms can easily convert into methane under anaerobic conditions. The loss of these molecules most probably reduced the methane production potential of SCG (Battista et al., 2021).

The ineffectiveness of the NMMO pretreatment on SCG is also linked to the high VS degradation observed for raw SCG. In fact, despite the considerable lignin percentage (i.e. 19%), 71% of the initial VS embedded in the raw SCG was degraded after AD, and the rate of

VS degradation did not significantly increase after NMMO pretreatment (Figure 4.6). The non-degraded solids include lignin, which barely changed after the NMMO pretreatment (Table 4.2 and Figure 4.2). The VS degradation rate observed for SCG is comparable with the result reported by Li et al. (2018) for a much easily biodegradable substrate, i.e. food waste. The lignin content and the VS degradation might suggest that not much further methane production potential can be gained from the investigated SCG. An alternative approach can lead to a better utilisation of the single component of this substrate, by, for instance, extracting valuable extractives from SCG before subjecting it to any pretreatment. The cascade approach would allow recovering molecules with high commercial value while providing a simpler substrate for AD (Rasi et al., 2019).

*4.4.2.3 Hazelnut skin*

The BMP of HS increased from 265.5 up to 400.4 mL $CH_4$/g VS after the NMMO pretreatment. The effectiveness is strongly correlated (r = 0.996) with the pretreatment time, with the 5 h NMMO pretreatment enhancing methane production up to 51% (Table 4.4 and Figure 4.5C). The increased total sugar content (r = 0.886) and WRC (r = 0.951) of pretreated HS were strongly correlated with the increase in BMP (Table 4.2, Table 4.3 and Table 4.4), following the results obtained by Kabir et al. (2014) with barley straw at a maximum pretreatment time of 7 h. The LOI of HS decreased from 3.90 to approximately 1.40, regardless of the pretreatment exposure (Table 4.3 and Figure 4.4), as previously observed by Purwandari et al. (2013) Moreover, the increased VS degradation (Figure 4.6) reflected the enhanced BMP achieved after the pretreatment.

The NMMO pretreatment altered the external surface of HS and exposed the swelled cellulose filaments, as enlightened in Figure 4.3J, 4.3K, and 4.3L. Similarly, the NMMO pretreatment is able to change the external surface of pinewood and oil palm empty fruit bunch enhancing the bioavailability of the cellulosic component of the LMs (Purwandari et al., 2013; Shafiei et al., 2014). The chemical structure of NMMO presents weak N-O polar bonds that can be easily broken to form new hydrogen bonds with cellulose in aqueous solutions. The NMMO solution penetrates the cell wall, increases its internal osmotic pressure, and expands the cellulosic fibers creating balloons. Inside the balloons, depending on the NMMO concentration and characteristics of the substrates, cellulose dissolution can occur. When the osmotic pressure exceeds the membrane resistance, the balloons explode, thus releasing dissolved cellulose (Wikandari et al., 2016).

The VFAs evolution (Figure 4.7C) revealed that the highest concentration (i.e. 211 mg $HAc_{eq}$/L) was observed at day 4 and corresponded to the 3 h pretreated HS, which was the pretreatment condition showing the best performance in terms of methane production at that time of the AD process (Figure 4.5C). After day 4, the VFAs concentration in the same bottles decreased and reflected the drop of methane production observed after day 14.

Mancini et al. (2016b) previously studied the effectiveness of NMMO pretreatment on HS under dissolution mode conditions (i.e. a NMMO concentration of 85%). In that case, no significant difference in methane production was observed between raw and pretreated HS. On the contrary, the swelling mode (i.e. 73%) was effective under all pretreatment conditions in the present study. This confirmed the result obtained with cotton by Jeihanipour et al. (2010), who observed an increased BMP only using 73 and 79% NMMO solutions during the pretreatment. Furthermore, Purwandari et al. (2013) showed that a 1 h 73% NMMO pretreatment was more effective than that performed at 85% for oil palm empty fruit bunch.

The effectiveness of the NMMO pretreatment here performed is attributable to lignin removal and, consequently, an increased sugars percentage (up to 112%). A moderate inverse correlation, i.e. r = - 0.708, was observed between the lignin content and methane production. In particular, the highest lignin removal (i.e. 29%) was observed after the 5 h pretreatment. Although lignin attack is not one of the expected effects of NMMO pretreatment (Mancini et al., 2016a), a long exposure time to the NMMO solution at high temperature (i.e. 120 °C) can remove part of the lignin. Other authors previously reported a significant lignin removal upon performing 75% NMMO pretreatment for 15 h, while shorter pretreatments using 85% NMMO solution did not remarkably affect the lignin content of forest residues (Aslanzadeh et al., 2014). Teghammar et al. (2012) reported a 34% lignin removal from triticale straw after a 15 h pretreatment with 85% NMMO solution, but no effect on the lignin content was observed when using a shorter pretreatment time. On the other hand, other authors did not report any change in lignin content from forest residues and barley straw after 30 h pretreatment using an 85% NMMO solution (Kabir et al., 2014). The results of the present study and the available literature suggest that lignin removal during NMMO pretreatment mainly depends on the specific characteristics of the substrate and is more likely to occur when performing the pretreatment at lower NMMO concentrations.

To the best of the authors' knowledge, the present work is the first study showing significant delignification (i.e. up to 29%) of highly lignified materials after short exposure time NMMO

pretreatment. Kabir et al. (2013) reported only a 7% lignin removal from forest residues after 15 h pretreatment. The effectiveness of lignin removal can be related to the high WRC of raw HS (i.e. 1.76 g $H_2O$/g TS), which allowed the solvent to penetrate the substrate faster than in other LMs (Oliva et al., 2021). Unfortunately, none of the authors who observed lignin removal after NMMO pretreatment reported substrate characterisation in terms of porosity. Thus, this hypothesis still needs confirmation with further studies.

The content and type of extractives also influence the biodegradability of LMs (Tajmirriahi et al., 2021a). Extractives include primary substrates for the AD process, such as non-structural sugars, proteins and fats, but also phenolic compounds, which negatively affected the AD of LMs (Tajmirriahi et al., 2021a, 2021b). In particular, Kayembe et al. (2013) showed that the number of hydroxyl groups on the aromatic compounds was inversely related to the toxicity of the phenolic monomers during AD. HS is indeed an extractive-rich LM (Table 4.2), with polyphenols representing 7% of the overall composition (Spagnuolo et al., 2021). A selective polyphenols removal from HS before AD can, thus, provide the dual benefit of recovering valuable compounds and removing inhibitors for the subsequent valorisation process (Covarrubias-García and Arriaga, 2022; Metsämuuronen and Sirén, 2019).

### *4.4.3 Scale-up perspective of the NMMO pretreatment: economical, energetic and environmental remarks*

In the present study, the NMMO pretreatment under improved operating conditions enhanced the BMP of AS and HS (Table 4.4). Nevertheless, a preliminary energy assessment demonstrated that a considerable extra methane production is required to counterbalance the pretreatment costs. This analysis showed that only the NMMO pretreated HS led to an energetic advantage (i.e. $\Delta E = 0.40$ kWh/kg VS, at best) in the bioconversion process (Table 4.5). On the other hand, Mancini et al. (2016b) did not achieve any energy gain by treating the same substrate with an 85% NMMO solution.

The energy gain obtained in the present study can be theoretically extended to the global production of hazelnuts, i.e. 512,100 tons/year (International Nut and Dried Fruit Council Foundation, 2021), considering a correction factor of 0.03 to take into account the percentage (*w/w*) of the whole fruit becoming a waste (Spagnuolo et al., 2021). A preliminary economic evaluation considering the energy average world price of 0.14 $/kWh (Bianco et al., 2021b) estimates an economic gain of roughly 75 million $/year by pretreating the HS under the operating conditions proposed in the present study.

A preliminary energetic and economic analysis is essential to evaluate the feasibility of using the NMMO pretreatment. Nevertheless, when evaluating the implementation of the pretreatment on an industrial scale, further aspects should be considered. For instance, the washing of the LMs and the recovery and reuse of the solvent are crucial aspects to reduce the costs of NMMO pretreatment. NMMO is indeed an expensive reagent, but has the advantage of being environmentally friendly and efficiently recoverable (up to 99%) (Satari et al., 2019). NMMO can be recovered by evaporating the extra water used to wash the LMs. Shafiei et al. (2011) showed that multistage evaporation units are up to 80% more efficient than a single stage for energy savings. In particular, the costs for water evaporation greatly increase when concentrating NMMO from 70 to 86% (Shafiei et al., 2011). The strong hydrogen bonds between water and NMMO require a further elevation of the evaporating temperature by 30 °C to obtain the 86% NMMO solution (Shafiei et al., 2011), increasing the process costs and the risk for NMMO degradation and side reactions (Guo et al., 2021). Therefore, using the 73% NMMO solution proposed in the present study rather than the most commonly investigated 85% NMMO solution for LMs pretreatment could offset the overall costs of the NMMO pretreatment process.

The effectiveness of recovered NMMO is still debated and seems to be related to the initial chemical composition of the LM. Recovered NMMO was effective on pure cellulose and barley straw (Jeihanipour et al., 2010; Kabir et al., 2014). On the other hand, the effectiveness was up to 55% lower for forest residues (Kabir et al., 2014). The lower performance of recovered NMMO seems to be related to the presence of extractives such as tannins, phenols and acid resins hydrolysed during the pretreatment. Therefore, the suggestion of recovering these compounds before pretreating the substrates for AD is furtherly endorsed. It is also fair to point out that Kabir et al. (2014) performed a much longer (i.e. 30 h) NMMO pretreatment compared to that of the present study, and the use of propyl gallate to stabilise the reaction was not reported in that study. Therefore, the failure of reusing the NMMO solution shown by Kabir et al. (2014) for forest residues is likely to be due to the solvent degradation caused by side reactions occurring during the pretreatment (Guo et al., 2021).

The techno-economic study proposed by Teghammar et al. (2014) revealed that the amount of LMs treated by the NMMO unit is another crucial aspect of the process. In that study, the pretreatment of at least 50000 tons (dried weight) of forest residues per year allowed an efficient NMMO pretreatment. Apart from the economic perspective, environmental impact is a critical

aspect when dealing with the pretreatment of LMs. In particular, NMMO pretreatment was compared with steam explosion via life cycle assessment, showing that the bioenergy gain due to NMMO pretreatment is more environmentally sustainable in terms of resources, climate change, ecosystem quality, and human health (Khoshnevisan et al., 2016).

The NMMO treatment also has the advantage of being already a well-known process on an industrial scale since it is worldwide used in the Lyocell process in the textile industry (Wikandari et al., 2016). To the best of the authors' knowledge, the NMMO pretreatment has not yet been implemented on an industrial scale for LMs pretreatment. Nevertheless, in that perspective, using a less concentrated NMMO solution would make the process for LMs pretreatment more similar to the Lyocell process, where the NMMO concentrations range from 60 to 75%, which means working with technologies already applied on an industrial scale (Wikandari et al., 2016).

### 4.5 Conclusion

Swelling mode (i.e. 73%) NMMO pretreatment is an effective technique to increase the methane production potential of AS and HS. The pretreatment time was a key parameter, resulting in different effects on chemical composition, physical characteristics and methane production potential of the LMs involved in the study. Of the three LMs, AS and HS were positively impacted after pretreatment improving the extraction of potential energy through methane production by 58 and 51%, respectively. The NMMO pretreatment increased the BMP of AS up to 86.1 mL $CH_4$/g VS. Nevertheless, the energy balance revealed that the extra methane produced did not compensate for the pretreatment costs. No significant change in the BMP of SCG was observed, despite the higher sugar percentage and WRC. On the other hand, NMMO pretreatment enhanced the AD from HS, increasing the methane production by 14, 31, and 51% after 1, 3, and 5 h pretreatment, respectively. The methane gain was the consequence of an increased sugar concentration, lower lignin content and LOI, and higher porosity. In addition, the loss of phenolic compounds may have positively influenced the AD process. The energetic balance revealed that the NMMO pretreatment is attractive for HS, showing a positive energy gain of 0.18 and 0.40 kWh/kg VS for 3 h and 5 h pretreated HS, respectively. This study opened new perspectives for the valorisation of emerging LMs, such as nut residues. In particular, the abundance of extractives in the LM here investigated is thus far an understudied aspect and will benefit from further studies on their role in AD.

## 4.6 References


Akoglu, H., 2018. User's guide to correlation coefficients. Turkish J. Emerg. Med. 18, 91–93. https://doi.org/10.1016/j.tjem.2018.08.001

Alonso-Fariñas, B., Oliva, A., Rodríguez-Galán, M., Esposito, G., García-Martín, J.F., Rodríguez-Gutiérrez, G., Serrano, A., Fermoso, F.G., 2020. Environmental assessment of olive mill solid waste valorization via anaerobic digestion versus olive pomace oil extraction. Processes 8. https://doi.org/10.3390/PR8050626

Annamalai, N., Elayaraja, S., Oleskowicz-Popiel, P., Sivakumar, N., Bahry, S. Al, 2020. Volatile fatty acids production during anaerobic digestion of lignocellulosic biomass, in: Recent Developments in Bioenergy Research. Elsevier, pp. 237–251. https://doi.org/10.1016/b978-0-12-819597-0.00012-x

Aslanzadeh, S., Berg, A., Taherzadeh, M.J., Sárvári Horváth, I., 2014. Biogas production from N-Methylmorpholine-N-oxide (NMMO) pretreated forest residues. Appl. Biochem. Biotechnol. 172, 2998–3008. https://doi.org/10.1007/s12010-014-0747-z

Ballesteros, L.F., Teixeira, J.A., Mussatto, S.I., 2014. Chemical, Functional, and Structural Properties of Spent Coffee Grounds and Coffee Silverskin. Food Bioprocess Technol. 7, 3493–3503. https://doi.org/10.1007/s11947-014-1349-z

Battista, F., Fino, D., Mancini, G., 2016. Optimization of biogas production from coffee production waste. Bioresour. Technol. 200, 884–890. https://doi.org/10.1016/j.biortech.2015.11.020

Battista, F., Zuliani, L., Rizzioli, F., Fusco, S., Bolzonella, D., 2021. Biodiesel, biogas and fermentable sugars production from Spent coffee Grounds: A cascade biorefinery approach. Bioresour. Technol. 342, 125952. https://doi.org/10.1016/j.biortech.2021.125952

Bianco, F., Monteverde, G., Race, M., Papirio, S., Esposito, G., 2020a. Comparing performances, costs and energy balance of ex situ remediation processes for PAH-contaminated marine sediments. Environ. Sci. Pollut. Res. https://doi.org/10.1007/s11356-020-08379-y

Bianco, F., Race, M., Forino, V., Pacheco-Ruiz, S., Rene, E.R., 2021a. Bioreactors for wastewater to energy conversion : from pilot to full scale, in: Waste Biorefinery. Elsevier Inc., pp. 103–124. https://doi.org/10.1016/B978-0-12-821879-2/00004-1

Bianco, F., Race, M., Papirio, S., Esposito, G., 2020b. Removal of polycyclic aromatic hydrocarbons during anaerobic biostimulation of marine sediments. Sci. Total Environ.

709. https://doi.org/10.1016/j.scitotenv.2019.136141

Bianco, F., Şenol, H., Papirio, S., 2021b. Enhanced lignocellulosic component removal and biomethane potential from chestnut shell by a combined hydrothermal–alkaline pretreatment. Sci. Total Environ. 762. https://doi.org/10.1016/j.scitotenv.2020.144178

Carrillo, F., Colom, X., Suñol, J.J., Saurina, J., 2004. Structural FTIR analysis and thermal characterisation of lyocell and viscose-type fibres. Eur. Polym. J. 40, 2229–2234. https://doi.org/https://doi.org/10.1016/j.eurpolymj.2004.05.003

Cheng, J., Zhang, J., Lin, R., Liu, J., Zhang, L., Cen, K., 2017. Ionic-liquid pretreatment of cassava residues for the cogeneration of fermentative hydrogen and methane. Bioresour. Technol. 228, 348–354. https://doi.org/10.1016/j.biortech.2016.12.107

Covarrubias-García, I., Arriaga, S., 2022. Adsorbents for the Detoxification of Lignocellulosic Wastes Hydrolysates to Improve Fermentative Processes to Bioenergy and Biochemicals Production, in: Renewable Energy Technologies for Energy Efficient Sustainable Development. Springer, pp. 63–83. https://doi.org/10.1007/978-3-030-87633-3_3

Cuissinat, C., Navard, P., 2006. Swelling and dissolution of cellulose part 1: Free floating cotton and wood fibres in N-methylmorpholine-N-oxide-water mixtures. Macromol. Symp. 244, 1–18. https://doi.org/10.1002/masy.200651201

Curry, N., Pillay, P., 2015. Integrating solar energy into an urban small-scale anaerobic digester for improved performance. Renew. Energy 83, 280–293. https://doi.org/10.1016/j.renene.2015.03.073

Dahunsi, O.S., Enyinnaya, M., 2019. The Bioenergy Potentials of Lignocelluloses, in: Energy Conversion - Current Technologies and Future Trends. https://doi.org/10.5772/intechopen.79109

Girotto, F., Lavagnolo, M.C., Pivato, A., 2018. Spent Coffee Grounds Alkaline Pre-treatment as Biorefinery Option to Enhance their Anaerobic Digestion Yield. Waste and Biomass Valorization 9, 2565–2570. https://doi.org/10.1007/s12649-017-0033-8

Gopal, L.C., Govindarajan, M., Kavipriya, M.R., Mahboob, S., Al-Ghanim, K.A., Virik, P., Ahmed, Z., Al-Mulhm, N., Senthilkumaran, V., Shankar, V., 2021. Optimization strategies for improved biogas production by recycling of waste through response surface methodology and artificial neural network: Sustainable energy perspective research. J. King Saud Univ. - Sci. 33, 101241. https://doi.org/10.1016/j.jksus.2020.101241

Gu, Y., Chen, X., Liu, Z., Zhou, X., Zhang, Y., 2014. Effect of inoculum sources on the anaerobic digestion of rice straw. Bioresour. Technol. 158, 149–155.

https://doi.org/10.1016/j.biortech.2014.02.011

Guo, Y., Cai, J., Sun, T., Xing, L., Cheng, C., Chi, K., Xu, J., Li, T., 2021. The purification process and side reactions in the N-methylmorpholine-N-oxide (NMMO) recovery system. Cellulose 28, 7609–7617. https://doi.org/10.1007/s10570-021-03929-0

Haldar, D., Purkait, M.K., 2021. A review on the environment-friendly emerging techniques for pretreatment of lignocellulosic biomass: Mechanistic insight and advancements. Chemosphere 264, 1–16. https://doi.org/10.1016/j.chemosphere.2020.128523

Hassan, M., Umar, M., Ding, W., Mehryar, E., Zhao, C., 2017. Methane enhancement through co-digestion of chicken manure and oxidative cleaved wheat straw: Stability performance and kinetic modeling perspectives. Energy 141, 2314–2320. https://doi.org/10.1016/j.energy.2017.11.110

Hernández-Shek, M.A., Mathieux, M., André, L., Peultier, P., Pauss, A., Ribeiro, T., 2020. Quantifying porosity changes in solid biomass waste using a disruptive approach of water retention curves (WRC) for dry anaerobic digestion. Bioresour. Technol. Reports 12, 100585. https://doi.org/10.1016/j.biteb.2020.100585

Holliger, C., Alves, M., Andrade, D., Angelidaki, I., Astals, S., Baier, U., Bougrier, C., Buffière, P., Carballa, M., De Wilde, V., Ebertseder, F., Fernández, B., Ficara, E., Fotidis, I., Frigon, J.C., De Laclos, H.F., Ghasimi, D.S.M., Hack, G., Hartel, M., Heerenklage, J., Horvath, I.S., Jenicek, P., Koch, K., Krautwald, J., Lizasoain, J., Liu, J., Mosberger, L., Nistor, M., Oechsner, H., Oliveira, J.V., Paterson, M., Pauss, A., Pommier, S., Porqueddu, I., Raposo, F., Ribeiro, T., Pfund, F.R., Strömberg, S., Torrijos, M., Van Eekert, M., Van Lier, J., Wedwitschka, H., Wierinck, I., 2016. Towards a standardization of biomethane potential tests. Water Sci. Technol. 74, 2515–2522. https://doi.org/10.2166/wst.2016.336

International Nut and Dried Fruit Council Foundation (INC), 2021. Nuts & dried fruits statistical yearbook 2020/2021.

Jeihanipour, A., Karimi, K., Taherzadeh, M.J., 2010. Enhancement of ethanol and biogas production from high-crystalline cellulose by different modes of NMO pretreatment. Biotechnol. Bioeng. 105, 469–476. https://doi.org/10.1002/bit.22558

Kabir, M.M., del Pilar Castillo, M., Taherzadeh, M.J., Horváth, I.S., 2013. Effect of the N-methylmorpholine-N-oxide (NMMO) pretreatment on anaerobic digestion of forest residues. BioResources 8, 5409–5423.

Kabir, M.M., Niklasson, C., Taherzadeh, M.J., Horváth, I.S., 2014. Biogas production from lignocelluloses by N-methylmorpholine-N-oxide (NMMO) pretreatment: Effects of

recovery and reuse of NMMO. Bioresour. Technol. 161, 446–450. https://doi.org/10.1016/j.biortech.2014.03.107

Kapoor, R., Ghosh, P., Tyagi, B., Vijay, V.K., Vijay, V., Thakur, I.S., Kamyab, H., Nguyen, D.D., Kumar, A., 2020. Advances in biogas valorization and utilization systems: A comprehensive review. J. Clean. Prod. 273, 123052. https://doi.org/10.1016/j.jclepro.2020.123052

Kayembe, K., Basosila, L., Mpiana, P.T., Sikulisimwa, P.C., Mbuyu, K., 2013. Inhibitory Effects of Phenolic Monomers on Methanogenesis in Anaerobic Digestion. Br. Microbiol. Res. J. 3, 32–41. https://doi.org/10.9734/bmrj/2013/2291

Khoshnevisan, B., Shafiei, M., Rajaeifar, M.A., Tabatabaei, M., 2016. Biogas and bioethanol production from pinewood pre-treated with steam explosion and N-methylmorpholine-N-oxide (NMMO): A comparative life cycle assessment approach. Energy 114, 935–950. https://doi.org/10.1016/j.energy.2016.08.024

Kim, J., Kim, H., Baek, G., Lee, C., 2017. Anaerobic co-digestion of spent coffee grounds with different waste feedstocks for biogas production. Waste Manag. 60, 322–328. https://doi.org/10.1016/j.wasman.2016.10.015

Kim, J. won, Jang, J.H., Yeo, H.J., Seol, J., Kim, S.R., Jung, Y.H., 2019. Lactic Acid Production from a Whole Slurry of Acid-Pretreated Spent Coffee Grounds by Engineered Saccharomyces cerevisiae. Appl. Biochem. Biotechnol. 189, 206–216. https://doi.org/10.1007/s12010-019-03000-6

Knapic, S., Oliveira, V., Machado, J.S., Pereira, H., 2016. Cork as a building material: a review. Eur. J. Wood Wood Prod. 74, 775–791. https://doi.org/10.1007/s00107-016-1076-4

Lama, G.F.C., Crimaldi, M., Pasquino, V., Padulano, R., Chirico, G.B., 2021a. Bulk drag predictions of riparian arundo donax stands through UAV-acquired multispectral images. Water (Switzerland) 13, 1–19. https://doi.org/10.3390/w13101333

Lama, G.F.C., Giovannini, M.R.M., Errico, A., Mirzaei, S., Padulano, R., Chirico, G.B., Preti, F., 2021b. Hydraulic efficiency of green-blue flood control scenarios for vegetated rivers: 1D and 2D unsteady simulations. Water (Switzerland) 13. https://doi.org/10.3390/w13192620

Lee, J., Kim, J.R., Jeong, S., Cho, J., Kim, J.Y., 2017. Long-term performance of anaerobic digestion for crop residues containing heavy metals and response of microbial communities. Waste Manag. 59, 498–507. https://doi.org/10.1016/j.wasman.2016.10.005

Lee, J., Park, K.Y., 2020. Impact of hydrothermal pretreatment on anaerobic digestion

efficiency for lignocellulosic biomass: Influence of pretreatment temperature on the formation of biomass-degrading byproducts. Chemosphere 256. https://doi.org/10.1016/j.chemosphere.2020.127116

Li, P., Liu, D., Pei, Z., Zhao, L., Shi, F., Yao, Z., Li, W., Sun, Y., Wang, S., Yu, Q., Chen, L., Liu, J., 2021. Evaluation of lignin inhibition in anaerobic digestion from the perspective of reducing the hydrolysis rate of holocellulose. Bioresour. Technol. 333, 125204. https://doi.org/10.1016/j.biortech.2021.125204

Li, W., Khalid, H., Zhu, Z., Zhang, R., Liu, G., Chen, C., Thorin, E., 2018. Methane production through anaerobic digestion: Participation and digestion characteristics of cellulose, hemicellulose and lignin. Appl. Energy 226, 1219–1228. https://doi.org/10.1016/j.apenergy.2018.05.055

Li, Y., Chen, Y., Wu, J., 2019. Enhancement of methane production in anaerobic digestion process: A review. Appl. Energy 240, 120–137. https://doi.org/10.1016/j.apenergy.2019.01.243

Li, Y., Jin, Y., Li, H., Borrion, A., Yu, Z., Li, J., 2018. Kinetic studies on organic degradation and its impacts on improving methane production during anaerobic digestion of food waste. Appl. Energy 213, 136–147. https://doi.org/10.1016/j.apenergy.2018.01.033

Li, Y., Zhang, R., Liu, G., Chen, C., He, Y., Liu, X., 2013. Comparison of methane production potential, biodegradability, and kinetics of different organic substrates. Bioresour. Technol. 149, 565–569. https://doi.org/10.1016/j.biortech.2013.09.063

Lo, S.L., Huang, Y.F., Chiueh, P. Te, Kuan, W.H., 2017. Microwave Pyrolysis of Lignocellulosic Biomass. Energy Procedia 105, 41–46. https://doi.org/10.1016/j.egypro.2017.03.277

Maestri, D., Cittadini, M.C., Bodoira, R., Martínez, M., 2020. Tree Nut Oils: Chemical Profiles, Extraction, Stability, and Quality Concerns. Eur. J. Lipid Sci. Technol. 122, 1–14. https://doi.org/10.1002/ejlt.201900450

Mancini, G., Papirio, S., Lens, P.N.L., Esposito, G., 2018a. Anaerobic Digestion of Lignocellulosic Materials Using Ethanol-Organosolv Pretreatment. Environ. Eng. Sci. 00, 1–8. https://doi.org/10.1089/ees.2018.0042

Mancini, G., Papirio, S., Lens, P.N.L., Esposito, G., 2018b. Increased biogas production from wheat straw by chemical pretreatments. Renew. Energy 119, 608–614. https://doi.org/10.1016/j.renene.2017.12.045

Mancini, G., Papirio, S., Lens, P.N.L., Esposito, G., 2016a. Solvent Pretreatments of

Lignocellulosic Materials to Enhance Biogas Production: A Review. Energy and Fuels 30, 1892–1903. https://doi.org/10.1021/acs.energyfuels.5b02711

Mancini, G., Papirio, S., Lens, P.N.L., Esposito, G., 2016b. Effect of N-methylmorpholine-N-oxide Pretreatment on Biogas Production from Rice Straw, Cocoa Shell, and Hazelnut Skin. Environ. Eng. Sci. 33, 843–850. https://doi.org/10.1089/ees.2016.0138

Mei, J., Shen, X., Gang, L., Xu, H., Wu, F., Sheng, L., 2020. A novel lignin degradation bacteria-Bacillus amyloliquefaciens SL-7 used to degrade straw lignin efficiently. Bioresour. Technol. 310, 123445. https://doi.org/10.1016/j.biortech.2020.123445

Metsämuuronen, S., Sirén, H., 2019. Bioactive phenolic compounds, metabolism and properties: a review on valuable chemical compounds in Scots pine and Norway spruce, Phytochemistry Reviews. https://doi.org/10.1007/s11101-019-09630-2

Nitsos, C., Matsakas, L., Triantafyllidis, K., Rova, U., Christakopoulos, P., 2015. Evaluation of mediterranean agricultural residues as a potential feedstock for the production of biogas via anaerobic fermentation. Biomed Res. Int. 2015. https://doi.org/10.1155/2015/171635

Oliva, A., Papirio, S., Esposito, G., Lens, P.N.L., 2022. Pretreatment of Lignocellulosic Materials to Enhance their Methane Potential, in: Sinharoy, A., Lens, P.N.L. (Eds.), Renewable Energy Technologies for Energy Efficient Sustainable Development, Applied Environmental Science and Engineering for a Sustainable Future. Springer, pp. 85–120. https://doi.org/10.1007/978-3-030-87633-3_4

Oliva, A., Tan, L.C., Papirio, S., Esposito, G., Lens, P.N.L., 2021. Effect of methanol-organosolv pretreatment on anaerobic digestion of lignocellulosic materials. Renew. Energy. https://doi.org/10.1016/j.renene.2020.12.095

Papirio, S., 2020. Coupling acid pretreatment and dosing of Ni and Se enhances the biomethane potential of hazelnut skin. J. Clean. Prod. 262, 121407. https://doi.org/10.1016/j.jclepro.2020.121407

Paul, S., Dutta, A., 2018. Challenges and opportunities of lignocellulosic biomass for anaerobic digestion. Resour. Conserv. Recycl. 130, 164–174. https://doi.org/10.1016/j.resconrec.2017.12.005

Purwandari, F.A., Sanjaya, A.P., Millati, R., Cahyanto, M.N., Horváth, I.S., Niklasson, C., Taherzadeh, M.J., 2013. Pretreatment of oil palm empty fruit bunch (OPEFB) by N-methylmorpholine-N-oxide (NMMO) for biogas production: Structural changes and digestion improvement. Bioresour. Technol. 128, 461–466. https://doi.org/10.1016/j.biortech.2012.10.088

Rasi, S., Kilpeläinen, P., Rasa, K., Korpinen, R., Raitanen, J.E., Vainio, M., Kitunen, V., Pulkkinen, H., Jyske, T., 2019. Cascade processing of softwood bark with hot water extraction, pyrolysis and anaerobic digestion. Bioresour. Technol. 292, 121893. https://doi.org/10.1016/j.biortech.2019.121893

Roy, S., Dikshit, P.K., Sherpa, K.C., Singh, A., Jacob, S., Chandra Rajak, R., 2021. Recent nanobiotechnological advancements in lignocellulosic biomass valorization: A review. J. Environ. Manage. 297, 113422. https://doi.org/10.1016/j.jenvman.2021.113422

Sanchez, A., Hernández-Sánchez, P., Puente, R., 2019. Hydration of lignocellulosic biomass. Modelling and experimental validation. Ind. Crops Prod. 131, 70–77. https://doi.org/10.1016/j.indcrop.2019.01.029

Satari, B., Karimi, K., Kumar, R., 2019. Cellulose solvent-based pretreatment for enhanced second-generation biofuel production: A review, Sustainable Energy and Fuels. Royal Society of Chemistry. https://doi.org/10.1039/c8se00287h

Schneider, W.D.H., Fontana, R.C., Baudel, H.M., de Siqueira, F.G., Rencoret, J., Gutiérrez, A., de Eugenio, L.I., Prieto, A., Martínez, M.J., Martínez, Á.T., Dillon, A.J.P., Camassola, M., 2020. Lignin degradation and detoxification of eucalyptus wastes by on-site manufacturing fungal enzymes to enhance second-generation ethanol yield. Appl. Energy 262, 114493. https://doi.org/10.1016/j.apenergy.2020.114493

Shafiei, M., Karimi, K., Taherzadeh, M.J., 2011. Techno-economical study of ethanol and biogas from spruce wood by NMMO-pretreatment and rapid fermentation and digestion. Bioresour. Technol. 102, 7879–7886. https://doi.org/10.1016/j.biortech.2011.05.071

Shafiei, M., Karimi, K., Zilouei, H., Taherzadeh, M.J., 2014. Enhanced ethanol and biogas production from pinewood by NMMO pretreatment and detailed biomass analysis. Biomed Res. Int. 2014. https://doi.org/10.1155/2014/469378

Sharma, P., Gaur, V.K., Sirohi, R., Larroche, C., Kim, S.H., Pandey, A., 2020. Valorization of cashew nut processing residues for industrial applications. Ind. Crops Prod. 152, 112550. https://doi.org/10.1016/j.indcrop.2020.112550

Shen, J., Yan, H., Zhang, R., Liu, G., Chen, C., 2018. Characterization and methane production of different nut residue wastes in anaerobic digestion. Renew. Energy 116, 835–841. https://doi.org/10.1016/j.renene.2017.09.018

Sluiter, A., Hames, B., Hyman, D., Payne, C., Ruiz, R., Scarlata, C., Sluiter, J., Templeton, D., Wolfe J., 2008a. Determination of Total Solids in Biomass and Total Dissolved Solids in Liquid Process Samples. Natl. Renew. Energy Lab. Tech. Rep. NREL/TP-510-42621.

Sluiter, A., Hames, B., Ruiz, R., Scarlata, C., Sluiter, J., Templeton, D., 2008b. Determination of Ash in Biomass. Natl. Renew. Energy Lab. Tech. Rep. NREL/TP-510-42622.

Sluiter, A., Hames, B., Ruiz, R., Scarlata, C., Sluiter, J., Templeton, D., Crocker, D., 2008c. Determination of Structural Carbohydrates and Lignin in Biomass. Natl. Renew. Energy Lab. Tech. Rep. NREL/ TP -510 -42618.

Sluiter, A., Ruiz, R., Scarlata, C., Sluiter, J., Templeton, D., 2008d. Determination of Extractives in Biomass. Natl. Renew. Energy Lab. Tech. Rep. NREL/TP-510-42619.

Spagnuolo, L., Posta, S. Della, Fanali, C., Dugo, L., De Gara, L., 2021. Antioxidant and antiglycation effects of polyphenol compounds extracted from hazelnut skin on advanced glycation end-products (Ages) formation. Antioxidants 10, 1–14. https://doi.org/10.3390/antiox10030424

Tajmirriahi, M., Karimi, K., Kumar, R., 2021a. Effects of pinewood extractives on bioconversion of pinewood. Fuel 283, 119302. https://doi.org/10.1016/j.fuel.2020.119302

Tajmirriahi, M., Momayez, F., Karimi, K., 2021b. The critical impact of rice straw extractives on biogas and bioethanol production. Bioresour. Technol. 319, 124167. https://doi.org/10.1016/j.biortech.2020.124167

Teghammar, A., Forgács, G., Sárvári Horváth, I., Taherzadeh, M.J., 2014. Techno-economic study of NMMO pretreatment and biogas production from forest residues. Appl. Energy 116, 125–133. https://doi.org/10.1016/j.apenergy.2013.11.053

Teghammar, A., Karimi, K., Sárvári Horváth, I., Taherzadeh, M.J., 2012. Enhanced biogas production from rice straw, triticale straw and softwood spruce by NMMO pretreatment. Biomass and Bioenergy 36, 116–120. https://doi.org/10.1016/j.biombioe.2011.10.019

Wainaina, S., Lukitawesa, Kumar Awasthi, M., Taherzadeh, M.J., 2019. Bioengineering of anaerobic digestion for volatile fatty acids, hydrogen or methane production: A critical review. Bioengineered 10, 437–458. https://doi.org/10.1080/21655979.2019.1673937

Wikandari, R., Millati, R., Taherzadeh, M.J., 2016. Pretreatment of Lignocelluloses With Solvent N-Methylmorpholine N-oxide, Biomass Fractionation Technologies for a Lignocellulosic Feedstock Based Biorefinery. Elsevier Inc. https://doi.org/10.1016/B978-0-12-802323-5.00012-8

Xu, N., Liu, S., Xin, F., Zhou, J., Jia, H., Xu, J., Jiang, M., Dong, W., 2019. Biomethane production from lignocellulose: Biomass recalcitrance and its impacts on anaerobic digestion. Front. Bioeng. Biotechnol. 7, 1–12. https://doi.org/10.3389/fbioe.2019.00191

Yazdani, M., Ebrahimi-Nik, M., Heidari, A., Abbaspour-Fard, M.H., 2019. Improvement of

biogas production from slaughterhouse wastewater using biosynthesized iron nanoparticles from water treatment sludge. Renew. Energy 135, 496–501. https://doi.org/10.1016/j.renene.2018.12.019

Yu, Q., Qin, L., Liu, Y., Sun, Y., Xu, H., Wang, Z., Yuan, Z., 2019. In situ deep eutectic solvent pretreatment to improve lignin removal from garden wastes and enhance production of bio-methane and microbial lipids. Bioresour. Technol. 271, 210–217. https://doi.org/10.1016/j.biortech.2018.09.056

Zeynali, R., Khojastehpour, M., Ebrahimi-Nik, M., 2017. Effect of ultrasonic pre-treatment on biogas yield and specific energy in anaerobic digestion of fruit and vegetable wholesale market wastes. Sustain. Environ. Res. 27, 259–264. https://doi.org/10.1016/j.serj.2017.07.001

Zoghlami, A., Paës, G., 2019. Lignocellulosic Biomass: Understanding Recalcitrance and Predicting Hydrolysis. Front. Chem. 7, 874. https://doi.org/10.3389/fchem.2019.00874

Zuo, X., Yuan, H., Wachemo, A.C., Wang, X., Zhang, L., Li, J., Wen, H., Wang, J., Li, X., 2020. The relationships among sCOD, VFAs, microbial community, and biogas production during anaerobic digestion of rice straw pretreated with ammonia. Chinese J. Chem. Eng. 28, 286–292. https://doi.org/10.1016/j.cjche.2019.07.015

*Chapter 5*

# Ultrasounds application for nut and coffee wastes valorisation via biomolecules solubilisation and methane production

A modified version of this chapter has been submitted for publication in *Waste Management* journal.

**Abstract**

Lignocellulosic materials (LMs) are abundant feedstocks with excellent potential for biofuels and biocommodities production. In particular, nut and coffee wastes are rich in biomolecules, e.g. sugars and polyphenols, the valorisation of which still has to be fully disclosed. This study investigated the effectiveness of ultrasounds coupled with hydrothermal (i.e. ambient temperature *vs* 80 °C) and methanol (MeOH)-based pretreatments for polyphenols and sugar solubilisation from hazelnut skin (HS), almond shell (AS), and spent coffee grounds (SCG). The liquid fraction obtained from the pretreated HS was the most promising in terms of biomolecules solubilisation. The highest polyphenols, i.e. 123.9 (± 2.3) mg/g TS, and sugar, i.e. 146.0 (± 3.4) mg/g TS, solubilisation was obtained using the MeOH-based medium. However, the MeOH-based media were not suitable for direct anaerobic digestion (AD) due to the MeOH inhibition during AD. The water-based liquors obtained from pretreated AS and SCG exhibited a higher methane production potential, i.e. 434.2 (± 25.1) and 685.5 (± 39.5) mL $CH_4$/g $glucose_{in}$, respectively, than the HS liquors despite having a lower sugar concentration. The solid residues recovered after ultrasounds pretreatment were used as substrates for AD as well. Regardless the pretreatment condition, the methane production potential of the ultrasounds pretreated HS, AS, and SCG was not improved, achieving maximally 255.4 (± 7.4), 42.8 (± 3.3), and 366.2 (± 4.2) mL $CH_4$/g VS, respectively. Hence, the solid and liquid fractions obtained from HS, AS, and SCG showed great potential either as substrates for AD or, in perspective, for biomolecules recovery in a biorefinery context.

## 5.1 Introduction

The search for alternative sources of energy is a crucial aspect to guarantee the sustainable development of human activities. In this perspective, recovery and valorisation of waste materials, e.g. lignocellulosic materials (LMs), offers a great opportunity (Velvizhi et al., 2022). LMs are abundant wastes produced during agricultural, municipal and industrial activities (Koupaie et al., 2019). LMs are mainly composed of cellulose, hemicellulose, and lignin linked together in a complex structure that hinders their decomposition and valorisation. In particular, the presence of lignin creates a physical barrier around cellulose and hemicellulose sugars (Xu et al., 2019). Apart from those three main biopolymers, depending on the specific characteristics of the LM, these substrates can be rich in valuable biomolecules, such as polyphenols, low molecular sugars, protein, and oils (Mirmohamadsadeghi et al., 2021).

Nuts and coffee wastes, in particular, are emerging as a new source of valuable products besides having a high methane production potential (Battista et al., 2021; Oliva et al., 2021; Shen et al., 2018). The cultivation of nut trees is mainly located in USA, Turkey and China. Nevertheless, nuts are exported worldwide, either with or without the shell (International Nut and Dried Fruit Council Foundation, 2021). The edible part of nuts only represents a small portion compared to the amount of wastes, i.e. shells, leaves, husks, and skins, generated during the harvesting season (Shen et al., 2018). In some cases, e.g. almonds, the shell represents over 50% of the overall fruit mass (Queirós et al., 2020). Coffee trees are mainly cultivated in Africa, South and Central America (International Coffee Organization (ICO), 2020). A considerable amount of waste is produced along the coffee production chain. Firstly, the outer skin, pulp, parchment, and silver skin are removed from the coffee beans, generally in the production country. After that, coffee is exported worldwide generally as green beans. Coffee beans are usually roasted and ground *in loco* before being packed to be sold (Murthy and Naidu, 2012). The waste production behind a cup of coffee continues with the beverage production. The spent coffee grounds generation amounts to roughly 6 million tons per year (Battista et al., 2021).

Anaerobic digestion (AD) is an advantageous and widely explored process for LMs valorisation. During the first stage of AD, carbohydrates, proteins and lipids are hydrolysed into sugars, amino acids, and long-chain fatty acids (Bianco et al., 2021a). The hydrolysis stage is considered the limiting step for AD of LMs due to recalcitrance caused by lignin protection and the complex bonds among cellulose, hemicellulose and lignin (Sawatdeenarunat et al., 2015). In the second stage, i.e. acidogenesis, the soluble monomers are fermented into alcohols,

volatile fatty acids, and hydrogen before being converted into acetate, carbon dioxide and hydrogen during the acetogenic stage. During the fourth and last phase, archaea utilise acetic acid and hydrogen to produce methane (Li et al., 2019).

The need to enhance the methane production from LMs has led to the development of several pretreatment methods that focus, in the first place, on removing the most recalcitrant components, but also on obtaining selected liquid or solid streams that can be further valorised following other patterns than AD (Oliva et al., 2022). In this perspective, the use of ultrasounds is a promising pretreatment technique. Ultrasounds have been widely used to enhance the methane production potential of sludge, digestate and manure (Garoma and Pappaterra, 2018; Ormaechea et al., 2018). In addition, this technique has been recently tested on LMs (Korai and Li, 2020; Zou et al., 2016b). Ultrasonic waves generate cavitation phenomena in the liquid medium that affect the lignocellulosic structure by removing part of the lignin and reducing the crystallinity and degree of polymerisation of cellulose. On the other hand, a partial sugar hydrolysis can occur (Bundhoo and Mohee, 2018). In addition, an ultrasounds pretreatment can be easily combined with other techniques, combining the effect of chemical and physical pretreatments (Oliva et al., 2022).

This study investigated the combination of ultrasounds with thermal and methanol (MeOH)-based pretreatment on nut and coffee residues, i.e. hazelnut skin (HS), almond shell (AS), and spent coffee grounds (SCG). The ultrasounds pretreatment was performed at ambient temperature ($T_{amb}$) and 80 °C, and the influence of different media, i.e. distilled water and a 50% (*v/v*) MeOH solution catalysed by sulfuric acid, on the chemical composition of the solid residues and the compounds released in the liquid fraction was studied. Several studies focused on obtaining methane via AD from the slurry obtained after a pretreatment. In contrast, this study aimed to disclose the optimal route for each solid and liquid fraction recovered after the pretreatment of HS, AS, and SCG, based on their specific composition. The liquid fraction obtained after ultrasounds pretreatment was characterised in terms of sugar and polyphenolic compounds before undergoing AD. The optimal pathway to valorise the liquid fraction obtained in the various pretreatment conditions was discussed depending on the specific characteristics of the liquor. Raw and pretreated solid residues were subjected to AD as well to understand the correlation between the various pretreatment conditions and the methane production potential of the solid residues.

## 5.2 Materials and methods

### *5.2.1 Substrates and inoculum*

The three substrates selected for the present study, i.e. HS, AS, and SCG, were obtained, prepared, and stored according to Oliva et al. (2021) before undergoing AD. Digestate from buffalo manure (DBM) was collected from a full-scale AD plant and degassed before being used as the inoculum for the experimental activities. The total (TS) and volatile (VS) solid content of the inoculum and raw LMs is shown in Table 5.1.

**Table 5.1 –** Characterisation of the inoculum, i.e. digestate from buffalo manure (DBM), and raw substrates, i.e. hazelnut skin (HS), almond shell (AS), and spent coffee grounds (SCG), in terms of total (TS) and volatile (VS) solid content.

| | **DBM** | **HS** | **AS** | **SCG** |
|---|---|---|---|---|
| **TS** [a] (%) | 5.8 ± 0.0 | 90.5 ± 0.1 | 90.2 ± 0.1 | 90.1 ± 0.2 |
| **VS** [a] (%) | 4.0 ± 0.0 | 87.9 ± 0.1 | 87.1 ± 0.8 | 88.5 ± 0.2 |
| **VS/TS** (g/g) | 0.70 | 0.97 | 0.96 | 0.98 |

[a]TS and VS are based on g/100 g wet matter.

### *5.2.2 Ultrasounds pretreatment*

The ultrasounds pretreatment was performed using a DL 510 H ultrasonic bath (Bandelin, Berlin, Germany) with frequency, nominal power, and amplitude of 35 kHz, 160 W, and 100%, respectively. Two different media were tested for ultrasonic waves diffusion, i.e. distilled water and 50% (*v/v*) water-MeOH solution catalysed by 0.1% (*w/v*) sulfuric acid (MeOH-based). The pretreatment was performed in 250 mL Duran bottles filled with 15 g of LM and 150 mL of medium. Four bottles at a time were placed in the ultrasonic bath. The ultrasounds pretreatment was performed for 1 h at $T_{amb}$ and 80 °C. The LMs were shaken manually every 10 min during the pretreatment. The energy density ($E_d$) was calculated following Eq. (5.1), as reported by Zou et al. (2016):

$$E_d = \frac{P \cdot t}{m \cdot TS_0} \quad (5.1)$$

where P (W) is the nominal ultrasonic power, t (min) is the pretreatment time exposure, m (kg) is the mass of LMs undergoing the pretreatment, and $TS_0$ (g/g) is the total solid content of the LMs before the pretreatment.

After the pretreatment, the solid residues were separated from the liquor using a textile cloth, washed with abundant distilled water, and dried at 40 °C before being used as the substrate for

AD. The liquor was taken for characterisation and stored at - 20 °C until evaluation of the methane production potential.

*5.2.3 Methane production potential assessment*

The methane production potential of raw and pretreated LMs, as well as the liquors obtained under the various pretreatment conditions, was evaluated by performing batch biochemical methane potential (BMP) tests in 250 mL serum bottles (OCHS, Bovenden, Germany). The bottles were kept under mesophilic, i.e. 37 (± 1) °C, conditions. The anaerobic conditions were ensured by flushing the reactors with Argon gas.

The first set of experiments aimed to evaluate the BMP of raw and the solid fraction of pretreated LMs. Each bottle was loaded with 1 g VS from raw or pretreated LMs (liquid phase decanted) and 1.5 g VS from DBM. A final solid content of 2.1% TS was achieved by adding demineralised water, reaching the final working volume of 150 mL. The second set of experiments evaluated the BMP of the liquor obtained after the pretreatment. Each bottle was filled with 30 mL of the liquor upon completion of the ultrasounds pretreatment, 1.5 g VS from DBM, i.e. 37.2 g, and an amount of demineralised water calculated to reach the same moisture as in the first set of experiments, i.e. 2.1% TS, regardless the working volume. Control biochemical tests were simultaneously carried out to evaluate the methane production potential of the inoculum. In the second experimental set, the methane production potential of the media was evaluated to account for the presence of MeOH during batch assays. All experiments were performed in triplicate, and the bottles were shaken manually once per day.

*5.2.4 Analytical methods and calculations*

The TS and VS content of the inoculum and raw and pretreated LMs was measured according to the standard methods (APHA AWWA, 2005). The chemical composition, i.e. total extractives, structural sugars, lignin, and ashes, of raw and pretreated substrates was determined by Celignis Limited (Limerick, Ireland), as previously described by Oliva et al. (2021).

The substrate solubilisation was calculated by comparing the amount of TS from raw and pretreated substrates following Eq. (5.2).

$$\text{Substrate solubilisation (\%)} = \frac{\text{TS}_{\text{raw}}\text{-TS}_{\text{pretreated}}}{\text{TS}_{\text{raw}}} \cdot 100 \quad (5.2)$$

where $TS_{raw}$ and $TS_{pretreated}$ is the amount (g) of TS from each substrate before and after the ultrasounds pretreatment.

A mass balance assessment was performed considering the percentage of substrate solubilised and the chemical composition measured before and after each pretreatment. The balance returns the amount (g) of each lignocellulosic component present in the raw substrate and the solid fraction recovered after the ultrasounds pretreatment.

The liquor obtained from the ultrasounds pretreatment was collected for pH measurement and determination of soluble polyphenols and sugar concentration. The pH of the liquor was measured with a HI-98103 pH meter (Hanna Instruments, Woonsocket, USA). The concentration of soluble polyphenols was determined following the Folin-Ciocalteu (F-C) method, according to Cubero-Cardoso et al. (2020). The absorbance was read at 655 nm using a V-530 UV/VIS spectrophotometer (Jasco, Tokyo, Japan). The total sugar concentration was measured according to the Dubois method (Dubois et al., 1956) using a 7600 UV-Vis spectrophotometer (Xylem, Weilheim, Germany) to read the absorbance at 492 nm. The polyphenols and sugar concentrations were determined using phenol crystals ($C_6H_6O$) and glucose ($C_6H_{12}O_6$) as the standards for the calibration curve, respectively.

The methane production from the first set of experiments was quantified volumetrically using a water displacement apparatus consisting of a Drechsel bottle and a glass cylinder (Glass Studio, Naples, Italy) connected by a capillary tube, as described by Papirio (2020). The Drechsel bottle was filled with a 12% NaOH solution used for carbon dioxide sequestration. The glass cylinder was used to measure the volume of water displaced by the methane that surpassed the carbon dioxide trap. The water displaced corresponds to the amount (mL) of methane produced between two measuring points (Filer et al., 2019). In the second set of experiments, a different method was used to measure the methane production from the liquor obtained after the ultrasounds pretreatment. The biogas production was evaluated manometrically, as described by Oliva et al. (2021). The gas composition was determined with a HPR-20 RD mass spectrometer (Hiden Analytical, Warrington, UK) equipped with a capillary tube heated at 140 °C and capable of analysing 0.8 ml/min of the gas mixture accumulated in the headspace of the serum bottles.

The net cumulative methane production from the two sets of experiments was calculated as the average of the biological triplicates after subtracting the average methane production of the controls. The methane production potential of the raw LMs and the solid residues recovered after ultrasounds pretreatment was expressed as mL $CH_4$/g VS, whereas the methane production from the liquors was reported as mL $CH_4$/100 mL liquor. The methane production potential of

the liquors was also calculated per grams of initial glucose from the liquid fraction (i.e. mL $CH_4$/g $glucose_{in}$) for a better understanding of the efficiency of the substrate utilisation during AD. Methane production was recorded regularly until the daily accumulation was below the negligible threshold in all bottles, i.e. 1% of the cumulative production (Holliger et al., 2016).

*5.2.5 Model fitting*

The experimental data obtained from the BMP tests digesting raw LMs and the solid residues recovered after the ultrasounds pretreatment were compared with a modified Gompertz model (Mancini et al., 2018). The kinetics of methane production were estimated following Eq. (5.3):

$$G(t) = G_m \cdot \exp\left\{-\exp\left[\frac{R_m \cdot e}{G_m} \cdot (\lambda - t) + 1\right]\right\} \quad (5.3)$$

where $G_m$ (mL $CH_4$/g VS) and $R_m$ (mL $CH_4$/g VS/d) are, respectively, the maximum specific methane production potential and rate assessed with the model, λ (d) is the lag phase time, t (d) is the time of the AD process, G(t) (mL $CH_4$/g VS) is the cumulative specific methane production achieved at t (d), and e = exp (1).

The model fitting was conducted using the Origin2018 software (OriginLab Corporation, Northampton, USA). The correlation coefficient ($r^2$) between experimental and model data was obtained with the Excel 2016 software (Microsoft Corporation, Redmond, USA).

*5.2.5 Statistical comparison*

The significance of the changes in BMP, as well as polyphenols and sugar solubilised, among the various pretreatment conditions was evaluated using Minitab 17 Statistical Software (Minitab LCC, USA). A one-way analysis of variance (ANOVA) was perfromed followed by the Tukey post hoc test. The difference was considered statistically significant when the p-value was below 0.05.

**5.3 Results**

*5.3.1 Polyphenols and sugar solubilisation using ultrasounds*

Table 5.2 shows that HS solubilisation increased with ultrasounds temperature and was higher when using the MeOH-based medium. The maximum solubilisation (i.e. 23.5%) was achieved when applying ultrasounds at 80 °C in the MeOH-based medium. In contrast, the application of ultrasounds did not affect AS solubilisation (Table 5.2). The highest solubilisation for AS was 6.4%. Regarding SCG (Table 5.2), increasing the pretreatment temperature enhanced the substrate solubilisation by 35 and 26% in water and MeOH-based medium, respectively. On

the contrary, the medium composition had only a minor impact for SCG. The maximum SCG solubilisation (i.e. 20.8%) was obtained at 80 °C in water. The pH of the liquors obtained after applying ultrasounds is reported in Table 5.2.

The HS liquor showed the highest concentration of released polyphenols and sugar. In particular, 11.48 (± 0.07) and 11.21 (± 0.21) g polyphenol/L were measured in the liquor when using the MeOH-based medium at $T_{amb}$ and 80 °C, respectively. On the other hand, the pretreatment temperature enhanced polyphenols solubilisation when using $H_2O$ as the medium. The polyphenols concentration was 4.83 (± 0.02) g/L after ultrasounds at $T_{amb}$, whereas it increased to 7.24 (± 0.11) g/L when the temperature was 80 °C. The sugar concentration measured in the liquor followed the same trend as polyphenols. Using the MeOH-based medium, ultrasounds solubilised 12.91 (± 0.23) and 13.22 (± 0.30) g sugar/L at $T_{amb}$ and 80 °C, respectively. Water was less effective than the MeOH-based medium, resulting in 6.49 (± 0.81) and 9.89 (± 0.33) g sugar/L at $T_{amb}$ and 80 °C, respectively.

Polyphenols solubilisation from AS was greatly influenced by the pretreatment temperature and medium composition, yet significantly lower than what achieved with HS ($p < 0.05$) (Table 5.2). The highest polyphenols concentration, i.e. 0.45 (± 0.01) g/L, was measured in the MeOH-based liquor obtained at 80 °C. At the same temperature, the water medium allowed to solubilise only 0.24 (± 0.01) g polyphenols/L from AS. A lower impact of the ultrasounds conditions was observed on the sugar solubilisation from AS (Table 5.2). The use of the MeOH-based medium at 80 °C was the most performing condition, resulting in 2.94 (± 0.08) g sugar/L, whereas water at $T_{amb}$ solubilised 1.96 (± 0.17) g sugar/L.

Polyphenols and sugar solubilisation from SCG was influenced by the temperature and medium during the ultrasounds pretreatment (Table 5.2). Similarly to AS, the use of the MeOH-based medium at 80 °C resulted in the highest polyphenols concentration in the liquor, i.e. 0.78 (± 0.02). On the contrary, using water at 80 °C was the most effective condition for sugar solubilisation from SCG, i.e. 2.72 (± 0.07) g sugar/L. The pretreatment temperature greatly influenced the solubilisation of polyphenols and sugar from SCG when using water as the medium, whereas it had a lower impact in the case of the MeOH-based medium (Table 5.2).

**Table 5.2 –** Substrate solubilisation efficiency after ultrasounds, pH of the liquor, and polyphenols and sugars solubilised through ultrasounds using different media, i.e. distilled water and a 50% (*v/v*) methanol (MeOH) solution catalysed by 0.1% (*w/v*) sulfuric acid, at different temperatures, i.e. ambient temperature ($T_{amb}$) and 80 °C. The polyphenols and sugars are expressed as concentration measured in the liquor and as milligrams of biomolecule solubilised per gram of dry lignocellulosic material undergoing ultrasounds pretreatment.

| **Substrate** | **Pretreatment condition** | **Substrate solubilisation** (%) | **pH** | **Polyphenols** (g/L) | **Polyphenols** (mg/g TS) | **Statistical information** [a] | **Sugars** (g glucose/L) | **Sugars** (mg glucose/g TS) | **Statistical information** [a] |
|---|---|---|---|---|---|---|---|---|---|
| Hazelnut skin | $H_2O$ $T_{amb}$ | 14.6 ± 1.4 | 5.4 | 4.83 ± 0.02 | 53.4 ± 0.2 | c | 6.49 ± 0.81 | 71.7 ± 9.0 | c |
| | $H_2O$ 80 °C | 17.2 ± 0.2 | 5.1 | 7.24 ± 0.11 | 80.0 ± 1.2 | b | 9.89 ± 0.33 | 109.3 ± 3.7 | b |
| | MeOH $T_{amb}$ | 19.3 ± 0.1 | 3.7 | 11.48 ± 0.07 | 126.9 ± 0.7 | a | 12.91 ± 0.23 | 142.6 ± 2.5 | a |
| | MeOH 80 °C | 23.5 ± 0.4 | 4 | 11.21 ± 0.21 | 123.9 ± 2.3 | a | 13.22 ± 0.30 | 146.0 ± 3.4 | a |
| Almond shell | $H_2O$ $T_{amb}$ | 5.7 ± 0.2 | 5.1 | 0.07 ± 0.00 | 0.7 ± 0.0 | d | 1.96 ± 0.17 | 21.7 ± 1.8 | c |
| | $H_2O$ 80 °C | 5.6 ± 0.0 | 4.9 | 0.19 ± 0.00 | 2.1 ± 0.0 | c | 2.47 ± 0.06 | 27.3 ± 0.6 | b |
| | MeOH $T_{amb}$ | 5.6 ± 0.0 | 2.4 | 0.24 ± 0.01 | 2.7 ± 0.1 | b | 2.04 ± 0.04 | 22.6 ± 0.5 | c |
| | MeOH 80 °C | 6.4 ± 0.1 | 2.5 | 0.45 ± 0.01 | 5.0 ± 0.1 | a | 2.94 ± 0.08 | 32.6 ± 0.8 | a |
| Spent coffee grounds | $H_2O$ $T_{amb}$ | 15.4 ± 0.2 | 5.2 | 0.34 ± 0.02 | 3.8 ± 0.2 | d | 1.50 ± 0.08 | 16.7 ± 0.9 | c |
| | $H_2O$ 80 °C | 20.8 ± 0.3 | 4.6 | 0.57 ± 0.02 | 6.3 ± 0.2 | c | 2.72 ± 0.07 | 30.2 ± 0.8 | a |
| | MeOH $T_{amb}$ | 15.1 ± 0.5 | 3.3 | 0.65 ± 0.01 | 7.2 ± 0.1 | b | 1.72 ± 0.07 | 19.1 ± 0.7 | b |
| | MeOH 80 °C | 19.1 ± 0.1 | 3.2 | 0.78 ± 0.02 | 8.6 ± 0.2 | a | 1.89 ± 0.07 | 21.0 ± 0.8 | b |

[a] Significant difference, i.e. $p < 0.05$, occurs when two conditions do not share letters.

*5.3.2 Liquor valorisation through anaerobic digestion*

The liquor recovered after the ultrasounds pretreatment was used as the substrate for AD. Despite the low pH of the liquors (Table 5.2), once mixed with the inoculum, all BMP tests started at a pH ranging between 7.6 and 8.0 (Table 5.3). The gas compositional analysis revealed that only methane and carbon dioxide were produced during AD (data not shown). The BMP of water-based liquors significantly increased with the pretreatment temperature ($p < 0.05$) for AS and SCG, whereas no significant difference for HS ($p > 0.05$) was observed (Figure 5.1). The water-based liquors recovered after the HS pretreatment produced 85.3 (± 12.2) and 79.9 (± 5.6) mL $CH_4$/100 mL liquor when the ultrasounds pretreatment was performed at $T_{amb}$ and 80 °C, respectively (Figure 5.1). The water-based liquors obtained from AS and SCG showed an increased BMP by 27 and 56% when the pretreatment occurred at 80 °C, achieving 107.0 (± 6.2) and 160.9 (± 16.6) mL $CH_4$/100 mL liquor, respectively (Figure 5.1). The cumulative production (Figure 5.1) showed that no methane was produced when the MeOH-based medium was used for ultrasounds diffusion, regardless the LM and the temperature used during the ultrasounds pretreatment.

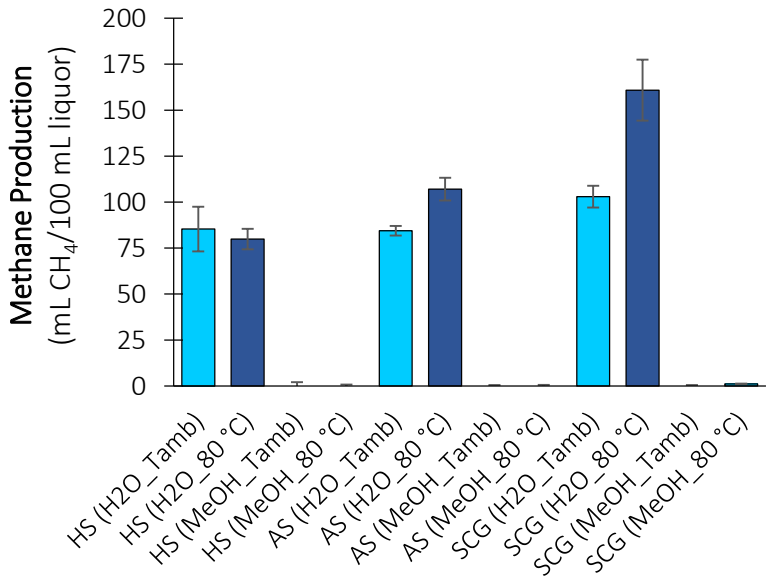


**Figure 5.1 –** Methane production potential of the liquor recovered after the ultrasounds pretreatment of hazelnut skin (HS), almond shell (AS), and spent coffee grounds (SCG) performed at ambient temperature ($T_{amb}$) and 80 °C using different media, i.e. distilled water and a 50% (*v/v*) methanol (MeOH) solution catalysed by 0.1% (*w/v*) sulfuric acid.

**Table 5.3 –** pH measured in the bottles digesting the liquid fraction from ultrasounds pretreatment at day 0 of observation and methane production potential with related statistical information of the liquid fractions expressed either as methane per 100 mL of liquor or as methane per gram of glucose added from the liquor.

| **Substrate** | **Pretreatment condition** | **Initial pH** | **Methane production potential** (mL/100 mL liquor) | **Statistical information** [a] | **Liquor$_{in}$** (mL) | **Glucose$_{in}$** (g) | **Methane production potential** (mL/g glucose$_{in}$) | **Statistical information** [a] |
|---|---|---|---|---|---|---|---|---|
| Hazelnut Skin liquor | $H_2O$ $T_{amb}$ | 8.0 ± 0.0 | 85.3 ± 12.2 | a | 30 | 0.19 | 131.5 ± 18.7 | a |
| | $H_2O$ 80 °C | 7.9 ± 0.1 | 79.9 ± 5.6 | a | 30 | 0.30 | 80.8 ± 5.6 | b |
| | MeOH $T_{amb}$ | 7.8 ± 0.1 | 0.0 ± 2.0 | b | 30 | 0.39 | 0.0 ± 1.6 | c |
| | MeOH 80 °C | 7.9 ± 0.1 | 0.0 ± 0.7 | b | 30 | 0.40 | 0.0 ± 0.6 | c |
| Almond Shell liquor | $H_2O$ $T_{amb}$ | 7.9 ± 0.1 | 84.4 ± 2.6 | b | 30 | 0.06 | 431.6 ± 13.2 | a |
| | $H_2O$ 80 °C | 7.9 ± 0.1 | 107.0 ± 6.2 | a | 30 | 0.07 | 434.2 ± 25.1 | a |
| | MeOH $T_{amb}$ | 7.7 ± 0.1 | 0.0 ± 0.5 | c | 30 | 0.06 | 0.0 ± 2.3 | b |
| | MeOH 80 °C | 7.7 ± 0.1 | 0.0 ± 0.6 | c | 30 | 0.09 | 0.0 ± 2.1 | b |
| Spent Coffee Grounds liquor | $H_2O$ $T_{amb}$ | 7.9 ± 0.1 | 102.9 ± 5.9 | b | 30 | 0.05 | 685.5 ± 39.5 | a |
| | $H_2O$ 80 °C | 7.9 ± 0.0 | 160.9 ± 16.6 | a | 30 | 0.08 | 590.5 ± 60.8 | a |
| | MeOH $T_{amb}$ | 7.7 ± 0.1 | 0.0 ± 0.5 | c | 30 | 0.05 | 0.0 ± 2.7 | b |
| | MeOH 80 °C | 7.8 ± 0.1 | 1.2 ± 0.1 | c | 30 | 0.06 | 6.1 ± 0.6 | b |

[a] Not sharing letters means that the condition was significantly different ($p < 0.05$) than the compared condition.

*5.3.3 Impact of ultrasounds on the chemical composition of hazelnut skin, almond shell and spent coffee grounds solid residues*

The compositional analysis (Table 5.4) revealed that, among the three untreated LMs, HS and AS have the highest lignin content, i.e. 39.7 (± 0.1) and 37.0 (± 0.4) g/100 g TS, respectively, whereas SCG has a lignin content of 18.7 (± 0.4) g/100 g TS. On the other hand, the untreated SCG is rich in structural sugars, i.e. 43.2 (± 0.1) g/100 g TS, with mannan (i.e. 54.4%), glucan (i.e. 21.8%), and galactan (i.e. 19.9%) being the most abundant. The overall sugar content of AS is 41.2 (± 0.1) g/100 g TS. The sugar speciation showed that xylan (i.e. 63.8%) is dominant in AS, and glucan (i.e. 31.3%) is the second most abundant sugar. The untreated HS has only 13.7 (± 0.1) g/100 g TS of structural sugars, mainly glucan (i.e. 74.5%). Apart from lignin and structural sugars, the total extractives represent 35.0 (± 0.0) and 29.0 (± 0.5) g/100 g TS of the overall dry matter of untreated HS and SCG, respectively. On the contrary, the total extractives content of untreated AS is 7.5 (± 0.1) g/100 g TS.

The ultrasounds pretreatment removed up to 13.1% of the total extractives from HS (Table 5.4). The increase in the pretreatment temperature enhanced the removal of total extractives from HS ($p < 0.05$), regardless the medium. The lignin content in the pretreated HS decreased ($p < 0.05$) up to 10.5%. Consequently, the content of structural sugars increased ($p < 0.05$) up to 17.1 (± 0.1) g/100 g TS after ultrasounds pretreatment of HS at 80 °C (Table 5.4). The mass balance assessment (Table 5.5) confirmed the solubilisation of extractives and lignin from HS under all the pretreatment conditions tested in this study. On the other hand, the solubilisation of structural sugars from HS was observed only at $T_{amb}$ (Table 5.5).

Regarding AS and SCG (Table 5.4), the ultrasounds pretreatment reduced by 50.7 ($p < 0.05$) and 18.6% ($p < 0.05$) the extractives percentage, respectively (Table 5.4). On the other hand, structural sugars and lignin concentrations measured in the pretreated AS and SCG were higher ($p < 0.05$) or comparable ($p > 0.05$) with the raw substrates, regardless the pretreatment condition (Table 5.4). The mass balance assessment (Table 5.5) showed that the lignin removal from AS and SCG was minimal compared to HS. In contrast, all pretreatment conditions enabled the removal of total extractives from AS and SCG. The solubilisation of structural sugars from SCG increased with the pretreatment temperature and was higher when using the MeOH-based medium (Table 5.5). On the other hand, the trend for the solubilisation of structural sugars from AS was not clearly identified.

*5.3.4 Methane production potential of the substrates before and after ultrasounds pretreatment*

The solid residues obtained after the ultrasounds pretreatment were used as the substrates for AD and compared with the raw LMs. The pretreated HS showed a lower BMP than raw HS (Figure 5.2A). Raw HS produced 255.5 (± 2.8) mL $CH_4$/g VS. The HS pretreated using water as the medium for the ultrasounds pretreatment at $T_{amb}$ and 80 °C lost 10 and 9% of the BMP ($p < 0.05$), achieving 228.9 (± 8.4) and 232.6 (± 6.4) mL $CH_4$/g VS, respectively. On the other hand, the ultrasounds pretreatment in the MeOH-based medium did not significantly ($p > 0.05$) affect the BMP of HS. The AD kinetic parameters did not improve after the applied ultrasounds pretreatment, being comparable to or worse than those obtained with the raw HS (Table 5.6).

The highest methane production from AS was obtained from the raw substrate, i.e. 50.6 (± 0.2) mL $CH_4$/g VS (Figure 5.2B). The AS residues after the ultrasounds pretreatment showed a significantly lower ($p < 0.05$) BMP than that of the raw substrate. No significant difference ($p > 0.05$) in the residual BMP from AS among the ultrasounds pretreatment conditions was observed, showing a decrease ranging from 15 to 22%. All kinetic parameters were negatively affected by the ultrasounds pretreatment. In particular, $\lambda$ was considerably higher than for raw AS (Table 5.6).

The SCG was the only solid residue in this study that benefited from the ultrasounds pretreatment. The highest methane production, i.e. 366.2 (± 4.2) mL $CH_4$/g VS, was measured from the SCG pretreated with ultrasounds in water at $T_{amb}$ (Figure 5.2C). Although the statistical comparison revealed that the difference in BMP was not significant ($p > 0.05$), the kinetic parameters showed an increase in the methane production rate from 9 to 13%, depending on the specific ultrasounds condition (Table 5.6).

**Table 5.4 –** Chemical composition of untreated and ultrasounds pretreated substrates expressed as total extractives, total structural sugars (i.e. glucan, xylan, mannan, arabinan, galactan, and rhamnan), total lignin, and ashes content. HS: hazelnut skin, AS: almond shell, and SCG: spent coffee grounds. Pretreatment media: distilled water and a 50% (*v/v*) methanol (MeOH) solution catalysed by 0.1% (*w/v*) sulfuric acid. Pretreatment temperature: ambient temperature ($T_{amb}$) and 80 °C.

| **Substrate** | **Pretreatment condition** | **Total Extractives** [a] (%) | **Total Structural Sugars** [a, b] (%) | **Total Lignin** [a, c] (%) | **Ashes** [a] (%) | **Unknown** [a, d] (%) | **Structural sugars speciation** | | | | | |
|---|---|---|---|---|---|---|---|---|---|---|---|---|
| | | | | | | | **Glucan** [a] (%) | **Xylan** [a] (%) | **Mannan** [a] (%) | **Arabinan** [a] (%) | **Galactan** [a] (%) | **Rhamnan** [a] (%) |
| HS | untreated | 35.0 ± 0.0 | 13.7 ± 0.1 | 39.7 ± 0.1 | 2.7 ± 0.1 | 8.9 ± 0.1 | 10.2 ± 0.1 | 1.0 ± 0.0 | 0.3 ± 0.0 | 0.7 ± 0.0 | 0.9 ± 0.0 | 0.7 ± 0.0 |
| | $H_2O$ $T_{amb}$ | 34.0 ± 0.0 | 14.0 ± 0.5 | 35.6 ± 0.2 | 2.1 ± 0.1 | 14.4 ± 0.14 | 10.6 ± 0.2 | 0.7 ± 0.0 | 0.2 ± 0.0 | 0.7 ± 0.1 | 1.0 ± 0.0 | 0.8 ± 0.1 |
| | $H_2O$ 80 °C | 32.3 ± 0.5 | 17.1 ± 0.5 | 38.5 ± 0.4 | 1.6 ± 0.1 | 10.5 ± 0.6 | 11.4 ± 0.2 | 1.9 ± 0.2 | 0.4 ± 0.0 | 1.2 ± 0.0 | 1.2 ± 0.0 | 1.0 ± 0.1 |
| | MeOH $T_{amb}$ | 33.8 ± 0.2 | 14.5 ± 0.6 | 36.2 ± 0.6 | 1.5 ± 0.0 | 14.1 ± 0.7 | 11.0 ± 0.4 | 0.8 ± 0.1 | 0.2 ± 0.0 | 0.7 ± 0.1 | 1.0 ± 0.0 | 0.8 ± 0.0 |
| | MeOH 80 °C | 30.4 ± 0.2 | 17.1 ± 0.1 | 36.4 ± 0.4 | 1.6 ± 0.1 | 14.5 ± 0.5 | 12.8 ± 0.1 | 1.0 ± 0.1 | 0.3 ± 0.1 | 0.8 ± 0.0 | 1.2 ± 0.1 | 0.9 ± 0.1 |
| AS | untreated | 7.5 ± 0.1 | 41.2 ± 0.1 | 37.0 ± 0.4 | 1.6 ± 0.1 | 12.6 ± 0.7 | 12.9 ± 0.2 | 26.3 ± 0.5 | 0.1 ± 0.0 | 0.7 ± 0.1 | 1.1 ± 0.1 | 0.2 ± 0.0 |
| | $H_2O$ $T_{amb}$ | 3.8 ± 0.1 | 40.6 ± 0.3 | 41.9 ± 0.3 | 0.5 ± 0.2 | 13.2 ± 0.4 | 12.4 ± 0.2 | 25.4 ± 0.1 | 0.0 ± 0.0 | 0.9 ± 0.0 | 1.3 ± 0.0 | 0.6 ± 0.0 |
| | $H_2O$ 80 °C | 6.5 ± 0.5 | 43.4 ± 0.2 | 39.0 ± 0.2 | 0.1 ± 0.0 | 10.9 ± 0.6 | 16.2 ± 0.1 | 24.1 ± 0.0 | 0.0 ± 0.0 | 1.3 ± 0.0 | 1.4 ± 0.0 | 0.5 ± 0.0 |
| | MeOH $T_{amb}$ | 3.7 ± 0.2 | 44.5 ± 0.3 | 41.1 ± 0.7 | 0.6 ± 0.2 | 10.2 ± 0.7 | 14.7 ± 0.1 | 27.4 ± 0.4 | 0.0 ± 0.0 | 0.9 ± 0.0 | 1.3 ± 0.0 | 0.3 ± 0.0 |
| | MeOH 80 °C | 4.0 ± 0.3 | 40.3 ± 0.1 | 41.8 ± 0.2 | 0.3 ± 0.1 | 13.7 ± 0.5 | 13.5 ± 0.1 | 24.9 ± 0.1 | 0.0 ± 0.0 | 0.6 ± 0.0 | 1.0 ± 0.0 | 0.3 ± 0.1 |
| SCG | untreated | 29.0 ± 0.5 | 43.2 ± 0.1 | 18.7 ± 0.4 | 1.4 ± 0.2 | 7.7 ± 0.7 | 9.4 ± 0.1 | 0.3 ± 0.1 | 23.5 ± 0.2 | 1.5 ± 0.0 | 8.6 ± 0.0 | 0.0 ± 0.0 |
| | $H_2O$ $T_{amb}$ | 24.5 ± 0.4 | 47.1 ± 0.2 | 21.6 ± 0.3 | 1.0 ± 0.1 | 5.9 ± 0.5 | 9.5 ± 0.0 | 0.1 ± 0.0 | 26.0 ± 0.2 | 1.7 ± 0.0 | 9.8 ± 0.0 | 0.0 ± 0.0 |
| | $H_2O$ 80 °C | 26.2 ± 0.2 | 43.5 ± 0.3 | 20.9 ± 0.4 | 0.6 ± 0.0 | 8.9 ± 0.5 | 9.2 ± 0.1 | 0.1 ± 0.0 | 23.8 ± 0.2 | 1.4 ± 0.1 | 9.0 ± 0.0 | 0.0 ± 0.0 |
| | MeOH $T_{amb}$ | 23.6 ± 0.0 | 48.6 ± 0.1 | 21.1 ± 0.3 | 0.1 ± 0.0 | 6.6 ± 0.5 | 9.6 ± 0.3 | 0.1 ± 0.0 | 26.8 ± 0.2 | 1.8 ± 0.0 | 10.2 ± 0.2 | 0.1 ± 0.0 |
| | MeOH 80 °C | 24.6 ± 0.1 | 46.0 ± 0.0 | 20.5 ± 0.0 | 0.1 ± 0.0 | 8.9 ± 0.6 | 9.8 ± 0.0 | 0.2 ± 0.1 | 25.3 ± 0.1 | 1.6 ± 0.0 | 9.1 ± 0.1 | 0.0 ± 0.0 |

[a] *Based on the dry matter (g/100 g TS).*

[a] *Total structural sugars are obtained as the sum of glucan, xylan, mannan, arabinan, galactan, and rhamnan.*

[b] *Total lignin is calculated as the sum of acid soluble lignin and Klason lignin* (Sluiter et al., 2008).

[c] *The unknown matter is calculated as the complement to 100 of the other components.*

**Table 5.5 –** Mass balance assessment considering the full extractives, total structural sugars, total lignin, ashes, and unknown matter measured before and after ultrasounds pretreatment.

| **Substrate** | **Pretreatment Condition** | **Initial substrate** (g) | **Substrate solubilisation** (%) | **Substrate loss** (g) | **Solid fraction recovered** (g) | **Full Extractives** (g) | **Total Structural Sugars** (g) | **Total Lignin** (g) | **Ashes** (g) | **Unknown** (g) |
|---|---|---|---|---|---|---|---|---|---|---|
| Hazelnut Skin | Raw | 15 | 0 | 0.0 | 15.0 | 5.3 | 2.1 | 5.9 | 0.4 | 1.3 |
| | $H_2O\_T_{amb}$ | 15 | 14.60 | 2.2 | 12.8 | 4.4 | 1.8 | 4.6 | 0.3 | 1.8 |
| | $H_2O$_80 °C | 15 | 19.33 | 2.9 | 12.1 | 3.9 | 2.1 | 4.7 | 0.2 | 1.3 |
| | $MeOH\_T_{amb}$ | 15 | 17.16 | 2.6 | 12.4 | 4.2 | 1.8 | 4.5 | 0.2 | 1.7 |
| | MeOH_80 °C | 15 | 23.51 | 3.5 | 11.5 | 3.5 | 2.0 | 4.2 | 0.2 | 1.7 |
| Almond Shell | Raw | 15 | 0.00 | 0.0 | 15.0 | 1.1 | 6.2 | 5.6 | 0.2 | 1.9 |
| | $H_2O\_T_{amb}$ | 15 | 5.74 | 0.9 | 14.1 | 0.5 | 5.7 | 5.9 | 0.1 | 1.9 |
| | $H_2O$_80 °C | 15 | 5.61 | 0.8 | 14.2 | 0.9 | 6.2 | 5.5 | 0.0 | 1.5 |
| | $MeOH\_T_{amb}$ | 15 | 5.61 | 0.8 | 14.2 | 0.5 | 6.3 | 5.8 | 0.1 | 1.4 |
| | MeOH_80 °C | 15 | 6.42 | 1.0 | 14.0 | 0.6 | 5.7 | 5.9 | 0.0 | 1.9 |
| Spent Coffee Grounds | Raw | 15 | 0.00 | 0.0 | 15.0 | 4.3 | 6.5 | 2.8 | 0.2 | 1.1 |
| | $H_2O\_T_{amb}$ | 15 | 15.36 | 2.3 | 12.7 | 3.1 | 6.0 | 2.7 | 0.1 | 0.8 |
| | $H_2O$_80 °C | 15 | 15.15 | 2.3 | 12.7 | 3.3 | 5.5 | 2.7 | 0.1 | 1.1 |
| | $MeOH\_T_{amb}$ | 15 | 20.75 | 3.1 | 11.9 | 2.8 | 5.8 | 2.5 | 0.0 | 0.8 |
| | MeOH_80 °C | 15 | 19.06 | 2.9 | 12.1 | 3.0 | 5.6 | 2.5 | 0.0 | 1.1 |

**Table 5.6 –** Methane production potential followed by statistical information and kinetic parameters, i.e. maximum specific methane production potential ($G_m$), maximum specific methane production rate ($R_m$), lag phase ($\lambda$), and correlation coefficient ($r^2$), obtained from the anaerobic digestion of raw and ultrasounds pretreated substrates using water ($H_2O$) and a 50% (*v/v*) methanol (MeOH) solution catalysed by 0.1% (*w/v*) sulfuric acid as the pretreatment media. HS: hazelnut skin, AS: almond shell, and SCG: spent coffee grounds. Pretreatment temperature: ambient temperature ($T_{amb}$) and 80 °C.

| **Substrate** | **Methane production potential** (mL $CH_4$/g VS) | **Statistical information** [a] | **$G_m$** [b] (mL $CH_4$/g VS·d) | **$R_m$** [b] (mL $CH_4$/g VS·d) | **$\lambda$** [b] (d) | **$r^2$** [c] |
|---|---|---|---|---|---|---|
| HS raw | 255.5 ± 2.8 | a | 254.3 | 15.76 | 3.9 | 0.9989 |
| HS $H_2O$ $T_{amb}$ | 228.9 ± 8.4 | b | 227.2 | 12.95 | 4.1 | 0.9982 |
| HS $H_2O$ 80 °C | 232.6 ± 6.4 | b | 230.8 | 13.35 | 3.9 | 0.9967 |
| HS MeOH $T_{amb}$ | 255.4 ± 7.4 | a | 253.4 | 15.61 | 3.7 | 0.9979 |
| HS MeOH 80 °C | 250.9 ± 1.9 | a | 248.9 | 14.15 | 3.5 | 0.9939 |
| AS raw | 50.6 ± 0.2 | a | 49.4 | 2.32 | 1.9 | 0.9945 |
| AS $H_2O$ $T_{amb}$ | 39.7 ± 1.7 | b | 39.0 | 1.90 | 4.5 | 0.9980 |
| AS $H_2O$ 80 °C | 40.2 ± 1.1 | b | 39.2 | 1.73 | 4.9 | 0.9966 |
| AS MeOH $T_{amb}$ | 42.8 ± 3.3 | b | 41.5 | 1.82 | 4.4 | 0.9962 |
| AS MeOH 80 °C | 41.1 ± 4.3 | b | 40.3 | 2.07 | 5.3 | 0.9990 |
| SCG raw | 345.1 ± 11.8 | ab | 345.1 | 19.61 | 5.6 | 0.9996 |
| SCG $H_2O$ $T_{amb}$ | 366.2 ± 4.2 | a | 365.1 | 21.31 | 5.6 | 0.9987 |
| SCG $H_2O$ 80 °C | 351.0 ± 4.9 | ab | 350.6 | 22.13 | 5.7 | 0.9972 |
| SCG MeOH $T_{amb}$ | 342.3 ± 12.1 | b | 341.2 | 21.36 | 5.4 | 0.9987 |
| SCG MeOH 80 °C | 352.5 ± 6.8 | ab | 351.3 | 21.49 | 5.4 | 0.9986 |

[a] Not sharing letters means that the condition was significantly different ($p < 0.05$) than the compared condition.

[b] Predicted by fitting the experimental data with a modified Gompertz model.

[c] Correlation coefficient between experimental and model data.

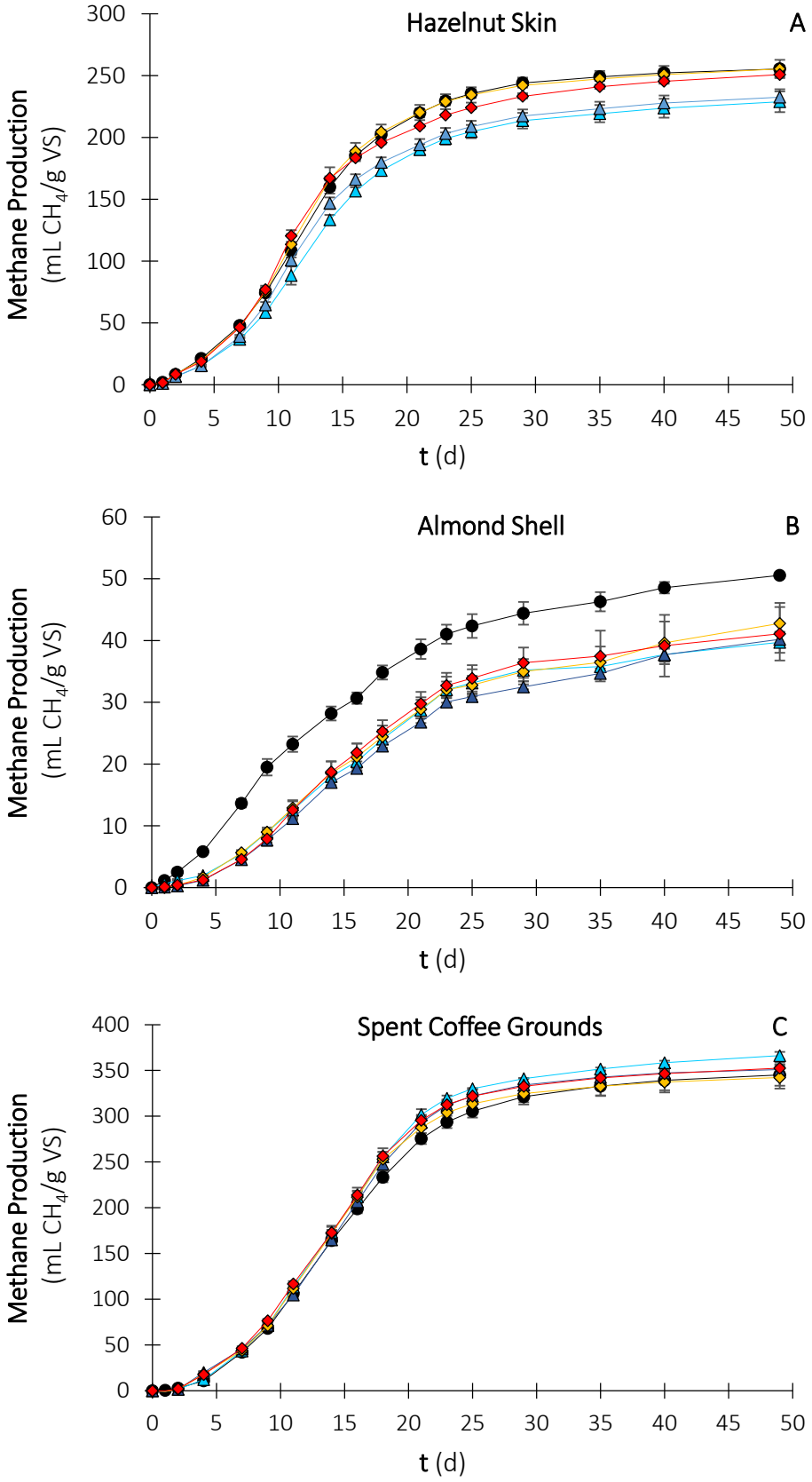


**Figure 5.2 –** Cumulative methane production obtained from the anaerobic digestion of raw and ultrasounds pretreated hazelnut skin (A), almond shell (B), and spent coffee grounds (C): raw (●), $H_2O$ at $T_{amb}$ (▲), $H_2O$ at 80 °C (▲), MeOH-based medium at $T_{amb}$ (◆), MeOH-based medium at 80 °C (◆).

## 5.4 Discussion

### *5.4.1 Biomass solubilisation during ultrasounds pretreatment*

This study showed for the first time a novel approach to valorise nut and coffee wastes through ultrasounds pretreatment. The available studies in the literature used the sonicated slurry (i.e. the mixture of the liquid and solid fractions) from ultrasound pretreatment of LMs as the substrate for methane production (Korai and Li, 2020; Qi et al., 2021). This approach can lead to the waste of valuable compounds that can be better valorised than via AD. Also, some of these compounds, e.g. polyphenols, can inhibit the AD process (Balasundaram et al., 2022). With the strategy here proposed, the optimal path for each fraction can be chosen by either using the solid and liquid fractions as the substrate for AD separately or, as a suggestion for future studies, using the liquid fraction for biomolecules recovery.

Ultrasound has been reported to be an effective technique for biomolecules extraction from algae, plants and fruit residues (Bhushan et al., 2020; de Sousa e Silva et al., 2017). In this study, the polyphenols and sugar solubilised from LMs through the ultrasounds pretreatment were quantified (Table 5.2). Polyphenols are generated from lignin disruption during the pretreatment (Covarrubias-García and Arriaga, 2022). The sugar solubilised through ultrasounds mainly come from the hemicellulose hydrolysis, whereas the cellulosic component of the biomass is generally unaffected by ultrasonic waves (Perrone et al., 2016). In addition, polyphenols and sugar are present in the non-bound matter of LMs, i.e. the extractives (Tajmirriahi et al., 2021).

#### *5.4.1.1 Polyphenols solubilisation*

HS is particularly rich in total extractives, i.e. 35.0% (Table 5.4). A considerable amount of the HS extractives are polyphenols, being mainly monomeric and oligomeric flavan-3-ols (Spagnuolo et al., 2021). The high polyphenols and lignin content resulted in 53.4 – 126.9 mg polyphenols/g TS solubilised from HS (Table 5.2), depending on the ultrasounds condition. The highest amount of polyphenols solubilised in this study is above the HS polyphenols content reported by Ivanović et al. (2020), i.e. 70 mg/g TS, indicating that part of the polyphenols measured come from the lignin disruption achieved during the ultrasounds pretreatment (Table 5.5). Similarly, polyphenols are the most abundant components of AS extractives (Queirós et al., 2020). However, the low total extractives content of AS (i.e. 7.5%) observed in this study (Table 5.4) and the scarce lignin removal (Table 5.5) resulted in a significantly lower polyphenols solubilisation from AS than HS ($p < 0.05$), i.e. 0.7 – 5.0 mg/g TS (Table 5.2). On

the contrary, despite the high total extractives content (i.e. 29.0%) of SCG (Table 5.4), polyphenols only represent a minor portion of the extractives in SCG (Sant'Anna et al., 2017). Therefore, considering the slight lignin removal during the pretreatment (Table 5.5), the polyphenols solubilised from SCG, i.e. 3.8 – 8.6 mg/g TS, were significantly lower than what was observed for HS ($p < 0.05$) (Table 5.2).

The capability of obtaining biomolecules from LMs depends on the chemical and physical properties of the substrate (Ibrahim et al., 2019). Oliva et al. (2021) showed that despite the recalcitrance caused by the high lignin content, HS is easily dented by solvent-based pretreatments due to its high porosity. On the other hand, the compact external surface and low porosity of AS made this LM particularly resistant to pretreatments (Oliva et al., 2021). In the present study, the pretreatment temperature was a key parameter for polyphenols solubilisation when distilled water was the medium for the ultrasounds pretreatment. Similarly, Tanase et al. (2018) reported an increment in polyphenols solubilisation when increasing the temperature of the medium during ultrasounds pretreatment from 40 to 60 °C. Ultrasounds generate hot spots due to bubble collapse, increasing the temperature of the medium (Bundhoo and Mohee, 2018). This facilitates cavitation phenomena, likely being the reason for the increased polyphenols solubilisation from all LMs here investigated (Table 5.2).

The impact of the pretreatment temperature on polyphenols solubilisation was lower when using the MeOH-based medium. An increase in the pretreatment temperature during ultrasounds pretreatment facilitates cavitation phenomena but may lower the power of bubble collapse. The vapour generation increases with the temperature of the solvent and fills the cavitation bubbles, reducing the energy released once collapsing (Bussemaker and Zhang, 2013). Therefore, the optimal pretreatment temperature depends on the given system. The boiling point of MeOH is lower than that of distilled water. Therefore, at 80 °C, the vapour production from the MeOH-based medium is expected to be greater than that from water, and to have a greater negative impact on the ultrasounds pretreatment. On the other hand, using low polarity liquids, such as organic solvents, offers the opportunity to combine the effects of organosolv and ultrasounds pretreatment. Juttuporn et al. (2018) investigated polyphenols removal from sugarcane bagasse using ultrasounds, showing that the ethanol (EtOH)-based medium was more efficient than water. MeOH and EtOH-based solutions are the most employed organic solvents for polyphenols removal through ultrasounds (Dzah et al., 2020). In

addition, MeOH may have a better impact than EtOH on lignin solubilisation (Sameni et al., 2017).

*5.4.1.2 Sugar solubilisation*

The pretreated HS solid residues has a higher content of structural sugars and lower lignin and total extractives content than the raw LM (Table 5.4). However, the sugar analysis showed that the liquor recovered after the ultrasounds pretreatment of HS had the highest sugar concentration among the LMs investigated (up to 146.0 mg/g TS). The sugar speciation (Table 5.4) showed that the main sugar in HS is glucan, which is associated with the cellulosic component of the biomass (Bulmer et al., 2021). On the contrary, the hemicellulose sugars are minor components of the HS. After the ultrasounds pretreatment, the glucan content slightly increased, indicating that mainly other components of HS were removed (Table 5.5). Therefore, the sugars present in the HS liquor were likely solubilised from the non-bound matter, i.e. extractives. Frankó et al. (2018) previously reported the presence of free sugars in the water-soluble extractives of LMs, i.e. spruce and pine softwood. Apart from the structural sugars, HS is rich in galacturonic acid, generated from pectin degradation during the roasting process (Košťálová and Hromádková, 2019).

The pretreatment temperature was a key parameter to enhance the sugar solubilisation from HS in water (Table 5.2). On the other hand, the MeOH-based medium at $T_{amb}$ was effective enough to remove all soluble sugars from HS under the ultrasounds conditions tested in this study. Therefore, no significant effect of the temperature was observed during the MeOH-based pretreatment. The importance of the temperature for sugar solubilisation in water was previously reported by da Silva Donadone et al. (2020) for peach palm residue. On the other hand, to the best of the authors' knowledge, the impact of the temperature on ultrasound-assisted solubilisation of sugar from LMs in the MeOH-based media has never been investigated before.

Similarly to other nut shells, AS showed a low free sugar content (Shen et al., 2018), in line with the low amount of sugar solubilised in the ultrasound liquors (Table 5.2). The highest pretreatment temperature increased the sugar removal. The highest sugar solubilisation, i.e. 32.6 mg/g TS, from AS was achieved at 80 °C in the MeOH-based medium. The amount of sugar here solubilised corresponded to over 90% of the overall non-structural sugar content of AS reported by Shen et al. (2018), suggesting that the extra potential for sugar solubilisation from AS is limited. Moreover, no significant change in sugar speciation was observed in the

pretreated AS (Table 5.4), suggesting that the sugars are mainly solubilised from the non-bound matter (Table 5.5).

The sugar solubilised from SCG at $T_{amb}$ in water (i.e. 16.7 mg/g TS) and MeOH-based medium (i.e. 19.1 mg/g TS) was slightly lower than that achieved by Ballesteros et al. (2015) via alkaline pretreatment at 25 °C, i.e. 23.8 mg/g TS. In this study, the ultrasound-assisted solubilisation lasted only 1 h, whereas Ballesteros et al. (2015) performed the alkaline pretreatment overnight. In addition, increasing the pretreatment temperature allowed the solubilisation of up to 30.2 mg sugars/g TS (Table 5.2). Contrary to HS and AS, the MeOH-based medium did not enhance the sugar solubilisation from SCG (Table 5.2). The sugar speciation of the pretreated SCG was similar to that of the raw SCG, and the lignin content barely changed after pretreatment (Table 5.4). In contrast, the total extractives content was lower (up to 19%) upon pretreatment (Table 3). The solubilisation of extractives was higher when using the MeOH-based medium, following the trend of polyphenols solubilisation, as discussed in Section 5.4.1.1. On the other hand, the solubilisation of polyphenols and sugar does not fully justify the high solubilisation percentage observed, i.e. 15 – 21%. Apart from the components investigated in this study, SCG is an oil-rich LM (Goh et al., 2020), likely being solubilised during the ultrasounds pretreatment as well and accounting for the solubilisation percentage here observed. In particular, MeOH has been widely used for oil extraction from SCG (Battista et al., 2021), which can explain the higher solubilisation percentage observed when using the MeOH-based medium for ultrasounds pretreatment.

### *5.4.2 Valorisation of ultrasounds pretreatment fractions via anaerobic digestion*

#### *5.4.2.1 Ultrasounds-resulting liquors*

The liquor from pretreated HS was rich in sugars, likely coming from the easily biodegradable non-bound matter (Table 5.5). The highest methane production, i.e. 85.3 (± 12.2) mL $CH_4$/100 mL liquor, was obtained from the water-based liquor at $T_{amb}$ (Figure 5.1). The water-based liquor obtained from the ultrasounds pretreatment at 80 °C showed a higher sugar content, i.e. 9.9 g/L, than at $T_{amb}$, i.e. 6.5 g/L, but gave a similar methane production (Figure 5.1). The failure to increase the BMP is likely attributed to the higher polyphenols concentration that may have partially inhibited the AD process (Balasundaram et al., 2022). The liquid fraction from the ultrasounds pretreated AS and SCG exhibited a similar performance as substrates for AD, with the liquors recovered after ultrasounds at 80 °C producing more methane (Figure 5.1). Contrary to HS, the sugars solubilised in the liquors from AS and SCG were significantly higher than the

polyphenols (Table 5.2), resulting in a higher methane production potential than the HS liquors despite the overall lower sugar concentration (Table 5.4). Xue et al. (2018) reported that increasing the concentration of phenolic compounds solubilised from LMs resulted in a lower sugar degradation in the fermentation of sugar-rich liquid substrates, which likely occurred in the AD of the HS liquors.

The lower polyphenols concentration in the liquid fractions resulted in a higher methane yield per gram of sugar added in the AD process (Table 5.3). The water-based liquors recovered from SCG pretreatment at $T_{amb}$ and 80 °C showed the highest methane yield among the LMs investigated, producing 685.5 (± 39.5) and 590.5 (± 60.8) mL $CH_4$/g $glucose_{in}$, respectively (Table 5.3). The water-based liquors recovered from the ultrasounds pretreatment of AS at $T_{amb}$ and 80 °C produced 431.6 (± 13.2) and 434.2 (± 25.1) mL $CH_4$/g $glucose_{in}$, respectively (Table 5.3). On the other hand, the inhibitory effect of polyphenols at high concentrations was confirmed by the low methane yield achieved from the HS liquor, i.e. 131.5 (± 18.7) and 80.8 (± 5.6) mL $CH_4$/g $glucose_{in}$, respectively (Table 5.3). The MeOH present in the liquors completely inhibited methane production, regardless the LM used (Figure 5.1). At moderate concentrations, MeOH is beneficial for the AD process, being a direct methanogenic substrate for methylotrophic methanogens (Feng et al., 2021). Nevertheless, higher MeOH concentrations without a proper microbial acclimation can hinder the methanogenic activity. Mancini et al. (2021) reported that 14.3 g VS/L is the half-maximal inhibitory concentration for methane production from MeOH-rich (i.e. 694 g MeOH/L) wastewater. Therefore, when using MeOH-based media for ultrasounds pretreatment, the recovery of the organic solvent is suggested to avoid AD inhibition and reduce the overall costs of the process. On the contrary, water-based liquors can be immediately subjected to AD.

*5.4.2.2 Ultrasounds pretreated solid substrates*

The solid HS residues after the ultrasounds pretreatment showed a high BMP (Table 5.6), despite the loss of sugar and polyphenols. The BMP of raw HS, i.e. 255.5 (± 2.8) mL $CH_4$/g VS, is comparable with previous studies (Mancini et al., 2016). The pretreated HS showed an increased structural sugar percentage while a lower lignin concentration was observed (Table 5.4). Nevertheless, the BMP of the HS obtained after the ultrasounds pretreatment in water was slightly lower than that of raw HS (Figure 5.2A). This can be attributed to the loss of non-structural sugars during ultrasounds, as discussed in Section 5.4.1.2. On the other hand, for the HS pretreated in the MeOH-based medium, the higher polyphenols removal (Table 5.2)

balanced the loss of fermentable sugars and returned a BMP similar to the raw HS (Table 5.6). The overall content of structural sugars measured in HS was significantly lower than that of other nut residues (Bianco et al., 2021b; Shen et al., 2018), reaching a maximum of 17.1% after the ultrasounds pretreatment. The high methane production compared to the low sugar content can be explained by the high porosity of the HS, which allows a proper microorganisms-substrate contact during AD (Oliva et al., 2021). In addition, the extractives of HS are reported to have a high protein and lipid content, i.e. 7.4 and 12.0 g/100 g TS (Ivanović et al., 2020), being additional substrates for methane production (Cheng and Brewer, 2021).

AS was the most recalcitrant among the LMs investigated in this study, and the ultrasounds pretreatment further lowered the BMP of AS (Figure 5.2B). Contrary to HS, the physical properties limit the biodegradation of AS, having low porosity and compact external surface (Oliva et al., 2021). The BMP of raw AS, i.e. 50.6 (± 0.2) mL $CH_4$/g VS, is comparable with that reported by Shen et al. (2018). Generally, the AD of nut shells lead to a lower methane production than other nut residues due to their coriaceous structure used to protect the edible fruit from grazers and the environment (Shen et al., 2018; Xiao et al., 2020). The ultrasounds pretreatment removed part of the extractives, whereas the structural components were barely touched (Table 5.4), resulting in a slight reduction of the BMP and a longer lag phase (Table 5.6), as previously observed when removing the extractives from AS by organosolv pretreatment (Oliva et al., 2021). The main structural sugars present in AS are xylan and glucan (Table 5.4), which are reported to be the most important substrate for AD of LMs (Zhong et al., 2015). Nevertheless, the high lignin content and the compact external surface strongly limit the hydrolysis of structural sugars from LMs (Xu et al., 2019).

The AD of SCG residues after ultrasounds showed a higher methane production rate than raw SCG (Table 5.6). The main changes in the chemical composition were the loss of extractives and the increment in mannan and lignin content (Table 5.4). The lower lignin content and increased contact surface, due to the powdery nature of the SCG, resulted in the highest BMP among the LMs investigated, i.e. 345.1 (± 11.8) mL $CH_4$/g VS (Figure 5.2C). Other authors reported a lower methane production from raw SCG, i.e. 220 mL $CH_4$/g VS (Battista et al., 2021). This difference in methane production potential can be attributed to the diversity in the coffee species, as well as in torrefaction and coffee brewing procedures.

*5.4.3 Perspectives of ultrasounds applications for lignocellulosic materials valorisation*

The optimal methodology for ultrasounds application is still debated. Recent studies showed an enhanced methane production potential using the sonicated slurry obtained after the ultrasounds pretreatment of corn stover (Hassan et al., 2017) and cannabis straw (Qi et al., 2021) as the substrates for AD. In contrast, this study evaluated separately the BMP of the liquid (Figure 1) and solid (Figure 2) fractions. Alternatively, Zou et al. (2016a, 2016b) pretreated dairy manure and wheat straw with ultrasounds before digesting the slurry. Therefore, the contribution in terms of the extra methane produced from the sole LM was thus far not fully disclosed in the literature.

The failure in increasing the BMP of the solid residues in this study could be due to the low $E_d$ applied during the pretreatment. An $E_d$ value of 10.6 MJ/kg TS (calculated using Eq. (5.1)) was applied, being significantly lower than that of Hassan et al. (2017), i.e. 88.5 MJ/kg VS, which increased the methane production potential of corn stover by 43%, using the sonicated slurry as the substrate. On the other hand, in this study, the ultrasounds pretreatment was carried out to improve the release of biomolecules present in LMs, that could be a further valorisation of the HS, AS, and SCG with a multi-product biorefinery approach.

This work demonstrated the viability of releasing high-value bioproducts while maintaining the high methane production potential of the solid residues. Organic agroindustrial wastes have been widely explored for biofuels production. Nevertheless, the interest in specific biomolecules recovery is recently increasing (Jain et al., 2022). In this perspective, ultrasounds pretreatment is a promising strategy offering several possibilities to regulate and optimise the process, e.g. temperature control, medium of diffusion, and energy density applied (Oliva et al., 2022). The future developments for ultrasounds applications seem to head toward the coupling with specific solvents to promote either the release of biomolecules or an increment of the methane production potential from the solid residues. Apart from the organic solvent investigated in this study, i.e. MeOH, ultrasounds were employed to assist alkaline pretreatment (Korai and Li, 2020) and dilute acid hydrolysis (Ríos-González et al., 2021) of LMs. A further suggestion may be to investigate ultrasounds assistance to other solvent-based pretreatments that do not require high temperature, i.e. over 100 °C, to activate the reaction, e.g. deep eutectic solvents (Wang and Lee, 2021). Nevertheless, investigating and optimising the valorisation of the liquid and solid fractions independently seems to be a more attractive approach, especially for the LMs rich in valuable bioproducts such as polyphenols, protein, and oils.

## 5.5 Conclusion

The liquid and solid fractions obtained from HS, AS, and SCG after ultrasounds pretreatment (using water and a MeOH-based medium at $T_{amb}$ and 80 °C) were investigated to determine their potential in terms of methane production and solubilisation of polyphenols and sugar. HS has the greatest potential for biomolecules solubilisation among the LMs investigated, achieving up to 126.9 and 146.0 mg/g TS of polyphenols and sugar solubilised, respectively. The liquors obtained from HS would benefit from further studies to investigate the selective recovery of specific biomolecules. On the other hand, the BMP of the HS liquors was limited compared to the amount of sugar solubilised. Polyphenols and sugar solubilised from AS and SCG were significantly lower than those obtained from HS, but the AS and SCG liquors showed a higher BMP. Thus, the water-based liquors from AS and SCG are suitable for direct AD, producing up to 107.0 and 160.9 mL $CH_4$/100 mL liquor, respectively. In contrast, the liquid fractions obtained using the MeOH-based medium would need a further step of MeOH removal to avoid the inhibition of methanogenesis. Apart from the liquid fractions, the solid residues obtained after the ultrasounds pretreatment showed a great potential for methane production for the three LMs investigated, although in most cases being comparable with the raw LMs.

## 5.6 References

APHA AWWA, W.E.F., 2005. Standard methods for the examination of water and wastewater. APHA WEF AWWA.

Balasundaram, G., Banu, R., Varjani, S., Kazmi, A.A., Tyagi, V.K., 2022. Recalcitrant compounds formation, their toxicity, and mitigation: Key issues in biomass pretreatment and anaerobic digestion. Chemosphere 291, 132930. https://doi.org/10.1016/j.chemosphere.2021.132930

Ballesteros, L.F., Cerqueira, M.A., Teixeira, J.A., Mussatto, S.I., 2015. Characterization of polysaccharides extracted from spent coffee grounds by alkali pretreatment. Carbohydr. Polym. 127, 347–354. https://doi.org/10.1016/j.carbpol.2015.03.047

Battista, F., Zuliani, L., Rizzioli, F., Fusco, S., Bolzonella, D., 2021. Biodiesel, biogas and fermentable sugars production from Spent coffee Grounds: A cascade biorefinery approach. Bioresour. Technol. 342, 125952. https://doi.org/10.1016/j.biortech.2021.125952

Bhushan, S., Kumar, A., Singh, N., Sheikh, J., 2020. Functionalization of wool fabric using lignin biomolecules extracted from groundnut shells. Int. J. Biol. Macromol. 142, 559–

563. https://doi.org/10.1016/j.ijbiomac.2019.09.130

Bianco, F., Race, M., Forino, V., Pacheco-Ruiz, S., Rene, E.R., 2021a. Bioreactors for wastewater to energy conversion : from pilot to full scale, in: Waste Biorefinery. Elsevier Inc., pp. 103–124. https://doi.org/10.1016/B978-0-12-821879-2/00004-1

Bianco, F., Şenol, H., Papirio, S., 2021b. Enhanced lignocellulosic component removal and biomethane potential from chestnut shell by a combined hydrothermal–alkaline pretreatment. Sci. Total Environ. 762. https://doi.org/10.1016/j.scitotenv.2020.144178

Bulmer, G.S., de Andrade, P., Field, R.A., van Munster, J.M., 2021. Recent advances in enzymatic synthesis of β-glucan and cellulose. Carbohydr. Res. 508, 108411. https://doi.org/10.1016/j.carres.2021.108411

Bundhoo, Z.M.A., Mohee, R., 2018. Ultrasound-assisted biological conversion of biomass and waste materials to biofuels: A review. Ultrason. Sonochem. 40, 298–313. https://doi.org/10.1016/j.ultsonch.2017.07.025

Bussemaker, M.J., Zhang, D., 2013. Effect of ultrasound on lignocellulosic biomass as a pretreatment for biorefinery and biofuel applications. Ind. Eng. Chem. Res. 52, 3563–3580. https://doi.org/10.1021/ie3022785

Cheng, F., Brewer, C.E., 2021. Conversion of protein-rich lignocellulosic wastes to bio-energy: Review and recommendations for hydrolysis + fermentation and anaerobic digestion. Renew. Sustain. Energy Rev. 146, 111167. https://doi.org/10.1016/j.rser.2021.111167

Covarrubias-García, I., Arriaga, S., 2022. Adsorbents for the Detoxification of Lignocellulosic Wastes Hydrolysates to Improve Fermentative Processes to Bioenergy and Biochemicals Production, in: Renewable Energy Technologies for Energy Efficient Sustainable Development. Springer, pp. 63–83. https://doi.org/10.1007/978-3-030-87633-3_3

Cubero-Cardoso, J., Trujillo-Reyes, Á., Marín-Ayllón, P., Rodríguez-Gutiérrez, G., Villa-Gomez, D., Serrano, A., Borja, R., Fermoso, F.G., 2020. Solubilization of phenols and sugars from raspberry extrudate by hydrothermal treatments. Processes 8, 1–16. https://doi.org/10.3390/pr8070842

da Silva Donadone, D.B., Giombelli, C., Silva, D.L.G., Stevanato, N., da Silva, C., Bolanho Barros, B.C., 2020. Ultrasound-assisted extraction of phenolic compounds and soluble sugars from the stem portion of peach palm. J. Food Process. Preserv. 44, 1–11. https://doi.org/10.1111/jfpp.14636

de Sousa e Silva, A., Moreira, L.M., de Magalhães, W.T., Farias, W.R.L., Rocha, M.V.P., Bastos, A.K.P., 2017. Extraction of biomolecules from Spirulina platensis using non-

conventional processes and harmless solvents. J. Environ. Chem. Eng. 5, 2101–2106. https://doi.org/10.1016/j.jece.2017.04.008

Dubois, M., Gilles, K., Hamilton, J.K., Rebers, P.A., Smith, F., 1956. Colorimetric method for determination of sugars and related substances. Anal. Chem. 28, 350–356. https://doi.org/10.1021/ac60111a017

Dzah, C.S., Duan, Y., Zhang, H., Wen, C., Zhang, J., Chen, G., Ma, H., 2020. The effects of ultrasound assisted extraction on yield, antioxidant, anticancer and antimicrobial activity of polyphenol extracts: A review. Food Biosci. 35, 100547. https://doi.org/10.1016/j.fbio.2020.100547

Feng, Y., Duan, J.L., Sun, X.D., Ma, J.Y., Wang, Q., Li, X.Y., Tian, W.X., Wang, S.G., Yuan, X.Z., 2021. Insights on the inhibition of anaerobic digestion performances under short-term exposure of metal-doped nanoplastics via Methanosarcina acetivorans. Environ. Pollut. 275, 115755. https://doi.org/10.1016/j.envpol.2020.115755

Filer, J., Ding, H.H., Chang, S., 2019. Biochemical methane potential (BMP) assay method for anaerobic digestion research. Water (Switzerland) 11. https://doi.org/10.3390/w11050921

Frankó, B., Carlqvist, K., Galbe, M., Lidén, G., Wallberg, O., 2018. Removal of water-soluble extractives improves the enzymatic digestibility of steam-pretreated softwood barks. Appl. Biochem. Biotechnol. 184, 599–615. https://doi.org/10.1007/s12010-017-2577-2

Garoma, T., Pappaterra, D., 2018. An investigation of ultrasound effect on digestate solubilization and methane yield. Waste Manag. 71, 728–733. https://doi.org/10.1016/j.wasman.2017.03.021

Goh, B.H.H., Ong, H.C., Chong, C.T., Chen, W.H., Leong, K.Y., Tan, S.X., Lee, X.J., 2020. Ultrasonic assisted oil extraction and biodiesel synthesis of spent coffee ground. Fuel 261, 116121. https://doi.org/10.1016/j.fuel.2019.116121

Hassan, M., Umar, M., Mamat, T., Muhayodin, F., Talha, Z., Mehryar, E., Ahmad, F., Ding, W., Zhao, C., 2017. Methane Enhancement through Sequential Thermochemical and Sonication Pretreatment for Corn Stover with Anaerobic Sludge. Energy and Fuels 31, 6145–6153. https://doi.org/10.1021/acs.energyfuels.7b00478

Holliger, C., Alves, M., Andrade, D., Angelidaki, I., Astals, S., Baier, U., Bougrier, C., Buffière, P., Carballa, M., De Wilde, V., Ebertseder, F., Fernández, B., Ficara, E., Fotidis, I., Frigon, J.C., De Laclos, H.F., Ghasimi, D.S.M., Hack, G., Hartel, M., Heerenklage, J., Horvath, I.S., Jenicek, P., Koch, K., Krautwald, J., Lizasoain, J., Liu, J., Mosberger, L., Nistor, M., Oechsner, H., Oliveira, J.V., Paterson, M., Pauss, A., Pommier, S., Porqueddu, I., Raposo,

F., Ribeiro, T., Pfund, F.R., Strömberg, S., Torrijos, M., Van Eekert, M., Van Lier, J., Wedwitschka, H., Wierinck, I., 2016. Towards a standardization of biomethane potential tests. Water Sci. Technol. 74, 2515–2522. https://doi.org/10.2166/wst.2016.336

Ibrahim, M.I.J., Sapuan, S.M., Zainudin, E.S., Zuhri, M.Y.M., 2019. Extraction, chemical composition, and characterization of potential lignocellulosic biomasses and polymers from corn plant parts. BioResources 14, 6485–6500. https://doi.org/10.15376/biores.14.3.6485-6500

International Coffee Organization (ICO), 2020. Annual review: coffee year 2019/2020.

International Nut and Dried Fruit Council Foundation, 2021. Nuts & dried fruits statistical yearbook 2020/2021.

Ivanović, S., Avramović, N., Dojčinović, B., Trifunović, S., Novaković, M., Tešević, V., Mandić, B., 2020. Contents and Antioxidant Activity as Nutritive Potential of Roasted Hazelnut Skins (Corylus avellana L.). Foods 9, 1–14. https://doi.org/doi:10.3390/foods9040430

Jain, A., Sarsaiya, S., Kumar Awasthi, M., Singh, R., Rajput, R., Mishra, U.C., Chen, J., Shi, J., 2022. Bioenergy and bio-products from bio-waste and its associated modern circular economy: Current research trends, challenges, and future outlooks. Fuel 307, 121859. https://doi.org/10.1016/j.fuel.2021.121859

Juttuporn, W., Thiengkaew, P., Rodklongtan, A., Rodprapakorn, M., Chitprasert, P., 2018. Ultrasound-Assisted Extraction of Antioxidant and Antibacterial Phenolic Compounds from Steam-Exploded Sugarcane Bagasse. Sugar Tech 20, 599–608. https://doi.org/10.1007/s12355-017-0582-y

Korai, R.M., Li, X., 2020. Effect of ultrasonic assisted KOH pretreatment on physiochemical characteristic and anaerobic digestion performance of wheat straw. Chinese J. Chem. Eng. 28, 2409–2416. https://doi.org/10.1016/j.cjche.2020.06.022

Košťálová, Z., Hromádková, Z., 2019. Structural characterisation of polysaccharides from roasted hazelnut skins. Food Chem. 286, 179–184. https://doi.org/10.1016/j.foodchem.2019.01.203

Koupaie, E.H., Dahadha, S., Bazyar Lakeh, A.A., Azizi, A., Elbeshbishy, E., 2019. Enzymatic pretreatment of lignocellulosic biomass for enhanced biomethane production-A review. J. Environ. Manage. 233, 774–784. https://doi.org/10.1016/j.jenvman.2018.09.106

Li, Y., Chen, Y., Wu, J., 2019. Enhancement of methane production in anaerobic digestion process: A review. Appl. Energy 240, 120–137.

https://doi.org/10.1016/j.apenergy.2019.01.243

Mancini, E., Tian, H., Angelidaki, I., Fotidis, I.A., 2021. The implications of using organic-rich industrial wastewater as biomethanation feedstocks. Renew. Sustain. Energy Rev. 144, 110987. https://doi.org/10.1016/j.rser.2021.110987

Mancini, G., Papirio, S., Lens, P.N.L., Esposito, G., 2018. Increased biogas production from wheat straw by chemical pretreatments. Renew. Energy 119, 608–614. https://doi.org/10.1016/j.renene.2017.12.045

Mancini, G., Papirio, S., Lens, P.N.L., Esposito, G., 2016. Effect of *N* -methylmorpholine- *N* -oxide Pretreatment on Biogas Production from Rice Straw, Cocoa Shell, and Hazelnut Skin. Environ. Eng. Sci. 33, 843–850. https://doi.org/10.1089/ees.2016.0138

Mirmohamadsadeghi, S., Karimi, K., Azarbaijani, R., Parsa Yeganeh, L., Angelidaki, I., Nizami, A.S., Bhat, R., Dashora, K., Vijay, V.K., Aghbashlo, M., Gupta, V.K., Tabatabaei, M., 2021. Pretreatment of lignocelluloses for enhanced biogas production: A review on influencing mechanisms and the importance of microbial diversity. Renew. Sustain. Energy Rev. 135. https://doi.org/10.1016/j.rser.2020.110173

Murthy, P.S., Naidu, M.M., 2012. Resources , Conservation and Recycling Sustainable management of coffee industry by-products and value addition — A review. Resour. Conserv. Recycl. 66, 45–58. https://doi.org/10.1016/j.resconrec.2012.06.005

Oliva, A., Papirio, S., Esposito, G., Lens, P.N.L., 2022. Pretreatment of Lignocellulosic Materials to Enhance their Methane Potential, in: Sinharoy, A., Lens, P.N.L. (Eds.), Renewable Energy Technologies for Energy Efficient Sustainable Development, Applied Environmental Science and Engineering for a Sustainable Future. Springer, pp. 85–120. https://doi.org/10.1007/978-3-030-87633-3_4

Oliva, A., Tan, L.C., Papirio, S., Esposito, G., Lens, P.N.L., 2021. Effect of methanol-organosolv pretreatment on anaerobic digestion of lignocellulosic materials. Renew. Energy 169, 1000–1012. https://doi.org/10.1016/j.renene.2020.12.095

Ormaechea, P., Castrillón, L., Suárez-Peña, B., Megido, L., Fernández-Nava, Y., Negral, L., Marañón, E., Rodríguez-Iglesias, J., 2018. Enhancement of biogas production from cattle manure pretreated and/or co-digested at pilot-plant scale. Characterization by SEM. Renew. Energy 126, 897–904. https://doi.org/10.1016/j.renene.2018.04.022

Papirio, S., 2020. Coupling acid pretreatment and dosing of Ni and Se enhances the biomethane potential of hazelnut skin. J. Clean. Prod. 262, 121407. https://doi.org/10.1016/j.jclepro.2020.121407

Perrone, O.M., Colombari, F.M., Rossi, J.S., Moretti, M.M.S., Bordignon, S.E., Nunes, C. da C.C., Gomes, E., Boscolo, M., Da-Silva, R., 2016. Ozonolysis combined with ultrasound as a pretreatment of sugarcane bagasse: Effect on the enzymatic saccharification and the physical and chemical characteristics of the substrate. Bioresour. Technol. 218, 69–76. https://doi.org/10.1016/j.biortech.2016.06.072

Qi, N., Zhao, X., Zhang, L., Gao, M., Yu, N., Liu, Y., 2021. Performance assessment on anaerobic co-digestion of Cannabis ruderalis and blackwater: Ultrasonic pretreatment and kinetic analysis. Resour. Conserv. Recycl. 169, 105506. https://doi.org/10.1016/j.resconrec.2021.105506

Queirós, C.S.G.P., Cardoso, S., Lourenço, A., Ferreira, J., Miranda, I., Lourenço, M.J. V., Pereira, H., 2020. Characterization of walnut, almond, and pine nut shells regarding chemical composition and extract composition. Biomass Convers. Biorefinery 10, 175–188. https://doi.org/10.1007/s13399-019-00424-2

Ríos-González, L.J., Medina-Morales, M.A., Rodríguez-De la Graza, J.A., Romero-Galarza, A., Dávila Medina, D., Morales-Martínez, T.K., 2021. Comparison of dilute acid pretreatment of agave assisted by microwave versus ultrasound to enhance enzymatic hydrolysis. Bioresour. Technol. 319, 124099. https://doi.org/10.1016/j.biortech.2020.124099

Sameni, J., Krigstin, S., Sain, M., 2017. Solubility of Lignin and Acetylated Lignin in Organic Solvents. BioResources 12. https://doi.org/10.15376/biores.12.1.1548-1565

Sant'Anna, V., Biondo, E., Kolchinski, E.M., da Silva, L.F.S., Corrêa, A.P.F., Bach, E., Brandelli, A., 2017. Total Polyphenols, Antioxidant, Antimicrobial and Allelopathic Activities of Spend Coffee Ground Aqueous Extract. Waste and Biomass Valorization 8, 439–442. https://doi.org/10.1007/s12649-016-9575-4

Sawatdeenarunat, C., Surendra, K.C., Takara, D., Oechsner, H., Khanal, S.K., 2015. Anaerobic digestion of lignocellulosic biomass: Challenges and opportunities. Bioresour. Technol. 178, 178–186. https://doi.org/10.1016/j.biortech.2014.09.103

Shen, J., Yan, H., Zhang, R., Liu, G., Chen, C., 2018. Characterization and methane production of different nut residue wastes in anaerobic digestion. Renew. Energy 116, 835–841. https://doi.org/10.1016/j.renene.2017.09.018

Sluiter, A., Hames, B., Ruiz, R., Scarlata, C., Sluiter, J., Templeton, D., Crocker, D., 2008. Determination of Structural Carbohydrates and Lignin in Biomass. Natl. Renew. Energy Lab. Tech. Rep. NREL/ TP -510 -42618.

Spagnuolo, L., Posta, S. Della, Fanali, C., Dugo, L., De Gara, L., 2021. Antioxidant and antiglycation effects of polyphenol compounds extracted from hazelnut skin on advanced glycation end-products (Ages) formation. Antioxidants 10, 1–14. https://doi.org/10.3390/antiox10030424

Tajmirriahi, M., Momayez, F., Karimi, K., 2021. The critical impact of rice straw extractives on biogas and bioethanol production. Bioresour. Technol. 319, 124167. https://doi.org/10.1016/j.biortech.2020.124167

Tanase, C., Domokos, E., Coşarcă, S., Miklos, A., Imre, S., Domokos, J., Dehelean, C.A., 2018. Study of the ultrasound-assisted extraction of polyphenols from beech (Fagus sylvatica L.) bark. BioResources 13, 2247–2267. https://doi.org/10.15376/biores.13.2.2247-2267

Velvizhi, G., Goswami, C., Shetti, N.P., Ahmad, E., Kishore Pant, K., Aminabhavi, T.M., 2022. Valorisation of lignocellulosic biomass to value-added products: Paving the pathway towards low-carbon footprint. Fuel 313, 122678. https://doi.org/10.1016/j.fuel.2021.122678

Wang, W., Lee, D.J., 2021. Lignocellulosic biomass pretreatment by deep eutectic solvents on lignin extraction and saccharification enhancement: A review. Bioresour. Technol. 339, 125587. https://doi.org/10.1016/j.biortech.2021.125587

Xiao, N., Bock, P., Antreich, S.J., Staedler, Y.M., Schönenberger, J., Gierlinger, N., 2020. From the Soft to the Hard: Changes in Microchemistry During Cell Wall Maturation of Walnut Shells. Front. Plant Sci. 11, 1–14. https://doi.org/10.3389/fpls.2020.00466

Xu, N., Liu, S., Xin, F., Zhou, J., Jia, H., Xu, J., Jiang, M., Dong, W., 2019. Biomethane production from lignocellulose: Biomass recalcitrance and its impacts on anaerobic digestion. Front. Bioeng. Biotechnol. 7, 1–12. https://doi.org/10.3389/fbioe.2019.00191

Xue, S., Jones, A.D., Sousa, L., Piotrowski, J., Jin, M., Sarks, C., Dale, B.E., Balan, V., 2018. Water-soluble phenolic compounds produced from extractive ammonia pretreatment exerted binary inhibitory effects on yeast fermentation using synthetic hydrolysate. PLoS One 13, 1–18. https://doi.org/10.1371/journal.pone.0194012

Zhong, Y., Ruan, Z., Zhong, Y., Archer, S., Liu, Y., Liao, W., 2015. A self-sustaining advanced lignocellulosic biofuel production by integration of anaerobic digestion and aerobic fungal fermentation. Bioresour. Technol. 179, 173–179. https://doi.org/10.1016/j.biortech.2014.12.013

Zou, S., Wang, H., Wang, X., Zhou, S., Li, X., Feng, Y., 2016a. Application of experimental design techniques in the optimization of the ultrasonic pretreatment time and enhancement

of methane production in anaerobic co-digestion. Appl. Energy 179, 191–202. https://doi.org/10.1016/j.apenergy.2016.06.120

Zou, S., Wang, X., Chen, Y., Wan, H., Feng, Y., 2016b. Enhancement of biogas production in anaerobic co-digestion by ultrasonic pretreatment. Energy Convers. Manag. 112, 226–235. https://doi.org/10.1016/j.enconman.2015.12.087

*Chapter 6*

# Fed-batch anaerobic digestion of raw and pretreated hazelnut skin over long-term operation

A modified version of this chapter has been accepted for publication as:

Oliva A., Tan L.C., Papirio S., Esposito G., Lens P.N.L., 2022. Fed-batch anaerobic digestion of raw and pretreated hazelnut skin over long-term operation, Bioresource Technology (In press). https://doi.org/10.1016/j.biortech.2022.127372.

**Abstract**

This study provided important insights on the anaerobic digestion (AD) of hazelnut skin (HS) by operating a fed-batch AD reactor over 240 days and focusing on several factors impacting the process in the long term. An efficient reactor configuration was proposed to increase the substrate load while reducing the solid retention time during the fed-batch AD of HS. Raw HS produced maximally 19.29 mL $CH_4$/g $VS_{add}$/d. Polyphenols accumulated in the reactor and the use of NaOH to adjust the pH likely inhibited AD. Maceration and methanol-organosolv pretreatments were, thus, used to remove polyphenols from HS (i.e. 82 and 97%, respectively) and improve HS biodegradation. Additionally, organosolv pretreatment removed 9% of the lignin. The organosolv-pretreated HS showed an increment in methane production of 21%, while macerated HS produced less methane than the raw substrate, probably due to the loss of non-structural sugars during maceration.

## 6.1 Introduction

The impact of fossil fuels on the environment and climate has led to the development of alternative strategies for energy production (Martins et al., 2019). The methane produced from renewable materials emerges as a great alternative to fossil fuels due to its high calorific value, low pollutant emission, and flexible use at different purity for various applications (Oliva et al., 2022). Methane can be produced via anaerobic digestion (AD) through different consortia of microorganisms, classified into hydrolytic, acetogenic, acidogenic, and methanogenic. Each group of microorganisms is responsible for a different phase of the AD process, i.e. hydrolysis, acetogenesis, acidogenesis, and methanogenesis. The balance between the various stages is the key for an efficient AD process (Pasalari et al., 2021).

Recently, the concept of AD evolved from a mere treatment to purify urban and industrial wastewater or sludge to an ad-hoc strategy to produce energy from undervalued waste materials (Silvestre et al., 2015). In this perspective, lignocellulosic materials (LMs) are an extraordinary opportunity for AD due to their abundance, low cost, and high organic content. Besides, agricultural, municipal, and industrial activities produce LMs that need a new destination, which needs to be more environmentally friendly than combustion or landfilling (Xu et al., 2019). Several researchers focused on the most produced LMs, such as straws (Dai et al., 2020) and grass residues (Wen et al., 2015). Nevertheless, the global interest is recently expanding to LMs coming from seasonal harvesting or specific regional production (Lovrak et al., 2020). For instance, the market of nuts is expanding year by year (International Nut and Dried Fruit Council Foundation, 2021), resulting in a huge amount of LMs that can be used for energy production without competing with the food industry. The harvesting and manufacturing of nuts produce different LMs, such as shells, skin, and husks (Shen et al., 2018). The most widely consumed nuts are peanuts, almonds, walnuts, cashews, pistachios, and hazelnuts, with the major producers being the USA, China, Turkey, and India. Nevertheless, nuts are exported worldwide, both shelled and unshelled, meaning that the issue of waste management travels with the product and affects any importer country (International Nut and Dried Fruit Council Foundation, 2021). In particular, the global hazelnut production achieved 512000 metric tons in the 2020/2021 harvesting season. Turkey (62%) and Italy (15%) were the leading producers, whereas hazelnuts are mainly exported to EU countries, China, and Canada (International Nut and Dried Fruit Council Foundation, 2021).

Most recent studies focused on optimising the AD of such residues to enhance their methane production potential (Bianco et al., 2021; Şenol, 2019). The optimisation of AD for LMs often involves pretreatments to overcome the recalcitrant structure of these substrates. The main components of LMs are cellulose, hemicellulose and lignin. The presence of lignin, together with physical characteristics, such as porosity and crystallinity degree of the cellulose, hinders the hydrolytic bacteria attacking the LMs, resulting in a low hydrolysis rate and inefficient AD in terms of methane production (Xu et al., 2019).

Great progress has been made in the valorisation of LMs. However, most studies focused on small-batch applications, which require further investigation before implementation on a pilot or industrial scale. In this perspective, this article aims to close the gap between batch and fed-batch applications, providing attractive insights for the AD of hazelnut residues, i.e. hazelnut skin (HS), investigated at lab-scale (i.e. 2 L working volume) in fed-batch operation. In particular, this study proposed an alternative reactor configuration that may allow more efficient feeding and process management for LMs under fed-batch AD operation. Different operating parameters were monitored and improved to enhance the methane production from HS, such as organic load, solid waste retention time (SWRT), and pH. Methane production, volatile fatty acids (VFAs) evolution, polyphenolic compounds accumulation, and alkalinity were monitored along with the reactor operation. The influence of pretreatments, i.e. maceration and organosolv, and the changes in the chemical composition of HS were investigated. In addition, the change in the microbial community along the variation of the operationg conditions was elucidated.

## 6.2 Materials and methods

### *6.2.1 Raw substrate and inoculum*

The raw HS used comes from Turkish imported hazelnuts (*Corylus avellana*). The hazelnuts were roasted, and the skin was separated from the kernel by a farming company located in the Campania region (Italy). The HS was sieved to select a range of particle sizes between 1.0 and 2.5 mm. The selected HS had a total (TS) and volatile solid (VS) content of 88.8 (± 0.2) and 86.1 (± 0.2)% (based on wet matter), respectively. A digestate from buffalo manure (DBM) coming from a full-scale anaerobic digester located in Eboli (Italy) was degassed to eliminate the endogenous biogas production before being used as the inoculum. The DBM showed a TS and VS content of 5.0 (± 0.0) and 3.4 (± 0.0)% (based on wet matter), respectively. The initial

pH of the inoculum was 7.7 (± 0.1), and the total alkalinity accounted for 10.7 (± 0.3) g $CaCO_3$/L.

*6.2.2 Maceration and organosolv pretreatment*

The HS maceration was preliminarily tested in 50 mL falcon tubes for 1, 3, 6, 24, 48 h, 1 and 2 weeks. The falcon tubes, filled with 1 g HS and 50 mL demineralised $H_2O$, were kept under agitation (i.e. 130 rpm) for the desired exposure time. The maceration time allowing the higher polyphenolic compound removal was performed on a larger scale, i.e. 2 L glass bottle, keeping a substrate to liquid (S/L) ratio of 1:50.

The organosolv pretreatment was carried out following the finest condition, i.e. pretreatment for 1 h at 130 °C using a 50% (*v/v)* water-methanol solution with 0.1% (*w/v*) $H_2SO_4$ as a catalyst, previously proposed in Chapter 3 (Oliva et al., 2021). In the present study, the selected S/L ratio was 1:15. Maceration and organosolv pretreatment were performed individually on raw HS. Macerated and organosolv-pretreated HS was dried at 45 °C before being used as the substrate for AD.

*6.2.3 Anaerobic digester design and methane production measurement*

The AD process was performed in a 2 L (working volume) borosilicate glass reactor (Figure 6.1A) designed by the authors and made by Glass Studio (Naples, Italy). The desired temperature (i.e. ~ 37 °C) was maintained using an ED (v.2) heating bath (Julabo, Seelbach, Germany) in the service of the reactor water jacket. The pH evolution was monitored with a pH electrode (VWR, Radnor, USA). pH correction was performed using a pH/ORP 300 controller (Cole-Parmer, Vernon Hills, USA) and an EVO45 pump (Verderflex, Castleford, UK) (Figure 6.1C) dosing an alkaline solution (Figure 6.1B) when the pH in the reactor went below the threshold value, which was chosen depending on the desired operating condition. Reactor agitation was guaranteed by magnetic stirring. The HS was kept inside a stainless steel mesh container (SSMC) (15 x 10 x 10 cm) (Figure 6.1D). The substrate container had an external grid with a mesh capable of retaining the HS, but allowing the digestate to penetrate and soak the HS. After each refeeding, the headspace of the reactor was flushed with Argon gas to ensure anaerobic conditions.

The methane production was monitored using a water displacement apparatus. The biogas produced flowed continuously through a $CO_2$ trap (Figure 6.1E) made by 12% NaOH solution using thymolphthalein as pH indicator (Sigma-Aldrich, St. Louis, USA). The $CO_2$ trap allowed

the methane only to displace the water in a 1.5 L glass cylinder (Figure 6.1F) (Glass Studio, Naples, Italy) for a volume equal to the amount of methane produced.

The specific methane production was calculated by dividing the daily methane production by the grams of VS from HS added ($VS_{add}$) in the reactor. The slope of the regression line fitting the experimental data of a single feeding cycle represents the methane production rate ($R_m$) for that cycle. The average rate ($R_{m,av}$) was obtained by averaging the rates obtained for each cycle of the same experimental phase.

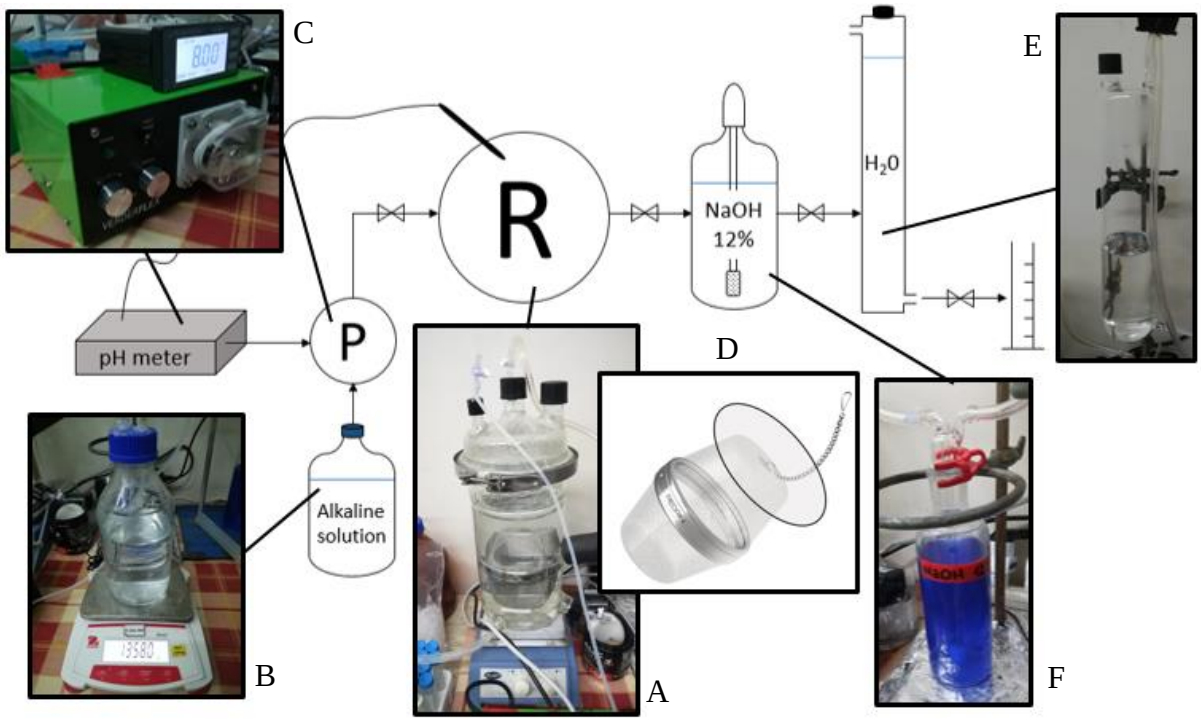


**Figure 6.1 –** Schematic representation of the experimental design including anaerobic digester (A), alkaline solution for pH control (B), pH controller and pump for alkaline solution dosing (C), stainless steel mesh container for lignocellulosic refeeding (D), carbon dioxide trap (E), and water cylinder for methane production measurement (F).

### *6.2.4 Reactor feeding and experimental phases*

The anaerobic reactor was initially filled with 697 g DBM and 1303 g $H_2O$, and 18.6 g HS were fed to reach an overall VS content of 20 g/L. The starting inoculum/substrate ratio was 1.5 g VS. The initial TS content was 2.6%. The operation of the reactor was divided into seven experimental phases (Table 6.1).

During Phase I, HS was fed every 14 days, replacing 50% of the overall VS from HS at a time, i.e. with a SWRT of 28 days, starting from HS load of 16.7 (± 0.7) g VS. In Phase II, the HS load increased by roughly 55%, reaching 26.0 (± 1.1) g VS, and the SWRT was kept at 28 days.

During Phase III, the SWRT was shortened to 20 days, using the same HS load as Phase II. Phases IV and V investigated the effectiveness of pretreatments on AD of HS, keeping the same HS load and SWRT selected in Phase III. In Phase IV, macerated HS was digested, while during Phase V an organosolv-pretreated HS was fed to the reactor.

During phases I to V of this study, the pH in the reactor was monitored and corrected online. Sodium hydroxide (NaOH) was used for pH correction until day 68. Afterwards, NaOH was replaced by sodium carbonate ($Na_2CO_3$). Nevertheless, due to a failure of the pumping system dosing the alkaline solution, the entire liquid phase of the reactor was contaminated on day 150, requiring the inoculation of fresh DBM and a standby phase of 28 days. During the standby phase, the reactor was fed regularly with raw HS, but methane production was not recorded.

The regular operation of the fed-batch reactor restarted with Phase VI, i.e. on day 195, by feeding raw HS with a shorter SWRT of 14 days and an organic HS load of 25.3 (± 0.8) g VS. Finally, in Phase VII (i.e. from day 216 to 237), organosolv-pretreated HS was used for AD, keeping the SWRT at 14 days.

**Table 6.1 –** Experimental design.

| **Operating parameters** | **Phase I** | **Phase II** | **Phase III** | **Phase IV** | **Phase V** | **Standby** | **Phase VI** | **Phase VII** |
|---|---|---|---|---|---|---|---|---|
| Timeline (day) | 0 - 56 | 56 - 105 | 105 - 125 | 125 - 145 | 145 - 167 | 167 - 195 | 195 - 216 | 216 - 237 |
| Substrate | Raw HS | Raw HS | Raw HS | Macerated HS | Pretreated HS | Raw HS | Raw HS | Pretreated HS |
| HS load (g VS) | 16.7 ± 0.7 | 26.0 ± 1.1 | 25.9 ± 0.7 | 25.2 ± 0.3 | 25.1 ± 1.0 | 24.4 ± 1.0 | 25.3 ± 0.8 | 25.0 ± 0.6 |
| Feeding percentage (% VS) | 50 | 50 | 50 | 50 | 50 | 50 | 50 | 50 |
| Solid retention time (days) | 28 | 28 | 20 | 20 | 14 | 28 | 14 | 14 |
| No. of cycles | 4 | 3 | 2 | 2 | 3 | 2 | 3 | 3 |
| Length of each cycle (days) | 14 | 14 | 10 | 10 | 7 | 14 | 7 | 7 |

*6.2.5 Microbial community analysis*

Samples for DNA analysis were taken on day 0 and at the end of each experimental phase (Table 6.1). Additionally, the reactor was sampled before and after the extra inoculations, i.e. on days 80 and 150. DNA extraction, sequencing and bioinformatics analysis were performed by FisaBio (Valencia, Spain). Before DNA extraction, samples were homogenised by adding 1 ml of phosphate-buffered saline (PBS) to 2 ml of sample and vortexed. After two centrifugation steps at 4 ºC (i.e. 2 min at 2000 rpm and 30 min at 13200 rpm), the pellet was recovered for DNA extraction.

DNA was extracted using a MAgNa Pure LC robot and a III 3264785001 isolation kit (Roche, Basel, Switzerland) according to the manufacturer's protocol. External lysis was performed before DNA extraction by adding 0.23 g of lysozyme. The DNA was quantified using a Qubit dsDNA High Sensitivity kit (Qiagen, Hilden, Germany) and normalised at 5 ng/ul to start the library preparation protocol. Polymerase chain reaction (PCR) amplification, sequencing, and PCR cleanup were performed according to the Illumina protocol (Illumina Inc., 2013) that targets the V3 and V4 regions of the 16S genes with the primers selected by Klindworth et al. (2013). The database used for the taxonomic assignation was Silva138.

*6.2.6 Analytical methods*

TS and VS of the inoculum, as well as raw, macerated and pretreated HS, were determined according to the standard methods (APHA AWWA, 2005) using a TCN115 convection oven (Argo Lab, Carpi, Italy) and a BWF 11/13 muffle furnace (Carbolite, Sheffield, UK), respectively. The HS degradation during the AD process was monitored by measuring the VS content of the digested HS before each refeeding cycle, using the same methods and equipment reported above. The water retention capacity (WRC) of raw, macerated and pretreated HS was measured as described by Sanchez et al. (2019). The chemical composition, i.e. extractives, polyphenols in the extractives, structural sugars, lignin, and ashes of the LMs was determined by Celignis Limited (Limerick, Ireland) following the NREL procedures (Sluiter et al., 2008b, 2008a). The cellulose content was considered equivalent to the glucan content. The hemicellulose content was obtained as the sum of xylan, mannan, arabinan, galactan, and rhamnan sugars. The unknown matter was calculated as the complement to 100 of the other components. The analysis of the structural sugars was performed using a ICS-3000 Ion Chromatography System (Dionex, Sunnyvale, USA) according to the company's protocol.

The liquid phase of the anaerobic digester was sampled regularly for alkalinity, VFAs, and soluble polyphenols analysis. Total (TA), partial (PA) and intermediate (IA) alkalinity were determined as described by Pontoni et al. (2015). PA is related to carbonate alkalinity, whereas IA refers to VFAs alkalinity. TA was obtained as the sum of PA and IA (Martín-González et al., 2013). The samples for VFAs analysis were stored and analysed according to Papirio (2020). Soluble polyphenols concentration was measured using a V-530 UV/VIS spectrophotometer (Jasco, Tokyo, Japan) following the Folin-Ciocalteu (F-C) procedure, as reported by Cubero-Cardoso et al. (2020).

## 6.3 Results and discussion

### *6.3.1 Anaerobic digestion of untreated hazelnut skin*

The AD process operated under fed-batch mode showed the potential of HS for methane production. Untreated HS was fed in Phase I, II, III, and VI, showing an $R_{m,av}$ of 12.9, 10.7, 19.3, and 16.0 mL $CH_4$/g $VS_{add}$/d, respectively (Table 6.2). The fed-batch operation here investigated allowed for fitting the experimental data with linear regression, whereas the cumulative methane production from LMs in batch experiments generally fits the first-order kinetic or a modified-Gompertz model (Mancini et al., 2018). These two models fit experimental data tending to a stationary phase after exponential growth. On the other hand, refeeding a reactor with fresh substrate more continuously than a batch system results in a more stable daily methane production, without experiencing methane production approaching zero after the biodegradation of the most available LM components (Shen et al., 2018).

During Phase I, four refeeding cycles were performed. The first cycle corresponded to the reactor start-up, with the entire amount of VS deriving from fresh HS. In the following cycles, 50% of digested HS was replaced with fresh HS up to the desired VS content of approximately 16.7 g VS. From the second cycle, a decreasing trend in methane production was observed (Figure 6.2). The methane production showed a peak after refeeding the reactor, likely due to the biodegradation of easily hydrolysable unbound compounds, i.e. free carbohydrates (Tao et al., 2019). The impact of extractives on AD largely depends on their composition, which varies with the LM (Tajmirriahi et al., 2021). After the first peak, the daily methane production decreased. Another peak was observed 5 - 7 days after refeeding the reactor (Figure 6.2). The second peak is likely attributed to the slower hydrolysis and subsequent degradation of the cellulose and hemicellulose sugars (Xu et al., 2019). In the first phase, no VFAs accumulation was observed (Figure 6.3A), and the total alkalinity was stable, ranging between 3.7 and 4.0 g

$CaCO_3$/L (Figure 6.3B), with the ratio IA/PA being below the suggested threshold value of 0.3 to digest organic wastes preserving stable reactor performance in terms of VFAs accumulation (Martín-González et al., 2013).

In Phase II, the feeding was increased to obtain an HS load of 26.0 g VS. Consequently, VFAs accumulation was observed in the reactor (Figure 6.3A), and the IA/PA ratio exceeded the threshold of 0.3, reaching the maximum value of 0.8 on day 79 (Figure 6.3B). Acetic acid was the only VFA detected until day 72 of operation (Figure 6.3A), resulting in pH drops and a frequent pH correction with NaOH (Figure 6.2B). The VFAs speciation partially switched to propionic acid in the second and third cycle of Phase II, reaching a concentration of 459 mg $HAc_{eq}$/L (Figure 6.3A). In previous works, propionic acid exceeding 410 mg $HAc_{eq}$ /L showed inhibitory effects on AD, which can explain the lower methane production measured in this study in the first two cycles of Phase II despite the higher HS load (Han et al., 2020).

Despite NaOH is one of the most employed pH adjusters, $Na^+$ ions have been reported to negatively affect the microbial activity during AD of LMs (Bianco et al., 2021; Feng et al., 2018). From day 56 to 80, the pH kept decreasing (Figure 6.2B), and VFAs accumulated (Figure 6.3A), suggesting that hydrolysis, acetogenesis, and acidogenesis proceeded regularly. On the other hand, methanogenic activity was inhibited albeit the increase of the HS load (Figure 6.2). The inhibition of methanogens can be attributed to the VFAs buildup above 1800 mg $HAc_{eq}$/L and $Na^+$ accumulation (Rocamora et al., 2020). Hence, $Na_2CO_3$ was used to control the pH from day 80, and 200 mL of fresh DBM were added to restart the reactor operation. $Na_2CO_3$ has also the advantage of increasing the carbonate alkalinity (Jos et al., 2020). Figure 6.3B shows that total alkalinity increased from day 80, and the optimal IA/PA ratio, i.e. 0.3, was established again. After day 80, the methane production restarted, allowing the reactor to work steadily with a higher organic load than that used in Phase I (Figure 6.2).

The retention time of HS was reduced from 28 to 20 days in Phase III. Consequently, the reactor was fed every 10 days. During the first two phases, the daily methane production decreased over time in each feeding cycle. This trend suggests that the easily biodegradable matter was hydrolysed in the first days of the AD process (Xu et al., 2019). Therefore, shortening the SWRT aimed to enhance the AD process by increasing the $R_{m,av}$ and preventing methane production from tending to zero. The peak in methane production further increased in Phase III, reaching 27.7 ml $CH_4$/g $VS_{add}$ (Figure 6.2). Nevertheless, a decrease in the daily methane production was observed in the subsequent days. During Phase III, the VFAs concentration was

lower than in Phase II, and no significant propionic acid accumulation was observed, i.e. 46 mg $HAc_{eq}$/L at most (Figure 6.3A).

The AD performance in Phase III can also be compared with that obtained in Phase VI, where raw HS was used as the substrate and the SWRT was further reduced to 14 days. Nevertheless, this comparison is influenced by the inoculation of fresh DBM on day 150. The methane production observed in Phase VI was lower than in Phase III, suggesting that the microorganisms' adaptation during the first 150 days played a relevant role in enhancing the AD process (Pasalari et al., 2021). On the contrary, the VFAs accumulation in Phase VI was slightly higher than that observed in Phase III (Figure 6.3A), and the pH correction (Figure 6.2B) was more frequent than in the previous phases. Consequently, the carbonate alkalinity in the reactor increased because of the buffer capacity of $Na_2CO_3$ (Figure 6.3A).

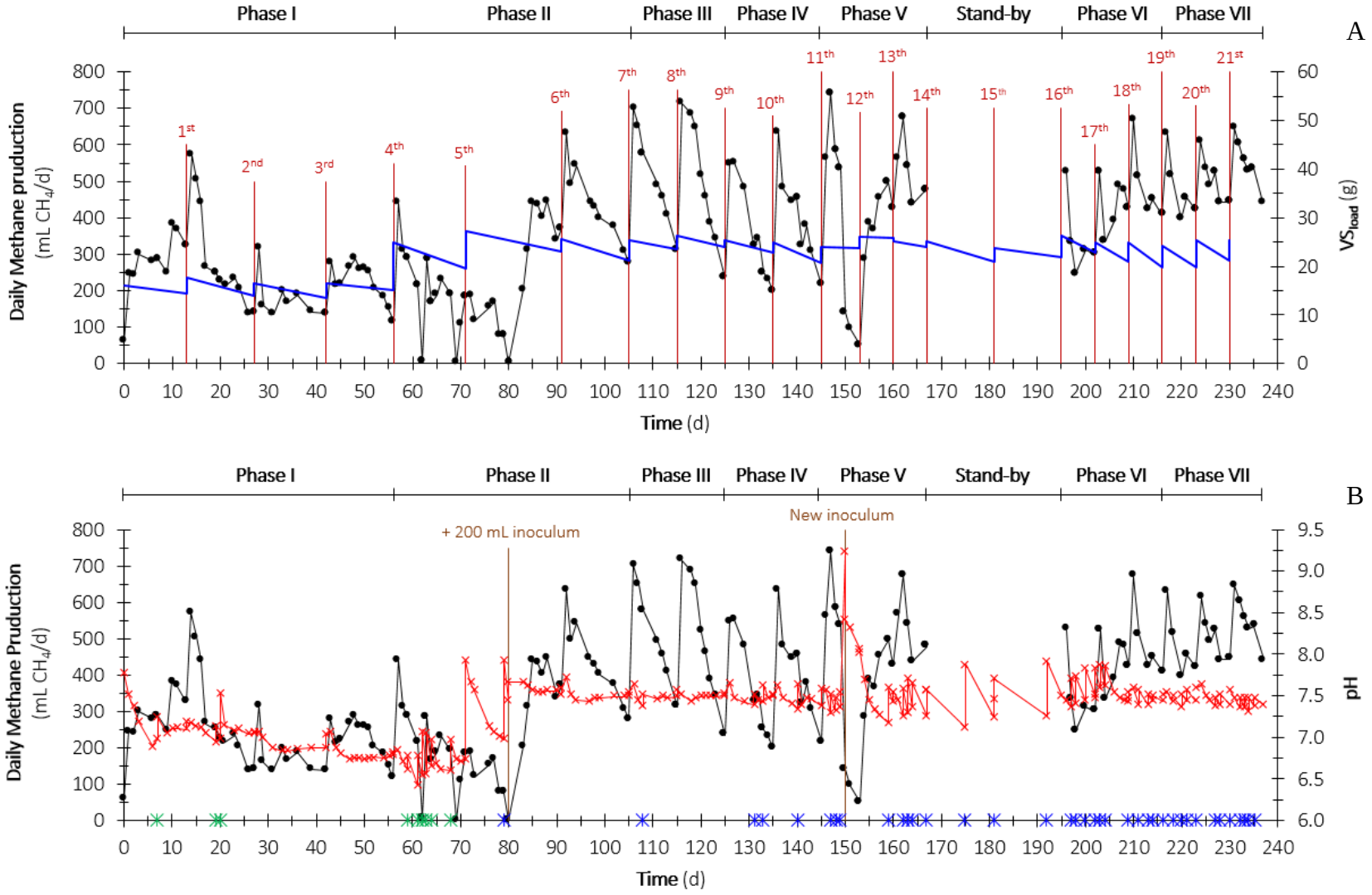


**Figure 6.2 –** Daily methane production (●) as a function of hazelnut skin refeeding (▮) (A), volatile solid content (▬) (A), pH (✖) (B), pH adjustment with NaOH (*) or $Na_2CO_3$ (*) (B), and extra inoculation (▮) (B) during the different cycles and experimental phases.

**Table 6.2 –** Average methane production rate ($R_{m,av}$) and R Square ($R^2$) obtained by fitting the experimental data with the linear regression function in each cycle and phase of the AD process.

| Phase | Cycle 1 | | Cycle 2 | | Cycle 3 | | Cycle 4 | | $R_{m,av}$ (mL $CH_4$/g VS/d) | |
|---|---|---|---|---|---|---|---|---|---|---|
| | $R_m$ (mL $CH_4$/g VS/d) | $R^2$ | $R_m$ (mL $CH_4$/g VS/d) | $R^2$ | $R_m$ (mL $CH_4$/g VS/d) | $R^2$ | $R_m$ (mL $CH_4$/g VS/d) | $R^2$ | Average | St. Dev. |
| I | 18.10[a] | 0.997[a] | 14.62 | 0.960 | 10.00 | 0.995 | 14.09 | 0.992 | 12.90 | 2.53 |
| II | 7.58[b] | 0.976[b] | 8.37[b] | 0.932[b] | 16.15 | 0.991 | - | - | 10.70 | 4.74 |
| III | 19.43 | 0.988 | 19.14 | 0.963 | - | - | - | - | 19.29 | 0.21 |
| IV | 14.76 | 0.978 | 15.83 | 0.980 | - | - | - | - | 15.30 | 0.76 |
| V | 15.02[c] | 0.854[c] | 16.35 | 0.994 | 20.72 | 0.995 | - | - | 17.36 | 2.98 |
| Standby | - | - | - | - | - | - | - | - | - | - |
| VI | 12.16 | 0.991 | 17.16 | 0.998 | 18.55 | 0.994 | - | - | 15.96 | 3.36 |
| VII | 18.55 | 0.995 | 19.63 | 0.997 | 21.1 | 0.995 | - | - | 19.76 | 1.28 |

[a]Data referring to the start-up cycle described in Section 6.3.1

[b]Data affected by the inhibition caused by NaOH dosing described in Section 6.3.1.

[c]Data affected by the inoculation of fresh digestate from buffalo manure described in Sections 6.2.3 and 6.3.2.

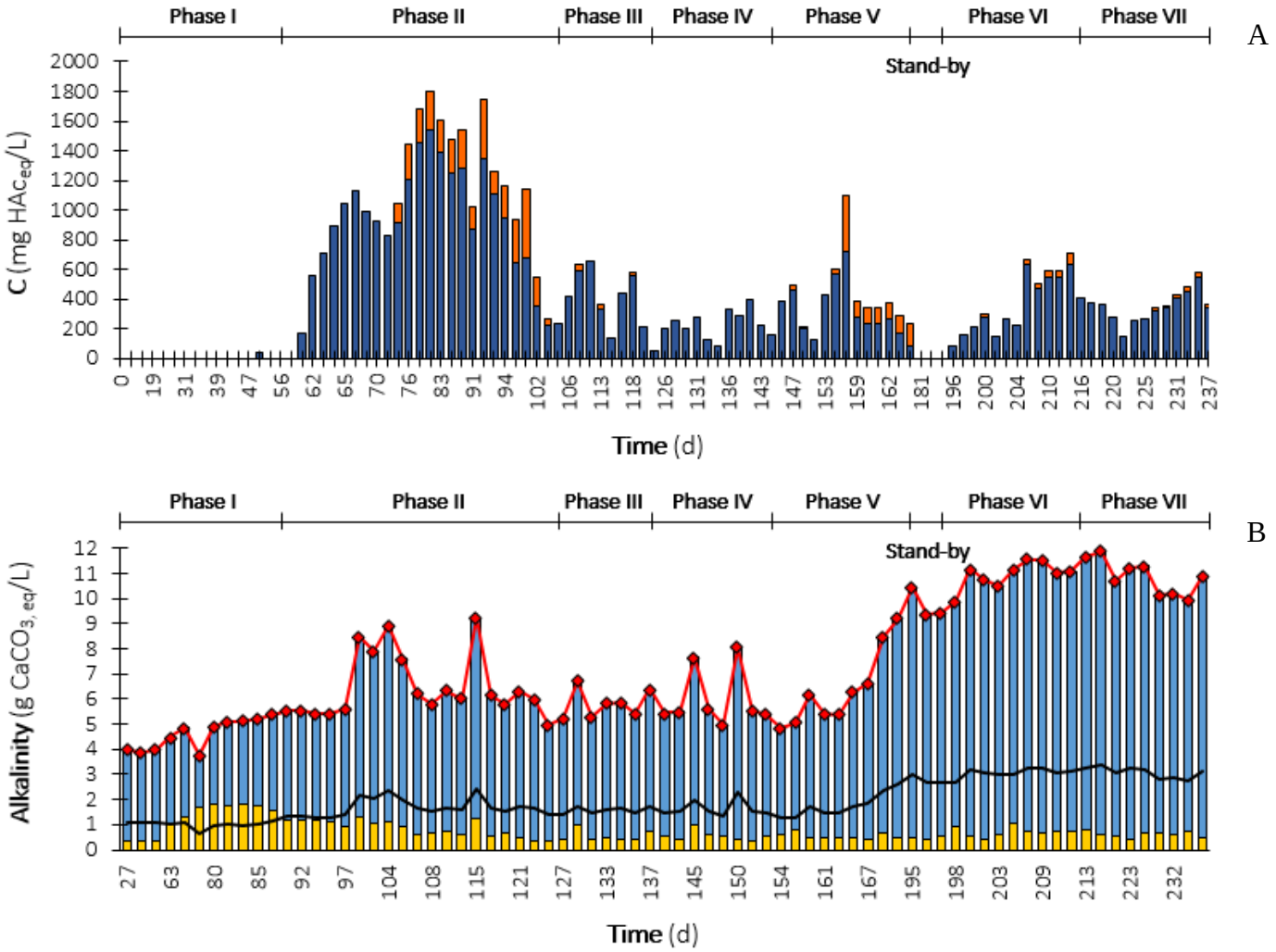


**Figure 6.3 –** Volatile fatty acids evolution (A) expressed as equivalent acetic acid: acetic acid (■) and propionic acid (■). Alkalinity evolution (B) expressed as total (◆), partial (■), and intermediate (■) alkalinity in comparison with the threshold value (▬), i.e. partial/intermediate alkalinity = 0.3, suggested in the literature (Martín-González et al., 2013).

*6.3.2 Impact of polyphenolic content and pH adjustment on anaerobic digestion of hazelnut skin*

The polyphenols concentration in the reactor was constantly monitored along the different operating conditions. Figure 6.4A shows that a background polyphenols concentration of approximately 329.6 mg/L was observed in the reactor on day 0, i.e. prior to feeding HS. Buffalo manure is rich in acid-soluble lignin (Zeb et al., 2022). This type of lignin can be broken down into polyphenolic compounds during the AD process. Nevertheless, the complete degradation of these compounds is unlikely to occur without specific strategies, such as microaeration (Zeb et al., 2022). Therefore, the initial polyphenols concentration observed in the reactor is likely associated with the DBM used. Regarding LMs, polyphenolic compounds are generated from lignin degradation during pretreatments (Ferreira and Taherzadeh, 2020). HS is rich in Klason lignin, with the acid-soluble fraction being a minor component of the total lignin (Oliva et al., 2021). Only fungi and selected strains of bacteria can degrade lignin from LMs. In contrast, the microorganisms involved in the AD process are unlikely to degrade lignin from LMs (Oliva et al., 2022). In addition, polyphenols are also present in the extractives of HS (Ivanović et al., 2020).

Section 6.3.1 explained the role of $Na^+$ in the AD process. In addition to that, $Na^+$ can bind with phenols and form sodium phenolate (Li et al., 2014). Sodium phenolate inhibits microbial growth, explaining the drop in methane production observed until day 80 when NaOH was dosed in the reactor (Gellert and Stommel, 1999). The formation of sodium phenolate can also be responsible for the fluctuation of the polyphenols concentration until day 80 (Li et al., 2014). Moreover, the refeeding before day 80 corresponded to the highest polyphenols concentration observed in this study, i.e. 479.7 mg phenol/L, suggesting that the reactor acidification also inhibited the polyphenols degradation. Figure 6.4A shows that polyphenols did not accumulate above the background concentration in Phase I when the organic load was 16 g VS from HS. In Phase II, the polyphenols content increased after each feeding, whereas it was lower at the end of a cycle. This trend suggests that the microbial community present in the reactor was probably capable of degrading part of the polyphenolic compounds (Zeb et al., 2022). On day 80, after inoculating 200 mL of fresh DBM, the methanogenic activity restarted along with the polyphenols degradation.

Apart from replacing NaOH with $Na_2CO_3$ for pH adjustment, maceration and organosolv pretreatments were tested to reduce the presence of polyphenols in the AD process. HS is indeed

a polyphenol-rich substrate, the solubilisation of which can hinder the AD process by inhibiting the hydrolytic bacteria (Ivanović et al., 2020; Milledge et al., 2019). The polyphenol measurement in the liquor showed that 3 hours of maceration led to the highest polyphenolic compounds extraction from HS. The 3 hours maceration was repeated on a larger scale, resulting in 47.3 mg of phenols removed per gram of HS (Figure 6.4B). Figure 6.4A shows that the polyphenols concentration spiked up after each refeeding with macerated HS in Phase IV, despite the significant removal via maceration (Figure 6.4B). The polyphenolic compounds hydrolysed from macerated HS were partially degraded during AD until reaching the background concentration mentioned previously. On the contrary, the feeding of organosolv-pretreated HS significantly reduced the polyphenols present in the reactor in Phase V (Figure 6.4B). During Phase VI, the polyphenols content increased again when feeding raw HS. Finally, in Phase VII, the lowest polyphenols concentration of the entire AD operation was observed, i.e. 180.1 mg phenol/L, confirming that methanol is an excellent solvent for polyphenols extraction (Vijayalaxmi et al., 2015).

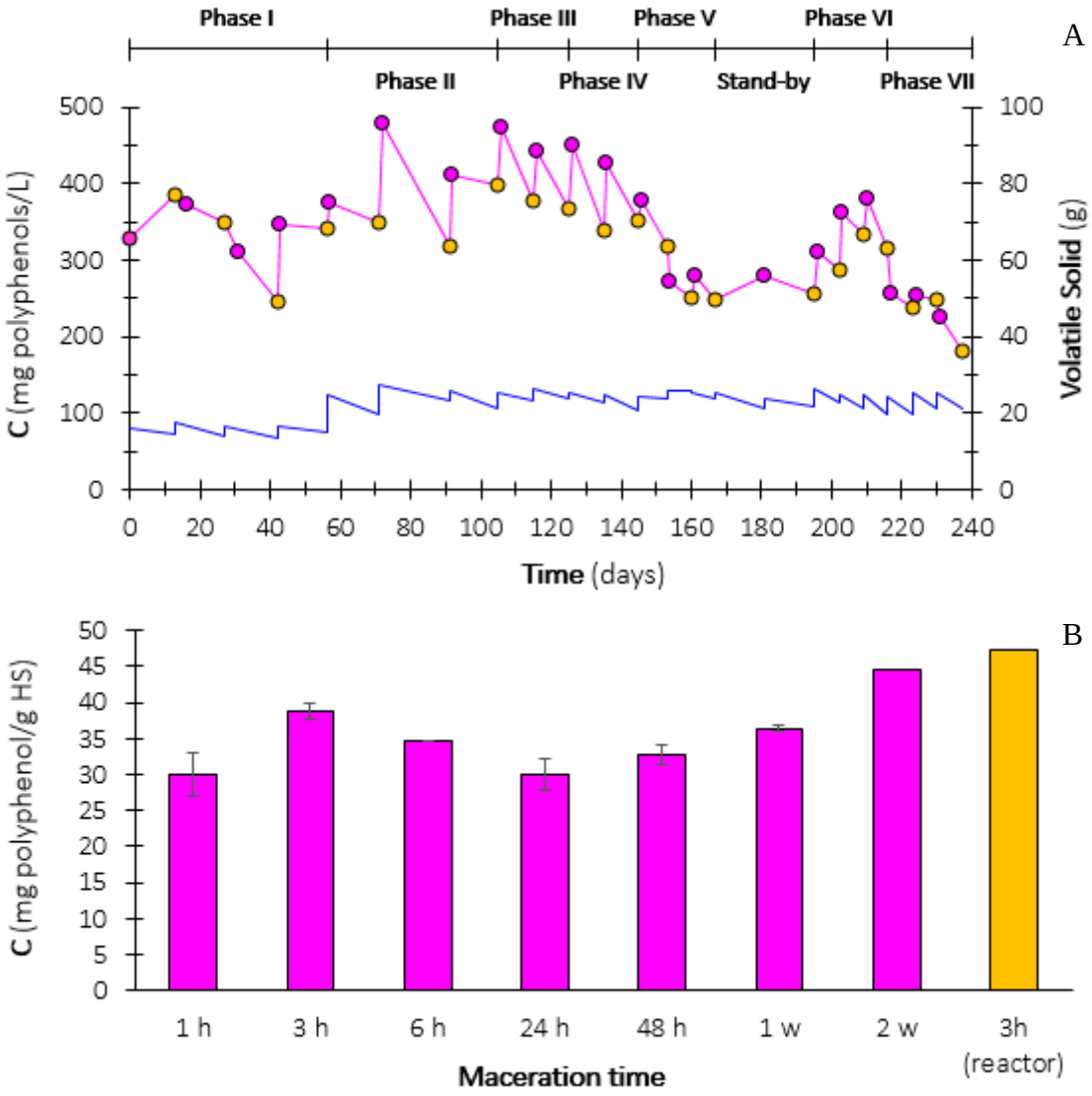


**Figure 6.4 –** Soluble polyphenols evolution during anaerobic digestion (A): polyphenols concentration at the beginning (●) and at the end (●) of each feeding cycle and evolution of the volatile solid content from hazelnut skin (▬). Polyphenols removed by maceration (B) at different exposure times on a small scale (■) and on a larger scale for the optimal condition (■).

### *6.3.3 Effect of maceration and organosolv pretreatment on chemical composition, porosity, and methane production potential of hazelnut skin*

The compositional analysis (Table 6.3) revealed that raw HS is particularly rich in lignin, i.e. 39.7 (± 0.1) g/100 g TS. The second most abundant components were the extractives, i.e. 35.0 (± 0.0) g/100 g TS. Extractives are usually a minor component in the LMs composition (Xu et al., 2019). Nevertheless, their abundance in HS suggests that extractives might have a crucial role during the AD process. In particular, the polyphenolic content of raw HS, expressed as equivalent gallic acid (GAE), was 106.0 (± 3.9) mg/g TS (Table 6.3). The cellulose and hemicellulose content was 10.2 (± 0.1) and 3.6 (± 0.0) g/100 g TS, respectively. The chemical

composition here reported is in line with the previous study of Mancini et al. (2018). As for the porosity index, the WRC of raw HS was 1.82 (± 0.08) g $H_2O$/g HS (Table 6.3). The chemical composition confirmed the high recalcitrance of HS, which prompted testing various pretreatments to unlock the full potential of this substrate.

Maceration is a physical pretreatment that can enhance the biodegradation of LMs by shearing the lignocellulosic fibers and reducing the particle size of LMs with limited energy consumption and overall costs (Ariunbaatar et al., 2014). In this study, maceration of HS was performed to reduce the release of polyphenolic compounds from the hydrolysis of HS extractives in the AD process. The 3 h maceration reduced the extractives content of HS by 11%, with no relevant effect on the other components (Table 6.3). The polyphenolic content of macerated HS was 19.3 (± 0.0) mg GAE/g TS, being significantly lower than the raw substrate (Table 6.3). On the other hand, the WRC of macerated HS was 25% lower than raw HS, i.e. 1.37 (± 0.12) g $H_2O$/g HS (Table 6.3). Macerated HS underwent AD in Phase IV, showing a 20% lower methane production than that observed in Phase III, with an $R_{m,av}$ of 15.3 mL $CH_4$/g VS/d (Table 6.2). The VFAs concentration was slightly lower than in Phase III, and the IA/PA ratio was constantly below the threshold value (Figure 6.3). It is reasonable that maceration, besides polyphenols, removed other valuable water-soluble molecules, such as free sugars, entailing a lower methane production potential of HS (Tao et al., 2019). Additionally, as an indicator of porosity, the lower WRC negatively influenced the biodegradation of LMs by reducing the substrate to microorganism contact (Mancini et al., 2018).

Organosolv pretreatment acts to reduce the lignin content of LMs. Additionally, depending on pretreatment parameters, hemicellulose hydrolysis and an increase in porosity can occur (Ferreira and Taherzadeh, 2020). Methanol-organosolv pretreatment greatly enhanced the AD of HS in a previous study conducted with batch bioassays (Oliva et al., 2021). In this study, the organosolv pretreatment reduced the lignin and extractives content of HS by 9 and 6%, respectively (Table 6.3). In particular, the pretreatment removed 97% of the overall polyphenols from raw HS, resulting in 3.1 (± 0.0) mg GAE/g TS in the organosolv-pretreated HS (Table 6.3). The pretreatment may have benefited from the S/L ratio of 1:15, whereas the most commonly employed ratio reported in the literature is 1:10 (Ferreira and Taherzadeh, 2020). The impact of S/L on organosolv pretreatment is still unclear and underinvestigated (Ferreira and Taherzadeh, 2020). Nevertheless, HS pretreatment may require a high S/L to completely soak HS during the pretreatment due to its high porosity. The organosolv-pretreated HS was

fed to the reactor in Phase V. After 4 days of operation under these operating conditions, the $R_{m,av}$ was 25.6 mL $CH_4$/g $VS_{add}$/d. Nevertheless, technical issues with the $Na_2CO_3$ dosing demanded to replace the entire liquid phase of the reactor with a fresh DBM on day 150. The overdosing of $Na_2CO_3$ increased the pH up to 9.2 (Figure 6.2B), being considerably above the optimal range (i.e. 6.5 - 7.5) for methanogenic activity (Borth et al., 2022). The performance of the reactor decreased with the new inoculation of DBM, probably due to the lack of proper microbial community adaptation to degrade HS. After two feeding cycles with the organosolv-pretreated HS, the reactor performance was restored (Figure 6.2A).

After Phase V, the reactor was readapted to the LM from day 167 to 195. During this period, the reactor was fed regularly with raw HS, the pH was monitored and adjusted, but the methane production was not recorded. This standby phase represented a new baseline necessary to compare the methane production from raw and organosolv pretreated HS. In Phase VI, the methane production from raw HS was lower than in Phase III, as described in Section 6.3.1 (Figure 6.2). In total, 8.65 L of methane were produced in Phase VI. In Phase VII, organosolv-pretreated HS was again used, keeping the refeeding time at 7 days. The overall methane production, i.e. 10.48 L, was 21% higher than in Phase VI, confirming the effectiveness of the methanol-organosolv pretreatment on HS (Oliva et al., 2021). The $R_{m,av}$ in Phase VII was 19.8 mL $CH_4$/g VS/d, against 16.0 mL $CH_4$/g VS/d measured in Phase VI (Table 6.2). On the other hand, no significant change in VFAs accumulation and alkalinity was observed. The increment in methane production can be attributed to the changes in chemical composition, e.g. lower lignin content, and loss of inhibitory compounds, i.e. polyphenols (Ferreira and Taherzadeh, 2020; Milledge et al., 2019). Moreover, the WRC of pretreated HS (Table 6.3), i.e. 1.72 (± 0.09) g $H_2O$/g HS, was comparable with the untreated substrate and is therefore not correlated with the increment in methane production.

**Table 6.3 –** Chemical composition, i.e. extractives, cellulose, hemicellulose, lignin, and ashes content, polyphenols in the extractives, and water retention capacity of raw, macerated, and organosolv-pretreated hazelnut skin (HS).

| **Substrate** | **Extractives** (g/100 g TS) | **Cellulose** [a] (g/100 g TS) | **Hemicellulose** [b] (g/100 g TS) | **Lignin** [c] (g/100 g TS) | **Ashes** (g/100 g TS) | **Unknown** [d] (g/100 g TS) | **Polyphenols** [e] (mg GAE/g TS) | **Water retention capacity** (g $H_2O$/g TS) |
|---|---|---|---|---|---|---|---|---|
| Raw HS | 35.0 ± 0.0 | 10.2 ± 0.1 | 3.6 ± 0.0 | 39.7 ± 0.1 | 2.7 ± 0.1 | 8.9 ± 0.1 | 106.0 ± 3.9 | 1.82 ± 0.08 |
| Macerated HS | 31.2 ± 0.6 | 10.4 ± 0.0 | 3.4 ± 0.1 | 39.5 ± 0.1 | 2.9 ± 0.1 | 12.1 ± 0.5 | 19.3 ± 0.0 | 1.37 ± 0.12 |
| Organosolv pretreated HS | 32.9 ± 0.2 | 11.8 ± 0.0 | 3.8 ± 0.1 | 36.0 ± 0.1 | 1.5 ± 0.1 | 13.9 ± 0.2 | 3.1 ± 0.0 | 1.72 ± 0.09 |

[a] The cellulose content was considered equivalent to the glucan content.

[b] The hemicellulose content was obtained as the sum of xylan, mannan, arabinan, galactan, and rhamnan sugars.

[c] The lignin content was calculated as the sum of acid soluble and Klason lignin.

[d] The unknown matter was calculated as the complement to 100 of the other components.

[e] The content of polyphenols is expressed as mg of gallic acid quivalent (GAE) on the dry matter.

*6.3.4 Microorganisms involved in hazelnut skin degradation*

The taxonomic classification on day 0 revealed the abundance of *Firmicutes* (i.e. 38%), *Proteobacteria* (i.e. 18%), *Synergistota* (i.e. 14%) and *Bacteroidota* (i.e. 9%) phyla (Figure 6.5A). These are the most common phyla involved in hydrolysis, acetogenesis and acidogenesis phases (Pasalari et al., 2021). The DBM was a heterogeneous inoculum, with *Synergistaceae* (affiliated with the *Synergistota* phylum) being the only family above 10% of the overall microbial community (Figure 6.5B). *Firmicutes* and *Proteobacteria* phyla are resilient to extreme conditions, whereas the *Bacteroidota* phylum is more sensitive to operating conditions (Pasalari et al., 2021), which suggests that the DBM was in the endogenous phase when inoculated to the reactor.

On day 80, a fresh DBM was inoculated, resulting in a step backwards in the microbial enrichment, as shown in Figure 6.5A. Before adding the fresh DBM, the *Synergistaceae* (i.e. 26%) and *Bacteroidaceae* (affiliated with the *Bacteroidota* phylum) (i.e. 17%) families survived the critical operating conditions caused by the overload of HS (Figure 6.5B). Around day 80, the highest VFAs accumulation was observed, i.e. 1800 mg $HAc_{eq}$/L (Figure 6.3A). The abundance of the *Synergistaceae* family has been associated with high VFAs concentrations in the AD of corn straw (Zhu et al., 2022). In addition, enrichment (i.e. up to 6%) in the *Spirochaetota* phylum (Figure 6.5A) was observed when the propionic acid concentration increased in the reactor (Figure 6.3A). These bacteria can convert propionic, butyric and valeric acids into acetic acid, $H_2$ and $CO_2$, ensuring process stability (Borth et al., 2022). At the end of Phase II, once reactor stability was reached, the *Rikenellaceae* family (affiliated with the *Bacteroidota* phylum) enriched up to 24%. On the other hand, the percentage of *Synergistaceae* and *Bacteroidaceae* families dropped to 21 and 6%, respectively (Figure 6.5B).

In the first three phases of this study, raw HS was fed to the reactor (Table 6.1). At the end of Phase III, *Bacteroidota* (i.e. 33%) and *Synergistota* (i.e. 21%) were the most abundant phyla. On the contrary, the relative abundance of *Firmicutes* and *Proteobacteria* phyla decreased to 24 and 9%, respectively (Figure 6.5A). The most abundant families after Phase III were *Synergistaceae* (i.e. 21%) and *Rikenellaceae* (i.e. 15%) (Figure 6.5B). Lv et al. (2019) reported the dominance of the *Synergistaceae* and *Rikenellaceae* families in the AD of a similar substrate, i.e. straw. The abundance of the *Synergistota* phylum has been recently reported in a phenol-degrading study working with concentrations comparable with this study (Li et al.,

2022). The enrichment in the *Synergistota* phylum could be associated with the polyphenols released from HS. Nevertheless, further studies are required to confirm this hypothesis.

In Phase IV, macerated HS was fed to the reactor (Table 6.1). In this phase, the *Rikenellaceae* and *Dysgonomonadaceae* families (affiliated with the *Bacteroidota* phylum) enriched (Figure 6.5B), resulting in a 41% relative abundance of the *Bacteroidota* phylum (Figure 6.5A). In particular, the *Dysgonomonadaceae* family was enriched from Phase III and increased until day 150 of operation, reaching 18% of the relative abundance (Figure 6.5B). The *Dysgonomonadaceae* family include hydrolytic genera capable of degrading recalcitrant polysaccharides, such as the carbohydrates of LMs (Owusu-Agyeman et al., 2022). As explained in Section 6.3.3, Phase V was affected by a new inoculation on day 150. The fresh DBM was abundant in *Rikenellaceae* (i.e. 14%), *Bacteroidaceae* (i.e. 14%), and *Synergistaceae* (i.e. 11%) families. The *Rikenellaceae* family enriched (i.e. 26%) until day 167 while feeding organosolv-pretreated HS. Nevertheless, this family gradually disappeared in the following phases to the benefit of the *Synergistaceae* family. The microbial community readapted to the substrate in the standby period. On day 195, the phyla present in the reactor were comparable with those present during Phase III (Figure 6.5A).

In Phase VI, feeding raw HS, the relative abundance of the *Proteobacteria* (i.e. 15%) and *Spirochaetota* (i.e. 6%) phyla increased. However, the most present phyla were *Bacteroidota* (i.e. 32%), *Synergistota* (i.e. 19%) and *Firmicutes* (i.e. 19%) (Figure 6.5A). At the family level, *Synergistaceae* (i.e. 19%) and *Dysgonomonadaceae* (i.e. 11%) were the most abundant (Figure 6.5B). The main difference with Phase III was the lower abundance of hydrolytic bacteria, which was likely the reason of the lower methane production (Pasalari et al., 2021). *Spirochaetaceae* (i.e. 6%) (Figure 6.5B), affiliated with the *Spirochaetota* phylum, is a family of complex polymer-oxidising bacteria that can be associated with the increased input of polyphenols along with the feeding of raw HS (Zhu et al., 2022). On the contrary, *Proteobacteria* was the dominant phylum after digesting raw and pretreated rice straw for 60 days (Mirmohamadsadeghi et al., 2021). The abundance of the *Proteobacteria* phylum was previously associated with the endogenous conditions occurring when the carbon source became scarce at the end of the AD process (Pasalari et al., 2021).

In Phase VII, organosolv-pretreated HS was fed to the reactor. *Bacteroidota* and *Synergistota* phyla reached 37 and 23%, respectively (Figure 6.5A). On the contrary, the *Firmicutes*, *Proteobacteria*, and *Spirochaetota* phyla decreased (Figure 6.5A). In particular, the

*Spirochaetota* decrement (i.e. below 2%) seems to confirm the correlation between polyphenols and the *Spirochaetota* phylum (Zhu et al., 2022). In Phase VII, the most abundant families were *Synergistaceae* (i.e. 23%), *Dysgonomonadaceae* (i.e. 15%), and *Lentimicrobiaceae* (i.e. 11%). The *Lentimicrobiaceae* family (affiliated with the *Bacteroidota* phylum) is associated with cellulase and xylanase activity (Jensen et al., 2021), which can be related to the higher HS degradation and subsequent methane production observed in Phase VII (Figure 6.5A).

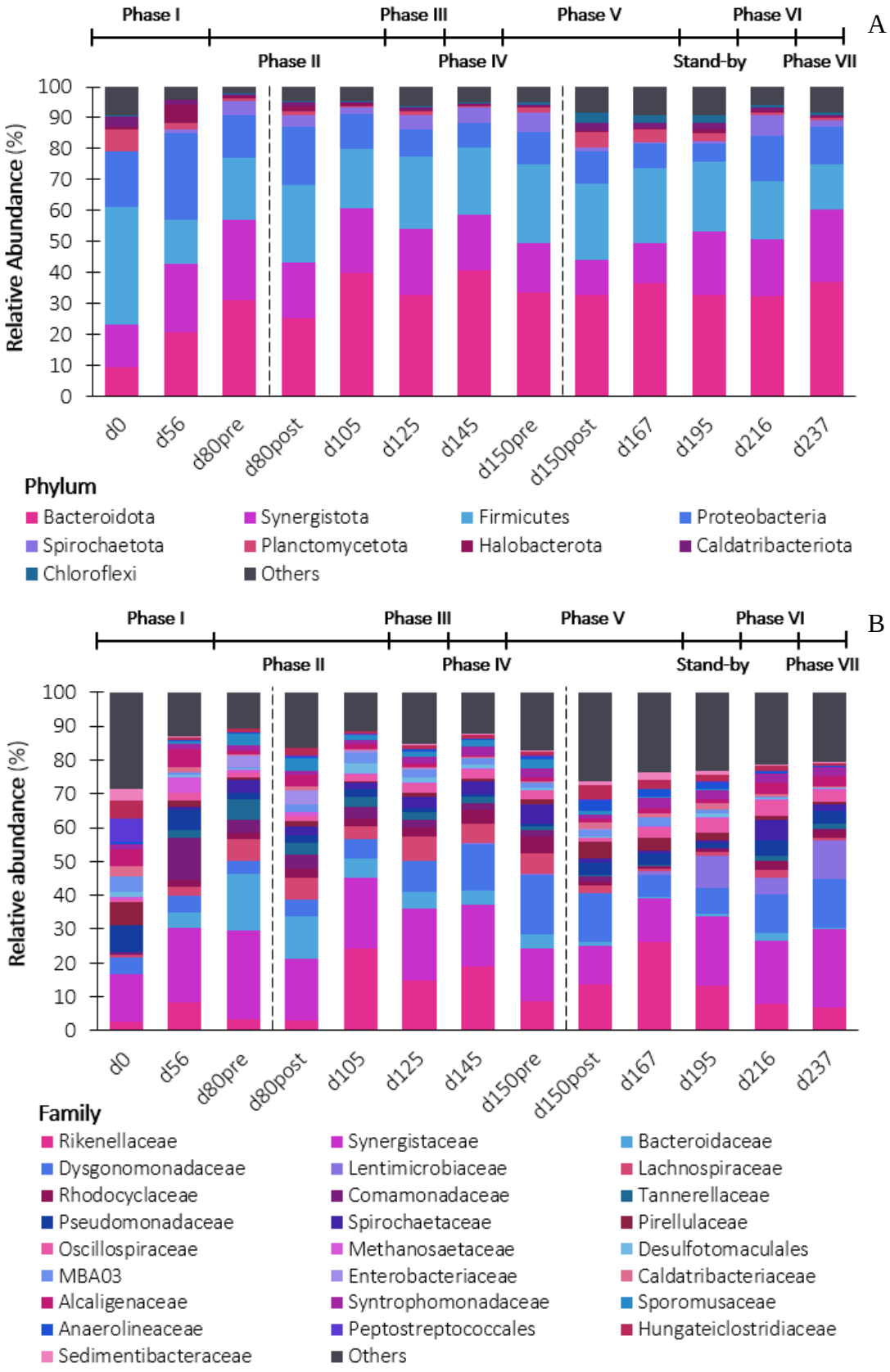


**Figure 6.5 –** Changes in the microbial community at phylum (A) and family (B) level during the anaerobic digestion of hazelnut skin under fed-batch mode operation. All the relative abundances below 3% were grouped as Others.

*6.3.5 Importance of reactor configuration for fed-batch anaerobic digestion*

The organic load and retention time of the substrate are crucial parameters for efficient AD, also affecting the economy of the entire process. When digesting liquid or semisolid substrates, such as sludge or slurries, organic loading rate and hydraulic retention time are more commonly used (Pasalari et al., 2021). In contrast, for solid substrates, such as LMs, the retention time, i.e. SWRT, should refer only to the solid matter.

Most of the studies investigating the AD of LMs under fed-batch operation used a stirred tank reactor and fed the reactor by replacing an aliquot of substrate and inoculum with a fresh amount of the same mixture (Lahboubi et al., 2020; Wang et al., 2021). In this study, an alternative reactor configuration was developed that decoupled the SWRT of the HS from the solid biomass retention time (SBRT), which allows microbial growth during the SBRT while shortening the SWRT (Okoye et al., 2022). A low SWRT is desirable to reduce the costs of AD. However, when SWRT and SBRT are coupled, shortening this time can lead to washout of microorganisms and imbalance of the microbial community at the expense of methanogens (Pasalari et al., 2021).

The core of the reactor proposed in this study is the SSMC used to retain the HS while being soaked in the reactor microbial biomass (Figure 6.1D). This configuration allowed to set the desired SWRT regardless the microbial biomass, which was left enriching for the entire operating time, apart from the liquid sampling and the extra inoculation on days 80 and 150 (Figure 6.2B). Microbial community acclimation is a crucial factor for AD, especially in the case of LMs, since hydrolytic bacteria need to adapt to the substrate and hydrolise it. Therefore, lowering the SBRT can result in ineffective AD (Pasalari et al., 2021; Xu et al., 2019). To the best of the authors' knowledge, the SSMC has never been used in AD to decouple SWRT and SBRT.

From the perspective of upscaling this configuration, a further advantage is the easy mixing of the reactor, most of the solids being retained in the SSMC. Mixing represents one of the highest operating costs, especially in dry and semidry AD. Additionally, feeding and withdrawal of the substrate are facilitated since no pumping is required. Also, the solid content of the digested LM is higher than a digestate obtained from a stirred tank reactor since it is mainly composed of undigested lignin from the LM, which reduces the costs of drying the digestate (Peng et al., 2020).

Despite the promising perspective, this configuration also raised some concerns, such as the risk of accumulating inhibitory compounds in the liquid phase of the reactor. In addition, to ensure an optimal inoculum to substrate contact, a highly porous substrate is required, such as HS. Finally, in view of upscaling this configuration, further studies are required to design a SSMC that guarantees the optimal inoculum to substrate contact once the volume of the SSMC and the amount of retained substrate are increased.

### 6.4 Conclusion

The AD of HS was improved over long-term fed-batch operation by reducing the SWRT and increasing the organic load. Polyphenols concentration and the pH control strategy were crucial to maintain an efficient AD. Methanol-organosolv pretreatment reduced the lignin and polyphenolic content of HS by 9 and 97%, respectively, resulting in a 21% increment of the methane production. Maceration removed 82% of the polyphenols, but negatively affected the methane production from HS. The reactor configuration here proposed allowed the enrichment of an efficient microbial community for HS degradation, but requires further optimisation before being implemented on a larger scale.

### 6.5 References

APHA AWWA, W.E.F., 2005. Standard methods for the examination of water and wastewater. APHA WEF AWWA.

Ariunbaatar, J., Panico, A., Esposito, G., Pirozzi, F., Lens, P.N.L., 2014. Pretreatment methods to enhance anaerobic digestion of organic solid waste. Appl. Energy 123, 143–156. https://doi.org/10.1016/j.apenergy.2014.02.035

Bianco, F., Şenol, H., Papirio, S., 2021. Enhanced lignocellulosic component removal and biomethane potential from chestnut shell by a combined hydrothermal–alkaline pretreatment. Sci. Total Environ. 762. https://doi.org/10.1016/j.scitotenv.2020.144178

Borth, P.L.B., Perin, J.K.H., Torrecilhas, A.R., Lopes, D.D., Santos, S.C., Kuroda, E.K., Fernandes, F., 2022. Pilot-scale anaerobic co-digestion of food and garden waste: Methane potential, performance and microbial analysis. Biomass and Bioenergy 157, 106331. https://doi.org/10.1016/j.biombioe.2021.106331

Cubero-Cardoso, J., Trujillo-Reyes, Á., Marín-Ayllón, P., Rodríguez-Gutiérrez, G., Villa-Gomez, D., Serrano, A., Borja, R., Fermoso, F.G., 2020. Solubilization of phenols and sugars from raspberry extrudate by hydrothermal treatments. Processes 8, 1–16.

https://doi.org/10.3390/pr8070842

Dai, X., Hua, Y., Liu, R., Chen, S., Li, H., Dai, L., Cai, C., 2020. Biomethane production by typical straw anaerobic digestion: Deep insights of material compositions and surface properties. Bioresour. Technol. 313, 123643. https://doi.org/10.1016/j.biortech.2020.123643

Feng, J., Li, Y., Zhang, E., Zhang, J., Wang, W., He, Y., Liu, G., Chen, C., 2018. Solid-State Co-digestion of NaOH-Pretreated Corn Straw and Chicken Manure Under Mesophilic Condition. Waste and Biomass Valorization 9, 1027–1035. https://doi.org/10.1007/s12649-017-9834-z

Ferreira, J.A., Taherzadeh, M.J., 2020. Improving the economy of lignocellulose-based biorefineries with organosolv pretreatment. Bioresour. Technol. 299, 122695. https://doi.org/10.1016/j.biortech.2019.122695

Gellert, G., Stommel, A., 1999. Influence of microplate material on the sensitivity of growth inhibition tests with bacteria assessing toxic organic substances in water and waste water. Environ. Toxicol. 14, 424–428. https://doi.org/10.1002/(SICI)1522-7278(1999)14:4<424::AID-TOX8>3.0.CO;2-4

Han, Y., Green, H., Tao, W., 2020. Reversibility of propionic acid inhibition to anaerobic digestion: Inhibition kinetics and microbial mechanism. Chemosphere 255, 126840. https://doi.org/10.1016/j.chemosphere.2020.126840

Illumina Inc., 2013. 16S Metagenomic Sequencing Library. Illumina.com 1–28.

International Nut and Dried Fruit Council Foundation (INC), 2021. Nuts & dried fruits statistical yearbook 2020/2021.

Ivanović, S., Avramović, N., Dojčinović, B., Trifunović, S., Novaković, M., Tešević, V., Mandić, B., 2020. Contents and Antioxidant Activity as Nutritive Potential of Roasted Hazelnut Skins (Corylus avellana L.). Foods 9, 1–14. https://doi.org/doi:10.3390/foods9040430

Jensen, M.B., de Jonge, N., Dolriis, M.D., Kragelund, C., Fischer, C.H., Eskesen, M.R., Noer, K., Møller, H.B., Ottosen, L.D.M., Nielsen, J.L., Kofoed, M.V.W., 2021. Cellulolytic and Xylanolytic Microbial Communities Associated With Lignocellulose-Rich Wheat Straw Degradation in Anaerobic Digestion. Front. Microbiol. 12, 1–13. https://doi.org/10.3389/fmicb.2021.645174

Jos, B., Sucipto, T.A., Pramianshar, A., Ikrimah, A.N., Sumardiono, S., 2020. Experimental and kinetic study of biogas production of fish processing industry in anaerobic digestion

as future renewable energy resources. AIP Conf. Proc. 2197. https://doi.org/10.1063/1.5140905

Klindworth, A., Pruesse, E., Schweer, T., Peplies, J., Quast, C., Horn, M., Glöckner, F.O., 2013. Evaluation of general 16S ribosomal RNA gene PCR primers for classical and next-generation sequencing-based diversity studies. Nucleic Acids Res. 41, 1–11. https://doi.org/10.1093/nar/gks808

Lahboubi, N., Kerrou, O., Karouach, F., Bakraoui, M., Schüch, A., Schmedemann, K., Stinner, W., El Bari, H., Essamri, A., 2020. Methane production from mesophilic fed-batch anaerobic digestion of empty fruit bunch of palm tree. Biomass Convers. Biorefinery. https://doi.org/10.1007/s13399-020-00864-1

Li, Y., Wang, M., Qian, J., Hong, Y., Huang, T., 2022. Enhanced degradation of phenolic compounds in coal gasification wastewater by an iron-carbon micro-electric field coupled with anaerobic co-digestion. Sci. Total Environ. 819, 151991. https://doi.org/10.1016/j.scitotenv.2021.151991

Li, Z., Mumford, K.A., Smith, K.H., Wang, Y., Stevens, G.W., 2014. Extraction of Phenol by Toluene in the Presence of Sodium Hydroxide. Sep. Sci. Technol. 49, 2913–2920. https://doi.org/10.1080/01496395.2014.952748

Lovrak, A., Pukšec, T., Duić, N., 2020. A Geographical Information System (GIS) based approach for assessing the spatial distribution and seasonal variation of biogas production potential from agricultural residues and municipal biowaste. Appl. Energy 267, 115010. https://doi.org/10.1016/j.apenergy.2020.115010

Lv, Z., Chen, Z., Chen, X., Liang, J., Jiang, J., Loake, G.J., 2019. Effects of various feedstocks on isotope fractionation of biogas and microbial community structure during anaerobic digestion. Waste Manag. 84, 211–219. https://doi.org/10.1016/j.wasman.2018.11.043

Mancini, G., Papirio, S., Lens, P.N.L., Esposito, G., 2018. Anaerobic Digestion of Lignocellulosic Materials Using Ethanol-Organosolv Pretreatment. Environ. Eng. Sci. 00, ees.2018.0042. https://doi.org/10.1089/ees.2018.0042

Martín-González, L., Font, X., Vicent, T., 2013. Alkalinity ratios to identify process imbalances in anaerobic digesters treating source-sorted organic fraction of municipal wastes. Biochem. Eng. J. 76, 1–5. https://doi.org/10.1016/j.bej.2013.03.016

Martins, F., Felgueiras, C., Smitkova, M., Caetano, N., 2019. Analysis of fossil fuel energy consumption and environmental impacts in european countries. Energies 12, 1–11. https://doi.org/10.3390/en12060964

Milledge, J.J., Nielsen, B. V., Maneein, S., Harvey, P.J., 2019. A brief review of anaerobic digestion of algae for BioEnergy. Energies 12, 1–22. https://doi.org/10.3390/en12061166

Okoye, F., Kakar, F.L., Elbeshbishy, E., Bell, K., Muller, C., Jimenez, J., Al-Omari, A., Santoro, D., Jang, E., Walton, J., Bahreini, G., Zaman, M., Nakhla, G., Hazi, F., Takacs, I., Murthy, S., Rosso, D., 2022. A proof-of-concept experimental study for vacuum-driven anaerobic biosolids fermentation using the IntensiCarb technology. Water Environ. Res. 94, 1–12. https://doi.org/10.1002/wer.10694

Oliva, A., Papirio, S., Esposito, G., Lens, P.N.L., 2022. Pretreatment of Lignocellulosic Materials to Enhance their Methane Potential, in: Sinharoy, A., Lens, P.N.L. (Eds.), Renewable Energy Technologies for Energy Efficient Sustainable Development, Applied Environmental Science and Engineering for a Sustainable Future. Springer, pp. 85–120. https://doi.org/10.1007/978-3-030-87633-3_4

Oliva, A., Tan, L.C., Papirio, S., Esposito, G., Lens, P.N.L., 2021. Effect of methanol-organosolv pretreatment on anaerobic digestion of lignocellulosic materials. Renew. Energy. https://doi.org/10.1016/j.renene.2020.12.095

Owusu-Agyeman, I., Plaza, E., Cetecioglu, Z., 2022. Long-term alkaline volatile fatty acids production from waste streams: Impact of pH and dominance of Dysgonomonadaceae. Bioresour. Technol. 346, 126621. https://doi.org/10.1016/j.biortech.2021.126621

Papirio, S., 2020. Coupling acid pretreatment and dosing of Ni and Se enhances the biomethane potential of hazelnut skin. J. Clean. Prod. 262, 121407. https://doi.org/10.1016/j.jclepro.2020.121407

Pasalari, H., Gholami, M., Rezaee, A., Esrafili, A., Farzadkia, M., 2021. Perspectives on microbial community in anaerobic digestion with emphasis on environmental parameters: A systematic review. Chemosphere 270. https://doi.org/10.1016/j.chemosphere.2020.128618

Peng, W., Lü, F., Hao, L., Zhang, H., Shao, L., He, P., 2020. Digestate management for high-solid anaerobic digestion of organic wastes: A review. Bioresour. Technol. 297, 122485. https://doi.org/10.1016/j.biortech.2019.122485

Pontoni, L., Panico, A., Salzano, E., Frunzo, L., Iodice, P., Pirozzi, F., 2015. Innovative parameters to control the efficiency of anaerobic digestion process. Chem. Eng. Trans. 43, 2089–2094. https://doi.org/10.3303/CET1543349

Rocamora, I., Wagland, S.T., Villa, R., Simpson, E.W., Fernández, O., Bajón-Fernández, Y., 2020. Dry anaerobic digestion of organic waste: A review of operational parameters and

their impact on process performance. Bioresour. Technol. 299. https://doi.org/10.1016/j.biortech.2019.122681

Sanchez, A., Hernández-Sánchez, P., Puente, R., 2019. Hydration of lignocellulosic biomass. Modelling and experimental validation. Ind. Crops Prod. 131, 70–77. https://doi.org/10.1016/j.indcrop.2019.01.029

Şenol, H., 2019. Biogas potential of hazelnut shells and hazelnut wastes in Giresun City. Biotechnol. Reports 24, 0–5. https://doi.org/10.1016/j.btre.2019.e00361

Shen, J., Yan, H., Zhang, R., Liu, G., Chen, C., 2018. Characterization and methane production of different nut residue wastes in anaerobic digestion. Renew. Energy 116, 835–841. https://doi.org/10.1016/j.renene.2017.09.018

Silvestre, G., Fernández, B., Bonmatí, A., 2015. Significance of anaerobic digestion as a source of clean energy in wastewater treatment plants. Energy Convers. Manag. 101, 255–262. https://doi.org/10.1016/j.enconman.2015.05.033

Sluiter, A., Hames, B., Ruiz, R., Scarlata, C., Sluiter, J., Templeton, D., Crocker, D., 2008a. Determination of Structural Carbohydrates and Lignin in Biomass. Natl. Renew. Energy Lab. Tech. Rep. NREL/ TP -510 -42618.

Sluiter, A., Ruiz, R., Scarlata, C., Sluiter, J., Templeton, D., 2008b. Determination of Extractives in Biomass. Natl. Renew. Energy Lab. Tech. Rep. NREL/TP-510-42619.

Tajmirriahi, M., Momayez, F., Karimi, K., 2021. The critical impact of rice straw extractives on biogas and bioethanol production. Bioresour. Technol. 319, 124167. https://doi.org/10.1016/j.biortech.2020.124167

Tao, J., Rajan, K., Ownley, B., Gwinn, K., D'Souza, D., Moustaid-Moussa, N., Tschaplinski, T.J., Labbé, N., 2019. Natural variability and antioxidant properties of commercially cultivated switchgrass extractives. Ind. Crops Prod. 138, 111474. https://doi.org/10.1016/j.indcrop.2019.111474

Vijayalaxmi, S., Jayalakshmi, S.K., Sreeramulu, K., 2015. Polyphenols from different agricultural residues: extraction, identification and their antioxidant properties. J. Food Sci. Technol. 52, 2761–2769. https://doi.org/10.1007/s13197-014-1295-9

Wang, R., Zhang, Y., Jia, S., Chen, J., Qi, C., Han, Y., Shan, M., Li, G., Li, Y., 2021. Comparison of batch and fed-batch solid-state anaerobic digestion of on-farm organic residues: Reactor performance and economic evaluation. Environ. Technol. Innov. 24, 101977. https://doi.org/10.1016/j.eti.2021.101977

Wen, B., Yuan, X., Li, Q.X., Liu, J., Ren, J., Wang, X., Cui, Z., 2015. Comparison and

evaluation of concurrent saccharification and anaerobic digestion of Napier grass after pretreatment by three microbial consortia. Bioresour. Technol. 175, 102–111. https://doi.org/10.1016/j.biortech.2014.10.043

Xu, N., Liu, S., Xin, F., Zhou, J., Jia, H., Xu, J., Jiang, M., Dong, W., 2019. Biomethane production from lignocellulose: Biomass recalcitrance and its impacts on anaerobic digestion. Front. Bioeng. Biotechnol. 7, 1–12. https://doi.org/10.3389/fbioe.2019.00191

Zeb, I., Yousaf, S., Ali, M., Yasmeen, A., Khan, A.Z., Tariq, J.A., Zhao, Q., Abbasi, A.M., Ahmad, R., Khalil, T.M., Yaqoob, A., Bilal, M., 2022. In-situ microaeration of anaerobic digester treating buffalo manure for enhanced biogas yield. Renew. Energy 181, 843–850. https://doi.org/10.1016/j.renene.2021.09.089

Zhu, R., Wang, D.H., Zheng, Y., Zou, H., Fu, S.F., 2022. Understanding the mechanisms behind micro-aeration to enhance anaerobic digestion of corn straw. Fuel 318, 123604. https://doi.org/10.1016/j.fuel.2022.123604

*Chapter 7*

# General discussion and future perspectives

## 7.1 Introduction

This thesis focused on the development of efficient strategies to valorise highly recalcitrant lignocellulosic materials (LMs). The main goal was to enhance methane production through anaerobic digestion (AD) while studying the impact of chemical and physical characteristics of LMs on the AD process. Three different substrates in terms of chemical composition and physical properties were selected, i.e. hazelnut skin (HS), almond shell (AS), and spent coffee grounds (SCG). HS is an abundant waste from hazelnut harvesting. In the last season, i.e. 2020 – 2021, 0.5 billion tons of hazelnuts were collected (International Nut and Dried Fruit Council Foundation, 2021). HS represents only 3% of the overall hazelnut weight (Spagnuolo et al., 2021). Nevertheless, HS has an extremely high bulk density that creates disposal problems for the confectionery industry. Similarly, almonds relate to the food processing industry, but the global almond production is much higher than that of hazelnuts, i.e. 1.7 billion tons per year (International Nut and Dried Fruit Council Foundation, 2021), and the shell represents over 50% of the entire fruit mass (Queirós et al., 2020). Finally, SCG are the end waste of the coffee supply chain, reaching over 6 million tons produced per year (Torres-Valenzuela et al., 2019).

The three substrates widely differ in chemical composition and physical characteristics. HS is particularly rich in lignin, i.e. 40 - 44%, whereas it is poor in structural sugars, mainly being glucan, i.e. 10%. On the other hand, AS is more balanced among lignin, i.e. 29 - 37%, cellulose (mainly glucan), i.e. 13 - 23%, and hemicellulose (mainly xylan), i.e. 21 - 28%. SCG is particularly rich in hemicellulose sugars (mainly mannan and galactan), i.e. 34%, and lignin, i.e. 19 - 20%, but poor in cellulose, i.e. 9%. Among the three, AS and SCG, having a high sugar content, are the most promising for biofuel production. Nevertheless, the experimental activities performed in this thesis demonstrated that other factors are involved in the biodegradation of LMs. For instance, the porosity index, evaluated through the water retention capacity (Tables 3.5 and 4.3), and the scanning electron microscopic (SEM) images (Figures 3.5 and 4.3), revealed that AS is hardly attackable by microorganisms due to its low porosity index and coriaceous external surface (Chapters 3 and 4).

An important pillar of this thesis was the impact of non-structural compounds on the AD process (Chapters 5 and 6). Non-structural compounds, i.e. extractives, are generally overlooked when investigating LMs. This blind zone originates from the idea that extractives only represent 5 - 10% of the overall chemical composition (Tajmirriahi et al., 2021). This extractives content is truthful in the case of the most and primarily investigated LMs, i.e. straws

and wood residues (Balat, 2011). On the other hand, the growing search for alternative biomass for energy production has led to the study of different LMs. The nut and coffee residues investigated in this thesis are particularly rich in non-structural compounds (Chapters 3, 4, and 5). In particular, HS and SCG are composed of 28 - 35 and 29 - 30% of extractives (Tables 3.4, 4.2, and 5.3), respectively. On the other hand, the extractives content in AS falls in the 10% range (Tables 3.4, 4.2, and 5.3).

Given the different chemical and physical characteristics among the three LMs, various pretreatments, i.e. organosolv (Chapter 3), N-Methylmorpholine N-Oxide (NMMO) (Chapter 4), and ultrasounds (Chapter 5), were tested to enhance the biodegradation of HS, AS, and SCG (Figure 7.1). Several pretreatment conditions, i.e. temperature, catalyst addition, exposure time, and type of medium, were tested, depending on the pretreatment technique. The last experimental activity (Chapter 6) aimed to scale up the process to a lab-scale bioreactor operated in fed-batch mode (Figure 7.1). The fed-batch operation provided further insights into the AD of raw and pretreated LMs. This study highlighted the impact of non-structural compounds on the AD of extractives-rich LMs, showing the importance of the reactor configuration and adaptation of the microbial community to the LM.

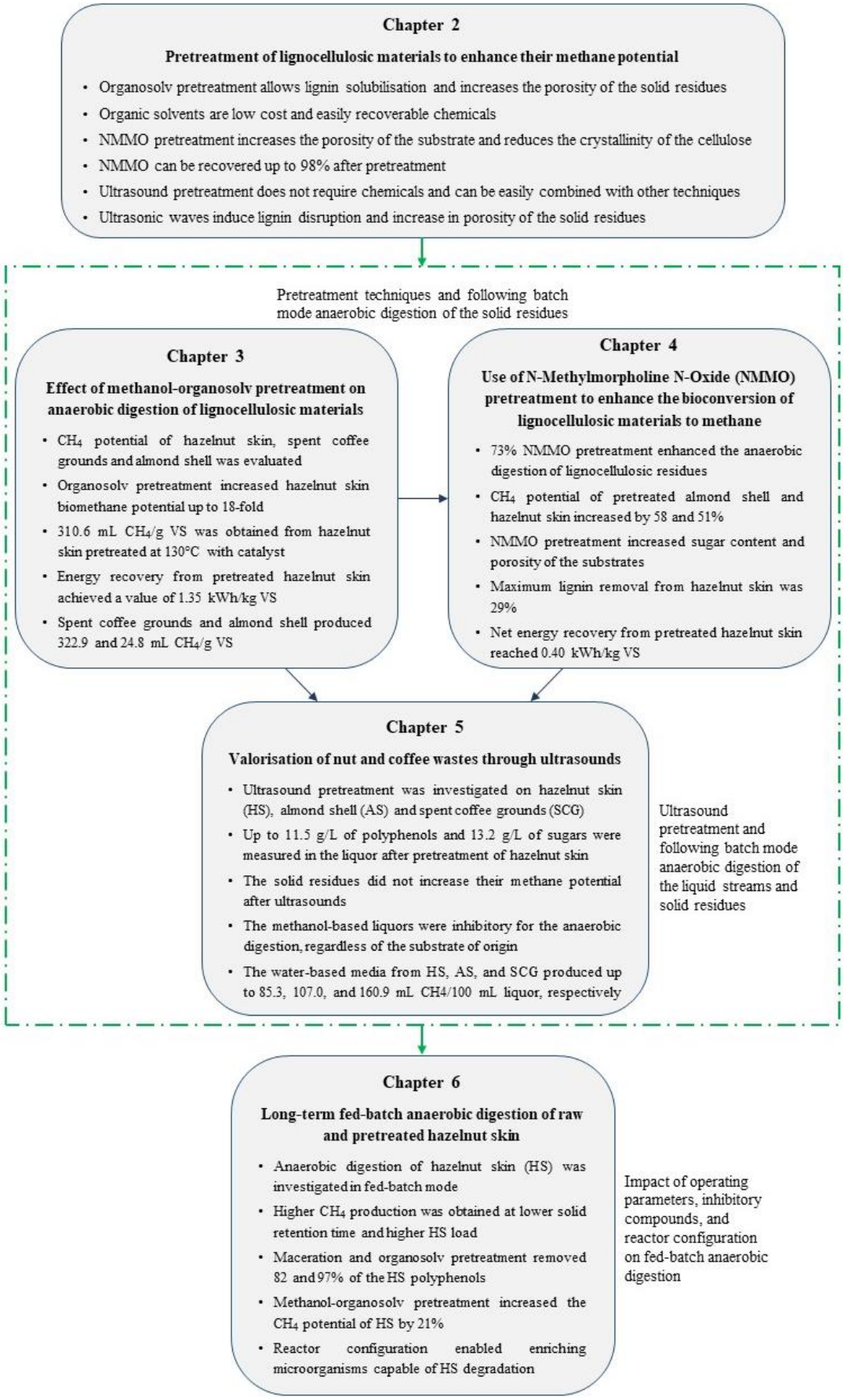


**Figure 7.1 –** Main findings achieved from the different chapters of this PhD thesis.

## 7.2 Main findings and comprehensive discussion

### *7.2.1 Hazelnut skin*

The experimental activities performed in batch mode (Chapters 3, 4, and 5) revealed that a deep characterisation of the substrate is required to select the most appropriate pretreatment of HS. HS has a less favourable composition for methane production than AS and SCG. However, its high porosity index (Tables 3.5 and 4.3) enabled the maximal effectiveness of solvent-based pretreatments (Chapters 3 and 4). Having a high porosity allows the solvents to easily soak the HS, with great solvent-substrate contact. In particular, the organosolv pretreatment performed in Chapter 3 greatly enhanced the methane production from HS (Figure 7.2). The pretreatment was performed using a 50% (*v/v*) methanol (MeOH) solution heated at 130, 160, and 200 °C, with or without catalyst addition. The baseline biochemical methane potential (BMP) of raw HS reported in Chapter 3, i.e. 17.3 (± 32.3) $CH_4$/g VS, was also affected by the scarce microorganisms-substrate contact obtained using a granular sludge as the inoculum. However, the organosolv pretreatment overcame this issue, yielding an easier biodegradable pretreated HS. The MeOH-organosolv pretreated HS achieved 310.6 (± 22.2) $CH_4$/g VS, at best (Chapter 3). The most performing pretreatment condition was 130 °C using 0.01M $H_2SO_4$ to enhance the reaction. The catalyst addition resulted in a 20% further increment of methane production and lowered the required pretreatment temperature (Figure 3.2), resulting in significant energy recovery (up to 1.35 kWh/kg VS). The enhanced BMP was attributed to the lignin removal (up to 12%) and exposure of the cellulosic fibers shown by the SEM images (Figure 3.5).

Chapter 4 discussed the effect of NMMO pretreatment on LMs. In this study, a different inoculum, i.e. digestate from buffalo manure (DBM), was used to guarantee a greater microorganisms-substrate contact. For HS, in particular, the inoculum turned out to be a key factor. The raw HS produced 265.5 (± 10.4) $CH_4$/g VS, being significantly higher than what was observed in Chapter 3 with anaerobic granular sludge. This result showed that the type of inoculum and its capability of reaching the substrate also affects the AD process. Changing the inoculum also resulted in different model employed to fit the experimental data. The granular sludge used in Chapter 3 hardly attacked the HS, resulting in a first stage, where the easily biodegradable matter, i.e. free sugars, was converted to methane, and a second step, where the structural sugars were digested. In contrast, the DBM allowed a greater contact with the HS, with the experimental data of the methane production fitting the typical, i.e. one-stage, modified Gompertz model. Once again, the BMP of HS was positively affected by the pretreatment. NMMO pretreatment was performed at 120 °C for 1, 3, and 5 hours (Figure 7.3). All the tested

conditions enhanced the BMP of HS, achieving a maximal production of 400.4 (± 9.5) mL $CH_4$/g VS for the 5 h pretreated HS (Figure 4.5). NMMO pretreatment acted on the cellulosic component of HS by reducing the lateral order index (LOI), meaning that easily accessible cellulose was returned after pretreatment (Table 4.3). Additionally, the water retention capacity (WRC) increased after pretreatment (Table 4.3). Interestingly, the NMMO pretreatment also reduced the lignin content of HS (up to 29%) (Table 4.2), most likely due to the extremely high porosity of HS, which enabled a perfect soak of this substrate in the solvent during the pretreatment. The loss of lignin resulted in a higher sugar content (up to 120%) (Table 4.2). The changes in chemical and physical characteristics resulted in an increased BMP and higher volatile solid (VS) degradation (up to 54%) during the AD process (Figure 4.6).

In Chapter 5, ultrasound pretreatment was carried out using different media, i.e. distilled water and 50% (*v/v*) catalysed (i.e. 0.01M $H_2SO_4$) MeOH solution, at ambient temperature (i.e. 20 °C) and 80 °C (Figure 7.4). The pretreated HS residues showed lower lignin (up to 10%) and extractives (up to 13%) content (Table 5.3). Consequently, the sugar content increased by 25%, at best (Table 5.3). Despite the most favourable lignocellulosic composition, none of the pretreatment conditions enhanced the BMP of HS (Figure 5.2). On the other hand, the liquid stream recovered after pretreatment was particularly rich in valuable biomolecules (Table 5.2). The polyphenols concentration in the liquor reached 11.5 (± 0.1) g/L, being significantly higher when using the MeOH solution as the medium (Table 5.2). The polyphenols extracted resulted either from the lignin disruption due to ultrasonic waves or from the free polyphenols present in the extractives of HS (Chapter 6). Apart from polyphenols, the liquor obtained from HS after ultrasound treatment was extremely rich in sugars (Table 5.2). A higher sugar concentration, i.e. 13.2 (± 0.3) g glucose/L, was measured in the MeOH-based medium recovered after ultrasound pretreatment (Table 5.2). The sugars extracted and the substrate solubilisation (ranging from 15 to 24%) explain the failure to increase the BMP of HS. The liquor offers several opportunities, such as the selective recovery of the valuable molecules solubilised, which can be an attractive perspective for further studies. In addition, the water-based liquor was used as the substrate for AD, producing 85.3 (± 12.2) mL $CH_4$/100 mL liquor at best (Figure 5.1). On the other hand, the AD of the MeOH-based liquor was inhibited by the presence of MeOH and did not show any methane production (Figure 5.1).

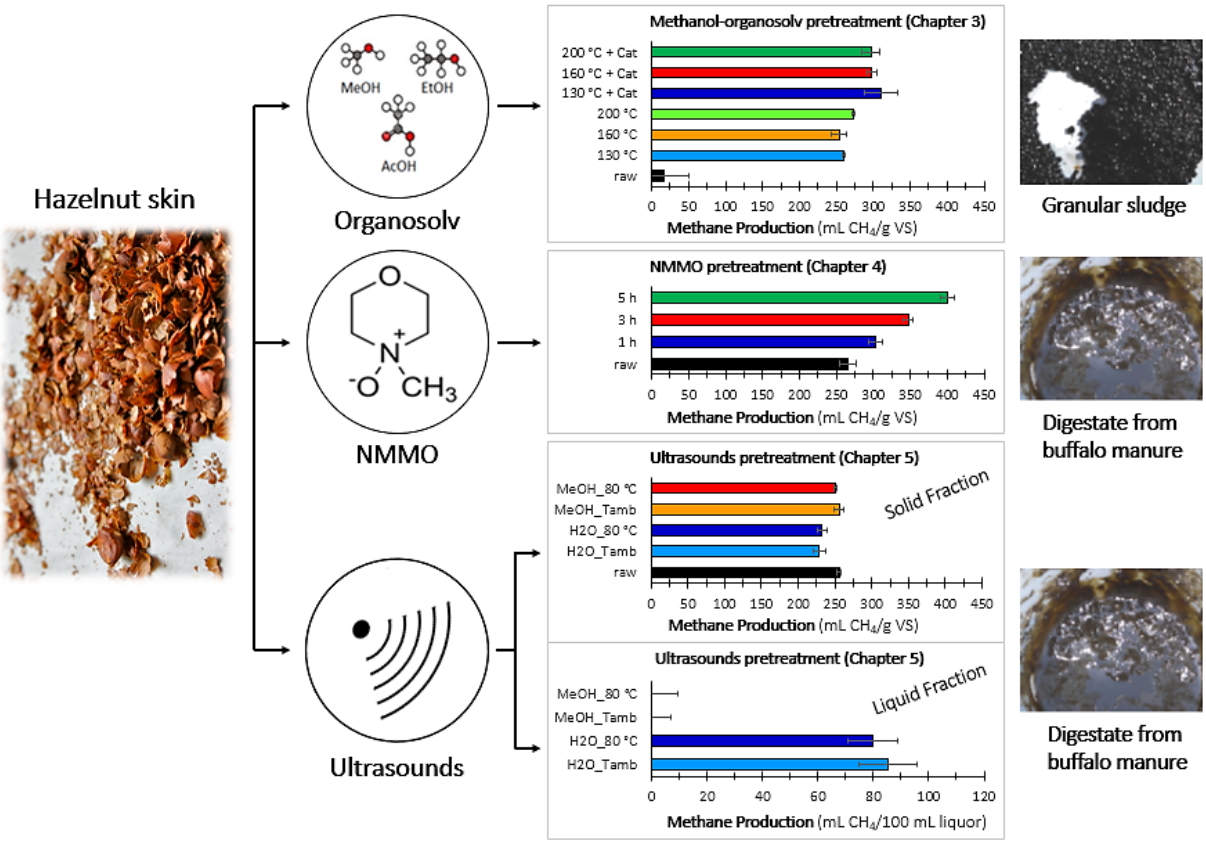


**Figure 7.2 –** Impact of methanol-organosolv (Chapter 3), NMMO (Chapter 4), and ultrasounds (Chapter 5) pretreatments on methane production potential of hazelnut skin.

### *7.2.2 Almond shell*

AS was the most recalcitrant substrate among the three studied in this PhD thesis. Despite the high sugar content, i.e. 43 - 45% (Tables 3.4, 4.2, and 5.3), the physical properties hindered AS biodegradation. The WRC of raw AS, i.e. 0.53 g $H_2O$/g TS (Table 4.3), is an index of the low porosity of this substrate. Low porosity negatively influences the effectiveness of solvent-based pretreatments and the microorganisms-substrate contact during AD. Additionally, the cellulose present in AS showed a high LOI, indicating that crystalline regions prevail over amorphous areas. Crystalline cellulose is hardly biodegradable during AD (Xu et al., 2019). In Chapter 3, the maximum methane production from AS was 24.8 (± 2.6) mL $CH_4$/g VS (Figure 7.2), and none of the investigated pretreatment conditions significantly increased this yield (Figure 3.2). The SEM images showed the hard and compact external surface of AS, which was not impacted by the pretreatment (Figure 3.5). Apart from the extractives removal, AS did not show significant changes after organosolv pretreatment, neither in lignocellulose composition nor in porosity index (Table 3.4).

Chapter 4 confirmed the importance of the type of inoculum previously enlightened for HS. The low methane production observed in Chapter 3 did not allow to fit the experimental data with a model. On the other hand, the trend in methane production observed when DBM was used as the source of microorganisms followed the typical "S" shape fitting the modified Gompertz model. Using the DBM as the inoculum increased the BMP of raw AS up to 54.7 (± 5.3) mL $CH_4$/g VS (Table 4.4). Contrary to the organosolv, NMMO pretreatment was effective on AS (Figure 7.3). In particular, the 5 h NMMO pretreatment increased the BMP of AS by 58% (Figure 4.5). The improvement in BMP was likely due to the LOI reduction and WRC increment (Table 4.3). Nevertheless, the enhanced methane production obtained from AS is still far from the theoretical maximum methane production, i.e. 490 mL $CH_4$/g VS, as confirmed by the VS degradation during AD, which reached 21% at best (Figure 4.6).

The ultrasound pretreatment performed in Chapter 5 resulted in two streams, i.e. liquor and solid residues (Figure 7.4). The solid residues showed a lower extractives content, but no significant changes in lignin or sugar content (Table 5.3). The BMP of pretreated AS was constantly below that of raw AS (Figure 5.2). The solubilisation percentage calculated after pretreatment (i.e. 6%) was significantly lower than that observed for HS, i.e. 15 - 24% (Table 5.2). The low solubilisation is likely due to the leathery and resistant structure of the AS, which did not allow the ultrasonic waves to penetrate the substrate. The polyphenols and sugars concentration measured in the liquor obtained from AS was higher in the MeOH-based media and increased with the pretreatment temperature (Table 5.2). The maximum concentrations of extracted polyphenols and sugars measured in the liquor were 0.5 (± 0.0) and 2.9 (± 0.1) g/L, respectively (Table 5.2). Similarly to HS, the presence of MeOH inhibited the AD of the liquor from AS (Figure 5.1), whereas the water-based liquors obtained at ambient temperature and 80 °C produced 84.4 (± 2.6) mL and 107.0 (± 6.2) mL $CH_4$/100 mL liquor, respectively (Figure 5.1).

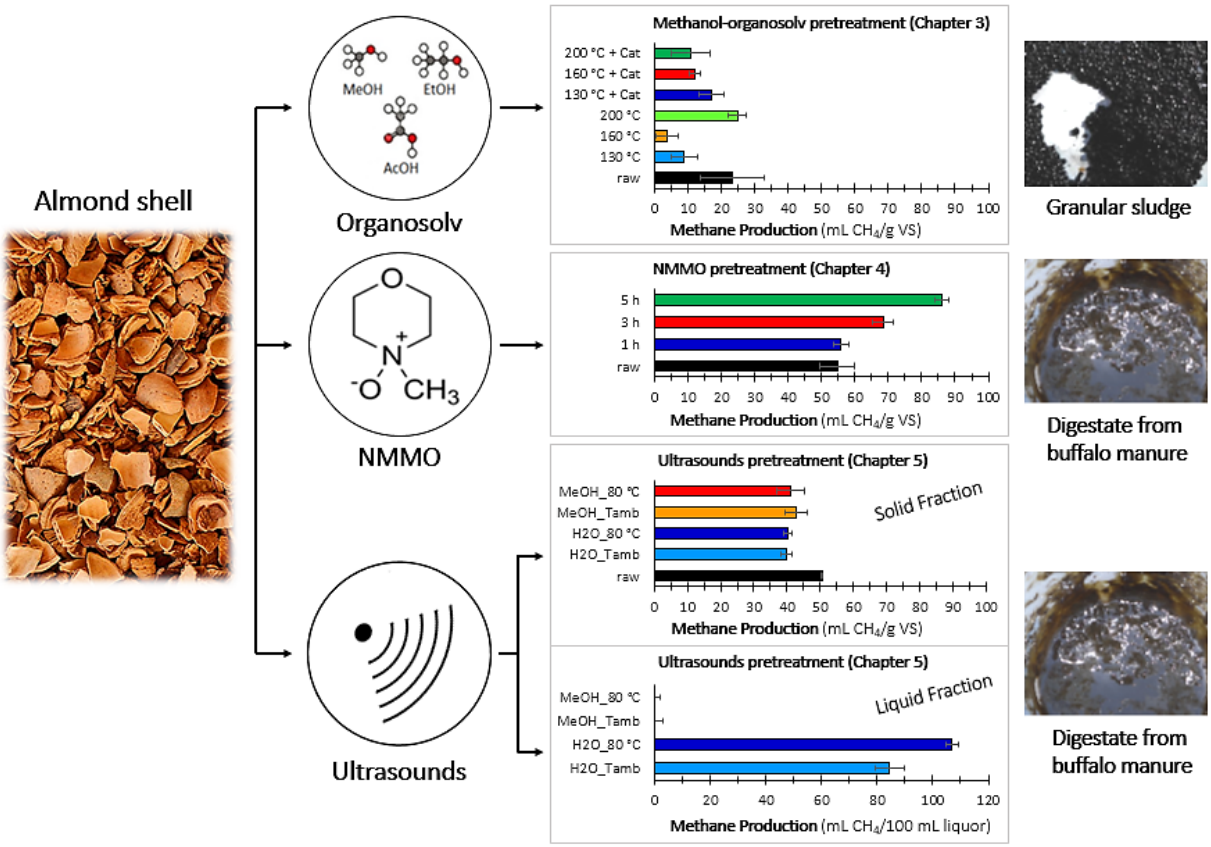


**Figure 7.3 –** Impact of methanol-organosolv (Chapter 3), NMMO (Chapter 4), and ultrasounds (Chapter 5) pretreatments on methane production potential of almond shell.

*7.2.3 Spent coffee grounds*

Contrary to the nut residues, the type of inoculum was found not to significantly affect the AD of SCG (Figure 7.2). The BMP of raw SCG observed in Chapter 3 and Chapter 4 was 293.4 (± 46.6) and 337.4 (± 16.5) mL $CH_4$/g VS, respectively (Tables 3.3 and 4.4). This result is likely due to the small particle size of SCG. The SCG, being a powder, guarantee an adequate contact with the inoculum, despite the physical limitation of the granular sludge. Nevertheless, similarly to HS, the trend of methane production from SCG using a granular sludge as the inoculum was characterised by two stages, whereas using the DBM allowed a more stable AD process, with a lag phase followed by an exponential increase in methane production before reaching the steady state.

The organosolv pretreatment performed in Chapter 3 resulted in a lower lignin and extractives content (Table 3.4) and increased porosity index of the pretreated SCG (Table 3.5). However, these changes did not translate in significant increment of the BMP, with the maximum production, i.e. 322.9 (± 19.5) mL $CH_4$/g VS (Figure 3.2), being statistically comparable with the raw SCG. Similarly, the NMMO pretreatment investigated in Chapter 4 (Figure 7.3)

increased the WRC of SCG (Table 4.3), but did not significantly increase the BMP of this substrate (Figure 4.5). After AD, the analysis of degraded VS showed that the raw SCG was already highly biodegradable (i.e. 71%) (Figure 4.6), leaving little extra potential to be unlocked with pretreatments. For this reason, further investigation should be focused on the valorisation of the components not being degraded during AD, i.e. lignin, and on the valuable biomolecules present in the extractives.

Chapter 5 focused on both liquid and solid streams recovered after ultrasound pretreatment (Figure 7.4). The substrate solubilisation increased with the pretreatment temperature, up to 21% (Table 5.2). The compositional analysis of pretreated SCG showed that only the extractives content was significantly lower than that of raw SCG (Table 5.3). The polyphenols solubilisation increased with pretreatment severity, i.e. highest temperature and use of MeOH solution as the medium (Table 5.2). On the other hand, the maximal sugar extraction was observed in water-based liquor pretreated with ultrasounds at 80 °C (Table 5.2). The highest concentrations of polyphenols and sugars measured in the liquor were 0.8 (± 0.0) and 2.7 (± 0.1) g/L, respectively (Table 5.2). The BMP of the water-based liquors obtained at ambient temperature and 80 °C were 102.9 (± 5.9) mL and 160.9 (± 16.6) mL $CH_4$/100 mL liquor, respectively (Figure 5.1). The BMP of SCG recovered after ultrasound pretreatment was comparable with the raw substrate, achieving 366.2 (± 4.2) mL $CH_4$/g VS (Figure 5.2). However, the methane production rate slightly increased by 13% (Table 5.4).

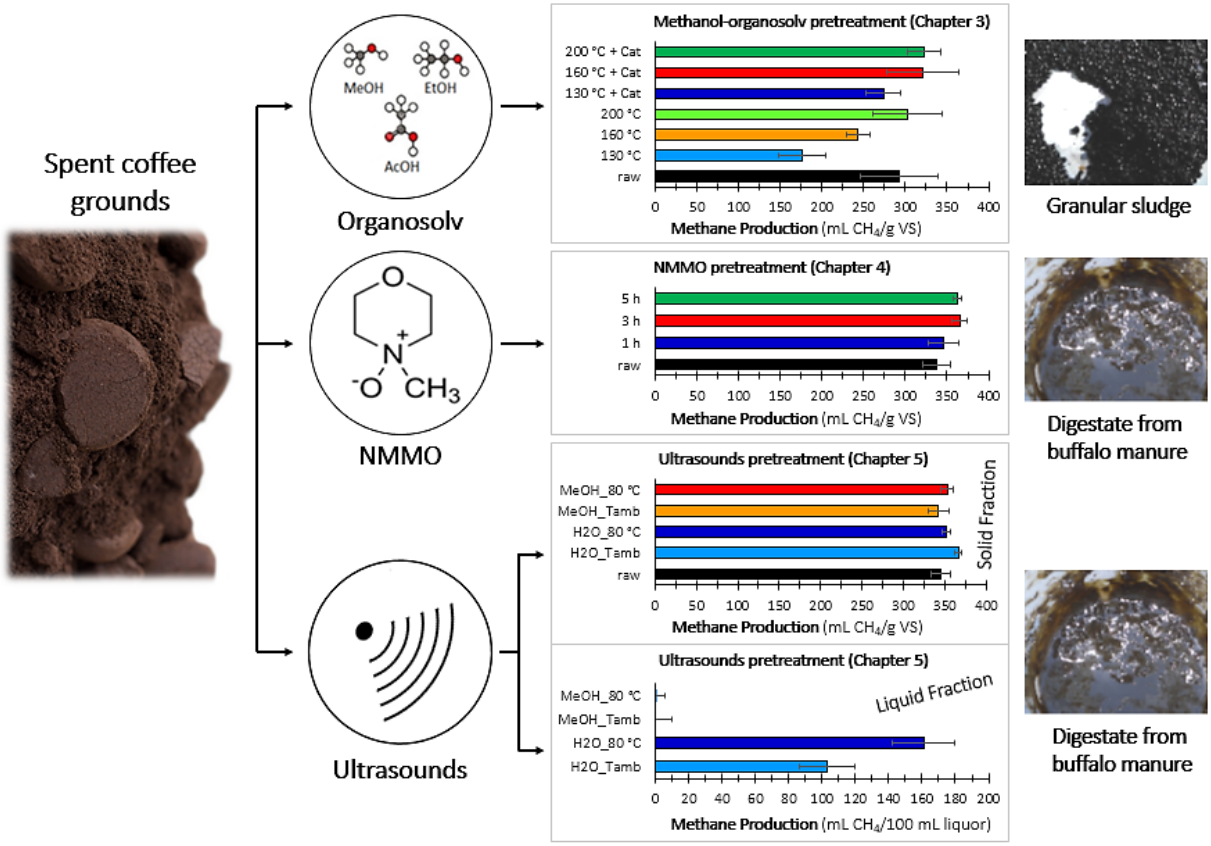


**Figure 7.4 –** Impact of methanol-organosolv (Chapter 3), NMMO (Chapter 4), and ultrasounds (Chapter 5) pretreatments on methane production potential of spent coffee grounds.

### *7.2.4 Fed-batch anaerobic digestion of hazelnut skin*

Among the three substrates investigated in this thesis, HS was the most interesting for its lignocellulosic composition, extractives content, and response to pretreatments. Therefore, HS was chosen to investigate the impact of long-term AD in fed-batch mode (Figure 7.5) (Chapter 6). A novel reactor configuration was proposed to decouple the solid waste retention time (SWRT) from the solid biomass retention time (SBRT). A stainless steel mesh container (SSMC) (Figure 6.1) was used to retain the HS while being soaked in the liquid phase of the reactor, where the microorganisms were enriched over long-term operation (Figure 6.5). A short SWRT is desirable to reduce the operating costs of the AD process. On the contrary, microorganisms may require a longer time to adapt to the LM. The microbial community analysis showed the enrichment of microbial phyla capable of degrading highly recalcitrant substrates, such as HS (Figure 6.5). The reactor configuration allowed increasing the HS load while reducing the SWRT. Raw HS produced maximally 19.29 mL $CH_4$/g $VS_{add}$/d (Figure 6.2).

Interestingly, the accumulation of polyphenolic compounds in the liquid phase of the reactor (Figure 6.4A) turned out to be an inhibitory factor for AD. On the contrary, this factor did not

emerge in batch mode (Chapters 3, 4, 5). Once the HS load was increased and the SWRT shortened, pH correction was required to maintain the reactor under optimal conditions for methane production. The use of NaOH for pH correction negatively affected the reactor operation, likely due to the reaction with the accumulated polyphenols and the formation of sodium phenolate. Sodium phenolate is an antiseptic and disinfectant aromatic alcohol that inhibits microorganisms' growth (Prado Martin et al., 2013). NaOH was replaced with $Na_2CO_3$ for pH control, and no further issues were observed when dosing the alkaline solution.

Although the formation of sodium phenolate was averted, the accumulation of polyphenols or other compounds in the liquid phase of the reactor can still lead to AD failure in long-term operation. A 3 h maceration of the HS was tested before AD to overcome this issue. The maceration removed 82% of the polyphenols present in HS (Table 6.3). Nevertheless, the methane production potential of macerated HS was negatively affected by maceration (Figure 6.2). In addition, the polyphenols concentration in the liquid phase of the reactor was stable, despite switching to macerated AD as the reactor feeding (Figure 6.4A). Alternatively, the most performing MeOH-organosolv pretreatment from Chapter 3 was selected. Organosolv pretreated HS has a lower lignin (by 9%) and polyphenols (by 97%) content than raw HS (Table 6.3). When feeding organosolv pretreated HS, the polyphenols concentration in the liquid phase was reduced (Figure 6.4A), and the overall methane production increased by 21% (Figure 6.2).

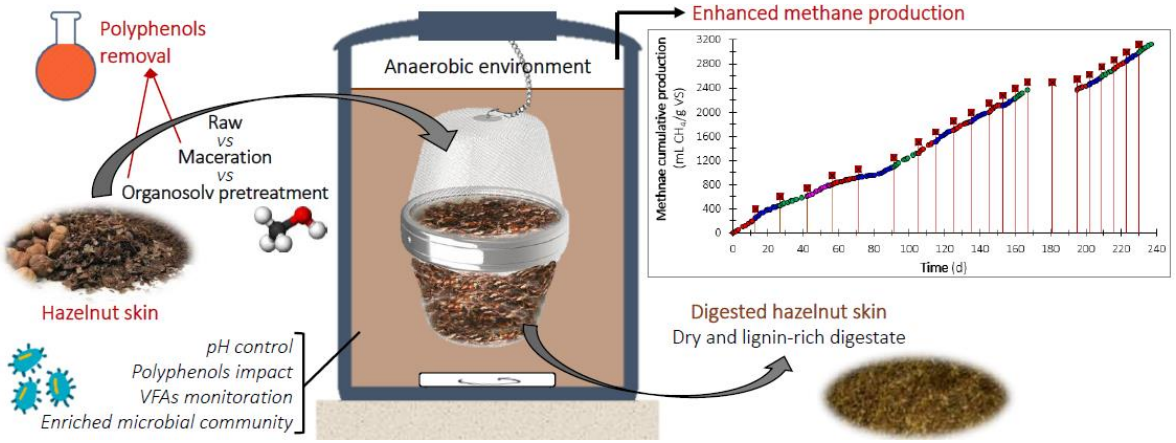


**Figure 7.5 –** Enhanced anaerobic digestion of raw, macerated, and organosolv-pretreated hazelnut skin in fed-batch mode (Chapter 6).

### 7.3 Conclusion of this thesis on valorisation of nut and coffee residues

The three pretreatments investigated in this thesis showed that MeOH-organosolv and NMMO pretreatment are the most effective techniques to enhance the AD of HS. On the other hand, only NMMO pretreatment enhanced the methane production potential of AS. Finally, none of

the investigated strategies unlocked extra methane production potential from SCG. However, the ultrasound pretreatment showed promising results to valorise the liquid streams of the three substrates. The common point between the three pretreatments was the removal of extractives from the three LMs. In particular, HS and SCG can be further investigated to explore the full potential of the non-structural valuable molecules representing a significant aliquot of their composition. On the other hand, another possibility to valorise highly resistant substrates, such as AS, can be co-digestion with other substrates depending on the availability in the surrounding region of the LM collection. Considering the example of confectionary industries, the co-digestion of the residues from nuts, coffee and cocoa should be investigated to mitigate the impact of the most recalcitrant fractions during AD.

## 7.4 Recommendations and future perspectives

### *7.4.1 Alternative pretreatment strategies for lignocellulosic materials*

Conventional and more severe strategies, such as steam explosion or acid pretreatment, may be tested to undermine the external barrier of AS. Steam explosion was effective for several LMs (Sarker et al., 2021). Nevertheless, it requires severe pretreatment conditions, such as high temperature (i.e. 160 - 260 °C) and pressure (i.e. 5 - 50 atm), which increase the overall cost of the pretreatment, and can lead to hemicellulose sugars loss (Amin et al., 2017). Acid pretreatment is one of the most studied techniques for LMs valorisation. However, the waste streams from acid pretreatment generally have a high environmental impact (Solarte-Toro et al., 2019).

Focusing on the pretreatments proposed in this thesis, other organic solvents may be explored for lignin dissolution. Lignin is highly soluble in pyridine and dimethyl sulfoxide (DMSO) (Sameni et al., 2017). However, the easy recovery, low cost, and lack of toxicity promoted the use of ethanol, methanol, and acetic acid (Ferreira and Taherzadeh, 2020). Among these, ethanol is the most studied organic solvent. Nevertheless, methanol showed promising results in this thesis for methane production from HS as well (Chapter 3). On the contrary, Mancini et al. (2018) failed to increase the methane production potential of HS using ethanol as the organic solvent. Acid catalysts are the most employed, with $H_2SO_4$ being the most performing on a wide range of LMs (Ferreira and Taherzadeh, 2020). Nevertheless, alternative catalysts, e.g. NaOH (Zhong et al., 2021) and oxalic acid (Sar et al., 2022), would benefit from further studies since they have only been tested on a few LMs. In any case, the economic viability of the pretreatment using these alternative compounds should be carefully evaluated.

The swelling-mode, i.e. 73% (*w/w*), NMMO pretreatment successfully enhanced the AD of HS and AS (Chapter 4). The exposure time may be further extended, but the energy demand and process costs will consequently increase. Other solvents acting on the cellulosic component of the biomass can be tested, aiming to undermine the most recalcitrant substrates, e.g. AS. Ionic liquids, e.g. 1-butyl-3-methylimidazolium chloride ([Bmim][Cl]), 1-allyl-3-methylimidazolium chloride ([Amim][Cl]), and 1-ethyl-3-methylimidazolium acetate ([Emim][OAc]), can dissolve cellulose, but the high costs of their synthesis limited the ionic liquids perspective till now (Chen et al., 2019). In particular, the synthesis of new ionic liquids with high hydrogen bonds accepting ability of cations and anions should be promoted, this property being positively correlated with the cellulose solubility in the solvent (Chen et al., 2019). In addition, more severe ultrasounds conditions (Chapter 5), e.g. higher energy density applied, as well as coupling the ultrasounds with other solvent-based pretreatments can be tested.

Pretreatments account for about 40% of the overall costs in the biorefinery of LMs (Haldar and Purkait, 2021). For this reason, emerging pretreatments involving recyclable solvents should be preferred over the traditional techniques mentioned above. Apart from the three pretreatments investigated in this PhD thesis, an innovative strategy is recently emerging and can be the starting point for future studies, i.e. deep eutectic solvents (DES) pretreatment. DES have been proposed as an alternative to NMMO and ionic liquids (Chen et al., 2019). DES are mixtures of two or three components, i.e. hydrogen bond donors and hydrogen bond acceptors, with a melting point lower than that of each component of the mixture (Isci and Kaltschmitt, 2021). Contrary to NMMO and ionic liquids, DES are more effective in lignin removal than cellulose dissolution (Wang and Lee, 2021). Nevertheless, this PhD thesis showed that the NMMO pretreatment is also effective on the lignin content when performed under specific pretreatment conditions (Chapter 4). DES can be approximately recovered by 90% (Isci and Kaltschmitt, 2021), which is lower than the NMMO recovery yield, i.e. 99% (Sayyed et al., 2019). On the other hand, DES are easily biodegradable and significantly less expensive than NMMO (Wang and Lee, 2021). At the current status, DES pretreatment has mainly been used for LMs fractionation, but only a few studies investigated the impact on the methane production potential of the solid residues (Olugbemide et al., 2021; Yu et al., 2019). Further studies may be proposed to select the optimal conditions for selective recovery of the lignin while leaving the structural sugars untouched for subsequent AD.

*7.4.2 Cascade process for advanced valorisation of lignocellulosic materials*

The present thesis showed how to valorise recalcitrant LMs through AD, choosing the most performing pretreatment technique depending on the lignocellulosic composition and physical properties of the LM. Nevertheless, the presence of biomolecules different from cellulose, hemicellulose, and lignin should also be considered when these represent a considerable amount of the overall substrate composition. In this thesis, it was observed that, despite the enhancement in methane production, well-established pretreatments, e.g. organosolv, barely changed the lignocellulosic composition of the LMs here investigated. This behaviour can be due to the abundance of other biomolecules, i.e. extractives, which likely undermined the pretreatment mechanisms once released in the aqueous solvent solution. This hypothesis will need further investigations and can be verified by performing a selective removal of these components.

In this perspective, the path proposed in Figure 7.6 can be followed when dealing with highly recalcitrant (i.e. high lignin content) and extractives-rich LMs. Partial or complete extractives removal can be achieved by maceration or performing pretreatments under milder conditions than usual, e.g. lower temperature, shorter duration, or lower solvent concentration. Mild pretreatment should avoid changes in the structural components, e.g. structural sugar hydrolysis, while removing the non-bound biomolecules. After that, a stronger pretreatment can be performed on the extractives-free LM. The third step can be the AD of the pretreated substrate. The present thesis showed that, despite pretreatments enhancing the biodegradability of LMs, they still exhibit a high non-biodegraded VS content after AD. In Chapter 4, the NMMO pretreatment enhanced the VS degradation from HS from 24 to 54%. The remaining VS are likely mainly lignin, a non-biodegradable component during AD. Therefore, the digested lignin-rich LM can undergo post-treatment, e.g. organosolv, for a full lignin recovery.

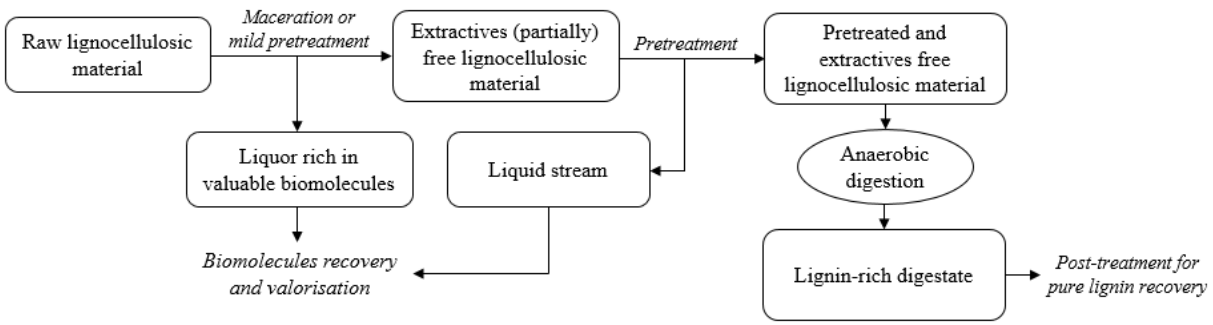


**Figure 7.6 –** Proposed pathway for advanced valorisation of extractives and lignin rich lignocellulosic materials.

*7.4.3 A zero solid waste approach for lignin-rich substrates*

The reactor configuration proposed in Chapter 6 for AD of HS biodegradation is based on the use of a SSMC to decouple the SWRT of the HS from the SBRT. This configuration allows obtaining a lignin-rich digestate with lower moisture content than the digestate from a stirred-tank reactor (STR). The digested LM recovered from the SSMC is likely to be mainly lignin due to the degradation of sugars during the AD process. The digestate is commonly used as a soil amendment (Mosa et al., 2018). However, a few studies reported that digested LMs are particularly profitable for biochar production (Ghysels et al., 2019; Inyang et al., 2010).

Biochar is emerging as an alternative to activated carbon due to the lower cost and great potential to enhance the AD process. The meta-analysis conducted by Alhashimi and Aktas (2017) showed that biochar production requires significantly lower energy than activated carbon (i.e. 6.1 MJ/kg *vs* 97.0 MJ/kg), which considerably reduces the overall costs. Biochar generally has lower specific surface and adsorption capacity than activated carbon but more abundant surface functional groups (Tan et al., 2017). On the other hand, biochar can be activated using physical (e.g. steam and gas activation) and chemical (e.g. alkali, acid and oxidation treatment) methods to increase its adsorption capacity (Tan et al., 2017). Biochar is produced via pyrolysis at 350 - 650 °C in an oxygen-free environment. Together with biochar, the main product from pyrolysis is syngas, mainly composed of CO, $CO_2$, and $CH_4$ (Zhao et al., 2021). The gaseous stream can be used for bioethanol or biobutanol production via solventogenesis (He et al., 2022, 2021a, 2021b).

Biochar is usually produced from raw LMs. However, producing biochar from digested LMs offers the advantage of generating extra biofuels during the preceding AD process. The biochar from digested LMs fits well with the idea of a zero solid waste approach to valorise lignin-rich LMs. The biochar can be reintegrated into the AD process to enhance the AD performance and can be used to upgrade the biogas to biomethane (Route1 in Figure 7.7) removing $CO_2$ and hydrogen sulfide impurities (Das et al., 2019; Zhao et al., 2021). An alternative to biogas upgrading for energetic purposes is to use methane-oxidizing bacteria to produce biofuels, e.g. methanol, biopolymers, e.g. polyhydroxyalkanoates (PHAs), and biomolecules, e.g. microbial proteins, from the methane generated from the AD process (Route 2 in Figure 7.7) (Patel et al., 2021). Previous studies demonstrated that upgraded biogas is more profitable than raw biogas for microbial protein production (+ 6% in protein content) (Acosta et al., 2020). Nevertheless,

the costs and benefits of upgrading the biogas before protein production should be carefully evaluated.

The biochar addition helps the AD stability by mitigating the impact of volatile fatty acids (VFAs) accumulation (Zhu et al., 2022). Also, biochar is an electron conductor, and its addition to the AD process can enhance the direct interspecies electron transfer (DIET) between syntrophic acetogens and methanogens (Qiu et al., 2019). In this perspective, the biochar addition is profitable when incomplete fermentation for VFAs production and chain elongation is desired (Liu et al., 2017; Lu et al., 2020). Nevertheless, biochar addition can also inhibit the AD process (Zhao et al., 2021), and further studies are required to disclose this aspect.

Apart from the well-known applications, biochar can be employed for polyphenols recovery. Abid et al. (2022) recently used the biochar from olive mill solid waste to adsorb the polyphenols from olive mill wastewater. This is an interesting perspective for substrates rich in lignin and polyphenols such as HS. Therefore, the biochar from the digested HS could be used to adsorb the polyphenols recovered in a mild pretreatment and mitigate the impact of polyphenols in fed-batch AD. Chapter 5 showed that it is difficult to extract valuable molecules selectively from LMs. For instance, after ultrasound treatment, the HS liquor was rich in sugars and polyphenols. The biochar produced from a lignin-rich digestate could address this issue due to its affinity with polyphenols, because of the abundance in phenolic functional groups into the biochar (Zhao et al., 2021). This hypothesis needs experimental evidence to be confirmed, which involves optimising the biochar production and the experimental conditions for a selective recovery of polyphenols. In the zero solid waste approach here proposed (Figure 7.7), the outlet biochar from AD will be regenerated and used as an amendment for agricultural purposes once exhausted. On the other hand, the biochar used for polyphenols adsorption can be regenerated and a polyphenol-rich solution can be obtained for further use in food chemistry, cosmetic, and technological applications (de Araújo et al., 2021; de Lima Cherubim et al., 2020).

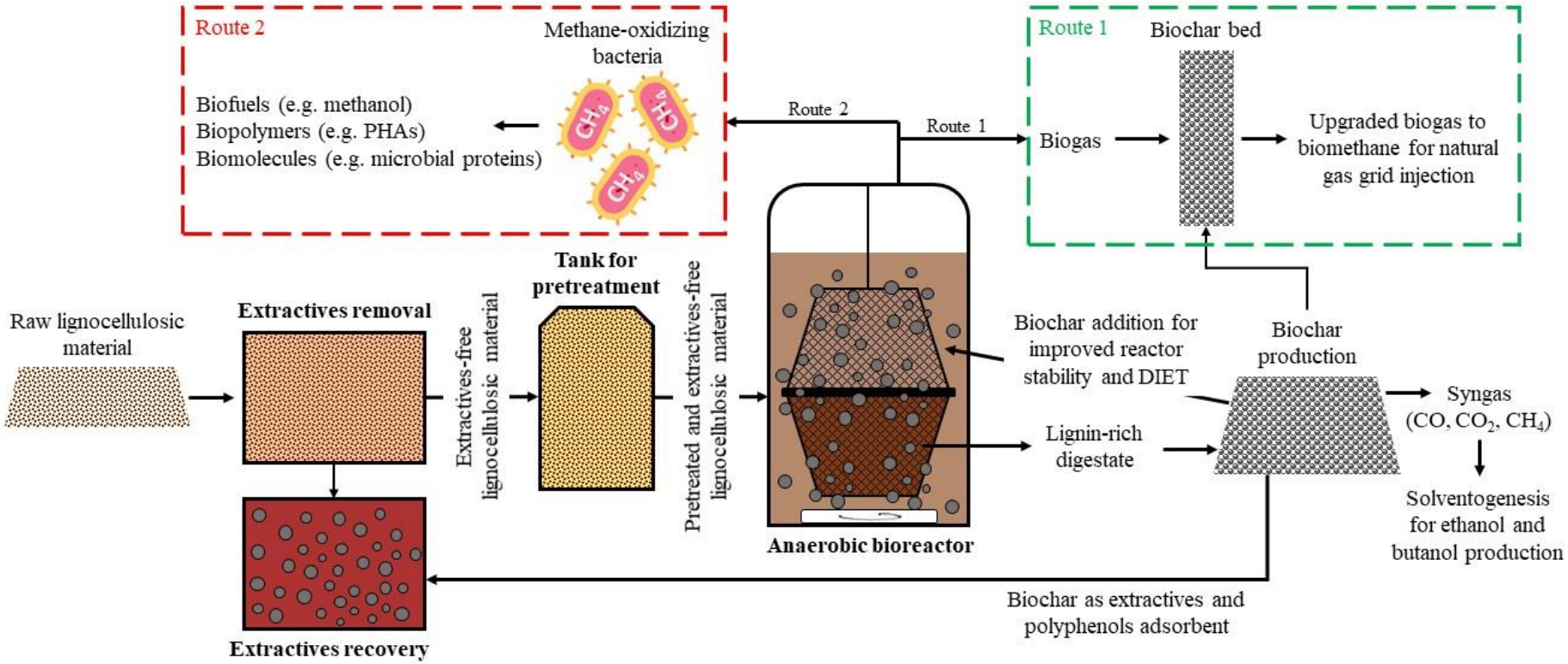


**Figure 7.7 –** Zero solid waste approach for a complete valorisation of lignocellulosic materials (LMs). The non-bound biomolecules are separated from the LM and selectively recovered using the biochar produced from the lignin-rich digestate after anaerobic digestion (AD). The extractives-free LMs are pretreated and, subsequently, used as the substrate for AD in a bioreactor equipped with the mesh container proposed in Chapter 6. The biogas produced during AD is upgraded to biomethane (Route 1) using the same biochar produced from the digested LM, whereas the syngas can be used for biofuels production through solventogenesis. Alternatively, biogas can be used as the substrate to produce biofuels, biopolymers, and biomolecules through methane-oxidizing bacteria (Route 2).

## 7.5 References


Abid, N., Masmoudi, M.A., Megdiche, M., Barakat, A., Ellouze, M., Chamkha, M., Ksibi, M., Sayadi, S., 2022. Biochar from olive mill solid waste as an eco-friendly adsorbent for the removal of polyphenols from olive mill wastewater. Chem. Eng. Res. Des. 181, 384–398. https://doi.org/10.1016/j.cherd.2022.02.029

Acosta, N., Sakarika, M., Kerckhof, F.M., Law, C.K.Y., De Vrieze, J., Rabaey, K., 2020. Microbial protein production from methane via electrochemical biogas upgrading. Chem. Eng. J. 391. https://doi.org/10.1016/j.cej.2019.123625

Alhashimi, H.A., Aktas, C.B., 2017. Life cycle environmental and economic performance of biochar compared with activated carbon: A meta-analysis. Resour. Conserv. Recycl. 118, 13–26. https://doi.org/10.1016/j.resconrec.2016.11.016

Amin, F.R., Khalid, H., Zhang, H., Rahman, S., Zhang, R., Liu, G., Chen, C., 2017. Pretreatment methods of lignocellulosic biomass for anaerobic digestion. AMB Express 7. https://doi.org/10.1186/s13568-017-0375-4

Balat, M., 2011. Production of bioethanol from lignocellulosic materials via the biochemical pathway: A review. Energy Convers. Manag. 52, 858–875. https://doi.org/10.1016/j.enconman.2010.08.013

Chen, Y.L., Zhang, X., You, T.T., Xu, F., 2019. Deep eutectic solvents (DESs) for cellulose dissolution: a mini-review. Cellulose 26, 205–213. https://doi.org/10.1007/s10570-018-2130-7

Das, J., Rene, E.R., Dupont, C., Dufourny, A., Blin, J., van Hullebusch, E.D., 2019. Performance of a compost and biochar packed biofilter for gas-phase hydrogen sulfide removal. Bioresour. Technol. 273, 581–591. https://doi.org/10.1016/j.biortech.2018.11.052

de Araújo, F.F., de Paulo Farias, D., Neri-Numa, I.A., Pastore, G.M., 2021. Polyphenols and their applications: An approach in food chemistry and innovation potential. Food Chem. 338, 127535. https://doi.org/10.1016/j.foodchem.2020.127535

de Lima Cherubim, D.J., Buzanello Martins, C.V., Oliveira Fariña, L., da Silva de Lucca, R.A., 2020. Polyphenols as natural antioxidants in cosmetics applications. J. Cosmet. Dermatol. 19, 33–37. https://doi.org/10.1111/jocd.13093

Ferreira, J.A., Taherzadeh, M.J., 2020. Improving the economy of lignocellulose-based biorefineries with organosolv pretreatment. Bioresour. Technol. 299, 122695. https://doi.org/10.1016/j.biortech.2019.122695

Ghysels, S., Ronsse, F., Dickinson, D., Prins, W., 2019. Production and characterization of slow pyrolysis biochar from lignin-rich digested stillage from lignocellulosic ethanol production. Biomass and Bioenergy 122, 349–360. https://doi.org/10.1016/j.biombioe.2019.01.040

Haldar, D., Purkait, M.K., 2021. A review on the environment-friendly emerging techniques for pretreatment of lignocellulosic biomass: Mechanistic insight and advancements. Chemosphere 264, 128523. https://doi.org/10.1016/j.chemosphere.2020.128523

He, Y., Cassarini, C., Marciano, F., Lens, P.N.L., 2021a. Homoacetogenesis and solventogenesis from H2/CO2 by granular sludge at 25, 37 and 55 °C. Chemosphere 265, 128649. https://doi.org/10.1016/j.chemosphere.2020.128649

He, Y., Lens, P.N.L., Veiga, M.C., Kennes, C., 2022. Selective butanol production from carbon monoxide by an enriched anaerobic culture. Sci. Total Environ. 806, 150579. https://doi.org/10.1016/j.scitotenv.2021.150579

He, Y., Lens, P.N.L., Veiga, M.C., Kennes, C., 2021b. Enhanced Ethanol Production From Carbon Monoxide by Enriched Clostridium Bacteria. Front. Microbiol. 12, 1–19. https://doi.org/10.3389/fmicb.2021.754713

International Nut and Dried Fruit Council Foundation, 2021. Nuts & dried fruits statistical yearbook 2020/2021.

Inyang, M., Gao, B., Pullammanappallil, P., Ding, W., Zimmerman, A.R., 2010. Biochar from anaerobically digested sugarcane bagasse. Bioresour. Technol. 101, 8868–8872. https://doi.org/10.1016/j.biortech.2010.06.088

Isci, A., Kaltschmitt, M., 2021. Recovery and recycling of deep eutectic solvents in biomass conversions: a review. Biomass Convers. Biorefinery. https://doi.org/10.1007/s13399-021-01860-9

Liu, Y., He, P., Shao, L., Zhang, H., Lü, F., 2017. Significant enhancement by biochar of caproate production via chain elongation. Water Res. 119, 150–159. https://doi.org/10.1016/j.watres.2017.04.050

Lu, J.H., Chen, C., Huang, C., Zhuang, H., Leu, S.Y., Lee, D.J., 2020. Dark fermentation production of volatile fatty acids from glucose with biochar amended biological consortium. Bioresour. Technol. 303, 122921. https://doi.org/10.1016/j.biortech.2020.122921

Mancini, G., Papirio, S., Lens, P.N.L., Esposito, G., 2018. Anaerobic Digestion of Lignocellulosic Materials Using Ethanol-Organosolv Pretreatment. Environ. Eng. Sci. 35,

953–960. https://doi.org/10.1089/ees.2018.0042

Mosa, A., El-Ghamry, A., Tolba, M., 2018. Functionalized biochar derived from heavy metal rich feedstock: Phosphate recovery and reusing the exhausted biochar as an enriched soil amendment. Chemosphere 198, 351–363. https://doi.org/10.1016/j.chemosphere.2018.01.113

Olugbemide, A.D., Oberlintner, A., Novak, U., Likozar, B., 2021. Lignocellulosic corn stover biomass pre-treatment by deep eutectic solvents (DES) for biomethane production process by bioresource anaerobic digestion. Sustain. 13. https://doi.org/10.3390/su131910504

Panagiotis, T., Benyamin, K., Xinyu, Z., Xiao, Z., Irini, A., 2019. Methane oxidising bacteria to upcycle effluent streams from anaerobic digestion of municipal biowaste. J. Environ. Manage. 251. https://doi.org/10.1016/j.jenvman.2019.109590

Patel, S.K.S., Shanmugam, R., Lee, J.K., Kalia, V.C., Kim, I.W., 2021. Biomolecules Production from Greenhouse Gases by Methanotrophs. Indian J. Microbiol. 61, 449–457. https://doi.org/10.1007/s12088-021-00986-8

Prado Martin, J.G., Porto, E., de Alencar, S.M., da Glória, E.M., Corrêa, C.B., Ribeiro Cabral, I.S., 2013. Antimicrobial activity of yerba mate (*Ilex paraguariensis* St. Hil.) against food pathogens. Rev. Argent. Microbiol. 45, 93–98. https://doi.org/10.1016/s0325-7541(13)70006-3

Qiu, L., Deng, Y.F., Wang, F., Davaritouchaee, M., Yao, Y.Q., 2019. A review on biochar-mediated anaerobic digestion with enhanced methane recovery. Renew. Sustain. Energy Rev. 115, 109373. https://doi.org/10.1016/j.rser.2019.109373

Queirós, C.S.G.P., Cardoso, S., Lourenço, A., Ferreira, J., Miranda, I., Lourenço, M.J. V., Pereira, H., 2020. Characterization of walnut, almond, and pine nut shells regarding chemical composition and extract composition. Biomass Convers. Biorefinery 10, 175–188. https://doi.org/10.1007/s13399-019-00424-2

Sameni, J., Krigstin, S., Sain, M., 2017. Solubility of Lignin and Acetylated Lignin in Organic Solvents. BioResources 12. https://doi.org/10.15376/biores.12.1.1548-1565

Sar, T., Arifa, V.H., Hilmy, M.R., Ferreira, J.A., Wikandari, R., Millati, R., Taherzadeh, M.J., 2022. Organosolv pretreatment of oat husk using oxalic acid as an alternative organic acid and its potential applications in biorefinery. Biomass Convers. Biorefinery. https://doi.org/10.1007/s13399-022-02408-1

Sarker, T.R., Pattnaik, F., Nanda, S., Dalai, A.K., Meda, V., Naik, S., 2021. Hydrothermal pretreatment technologies for lignocellulosic biomass: A review of steam explosion and

subcritical water hydrolysis. Chemosphere 284, 131372. https://doi.org/10.1016/j.chemosphere.2021.131372

Sayyed, A.J., Deshmukh, N.A., Pinjari, D. V., 2019. A critical review of manufacturing processes used in regenerated cellulosic fibres: viscose, cellulose acetate, cuprammonium, LiCl/DMAc, ionic liquids, and NMMO based lyocell. Cellulose 26, 2913–2940. https://doi.org/10.1007/s10570-019-02318-y

Solarte-Toro, J.C., Romero-García, J.M., Martínez-Patiño, J.C., Ruiz-Ramos, E., Castro-Galiano, E., Cardona-Alzate, C.A., 2019. Acid pretreatment of lignocellulosic biomass for energy vectors production: A review focused on operational conditions and techno-economic assessment for bioethanol production. Renew. Sustain. Energy Rev. 107, 587–601. https://doi.org/10.1016/j.rser.2019.02.024

Spagnuolo, L., Posta, S. Della, Fanali, C., Dugo, L., De Gara, L., 2021. Antioxidant and antiglycation effects of polyphenol compounds extracted from hazelnut skin on advanced glycation end-products (Ages) formation. Antioxidants 10, 1–14. https://doi.org/10.3390/antiox10030424

Tajmirriahi, M., Momayez, F., Karimi, K., 2021. The critical impact of rice straw extractives on biogas and bioethanol production. Bioresour. Technol. 319, 124167. https://doi.org/10.1016/j.biortech.2020.124167

Tan, X., Liu, S., Liu, Y., Gu, Y., Zeng, G., Hu, X., Wang, X., Liu, S., Jiang, L., 2017. Biochar as potential sustainable precursors for activated carbon production: Multiple applications in environmental protection and energy storage. Bioresour. Technol. 227, 359–372. https://doi.org/10.1016/j.biortech.2016.12.083

Torres-Valenzuela, L.S., Ballesteros-Gómez, A., Sanin, A., Rubio, S., 2019. Valorization of spent coffee grounds by supramolecular solvent extraction. Sep. Purif. Technol. 228, 115759. https://doi.org/10.1016/j.seppur.2019.115759

Wang, W., Lee, D.J., 2021. Lignocellulosic biomass pretreatment by deep eutectic solvents on lignin extraction and saccharification enhancement: A review. Bioresour. Technol. 339, 125587. https://doi.org/10.1016/j.biortech.2021.125587

Xu, N., Liu, S., Xin, F., Zhou, J., Jia, H., Xu, J., Jiang, M., Dong, W., 2019. Biomethane production from lignocellulose: Biomass recalcitrance and its impacts on anaerobic digestion. Front. Bioeng. Biotechnol. 7, 1–12. https://doi.org/10.3389/fbioe.2019.00191

Yu, Q., Qin, L., Liu, Y., Sun, Y., Xu, H., Wang, Z., Yuan, Z., 2019. In situ deep eutectic solvent pretreatment to improve lignin removal from garden wastes and enhance production of

bio-methane and microbial lipids. Bioresour. Technol. 271, 210–217. https://doi.org/10.1016/j.biortech.2018.09.056

Zhao, W., Yang, H., He, S., Zhao, Q., Wei, L., 2021. A review of biochar in anaerobic digestion to improve biogas production: Performances, mechanisms and economic assessments. Bioresour. Technol. 341. https://doi.org/10.1016/j.biortech.2021.125797

Zhong, L., Wang, C., Xu, M., Ji, X., Yang, G., Chen, J., Janaswamy, S., Lyu, G., 2021. Alkali-catalyzed organosolv pretreatment of lignocellulose enhances enzymatic hydrolysis and results in highly antioxidative lignin. Energy and Fuels 35, 5039–5048. https://doi.org/10.1021/acs.energyfuels.1c00320

Zhu, Y., Jin, Z., Yu, Q., Zhao, Z., Zhang, Y., 2022. Alleviating acid inhibition in anaerobic digestion of food waste: Coupling ethanol-type fermentation with biochar addition. Environ. Res. 212, 113355. https://doi.org/10.1016/j.envres.2022.113355

## Author information

### Biography

Armando Oliva started his PhD at the National University of Ireland Galway (NUIG) in December 2018, supported by the Science Foundation Ireland (SFI) through the SFI Research Professorship Programme *Innovative Energy Technologies for Biofuels, Bioenergy and a Sustainable Irish Bioeconomy* (IETSBIO$^3$). In August 2020, he moved to the University of Naples Federico II (Italy) for a PhD mobility. Earlier, Armando received a MSc degree in Environmental Engineering and a BSc degree in Civil and Environmental Engineering at the University of Cassino and Southern Lazio (Italy). He also worked at the Instituto de la Grasa in Seville (Spain) for a curricular internship in 2018. Armando's research interests include anaerobic digestion, solid waste management, pretreatment techniques, and bioprocess for solid waste and wastewater treatment.

### Publications

Alonso-Fariñas, B., **Oliva, A.**, Rodríguez-Galán, M., Esposito, G., García-Martín, J.F., Rodríguez-Gutiérrez, G., Serrano, A., Fermoso, F.G., 2020. Environmental assessment of olive mill solid waste valorization via anaerobic digestion versus olive pomace oil extraction. Processes 8. https://doi.org/10.3390/PR8050626

**Oliva, A.**, Tan, L.C., Papirio, S., Esposito, G., Lens, P.N.L., 2021. Effect of methanol-organosolv pretreatment on anaerobic digestion of lignocellulosic materials. Renew. Energy. https://doi.org/10.1016/j.renene.2020.12.095

**Oliva, A.**, Papirio, S., Esposito, G., Lens, P.N.L., 2022. Pretreatment of Lignocellulosic Materials to Enhance their Methane Potential, in: Sinharoy, A., Lens, P.N.L. (Eds.), Renewable Energy Technologies for Energy Efficient Sustainable Development, Applied Environmental Science and Engineering for a Sustainable Future. Springer, pp. 85–120. https://doi.org/10.1007/978-3-030-87633-3_4

**International conferences**

5th EurAsia Waste Managment Symposium (Online), organised by the Environmental Engineering Department of Yildiz Technical University and ISTAC Inc. in collaboration with the Ministry of Environment and Urbanization and International Waste Working Group (IWWG), Instanbul, Turkey (26.10.2020 - 28.10.2020).

3rd International Conference for Bioresource Technology for Bioenergy, Bioproducts & Environmental Sustainability (Biorestec) (Online), organised by Elsevier (17.05.2021 - 19.05.2021).

8th International Conference on sustainable solid waste management (Online), organised by the National Technical University of Athens, the Global WtERT Council (GWC) and the World Biogas Organization Thessaloniki, Greece (23.06.2021 – 26.06.2021).

**Courses and modules**

The table below reports the module completion (30 ECTS) as a part of the structured PhD at NUI Galway

| Code | Module Title | Session | ECTS | Status |
|---|---|---|---|---|
| GS515 | Research Paper Publication | 2020 - 2021 | 5 | Completed |
| GS514 | Research Placement 3 | 2020 - 2021 | 15 | Completed |
| GS501 | Seminar Programme | 2020 - 2021 | 5 | Completed |
| GS502 | Journal Club Programme | 2020 - 2021 | 5 | Completed |